

Copyright is owned by the Author of the thesis. Permission is given for a copy to be downloaded by an individual for the purpose of research and private study only. The thesis may not be reproduced elsewhere without the permission of the Author.

GEOLOGY AND ITS RELATIONSHIP TO EROSION  
IN THE SOUTHERN RUAHINE RANGE,  
NORTH ISLAND, NEW ZEALAND

A thesis presented in partial fulfilment of the requirements  
for the degree of Doctor of Philosophy in Soil Science  
at Massey University, Palmerston North

MICHAEL MARDEN

---

Volume I

---

July 1984

ABSTRACT

The structure and lithology of a sequence of Mesozoic greywackes comprising the Torlesse terrane within the southern Ruahine Range has been mapped. At a scale of 1:25 000 the sequence was subdivided into informal lithozones with one or more lithozones constituting a higher order lithostratigraphic unit here referred to as a Lithotype. Each of three recognised Lithotypes occupies a consistent stratigraphic position throughout a 40 km long mapped area. From east to west the three Lithotypes are: (1) the Tamaki Lithotype; (2) the Wharite Lithotype; and (3) the Western Lithotype. The easternmost Tamaki Lithotype and the westernmost Western Lithotype consist of a relatively undeformed flysch-type sequence of distal turbidites. The centrally located Wharite Lithotype structurally underlies the Tamaki Lithotype but overlies the Western Lithotype. It comprises a complex sequence of predominantly flysch-type sedimentary rocks, together with lithologically diverse, argillite-dominated, clast-bearing debris flow deposits; large sheet-like bodies of massive volcanics (and associated cherts) that have been emplaced by gravitational sliding; and intact pillow lava accumulations and horizons of red and green argillite of syndepositional origin.

Major and trace element analyses of volcanic lithologies indicate that most samples were erupted in a mid-ocean ridge or intraplate setting. None appear to have been derived from an island arc setting.

The bulk of the clastic sediments consist of reworked materials derived by the erosion of a mixed volcano-plutonic source and redeposited in a distal deep-water submarine fan environment. Blocks of allochthonous fossiliferous shallow-water lithologies indicate that the source terrane, in part, comprised rocks of Late Triassic age. Autochthonous fossils indicate that sedimentation continued until at least Late Jurassic time.

Part of the stratigraphic sequence was severely deformed along a low angle thrust zone in Early Cretaceous time at the onset of the Rangitata Orogeny. An early phase of ductile deformation resulted in plastically and permanently deformed rocks. Ductile deformation is restricted to strata comprising the Wharite Lithotype which, with its allochthonous debris, in part, constitutes an olistostrome that has undergone tectonic deformation and hence also constitutes a melange. Thus it may be regarded as a tectonised olistostrome. Ductile deformation was succeeded by the development of shear fractures during subsequent phases of brittle deformation that affected strata comprising all three Lithotypes. Brittle deformation

occurred in conjunction with episodes of faulting and folding during the second orogeny - the Kaikoura Orogeny in Pliocene to Recent times.

Active faults that were initiated during the early phase of ductile deformation continued to be sites of active fault displacement throughout Quaternary and Holocene time. Late Quaternary tectonic features along these major active faults have been mapped. Minimum rates of vertical fault displacements since Ohakean time approximate 1 mm/yr in this area.

Several phases of folding were recognised, including: (1) an early phase of syndepositional, highly asymmetric folds with well developed axial plane cleavage; and (2) three post-lithification phases of folding - e.g. (a) steeply plunging isoclinal folds; (b) subhorizontal, open asymmetric folds; and (c) steeply plunging open folds.

Contacts between the three Lithotypes are not thought to be major tectonic breaks but are instead of primary depositional origin and have become sites of subsequent fault movement in Quaternary time. The three Lithotypes may therefore represent a near complete eastward dipping, westward younging overturned stratigraphic sequence. They are not fault-bound terranes.

Metamorphism to prehnite pumpellyite grade, folding and rotation of the strata to its present steep attitude predates Late Cretaceous sedimentation. The westward rotation and imbrication of thrust sheets that are internally westward younging but form part of a regionally eastward younging succession of thrust sheets was the result of underthrusting at a convergent plate margin.

The relationship between structural and lithological characteristics of the Torlesse bedrock and the magnitude of valley slope erosion in the southern Ruahine Range is investigated. Comparison of aerial photographs spanning a 28 year period between 1946 and 1974 indicate that erosion has increased by 91%. The greatest proportion of this eroded area occurs on the steeper north- and west-facing slopes. Saturation of colluvium during major storm events is the prime triggering mechanism for the majority of shallow translational slope movements. Debris slides and debris avalanches predominate and result from failure at less than 1m depth at the colluvium-bedrock contact. Rock slides are few in number and are structurally controlled, failing along bedding plane surfaces at greater than 1m depth. Rock falls and rock topples are least numerous and only involve small quantities of material.

An erosion rate of  $1215\text{m}^3/\text{ha}/\text{yr}$  for the southern Ruahine Range is of the same order of magnitude as other New Zealand and overseas studies and although considered to be severe it is not unduly excessive.

Much of the forest deterioration in this area is due to the opening of the canopy by the successive removal of large tracts of forest vegetation through mass movement processes during episodes of increased rainfall.

Large-scale rotational and translational mass movement features including rock slumps, earth slumps, earth slides and ridge-top features (involving bedrock only), have been documented from 109 localities. A relationship between the incidence of rock slumps and major fault breccia zones has been established in this area. The majority of large-scale mass movement features failed in pre-historic time but two failed in historic time. The consequences of future mass movements upon lowland areas adjacent to the base of the Range is discussed.

A map showing the relative stability of slopes and the predominant forms of slope movement most likely to occur under the present seismic, climatic, physiographic and human conditions is presented.

\*\*\*\*\*

### ACKNOWLEDGEMENTS

The writer wishes to acknowledge the following for their assistance in various aspects related to this thesis.

Thanks are especially extended to the National Water and Soil Conservation Organisation, without whose financial assistance, over a 3½ year period, this thesis would not have been possible.

Particular thanks to Drs V E Neall, R B Stewart and P E H Gregg of the Soil Science Department, Massey University, who supervised, criticised and guided me through this study.

Gratitude is extended to the personnel of the Manawatu Catchment Board, the NZ Forest Service and to the Aokautere Science Centre, of Palmerston North, for their assistance in obtaining relevant materials and information.

Encouragement and financial assistance received from members of the NZ Geological Survey has made it possible to prepare some of the aspects of this research for publication. In particular, many thanks to G Lensen, A Hull and K Berryman of the Earth Deformation Studies group and to J E Simes, P Strong and H J Campbell for assistance with microfossil and macrofossil identifications.

Many thanks to Professor J A Grant-Mackie of the Geology Department, Auckland University, and Dr G R Stevens of the NZ Geological Survey, for identification and age determination of several macrofossil specimens and to Dr M Shepherd of the Geography Department, Massey University, who brought my attention to a rare fossiliferous boulder of limestone.

I am grateful to Mr J M C Boag of the Drainage Extension Service, Massey University, for assisting with the surveying of fault displacements.

The assistance of the District Engineers Office, NZ Railways, Wellington, for providing transportation and protection during mapping within the Manawatu Gorge is also acknowledged.

Thanks to Dr Barry Roser of Victoria University for carrying out major and trace element analyses on volcanic lithologies sampled from the study area.

A special thank you to Joy Watson for typing the many drafts of this thesis, for colouring in maps and for providing moral support.

I would also like to acknowledge the numerous farmers whose properties bordered the southern Ruahine Range. Each granted me access across their property and, in some cases, provided much needed accommodation in the field. In this respect, particular thanks must go to Mr J Inglis and Mr K W Cresswell.

Finally, I would like to thank my family, friends and fellow students, all of whom have assisted in a variety of ways. In particular, I appreciate the many hours spent by Drs J McArthur and R Thornton and Mrs C Hedley proof-reading the final script and also the assistance of Miss J McEwen in map colouring.

\*\*\*\*\*

T A B L E   O F   C O N T E N T S

(details of contents precede each chapter)

	<u>page</u>
ABSTRACT ... ..	ii
ACKNOWLEDGEMENTS . ... ..	v
TABLE OF CONTENTS ... ..	vii
LIST OF FIGURES .. ... ..	viii
LIST OF TABLES ... ..	xv
LIST OF MAPS ... ..	xvii
LIST OF APPENDICES ... ..	xviii

PART ONE : GEOLOGY OF THE SOUTHERN RUAHINE RANGE

CHAPTER 1: Introduction .. ... ..	1
CHAPTER 2: Stratigraphy and Lithology ... ..	21
CHAPTER 3: Sedimentary Structures and Palaeoenvironmental Analyses . ... ..	76
CHAPTER 4: Palaeontology . ... ..	106
CHAPTER 5: Petrography ... ..	117
CHAPTER 6: Late Quaternary Tectonics ... ..	142
CHAPTER 7: Structure and Deformation ... ..	190
CHAPTER 8: Geological History . ... ..	221
POTENTIAL RESEARCH ... ..	235

PART TWO : RELATIONSHIPS BETWEEN GEOLOGY AND EROSION -  
SOUTHERN RUAHINE RANGE

INTRODUCTION ... ..	237
CHAPTER 9: Slope Movement Types and Processes ... ..	238
CHAPTER 10: Factors that Influence Slope Stability . ... ..	251
CHAPTER 11: Late Quaternary Erosion Events ... ..	340
CHAPTER 12: Past, Present and Potential Patterns of Slope Stability ... ..	348
REFERENCES .. ... ..	386
APPENDICES .. ... ..	A1



LIST OF FIGURES

	<u>page</u>
FIGURE 1.1: Map showing position of study area in relation to the axial ranges of the North Island . . . . .	5
FIGURE 1.2: Southern Ruahine Range - location map . . . . .	6
FIGURE 2.1: A tectonic-stratigraphic subdivision of New Zealand, compiled after Landis & Bishop (1972), Speden (1975) and Coombs <i>et al.</i> (1976) . . . . .	22
FIGURE 2.2: Distribution of Torlesse bedrock and Plio-Pleistocene marine deposits, southern Ruahine Range . . . . .	27
FIGURE 2.3: Small sized conglomerate pebbles within a fine- to medium-grained sandstone matrix . . . . .	33
FIGURE 2.4: Coarser sized pebbles than in Figure 2.3 set within a medium-grained sandstone matrix . . . . .	33
FIGURE 2.5: Lenses of calcareous siltstone (arrowed) within an interbedded sequence of sandstone, siltstone and argillite comprising the Tamaki Lithotype . . . . .	35
FIGURE 2.6: Strata comprising Very Thin-Bedded Association of the Tamaki Lithotype exposed on Delaware Ridge at locality T23/664174 . . . . .	38
FIGURE 2.7: A representative example of the Thin-Bedded Association of the Tamaki Lithotype in Rokaiwhana Stream at locality T23/664157 . . . . .	38
FIGURE 2.8: Schematic diagram showing field relationships between mappable lithozones within Wharite Lithotype . . . . .	43
FIGURE 2.9: Pebble-dominated conglomerate containing predominantly clastic and volcanic lithologies set within a sandstone matrix . . . . .	47
FIGURE 2.10: Pebble-dominated conglomerate containing clastic and volcanic lithologies set within a muddy siltstone matrix . . . . .	47
FIGURE 2.11: Conglomerate comprising predominantly muddy siltstone matrix within which pebbles of clastic and volcanic lithologies are randomly scattered . . . . .	48

FIGURE 2.12:	Conglomerate consisting of rounded to subangular, light coloured, fine-coarse grained sandstone and siltstone pebbles set within a darker sandy matrix	48
FIGURE 2.13:	An autoclastic breccia comprising angular chips of sandstone with signs of internal quartz veining, set within an argillaceous matrix ... ..	50
FIGURE 2.14:	An autoclastic breccia consisting of stretched and attenuated thin beds of sandstone interbedded with argillite ... ..	50
FIGURE 2.15:	A slabbed sample of ?diorite containing large feldspar phenocrysts set within a dark fine-grained mafic matrix .. ...	52
FIGURE 2.16:	A slabbed sample of vesicular basalt containing amygdules of calcite .. ...	52
FIGURE 2.17:	Interbedded red and green argillites together with clasts of spilite (sp), chert (ct) and sandstone (sd), lithologies ... ..	53
FIGURE 2.18:	A variety of coloured chert lithologies found as thin discontinuous lenses within Foliated Lithozones or as discrete clasts within Diamictite Lithozones .. ...	55
FIGURE 2.19:	A clast of laminated, blue-green chert ... ..	55
FIGURE 2.20:	Sample of copper ore from Maharashtra Coppermine within Coppermine catchment, showing green efflorescence of copper carbonate (Malachite) ...	57
FIGURE 2.21:	Chert breccia, consisting of angular coloured chips of chert set in a microcrystalline siliceous cement, was found in Makohine catchment at locality T23/498050 . ... ..	58
FIGURE 2.22:	Autoclastic chert breccia comprising angular, white coloured chips of chert set within an indurated argillaceous matrix ... ..	58
FIGURE 2.23:	Calcareous conglomerate containing rounded pebbles with brown weathered exterior set in a calcareous sandstone matrix ... ..	60
FIGURE 2.24:	Foliated Lithozone within which once-bedded sandstone units have been pulled apart along strike, during deformation, into isolated lenses .. ...	66

FIGURE 2.25:	Diamictite which contains very angular chert clasts of small size range within a sheared argillaceous matrix ... ..	68
FIGURE 2.26:	Diamictite containing clasts of varying sizes and compositions, within a sheared argillaceous matrix . ... ..	68
FIGURE 2.27:	An outcrop of argillite that is essentially devoid of clasts and interbeds of competent lithologies and has been mapped as an Argillite Lithozone ..	73
FIGURE 3.1:	Ideal sequence of structures in a turbidite bed (the Bouma sequence), from Bouma (1962) and Blatt <i>et al.</i> (1972) ... ..	78
FIGURE 3.2:	Three upward grading $T_{a,e}$ units consisting of a basal siltstone and an upper argillite ... ..	79
FIGURE 3.3:	Slabbed rock sample of <i>in situ</i> siltstone containing whisps of argillite. The siltstone grades westward into an overlying bed of argillite ... ..	81
FIGURE 3.4:	Thin parallel laminations of alternating argillite (dark layers) and fine-grained siltstone (light layers) ... ..	82
FIGURE 3.5:	A variety of internal sedimentary structures including disrupted beds, load structure, argillite whisps and truncated cross-lamination .. ...	86
FIGURE 3.6:	Disrupted siltstone horizons interbedded within an argillaceous medium. The lenses of argillaceous material within the siltstone horizons are possibly injection structures as a result of syndepositional deformation . ... ..	86
FIGURE 4.1:	Specimens of <i>Retroceramus</i> ( <i>Retroceramus</i> ) <i>haasti</i> (Hochstetter) (T23/f3) found within Rokaiwhana catchment at T23/644142 ... ..	109
FIGURE 4.2:	Fossiliferous calcareous conglomerate containing fragments of foraminifera and ?bryozoa ... ..	111
FIGURE 4.3:	Radiolarian chert showing radiolaria with double ring structure ... ..	111
FIGURE 5.1:	$SiO_2$ variation diagram for volcanic samples from the southern Ruahine Range . ... ..	131

FIGURE 5.2:	Zr variation diagram for volcanic samples from the southern Ruahine Range . . . . .	132
FIGURE 5.3:	Ti-Zr-y discriminant plot .. . . .	134
FIGURE 5.4:	Zr/y-Zr discriminant plot .. . . .	134
FIGURE 5.5:	Ti-V plot of volcanic samples from the southern Ruahine Range . . . . .	135
FIGURE 6.1:	Reference map of the mapped region showing map-sheet boundaries, major faults and faulted monocline .. . . .	143
FIGURE 6.2:	Dextral transcurrent displacement of high level terrace surface of Porewan age on Wellington Fault trace . . . . .	152
FIGURE 6.3:	Cross-section at Ballantrae Research Station showing stratigraphy of localities from which radiocarbon dated samples of wood were collected, in relation to the trace of Wellington Fault . . .	157
FIGURE 6.4:	Stereoscopic pair showing a tilted wedge located at T24A/477899 on the trace of Wellington Fault . . .	163
FIGURE 6.5:	Diagrammatic sketch illustrating features of tectonic origin commonly found along active fault traces . . . . .	181
FIGURE 7.1:	Small-scale hinge zone of a steeply plunging isoclinal fold in Wharite Lithotype . . . . .	193
FIGURE 7.2:	Rose diagrams showing orientation of fold axes, faults and joints . . . . .	194
FIGURE 7.3:	Subhorizontal, open flexure involving eastward-dipping, thin-bedded strata comprising Tamaki Lithotype . . . . .	195
FIGURE 7.4:	Subhorizontal, near isoclinal fold comprising thin-bedded strata of the Tamaki Lithotype . . .	195
FIGURE 7.5:	Carbonate-cemented fault breccia (white colour) within a 30m wide fault zone . . . . .	199
FIGURE 7.6:	Thin beds showing slight thickness variations due to soft-sediment extension of competent sandstone beds and ductile behaviour of argillite beds . . .	201

FIGURE 7.7:	Extremely disrupted and mixed clasts of sandstone encompassed by argillaceous matrix ... ..	202
FIGURE 7.8:	Extensional shear fractures within lensed clasts of sandstone ... ..	205
FIGURE 7.9:	Post-metamorphic, non-mineralised shear surfaces with partings up to 0.01m width across the fracture	208
FIGURE 8.1:	Structural contour map of marine erosion surface preserved in the southern Ruahine and northern Tararua Ranges ... ..	230
FIGURE 9.1	Debris avalanche resulting from failure within bedrock ... ..	241
FIGURE 9.2:	Debris avalanche scars on steep valley slopes within Mangapuaka catchment .. ...	241
FIGURE 9.3:	A schematic block diagram showing the characteristic features of a typical slump in the southern Ruahine Range .. ...	248
FIGURE 10.1:	Extensive debris slide development within South Oruakeretaki catchment ... ..	256
FIGURE 10.2:	Close-up of debris slide scar within Mangapuaka catchment ... ..	256
FIGURE 10.3:	Torlesse bedrock overlain and in sharp contact with peaty loam .. ...	257
FIGURE 10.4:	Variations in the structural attitude of strata with respect to slope angle and direction, that largely determine the type of slope failure likely to occur in catchments underlain by the Tamaki Lithotype ... ..	258
FIGURE 10.5:	Variations in the structural attitude of foliated bedrock with respect to slope angle and direction, that largely determine the type of slope failure likely to occur in catchments underlain by the Wharite Lithotype ... ..	259
FIGURE 10.6:	A rock slide resulting from downslope movement along a bedding plane surface within bedrock comprising the Tamaki Lithotype ... ..	261

FIGURE 10.7:	An undisrupted rock slide resulting from downslope movement along a lithological contact within bedrock comprising the Wharite Lithotype ... ..	261
FIGURE 10.8:	Very shallow debris avalanches resulting from failure at the colluvium-bedrock contact .. ...	265
FIGURE 10.9:	Stereoscopic view of large-scale earth movements in the lower reaches of No. 1 Line and No. 2 Line Streams ... ..	267
FIGURE 10.10:	Schematic diagram illustrating variations in the structural attitude of joint surfaces, with respect to the free face of sandstone bluff, along which failure results in rock fall activity ... ..	268
FIGURE 10.11:	Rock fall resulting from failure along the north-south trending joint system ... ..	270
FIGURE 10.12:	Position of Wellington Fault trace in relation to rock slump at locality 36 .. ...	274
FIGURE 10.13:	Position of Wellington Fault in relation to rock slump at locality 30 .. ...	276
FIGURE 10.14:	Position of Wellington Fault trace in relation to rock slump at locality 11 .. ...	277
FIGURE 10.15:	Position of Ruahine Fault trace in relation to rock slump at locality 61 .. ...	279
FIGURE 10.16:	Position of Piripiri Fault trace in relation to rock slump at locality 2 ... ..	281
FIGURE 10.17:	Large-scale rock slump with well defined lateral and headwall scarps ... ..	283
FIGURE 10.18:	Small-scale rock slumps and debris slides involving disrupted bedrock lithologies of the Wharite Lithotype and thick accumulations of colluvium	283
FIGURE 10.19:	Stereoscopic photo-pair of large-scale earth slump at locality 108 .. ...	286
FIGURE 10.20:	Frequency and magnitude of flood events recorded in the upper Manawatu River catchment . ...	309
FIGURE 10.21:	Rilling within colluvium at the head of a debris slide scar .. ...	313

FIGURE 10.22:	A typical example of structurally controlled gully erosion within strata comprising the Tamaki Lithotype . . . . .	316
FIGURE 10.23:	An example of gully erosion within bedrock strata comprising the Wharite Lithotype . . . . .	316
FIGURE 11.1	Whiteywood Creek fan deposit in which at least three levels of gravel aggradation are recorded	342

L I S T   O F   T A B L E S

	<u>page</u>
TABLE 2.1: Strata of the Tamaki Lithotype comprise a Graded-Bedded Lithozone. This Lithozone is subdivided into Associations on the basis of average outcrop thickness of individual beds . . . . .	36
TABLE 2.2: Strata of the Wharite Lithotype are differentiated into seven distinct Lithozones. The Graded-Bedded Lithozone is further subdivided into Associations on the basis of average outcrop thickness of individual beds . . . . .	62
TABLE 2.3: Diagnostic features at outcrop scale of three major Lithozones comprising the Wharite Lithotype . . .	64
TABLE 2.4: Strata of the Western Lithotype comprise a Graded-Bedded Lithozone. This Lithozone is subdivided into Associations on the basis of average outcrop thickness of individual beds . . . . .	74
TABLE 4.1: Fossil record dates from study area . . . . .	107
TABLE 6.1: Upper Quaternary stratigraphy of the Upper Manawatu district immediately to the east of the southern Ruahine Range between Woodville and Ruaroa .. . . .	155
TABLE 9.1: Classification of slope movements in the southern Ruahine Range (after Varnes, 1978) . . . . .	238
TABLE 10.1: Percentage and type of shallow translational slope movement in the southern Ruahine Range resulting from failure at varying depths . . . . .	257
TABLE 10.2: Distribution of erosion scars with respect to altitude . . . . .	299
TABLE 10.3: Distribution of erosion scars with respect to aspect	300
TABLE 10.4a: Results of measurement of slope gradient, determined from unpublished 1:25 000 topographic maps, within the study area . . . . .	303
TABLE 10.4b: Measurements of slope gradient with respect to aspect	303
TABLE 11.1: Periods of erosion in the southern Ruahine Range and West Tamaki Basin .. . . .	340



TABLE 12.1:	Calculation and comparison of the area in actively eroding slips within upper catchments along the western flank of the southern Ruahine Range . . .	350
TABLE 12.2:	Calculation and comparison of the area in actively eroding slips within upper catchments along the eastern flank of the southern Ruahine Range . . .	351
TABLE 12.3:	Calculation of annual erosion rates 1946-74 . . .	357
TABLE 12.4:	Annual erosion rates, 1946-74, southern Ruahine Range . . . . .	359
TABLE 12.5:	Annual erosion and sediment transport rates, New Zealand and overseas . . . . .	359
TABLE 12.6:	Estimated volumes of material contained in large-scale, deep-seated mass movements . . . . .	368

L I S T   O F   M A P S

(contained in map pocket in Volume III)

- MAP ONE:           Lithological Outcrop Map of the Southern Ruahine Range.
- MAP TWO:           Field Observation Map of the Southern Ruahine Range.
- MAP THREE:         Structural Interpretation Map of the Southern Ruahine Range.
- MAP FOUR:          Late Quaternary Tectonic Map of the Southern Ruahine Range.
- MAP FIVE:          Distribution of Surficial Erosion Scars and Mass Movement Features - Southern Ruahine Range in the Years 1946 to 1949.
- MAP SIX:            Distribution of Surficial Erosion Scars and Mass Movement Features - Southern Ruahine Range in the Years 1974 to 1978.
- MAP SEVEN:         Map of Relative Slope Stability, Southern Ruahine Range.

L I S T   O F   A P P E N D I C E S

page

APPENDIX Ia:	Manawatu Catchment Board expenditure on erosion control and investigations into the erosion problem along the southeastern Ruahine Range front .. ...	A1
APPENDIX Ib:	Estimated government subsidies (on a basis of 3:1) required by the Board during the next five year period . ...	A1
APPENDIX IIa:	Forest Service expenditure on slope and streambed stabilisation in the southern Ruahine Range ...	A1
APPENDIX IIb:	Estimated future expenditure by the Forest Service on slope and streambed stabilisation . ...	A1
APPENDIX IIIa:	Faunal list for limestone block T23/f7530 . ...	A2
APPENDIX IIIb:	Comments on the identification, interpretation and significance of the faunal content of T23/f7530 (extracts from unpublished manuscript and/or pers coms)	A3
APPENDIX IIIc:	Conodont fauna from fossiliferous limestone block T23/f7530 ...	A6
APPENDIX IVa:	Abbreviations used to denote locality of rock samples and corresponding petrological slides ...	A7
APPENDIX IVb:	Rock sample and petrological slide localities ..	A8
APPENDIX IVc:	Major and trace element analyses of spilitic rocks from the southern Ruahine Range . ...	A9
APPENDIX Va:	Late Quaternary Tectonic Data ...	A11
APPENDIX Vb:	Radiocarbon dates collected from study area ...	A25
APPENDIX VI:	Changes in the state of activity of major mass movement features in the southern Ruahine Range between the years 1946 to 1949 and 1974 to 1978 ...	A26
APPENDIX VII:	Reference numbers of rock samples in the Massey University Reference Collection sampled from the southern Ruahine Range ...	A42

PART ONE

---

GEOLOGY OF THE SOUTHERN RUAHINE RANGE

---

C H A P T E R    1

---

---

INTRODUCTION

CONTENTS

	<u>page</u>
1.0 BACKGROUND    ... ..	1
1.1 OUTLINE OF STUDY    ... ..	3
1.2 LOCATION OF STUDY AREA    ... ..	4
1.3 SELECTION OF STUDY AREA    ... ..	4
1.4 FIELDWORK PROCEDURES    ... ..	7
1.5 PHYSIOGRAPHY    ... ..	9
1.6 PREVIOUS GEOLOGICAL RESEARCH    ... ..	12
1.7 VEGETATION    ... ..	17
1.8 CLIMATE    ... ..	18

# CHAPTER 1

## INTRODUCTION

### 1.0 BACKGROUND

Within the last decade a number of organisations have expressed concern that rates of erosion have markedly increased in the southern Ruahine Range, North Island, New Zealand. During this time the observed increase in erosion within the Range has led to aggradation of stream channels draining the Range with a consequent increased flood risk in adjacent lowland areas.

Streams draining the eastern flank of the southern Ruahine Range flow into the upper reaches of the Manawatu River. The Manawatu River then passes from the east to the west side of the Range through the Manawatu Gorge. At the western end of the Gorge, near the township of Ashhurst, the Manawatu River is joined by the Pohangina River, tributaries of which drain the western flank of the Range.

Fluvial transportation of bedload by the combined flow of these rivers has, in the past, built up much of the flood plain upon which Palmerston North City is situated. Within historic times this flood plain has been subjected to river flooding (Cowie & Osborn, 1977). Thus the current erosion problem, if left unchecked, could lead to an increased risk of flooding around Palmerston North City and the lower reaches of the Manawatu River. The seriousness of the increased erosion in the southern Ruahine Range became widely publicised in the 1970s when the chairman of the Soil Conservation and Rivers Control Council declared that the preservation of the Ruahine Range was far more important than saving Lake Manapouri (Poole, 1973).

Two local bodies immediately concerned with the problem were the Manawatu Catchment Board and the New Zealand Forest Service. Government funding allocated for works on erosion-related problems was received by the Manawatu Catchment Board in 1974. By 1976 the problem was considered to be serious enough to warrant a three-year investigative programme. This involved: (1) the collection and processing of hydrological data, measuring flood flows and observing flood flow responses (Martin, 1978); (2) an investigation of the origin, nature, amount and

movement of stored sediments in stream channels draining the south-eastern side of the Range (Mosley, 1977); and (3) an investigation into the hydraulic behaviour of these streams with the aim of assessing long term management needs and proposing viable work schemes (Brougham, 1977). In addition the Board invited Dr S A Schumm (Professor of Geology, Colorado State University, USA) to give an appraisal of conclusions presented by Mosley (1977) concerning the state of the erosion in the southern Ruahine Range (Schumm, 1977). Status quo and maintenance works were carried out by the Board during this period of investigative work. Expenditure during the years 1975-81 by the Manawatu Catchment Board is presented in Appendix Ia.

Corrective measures by the Board to ameliorate the risk of flooding downstream of the Range front have included the creation of gravel reserves to temporarily store and regulate the flow of detritus from the Range.

Simultaneously, the New Zealand Forest Service stepped up a revegetation programme within the Range which involved the hand planting and direct seeding of pines and aerial sowing of herbaceous plants. The cost of this programme peaked during the 1977-78 financial year (Appendix IIa). In conjunction with the revegetation programme, the culling of deer from helicopters began and poisoning of opossums was conducted on a large scale in an attempt to lessen the destructive effects of these browsing animals upon the vegetation cover.

With the completion of its investigative programme, the Manawatu Catchment Board's aim during the five-year period 1980-85 is to: (1) maintain drainage channels by tree planting, extract metal from stream channels, realign channels and repair bank erosion; and (2) continue to monitor movement of stream bedload. Many of the proposed work schemes outlined in Blakely (1978) for streams draining the southeastern Ruahine Range have been approved by the Board, some of which will be implemented during this period. Government funding for this period has been approved and the yearly amounts allocated as a subsidy are shown in Appendix Ib.

The New Zealand Forest Service continues its efforts to stabilise eroded slopes principally by aerial sowing, since hand planting on a large scale is too expensive. Throughout this campaign to stabilise eroded slopes, the problem areas have been clearly defined as occurring on the southeastern flank of the Range. This becomes particularly evident when

comparing the cost of revegetating eroded slopes on the western flank of the Range with the cost of revegetating the eastern flank (Appendix IIa). Predicted rates of expenditure on these activities by the Forest Service over the next few years is given by Appendix IIb.

The reasons for these increased erosion rates are not well understood. Avenues of research to date have suggested causes that involve only the surficial geology and soils of the Range. These are centred on the effects of intense rainstorms, the influence of browsing animals, strong winds, fires, and drought on the vegetation cover which, if depleted, causes slope instability. In the majority of cases, a prime factor has been advanced as being the reason for the increased erosion rather than several factors operating simultaneously. However, it is clear that many, if not all, of the factors mentioned by previous workers have influenced the increased erosion rates to some extent. The degree to which each compounds the problem varies considerably being largely dependent upon the location of the erosion site. Only by specific investigation of each erosion site involving slope movement can factors and processes causing slope movement be understood.

With the aid of a grant from the National Water and Soil Conservation Organisation (NWASCO), this study was initiated to understand more fully the problem of increased erosion rates in the southern Ruahine Range.

Attention was initially directed towards the geological structure and physiographical aspects of the southern Ruahine Range as it is in these fields that least information is available. As the lithological make-up and structures within the bedrock had not previously been mapped in this area, research was directed towards determining if relationships existed between bedrock structures and lithologies and the types of slope movement observed today on valley slopes within the Range. It was anticipated that the information obtained from this work would enable the identification of sites which are prone to future erosion and for which some protective measures might be possible before larger scale movements occur.

### 1.1 OUTLINE OF STUDY

This study comprises two principal parts. The first part concerns a detailed 1:25 000 geological survey of the study area, which depicts: (1) bedrock mapping of lithotypes; (2) determination of age, superposition, mode of deposition and provenance of sediments; (3) petro-



graphic examination of lithologic constituents; (4) mapping of major fault zones, splay and cross faults; and (5) an interpretation of the structure, deformation and tectonic setting of the southern Ruahine Range.

The second part discusses erosion in the study area and includes:

(1) classification of slope movement types; (2) factors of geologic, physiographic, climatic, seismic and human origin that influence slope stability; (3) a chronological account of episodes of upper Quaternary slope movement and subsequent fluvial aggradation; (4) a comparative study of historical changes in extent and location of sites of active slope movement spanning a 28 year period; and finally (5) an interpretative evaluation of areas of potential slope movement.

## 1.2 LOCATION OF STUDY AREA

The Ruahine and Tararua Ranges form part of an extensive series of axial ranges stretching the length of the North Island between Wellington and East Cape, a distance of 510 km (Fig. 1.1). The area delineated for this study comprises that part of the southern Ruahine Range extending southwards from where the Pohangina River is incised within a natural gorge, cut at right angles to the long axis of the Range at Lat.  $40^{\circ} 02' 30''$ S, to immediately south of the Manawatu Gorge to include part of the northern tip of the Tararua Range at Lat.  $40^{\circ} 21''$ S (Fig. 1.2). This area lies between longitudes  $175^{\circ} 45$ E to  $176^{\circ} 06$ E.

The study area is largely within the boundaries of the Ruahine State Forest Park. The Range is widest at its northern end where it is approximately 13 km across and tapers southward to barely 7.5 km across where the Ruahine and Tararua Ranges approach each other at the Manawatu Gorge. The eastern boundary of the study area has been defined to parallel Top Grass and Pinfold Roads and the western boundary has been drawn along the left bank of the Pohangina River. The eastern and western boundaries have thus been delineated beyond the state forest boundary to include several important geological findings within Quaternary aged deposits that flank the Range. The total length of the study area is approximately 40 km and encompasses an area of approximately  $510 \text{ km}^2$  of which  $212 \text{ km}^2$  is forested.

## 1.3 SELECTION OF STUDY AREA

Selection of the study area was based on the following factors, listed

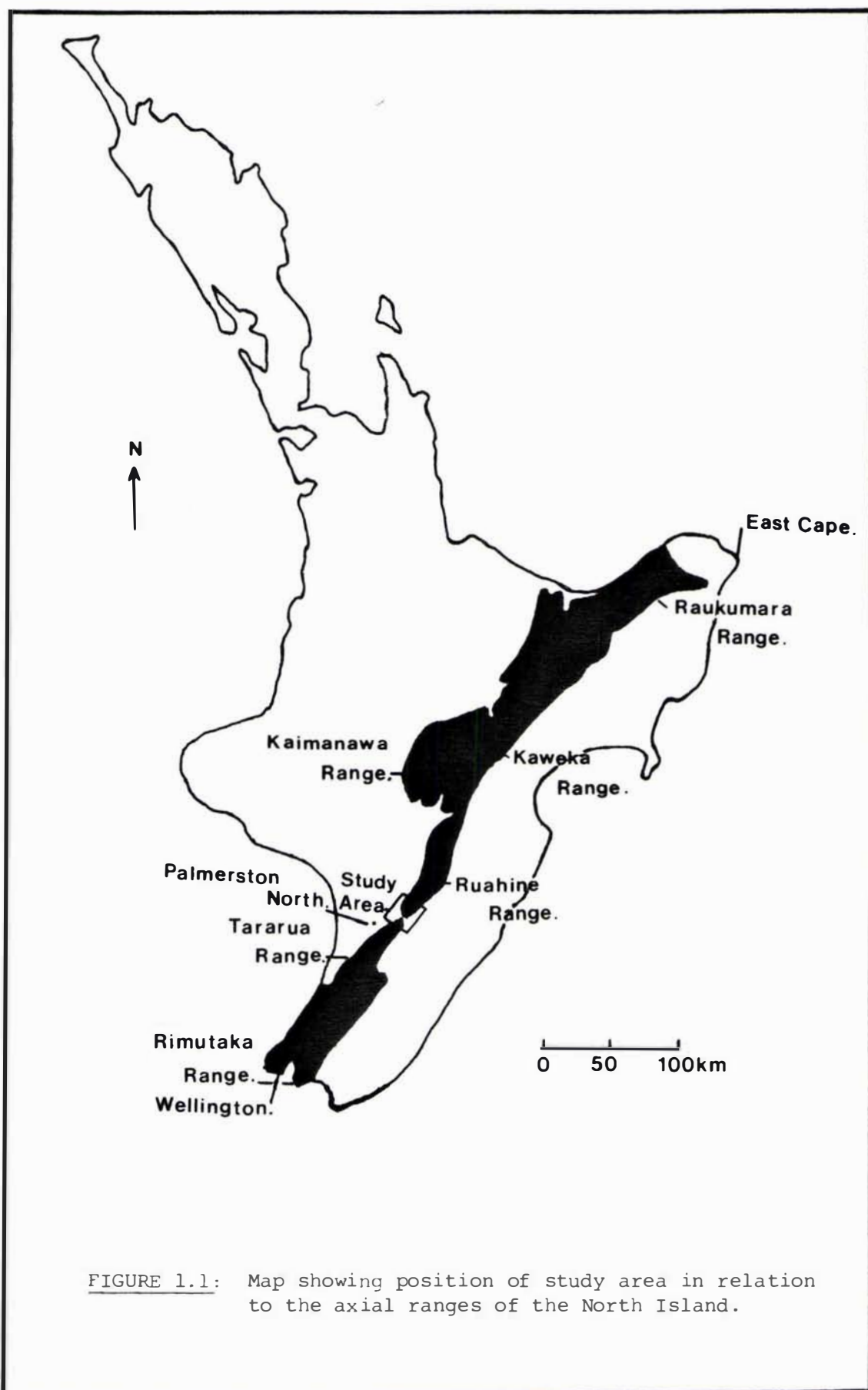


FIGURE 1.1: Map showing position of study area in relation to the axial ranges of the North Island.

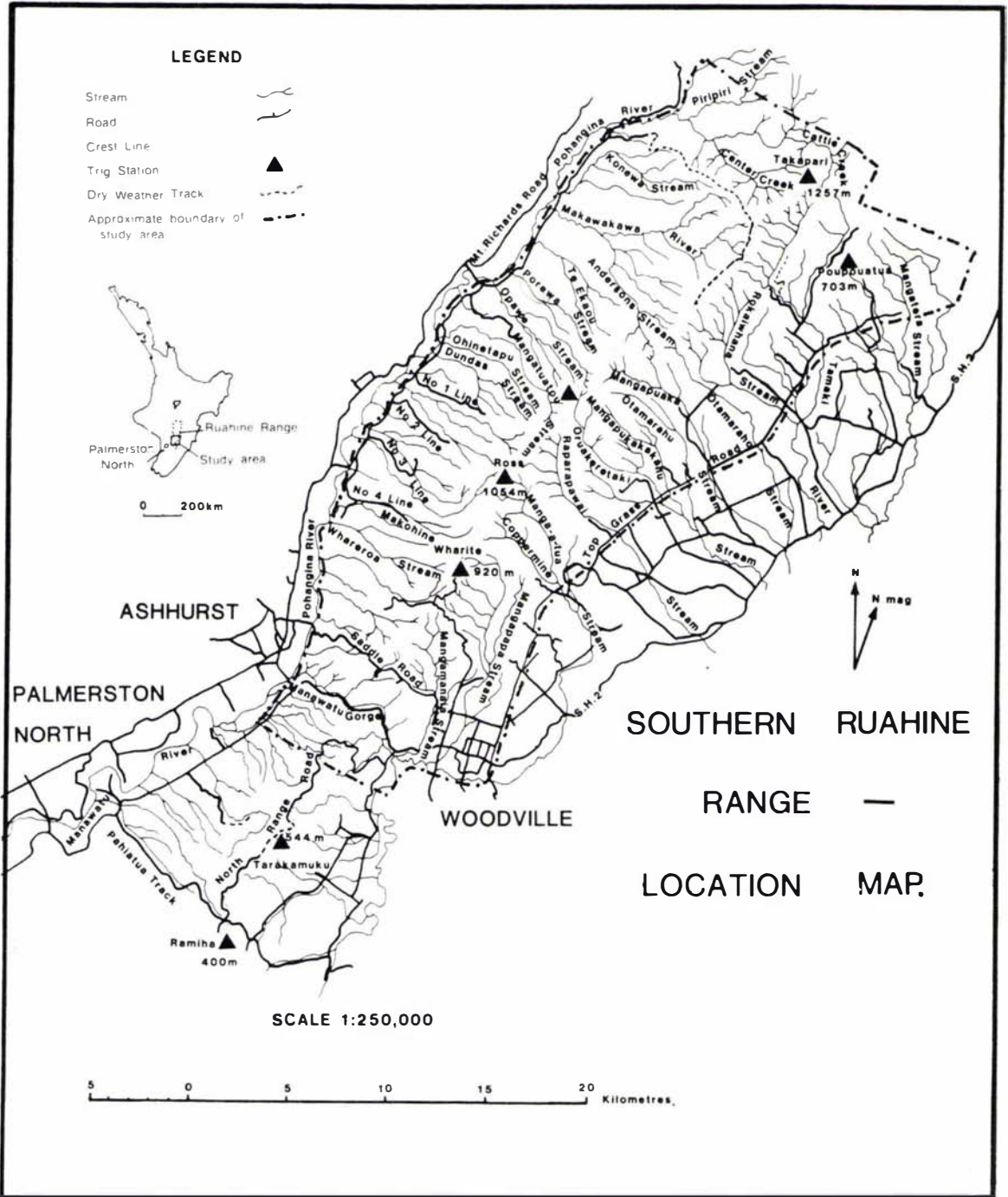


FIGURE 1.2: Location map showing major streams, roads, trigonometrical stations and towns within and adjacent to the study area.

in order of importance:

- (1) At the commencement of this study, the Manawatu Catchment Board was investigating erosion and sedimentation problems associated with rivers draining the southeastern part of the Ruahine Range. This work, together with research conducted by two government agencies, the Soil and Water Division of the Ministry of Works and Development and the New Zealand Forest Service, provided considerable background information which was relevant and helpful to further research investigations.
- (2) Several useful geological investigations have involved mapping of the greywacke bedrock in areas to the north (Sporli & Bell, 1976; Munday, 1977) and in the extreme south (Zutelija, 1974) of the study area. In addition theses have detailed the Late Cenozoic sediments in and around the Manawatu Gorge - Saddle Road region (Piyasin, 1966; Grammer, 1971) and along the margins of the study area (Ower, 1943; Carter, 1963).
- (3) The northern and southern boundaries were selected where two naturally formed gorges traverse the Range, thereby providing almost complete cross-sections of the bedrock strata comprising the Range. At the southern extremity, the structure and lithology of the Manawatu Gorge had been investigated by Zutelija (1974) so some preliminary information was available at the commencement of this study.
- (4) A network of secondary roads bounding the Range (Fig. 1.2) and tracks prepared by the New Zealand Forest Service within the Range allow ready access to much of the study area. One dry-weather access road penetrates to the crest of the Range, at Delaware Ridge.\*

#### 1.4 FIELDWORK PROCEDURES

Fieldwork was carried out between 1976 and 1982, mainly during the summer months. The heavily bush clad slopes of the Range reveal few geological outcrops. Much of the structural and lithological information has been obtained from exposures along river courses although outcrop exposure is seldom continuous throughout the length of most stream channels. Some stream channels have very few exposures due to dense vegetation cover or excessive accumulations of stream detritus, particularly in upper catchment reaches. Recently formed erosion scars have provided

---

\* Not an approved National Geographic Board name

useful insights into the structure of bedrock lithologies. Ridge-top exposures are few and are generally inaccessible on account of the dense forest cover. Most useful information, away from river courses, has been gleaned in foothill areas in the vicinity of Mangatera Stream and access roads to Wharite and Takapari trigonometrical stations (Fig. 1.2).

As a result of the intricate drainage network, many streams are not named. With the necessity to refer to numerous locations within the field area without ambiguity, a number of informal names have been used by the author which are not approved by the New Zealand Geographic Board and thus do not occur on any New Zealand Lands and Survey maps. Where possible, subdivision of named streams was accomplished with the use of prefixes, for example East Tamaki and North Oruakeretaki. Specific localities are referred to using grid references based on the 1:25000 metric map series (NZMS 270). The following NZMS 270 sheet numbers cover the study area: T23B, T23C, T23D, T24A, T24B, U23A and U23C. The study area is also covered by NZMS 1 based on the national thousand-yard grid of the 1:63360 topographical map series, sheets N144 (Feilding), N145 (Dannevirke) and N149 (Palmerston North). The only geological map of the area is at 1:250000 scale (Kingma, 1962).

At the commencement of field mapping, there existed a number of stereo aerial photograph series each of which offered only partial coverage of the study area. The earliest known series were photographed between 1946 and 1950 (SN 230 and SN 181) at a scale of 1:13600. Further series were photographed in 1968 (SN 4143) and 1974 (SN 3721) but again each only covers part of the study area required to be mapped.

Recent stereo aerial photograph coverage of the forested portion of the study area became available in 1977-78 with completion of SN 5163 at a scale of 1:10000 and SN 5026 at a scale of 1:50000. The most suitable means of recording field observations involved the use of tracing paper overlays upon photographic contact prints. Information from these overlays was then transferred onto work sheets. Fortunately, the completion of NZMS 270 work sheets coincided with the end of the fieldwork programme and were used to compile the final base map.

All rock samples, thin-sections and fossil specimens are held at the Department of Soil Science, Massey University, Palmerston North. The labelling of rock specimens and their corresponding thin-sections is explained in Appendix IVa. Radiocarbon dates and fossil specimens collected from the study area are listed in Appendix Vb.

## 1.5 PHYSIOGRAPHY

The physiography of the study area is closely related to the stratigraphic and tectonic history of the Ruahine and Tararua Ranges. Adkin (1930), in discussing deformation of the Tararua Range, commented "the Tararua segment . . . is regarded as a large upfold . . . plunging northward . . . and corrugated by a completed pattern of secondary flexures, longitudinal and transverse . . . At its northern end - near the Manawatu Gorge - the secondary longitudinals are reduced to one (as a result of converging and by plunging beneath the level of the adjacent lowlands), there giving the mountain axis the appearance of a simple arch" (p 28). This 'arch' structure extends northwards into the southern Ruahine Range where it was interpreted by Lillie (1953) as a "simple anticlinal flexure with southward plunge". The north-plunging Tararua Range and south-plunging Ruahine Range are separated by a physiographic depression referred to as the 'Manawatu Saddle'\* across which the Manawatu Gorge is incised. Both Ranges are flanked by en-echelon faults along their steep eastern limb, giving the flexure a marked asymmetry which is suggestive of a high, outstanding, tilted bedrock block, having a steep eastward-facing scarp and a longer back slope towards the west. Contouring that section of the axial range between Wellington and Hawkes Bay clearly indicates "a major anticline marked by two elongated domes . . . The southern domes represent the Rimutaka and Tararua Ranges and the northern dome the Ruahine Range". Furthermore, "There is little doubt that the structure shown by the contours is geologically significant, and they must represent a deformed surface that had considerably less relief than the present ranges have." (Wellman, 1948). This deformed surface which has been carved into greywacke bedrock of Triassic-Jurassic age has been referred to as a peneplain (*sensu stricto*). It may alternatively be a surface of marine erosion. Kingma (1957a) considered the surface to represent planation in Pareora time over the whole 'North Island Geanticline' with planation of the Ruahine block occurring again in Waitotaran time. It is this relict erosion surface that is now prominent at approximately 1000-1100m altitude along the Delaware Ridge, and at the Manawatu Gorge-Saddle Road area where it is exposed at the northern end of the Tararua Range and southern end of the Ruahine Range. Within the Manawatu Saddle a well-defined erosion surface is overlain by fossiliferous marine sediments of Waitotaran, Nukumaruan and Castlecliffian age. No residual deposits

---

\* Not an approved National Geographic Board name

of Cretaceous - Tertiary strata are known to occur upon the Delaware Ridge although occasional outliers of Waitotaran-aged limestone upon an even, unbroken broad plateau-like surface at Lessongs Monument (1095m altitude) and elsewhere in the northern Ruahine Range is proof of an episode of Late Tertiary marine planation. However, it is not clear if the southern Ruahine Range was submerged in Pareora times. There is only one known location within the study area at which marine sediments of Late Tertiary age occur, well within the confines of the Range and far removed from sediments of the same age flanking the Range. The outcrop occurs in a tributary of Centre Stream (T23/652222) at an altitude of 700m and consists of a basal conglomerate overlain by limestone and sand (Moore, 1975). The fossil content of the limestone indicates an Early Nukumaruan age (T23/f7529). The conglomerate suggests that part of the southern Ruahine Range was above sea level and eroding prior to Early Nukumaruan times.

To the south of the study area near the Pahiatua Track (Fig. 1.2) the peneplain reaches an axial culmination at Tarakamuku trig. (544m), before descending gradually northwards for the next 8 km to the Manawatu Gorge. This broad, smooth, north-sloping surface can be traced further northwards beyond the Manawatu Gorge with no sag at the Gorge itself. The lowest part in the curve of this surface is 3.5 km north of the Gorge where it is 153m above sea level. Marine sediments conceal this surface through much of the Manawatu Saddle area. Still further northwards the peneplain rises steeply again, and is preserved up to the summit of Wharite (920m) where it is seen to ". . . pass into the air, although summit concordance at a few points along the Range may indicate its former extent" (Lillie, 1953). The southern part of the Ruahine Range between Wharite (920m) and Maharahara (1095m) portrays a rugged saw-toothed crest, severely eroded with sharp peaks and low saddles. When viewed from either the west or the east the silhouette of this section of the Range exhibits a general northward increase in altitude which is reflected in the heights of trigonometrical stations from Wharite (920m), two unnamed stations (968m and 1013m), Ross (1054m), unnamed (1021m), Matanginui (1074m) and Maharahara (1095m). It is thought that the crest of this section of the Range has been dissected to a greater extent thereby largely destroying evidence of the former peneplain. A distinctly different axial profile extends northwards from Mangapuaka Stream to the northern boundary of the study area. This profile is near planar with little relief, and is gently inclined towards the south and west. This area referred to as 'Delaware Ridge' extends over several

hundred hectares and comprises several levels, suggestive of marine planation. The trigonometrical stations Maharahara and Matanginui are considered to be the southernmost remnants of this section of the peneplain which increases in altitude and width towards the north from 1005m altitude at the north bank of Mangapuaka Stream to 1066m altitude at the northern edge of the study area. This level of planation is the most extensive, above which isolated higher levels of planation rise to approximately 1158m altitude. Three such "highs" are separated by two low saddles that cross the Range at an altitude of 1000m. The southernmost saddle separates headwater reaches of a tributary of West Tamaki River to the east from the headwaters of a tributary of Makawakawa Stream to the west, at T23/666174. The northernmost saddle separates the headwaters of a tributary of West Tamaki River from Centre Creek, a tributary of Pohangina River, at T23/694208.

The physiographic boundary between the steep mountain range and adjacent piedmont areas corresponds to the boundary between semi-consolidated sediments of Wanganui Series age to the east and west, with greywacke bedrock lithologies (see Chapter 2) of Triassic-Jurassic age comprising the southern Ruahine Range. Closer inspection of the piedmont areas shows that they consist of multiple surfaces, largely of depositional origin, representing aggradational floodplain remnants deposited during cool climate episodes of the Late Quaternary.

Streams draining the Range generally flow perpendicular to its axis. However, stream alignment along NE-SW trending fault lines is conspicuous in this area. Those streams draining the eastern flank of the Range are short and steep whilst those draining the western flank have longer channels with more gentle profiles. This reflects the asymmetric cross-sectional profile of the Range. A weak radial drainage pattern has formed upon peneplained bedrock surfaces at the southern end of the Ruahine Range and the northern end of the Tararua Range. Stream dissection here is minimal. Interfluvial areas are broad and smooth in relief. Locally, the radial pattern has been modified by faulting.

Valleys within the Range are deep, narrow and steep-sided as a result of rapid incision by rivers. In a detailed study of the Raparapawai Catchment, for example, Stephens (1975) estimated the mean slope-angle to be  $27^{\circ}$  with maximum slope angles of  $40^{\circ}$  to  $50^{\circ}$ , excluding vertical bluffs which are common. Valley-in-valley forms are a feature found



within the principal drainage catchments. Characteristically, these comprise inner valleys close to the water course, with slopes of 30-40°, within older valleys with slopes of 20-25°. These features clearly indicate a rejuvenated phase of dissection in a youthful, unstable landscape. Although rainfall is sufficient to maintain appreciable perennial flow in the mountain streams many of the smaller streams are ephemeral, drying up during the summer months. Where thick accumulations of bedload are characteristic some larger streams become ephemeral within the Range front due to percolation into the unconsolidated gravel. Beyond the eastern mountain front, valley depths decrease and valley widths increase markedly. Here, streams spread large quantities of alluvial gravel, sand and silt over weakly consolidated Plio-Pleistocene and Quaternary sediments. Some streams draining the eastern front are incised to 1m or 2m below the general level of the adjacent ground surface but many have aggraded so vigorously that they leave the mountain front at a higher level than the surrounding farmland, whereupon they deposit their bedload in the form of an alluvial fan. Excellent examples of these fans may be seen where Mangapuaka, Otamarahu and Mangapukakakahu Streams emerge from the Range. Streams draining the eastern front of the Range eventually flow into the Manawatu River which drains southward parallel to the southern Ruahine Range before flowing westward across the southernmost tip of the Ruahine Range, through the Manawatu Gorge. Streams draining the western front of the Range carry less bedload and upon emergence from the Range are incised to depths in excess of 150m within Plio-Pleistocene and Quaternary sediments. Stream channels are often confined within narrow, steep-walled canyons extending from the western flank of the Range to the Pohangina River. The Pohangina River drains southward parallel to the western front of the Range to join the Manawatu River, at the western end of the Manawatu Gorge, close to the township of Ashhurst (Fig. 1.2).

#### 1.6 PREVIOUS GEOLOGICAL RESEARCH

Many of the early geological expeditions to the southern Ruahine Range were concerned with the search for mineral deposits and much interest revolved around the Maharahara copper mines. Reports were prepared by Hector (1890, 1892 and 1894) and McKay (1888a, 1894 and 1901), Hector's (1890) report being accompanied by a plan and sections of the mine workings and lode. Thomson (1914) on visiting the Maharahara district considered the prospects for copper unpromising. Since then, unfavourable reports on the copper mines were made by Morgan (1920) and Ongley

& Williamson (1931b) and a comprehensive account of their prospecting history was prepared by Lillie (1953). At infrequent intervals gold and silver are reputed to have been found in the greywackes of the Range. However, not one of the claims has been verified. Park (1887) and Thomson (1914) visited "reefs" in the Pohangina River Valley, only to find they were not of quartz but of a whitish-grey limestone of good quality.

Numerous studies have dealt with aspects of the structure, stratigraphy and deformation of Tertiary-Quaternary sediments immediately adjacent to the eastern and western flanks of the southern Ruahine Range, including the Manawatu Gorge - Saddle Road area. McKay (1877) was the first to mention the presence of calcareous sands, conglomerates and limestones forming a "very incomplete" section overlying the greywackes at the eastern end of the Manawatu Gorge. Park (1887) examined "alternations of arenaceous and calcareous strata belonging to the Te Aute series (Upper Miocene)". Their relation to the older greywacke bedrock and mode of occurrence at the upper end of the Manawatu Gorge are illustrated by him in a cross-section (p 34). Hill (1893) drew attention to fossiliferous blue clays and conglomerates in the vicinity of Wharite, which he found up to altitudes of 360m above sea level lying in unconformable contact with the greywackes.

Two of the earliest and most comprehensive accounts of the Cenozoic stratigraphy around the margins of the study area were undertaken by the Superior Oil Company (Ower, 1943; Feldmeyer *et al.*, 1943). Since then Te Punga (1952), Lillie (1953) and Kingma (1957a, 1957b, 1958b and 1959) together with theses by Rich (1959), Piyasin (1966), Grammer (1971) and Carter (1963) have all contributed valuable information concerning the stratigraphic relationships of beds within the Wanganui Series and their relationship to the underlying greywacke bedrock in this region.

McKay, Park and Thomson provided the first, if somewhat sketchy, lithological descriptions of the greywacke bedrock in the study area. Park (1887), in a discussion of the bedrock of the Manawatu Gorge, described "red siliceous slaty shales" and "red cherty jaspers" that occur as large irregular masses within a unit that is highly sheared. Overlying this unit and to the east of it, he recognised compact, grey siliceous sandstones alternating with thin dark siliceous shales. McKay (1888b, 1888c) also noted these two distinct lithological units within the Manawatu Gorge (p 91). Thomson (1914) commented "The

core of the Ruahine Mountains and its northerly and southerly continuations is formed of the central group of greywackes and argillites with reddish jaspers, which appear at numerous points between Wellington and Norsewood, and may be clearly seen in the Manawatu Gorge". The Superior Oil Company report (Ower, 1943) considered that due to the prevalence of jointing and fracturing the greywackes could only be mapped as a "structureless mass". Lillie (1953) provided an up to date summary of the stratigraphy and structure of the greywackes as they were understood at that time, with particular attention being focussed upon the complexities surrounding the Maharahara copper deposits. On the 1:250000 Geological Map of New Zealand Series, Sheet 11 (Dannevirke) Kingma (1962) divides the lithologies of the Ruahine Range into two groups, the Wakarara Greywacke Group to the east and the Ruahine Greywacke Group to the west. Mapping of lithologies in the Ruahine Range in more recent times has involved detailed research studies of relatively small areas. Zuteliya (1974) investigated in detail the structures and lithologies of the greywackes in the Manawatu Gorge. Sporli & Bell (1976) concentrated their efforts in the Tukituki River - Moorcock's Stream area to the northeast of the area investigated in this present study and Munday (1977) mapped an area in the headwaters of Oroua River, to the northwest of the present study area.

Very few Mesozoic fossils have been found in the southern Ruahine Range during these surveys. Triassic fossils were first recorded from the Oroua River by Milne & Campbell (1969) which led Munday (1977) to work in the same area. He relocated the previous finds and established several additional fossil localities. Upper Jurassic spores and macrofossils have been found in the Wakarara Range (to the northeast of the study area) which is thought to be part of the same structural and lithological terrane (Kingma, 1962) comprising the southern Ruahine Range. Te Punga (1978) has recently recorded the finding of a belemnite of Upper Jurassic age in the northern Ruahine Range.

Prior to Kingma's (1957b) work, few geologists had discussed the tectonic setting of the Ruahine Range as being other than an axial structure of the North Island (Macpherson, 1946; Lillie, 1950; Wellman, 1956). Kingma (1957b) envisaged a 'North Island Geanticline', the axis of which lies further to the west of the Ruahine Range and corresponds with a belt of sub-schists that crop out in the western part of the Kaimanawa Range. These schists were considered by him to form the core of the 'North Island Geanticline'. "Taking the above points into account, the

setting of the Ruahine - Rimutaka Range . . . is apparently situated on the eastern flank of the Geanticline" (Kingma, 1957b). From his work, Kingma suggested that the Ruahine - Rimutaka Range is a horst, bounded to the east and west by major faults on which both vertical movement and dextral transcurrent movement has occurred.

Many of the earlier workers made mention and realised the significance of the major fault line between Wellington and Hawkes Bay along the eastern margin of the Rimutaka - Tararua - Ruahine Ranges. Ower (1943), Cotton (1956), Kingma (1957b), Lensen (1958) and Heine (1962) have all studied various aspects of faults in this area. Theses by Rich (1959), Piyasin (1966), Grammer (1971) and Zutelija (1974) contain additional information concerning smaller cross-faults in the Manawatu Gorge and Saddle Road area as well as giving their own interpretations on the position of major northeast trending faults.

Much literature has been written on the geological origin of the Manawatu Gorge - Saddle Road area. Here the Manawatu Gorge traverses the structural sag between the near continuous Tararua and Ruahine Ranges. However, the Gorge is not located at the exact position of minimum peneplain altitude which is 3.5 km to the north of the Gorge and has been covered by Plio-Pleistocene marine sediments. Consequently, much controversy surrounds the exact origin of the Manawatu Gorge, with Hill (1911), Marshall (1905, 1912), Petrie (1907), Morgan (1914), Thomson (1914), Cotton (1922) and Adkin (1930) all contributing hypotheses. These fall into two groups: Marshall, Hill and Adkin suggest that the Manawatu headwaters previously flowed to the east; and Petrie, Thomson, Morgan and Cotton suggest that the Manawatu River has maintained a former course through the tectonically rising Ranges. Ongley (1935) summarised all the previous theories and advanced a modified consequent theory for the Manawatu River. That is, in the vicinity of the southern Ruahine Range the Manawatu River is superposed at the Manawatu Gorge upon greywacke bedrock into which it gradually incised by the same downward cutting processes in evidence today. To account for the fact that the gorge is not situated at the lowest point of the greywacke surface, Ower (1943) postulated that the ancient Manawatu River was deflected southwards and eastwards by alluvial fans formed by eastward flowing streams draining the emergent Ruahine Range. Lillie (1950, 1953) proposed the idea that the Manawatu River follows the course of a "Tertiary Manawatu Strait" across the Range whilst Piyasin (1966) proposed the existence of a former "Woodville Lake" to the east of the Range that overflowed towards the west and incised the

present gorge.

There is a paucity of information on the type, extent and location of slope movements in evidence during the early period of settlement of the study area. Many of the early reports were very generalised and mostly referred to parts of the Ruahine Range outside the study area. In his accounts of visits to and during crossings of the Ruahine Range, Colenso (1884) made brief mention of some aspects of erosion but details of location are sketchy. McKay (1877) reported seeing large shingle slips in the Ruahines but, once again, locations are not specific.

Few mass movement studies have been conducted within the Ruahine Range. Cunningham (1966, 1967) and James (1973) provide the first specific comments on types of erosion in the study area and possible causal factors. Comparative studies of aerial photographs of the Pohangina Catchment taken in 1946 and then again in 1963 showed an increased frequency of mass movements (James, 1973). James attributed this increase to introduced browsing mammals having caused substantial changes in the composition and density of the forest. The existence of very large mass movement features within the southern Ruahine Range was given prominence by Stephens (1975) in a detailed study of the Raparapawai catchment. In addition, failure of a single recent mass movement feature in the Manga-a-tua Stream has been documented by Mosley & Blakely (1977).

Most of the more recent research pertaining specifically to the southern Ruahine Range has been conducted by the Manawatu Catchment Board and Regional Water Board. These Boards employed overseas researchers to elucidate the problems of erosion and sedimentation associated with several rivers draining the Range (Mosley, 1977). A report outlining channel improvement designs followed (Brougham, 1977), together with a consultant's appraisal of the previous reports commending the Boards for their investigative work (Schumm, 1977). These reports, together with those of Cunningham & Stribling (1977, 1978), Grant (1965, 1977), Holland (1975) and the Manawatu Catchment Board (1972, 1976), clearly indicate the seriousness of the erosion problem in the southern Ruahine Range and its implications on the farmed piedmont areas adjacent to the Range.

While the consensus of opinion indicates that erosion in the Ruahine Range has substantially increased during the last few decades, Mosley (1977) and Schumm (1977) stress that significant fluctuations in erosion rates occur naturally and may be part of a natural cyclical

process. For example, stream behaviour does not change progressively through geologic time but, rather, relatively brief periods of instability and incision are separated by longer periods of relative stability (Schumm, 1975). These authors thus envisage the present increased erosion rates in the Ruahine Range as being accounted for as a normal stage in the very complex denudational history of the landscape (Schumm, 1977).

### 1.7 VEGETATION

A comprehensive account of vegetation in the Range, based upon observations over a 30 year period, is presented by Elder (1965). In this work, Elder explains changes in the vegetation during the post-glacial period as being a response to climatic change. In historic times, detrimental effects on the vegetation have been caused by such factors as pre-European fires (Esler, 1963), burning and grazing (Cunningham & Stribling, 1977), increased storminess (Grant, 1977) and the influence of introduced mammals (James, 1973).

Throughout the southern Ruahine Range the vegetation is noticeably zonal in nature, each zone containing associations of vegetation that thrive under specific conditions of altitude, moisture, temperature and soil fertility. As the Range rises particularly steeply above the surrounding lowlands, the changes in temperature and moisture with altitude tend to be marked. Thus, the vegetation zones are correspondingly distinct despite considerable modification during at least three decades by domestic animal browsing, fires, droughts, cyclonic storms and introduced animals. The indigenous vegetation falls into three main (1 to 3) and two subsidiary (4 and 5) altitudinal zones as follows:

- (1) The lowest vegetation zone includes the river banks and the lowest slopes of the Range up to approximately 600m altitude. It comprises a podocarp/hardwood forest which is predominantly rimu (*Dacrydium cupressinum*), with smaller numbers of matai (*Podocarpus spicatus*) and miro (*P. ferrugineus*) associated with hardwoods and tree ferns. The major hardwood species are mahoe (*Melicytus ramiflorus*) pigeon wood (*Hedycarya aborea*), horopito (*Pseudowintera axillaris*), pepperwood (*P. colorata*) and rangiora (*Brachyglottis repanda*). The common tree ferns are *Cyathea* and *Dicksonia* species.
- (2) The middle vegetation zone, between 600-800m altitude is recognised where the lowest vegetation zone grades upward into a kamahi/rimu

association. It differs from the lower forest in its major component comprising kamahi (*Weinmannia racemosa*). This association used to contain abundant rata (*Metrosideros robusta*), but many have died in historic times. In the north of the study area, within West Tamaki catchment, occurs the southernmost extent of a kamahi/red beech (*Nothofagus fusca*) association which is more widespread northwards, particularly in the Pohangina catchment. Cedar (*Libocedrus bidwilli*) are present in small numbers.

- (3) Immediately above the kamahi/red beech and kamahi/rimu associations, at approximately 900m altitude, is a zone of cedar separating these forests from a zone of leatherwood (*Olearia colensoi*) above. This cedar forest with a subsidiary rimu component is considered by Elder (1965) to be "a ghost of a formation", as it is being replaced at its upper and lower margins by leatherwood and pepperwood.
- (4) Leatherwood scrub occupies the crest of the Range where it forms a dense impenetrable cover above the tree line. Associated with leatherwood at its lowest margin is fuschia (*Fuschia excorticata*) and pepperwood.
- (5) The tussock (*Chionochloa pallens*) at Maharahara (1095m) appears as strips dominating the better drained, exposed ridges within a sea of leatherwood. On flatter terrain with poor drainage, snowgrass is displaced by red tussock (*Chionochloa rubra*) in small isolated depressions of peat formation.

Adjacent foothill and lowland areas have been cleared of once dense podocarp/hardwood forest as a result of European settlement. Only a few isolated stands of original forest vegetation remain in an otherwise cleared and farmed landscape that extends to the foot of the southern Ruahine Range along both flanks. Milling of the forest within the Range has effectively depleted the taller stands to result in a forest cover characterised by a dense undergrowth of medium-height trees above which a few taller emergents can be seen. Many such trees are very prone to, and show obvious signs of, wind damage.

## 1.8 CLIMATE

The only meteorological station in the study area was established in 1966 at an altitude of 920m near Wharite, at the southern end of the Range. A network of rain gauges (storage and automatic) are now scattered throughout the Range and adjacent piedmont area. Coulter (1975) describes

the Range as having a cool climate, with high annual rainfalls and at times very heavy rains from the south or southeast.

One of the most important features of the climate is the occurrence of cyclonic storms bringing heavy rains lasting from two to four days. These storms are often locally very intense and may produce daily rainfalls of over 300 mm. They occur most frequently in summer and autumn. Ordinarily the wettest months extend from May to August and also include December, the latter having the highest monthly precipitation of the year. The number of rain days per annum is variable but generally ranges between 180 at the base of the Range to 250 at the highest altitudes. Daily rainfalls up to about 150 mm may be expected at any time of the year. Average annual precipitation varies from approximately 1500 mm at the base of the Range to over 3000 mm on the crest of the Range at the northern end of the study area. At Wharite Meteorological Station the average annual precipitation is approximately 2059 mm.

Despite the barrier-like appearance of the Range, the southeastern flank is considerably influenced by prevailing westerly and northwesterly winds. Northwest winds predominate (56% frequency) but southerlies and southeasterlies may also occur commonly on the eastern flank of the Range. Wind values are exceptionally high, with mean wind speeds of 827 km/day being recorded at Wharite during the years 1966-75. In comparison, Palmerston North (ten kilometres to the west of the Range) recorded 262 km/day during the same period. Wharite is reputed to be one of the windiest places in New Zealand (Cunningham & Stribling, 1978). The climate of the piedmont area contrasts sharply with that within the Range. Not only are there major differences in annual precipitation but also wind speeds and number of windy days are considerably less, and mean daily and monthly temperatures are considerably warmer in the piedmont areas. The mean daily temperature on the Range crest is estimated at approximately  $4.5^{\circ}\text{C}$  while that in the foothill areas is approximately  $10.5^{\circ}\text{C}$ .

Mean temperatures of the warmest months, January and February, vary between  $8.5^{\circ}\text{C}$  at the Range crest to  $15^{\circ}\text{C}$  in the foothill areas but often reach in excess of  $22^{\circ}\text{C}$  in the foothills. The lowest mean daily temperatures occur between June and August and vary between  $0^{\circ}\text{C}$  at the Range crest to  $6^{\circ}\text{C}$  in the foothills (Cunningham & Stribling, 1978).

Above 1100m elevation snowfall contributes 5-10% of the total precipitation (Grant, 1975) and may occur during any season of the year. Snow rarely



persists as ground cover for more than one month's duration.

One dominant feature of the climate of the study area is the large amount of cloud cover. Elder (1965, p 16) reports that during a 13 month period in 1940/41, cloud covered Maharahara trig. for 67% of the time and for a longer period around Wharite. Elder also estimated the percentage of substantially sunny days in the study area to be approximately 11%. At Wharite during 1972/75, fog (*i.e.* cloud whose base was below the station at 920m) was reported on 231 days per year (63% frequency). Similar observations are not available for the rest of the study area but it is known that frequency of cloudy days decreases away from the Range (Mosley, 1977).

In summary, the piedmont has an equable, temperate climate in which climatic extremes of temperature and precipitation are rare. Within the Range the climate is substantially more variable, extreme and severe.

C H A P T E R    2

STRATIGRAPHY AND LITHOLOGY

CONTENTS

	<u>page</u>
2.0 STRATIGRAPHIC TERMINOLOGY .. ... .. .	21
2.0.1 INTRODUCTION ... .. .	21
2.0.2 TORLESSE - DEFINITION AND USAGE ... .. .	24
2.0.3 LOCAL STUDIES OF TORLESSE ROCKS ... .. .	25
2.0.4 USE OF THE TERM 'GREYWACKE' ... .. .	25
2.1 LOCAL STRATIGRAPHY AND LITHOLOGY ... .. .	26
2.1.1 INTRODUCTION ... .. .	26
2.1.2 TAMAKI LITHOTYPE ... .. .	29
A. Distribution ... .. .	29
B. Nature ... .. .	29
C. Lithologic Components ... .. .	30
1. Sandstone ... .. .	30
2. Argillite ... .. .	31
3. Siltstone ... .. .	31
4. Intraformational Conglomerate ... .. .	32
5. Chert .. ... .. .	32
6. Calcareous Siltstone .. ... .. .	32
7. Pebbly Mudstone .. ... .. .	34
D. Mappable Lithozones within the Tamaki Lithotype ... .. .	34
1. Graded-bedded Lithozone ... .. .	34
(a) <i>Associations</i> ... .. .	37
(i) <i>Very Thin-Bedded Association</i> ..	37
(ii) <i>Thin-Bedded Association</i> .. ...	39
(iii) <i>Thick-Bedded Association</i> . ...	39
(iv) <i>Very Thick-Bedded Association</i>	40

2.1.3	WHARITE LITHOTYPE	...	...	...	...	...	...	40
	A.	Distribution	...	...	...	...	...	40
	B.	Nature	...	...	...	...	...	41
	C.	Preview	...	...	...	...	...	42
	D.	Lithologic Components	...	...	...	...	...	44
		1.	Black Argillite	...	...	...	...	44
		2.	Competent Lithologies	...	...	...	...	45
		(a)	<i>Clastic Lithologies</i>	...	...	...	...	45
			(i) <i>Bedded Clasts</i>	...	...	...	...	45
			(ii) <i>Sandstone and Siltstone Clasts</i>	...	...	...	...	46
			(iii) <i>Conglomerates</i>	...	...	...	...	46
			(iv) <i>Autoclastic Sandstone Breccias</i>	...	...	...	...	49
		(b)	<i>Volcanic Lithologies</i>	...	...	...	...	51
			(i) <i>Isolated Clasts</i>	...	...	...	...	51
			(ii) <i>Red and Green Argillite</i>	...	...	...	...	51
			(iii) <i>Pillow Lava</i>	...	...	...	...	54
		(c)	<i>Chert Lithologies</i>	...	...	...	...	54
			(i) <i>Non-laminated Cherts</i>	...	...	...	...	54
			(ii) <i>Laminated Cherts</i>	...	...	...	...	56
			(iii) <i>Chert Breccia</i>	...	...	...	...	56
			(iv) <i>Autoclastic Chert Breccia</i>	...	...	...	...	56
		(d)	<i>Calcareous Lithologies</i>	...	...	...	...	56
			(i) <i>Micritic Limestone</i>	...	...	...	...	56
			(ii) <i>Calcareous Siltstone</i>	...	...	...	...	59
			(iii) <i>Calcareous Conglomerate</i>	...	...	...	...	59
	E.	Mappable Lithozones within the Wharite Lithotype	...	...	...	...	...	59
		1.	Introduction	...	...	...	...	59
			(a) <i>Graded-Bedded Lithozones</i>	...	...	...	...	61
			(b) <i>Foliated Lithozones</i>	...	...	...	...	65
			(c) <i>Diamictite Lithozones</i>	...	...	...	...	67

	(i)	<i>Distinction between foliated Diamictite Lithozones and strongly fragmented Foliated Lithozones</i>	70
	(d)	<i>Sandstone Lithozones</i> ... ..	70
	(e)	<i>Chert Lithozones</i> ... ..	71
	(f)	<i>Volcanic Lithozones</i> ... ..	71
	(g)	<i>Argillite Lithozones</i> ... ..	72
2.2.4		WESTERN LITHOTYPE ... ..	72
	A.	Distribution ... ..	72
	B.	Nature ... ..	72
	C.	Lithologic Components ... ..	75
	D.	Mappable Lithozones within the Western Lithotype	75

## C H A P T E R 2

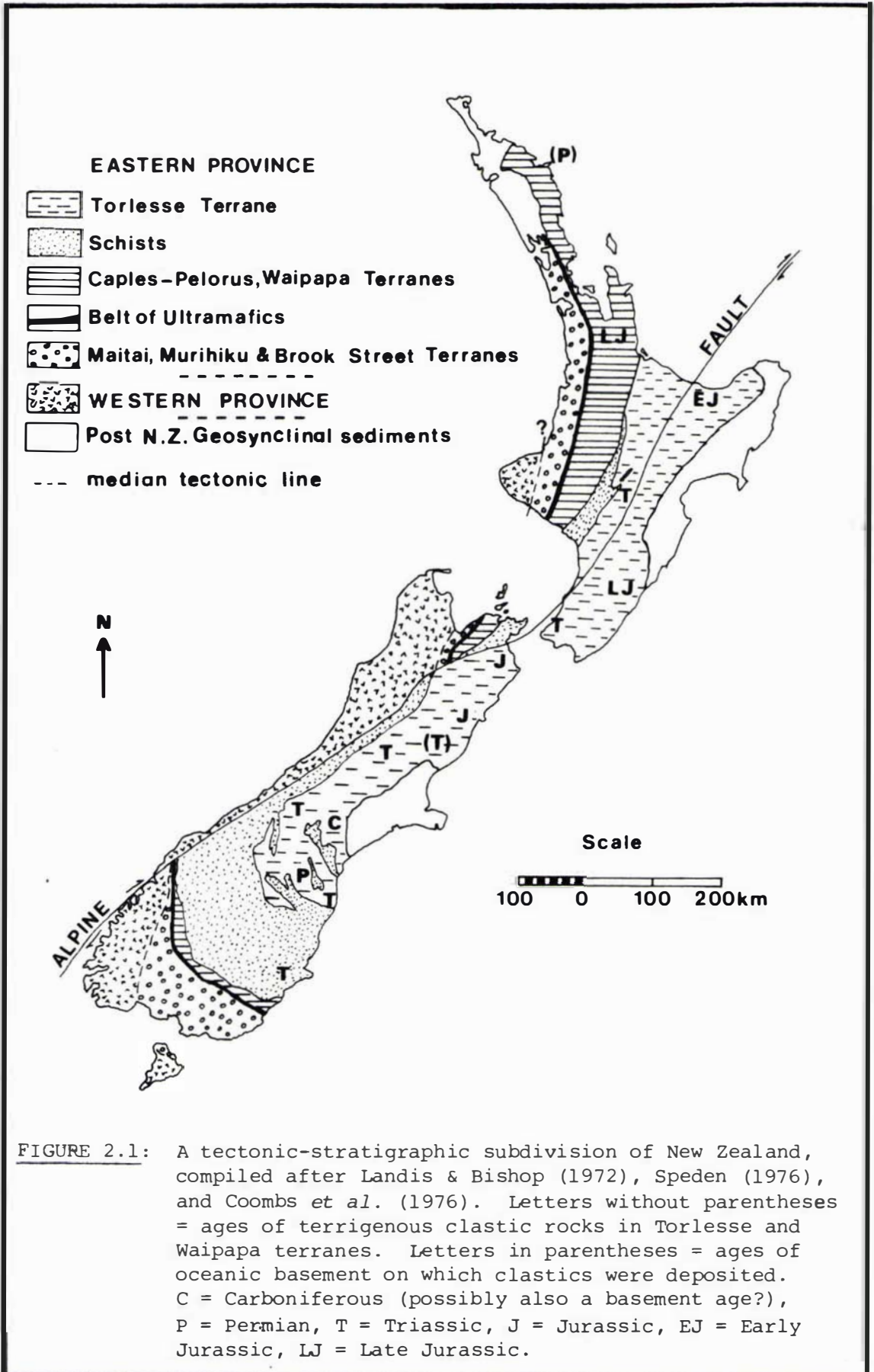
### STRATIGRAPHY AND LITHOLOGY

#### 2.0 STRATIGRAPHIC TERMINOLOGY

##### 2.0.1 INTRODUCTION

Large areas of both main islands of New Zealand are underlain by basement rocks of the Carboniferous to Jurassic Rangitata Orogen (New Zealand Geosyncline of earlier writers). These rocks have been divided into an Eastern and a Western Province (Landis & Coombs, 1967). The Eastern Province is divided into lithologic units referred to informally as terranes (see Carter *et al.*, 1974, 1978, for discussion of alternative stratigraphic nomenclature schemes). The terranes (Fig. 2.1) are of regional extent and are distinguished by differences in lithology, structure and deformation. Contacts between terranes are commonly but not always faulted. This differs from the "terrane concept" currently followed by many North American workers (for example, Jones *et al.*, 1981), where terranes are always fault-bounded entities (MacKinnon, 1983). The Eastern Province terranes are thought to have been part of an extensive, largely Mesozoic belt of clastic rocks deposited along the Austral-Antarctic margin of Gondwanaland (Fleming, 1974). This margin has had a long history of plate convergence (Craddock, 1975) and torsion. The Western Province (Fig. 2.1) consisting of Palaeozoic sedimentary rocks and a variety of crystalline rocks of Late Precambrian to Cretaceous age, is thought to have originally formed part of the Gondwana continental block (Cooper, 1975). The two provinces are separated by a tectonically complex zone marked by faulting and intrusions, referred to as the Median Tectonic Line by Landis & Coombs (1967).

In general, the terrane pattern in the North Island is analagous to that described from the South Island by Landis & Bishop (1972) and Coombs *et al.* (1976). A structurally simple belt of clastic and volcanic rocks (Murihiku, Matai and Brook Street terranes) rims the Western Province on its eastern side (Fig. 2.1). The Murihiku terrane is thought to represent forearc basin deposits and the Brook Street terrane a former volcanic arc (Coombs *et al.*, 1976). The Maitai terrane of the South Island has not been recognised in the North Island (Sporli, 1978). Immediately to the east of the Murihiku terrane lies a narrow belt of ultramafic rocks. Further east



lies the Waipapa terrane (North Island only) which, while probably considerably younger, is nevertheless in a tectonic position analagous to that of the Caples and Pelorus terranes of the South Island (Sporli, 1978). These terranes are thought to represent trench complex deposits. The eastern part of the North Island is underlain by the Torlesse terrane composed of highly deformed, sparsely fossiliferous clastic rocks, with minor but widespread spilite and associated chert and limestone. Torlesse rocks are considered to be convergent margin deposits (Coombs *et al.*, 1976).

The Haast Schists of the South Island are thought to extend to the North Island where they crop out as a narrow strip in the Kaimanawa Range (Grindley, 1960; Sporli & Barter, 1973; Stevens & Speden, 1978). The schists of the North Island separate the Torlesse and Waipapa terranes and as in the South Island are thought to constitute, in part, the metamorphic equivalent of these two terranes.

The Torlesse is clearly distinguished from the other Eastern Province terranes by differences in detrital composition and provenance. Whereas the quartzofeldspathic Torlesse was derived from a tectonically active continental-margin source, sediments comprising the other Eastern Province terranes were derived principally from a volcanic island arc. Both suites of sediment were originally thought to have been derived from a southwestern source. The source of the Torlesse terrane was considered by many previous workers to be the Western Province because of its proximity and appropriate composition (Landis & Bishop, 1972). However, the presence of volcanogenic terranes between the Western Province and the Torlesse, long considered a problem (Coombs *et al.*, 1959), has been emphasised in recent years, and most recent workers have considered other sources (Blake *et al.*, 1974). Most controversial is the proposal of an eastern unidentified continental source by Bradshaw & Andrews (1973) and by Andrews *et al.* (1976). Bradshaw *et al.* (1981) considers a possible source area to be Marie Byrd Land in Lesser (West) Antarctica. Recently a localised source area in Lesser Antarctica has been proposed but nearer the Antarctic Peninsula than is Marie Byrd Land (Korsh & Wellman, in press).

The depositional sites represented by the Torlesse and the other Eastern Province terranes with respective source areas must have been largely separated throughout their depositional histories. Despite this, there is evidence to suggest that their origins were not entirely unrelated because they are coeval, have similar faunal elements, and show a sympathetic relationship in depositional rates (MacKinnon, 1983). Sedimentation is

generally thought to have been terminated, or at least severely restricted, by the time of the Rangitata Orogeny in Late Jurassic and Early Cretaceous times (Kingma, 1959; Grindley, 1961; Waterhouse, 1975).

The Eastern Province non-Torlesse terranes of Triassic-Jurassic age have often been viewed as shallow water "shelf" facies (Wellman, 1956; Fleming, 1970; Kear, 1971), although recently some authors have suggested an off-shelf origin for some of the sediments (Blake & Landis, 1973). In contrast, the Torlesse terrane has long been regarded as a deep-water facies though marine, shallow-water shelf facies have been described from towards the southeast of the Torlesse terrane in the South Island (Ryburn, cited in Force, 1974). A shallow marine and even deltaic origin has been proposed for Torlesse rocks in the South Island described by Andrews (1974) and Bradshaw & Andrews (1973).

Within New Zealand a number of studies have established the general stratigraphy of the Eastern Province non-Torlesse terranes (summary and extensive bibliography appear in Fleming, 1970). The schists have, in part, been studied in some detail (Grindley, Harrington & Wood, 1959; Grindley, 1960; Sporli & Barter, 1973). However, in contrast the non-schistose rocks of the Torlesse terrane were poorly understood prior to the 1970s, particularly in the North Island. It is the Torlesse terrane to which all the rocks of the study area belong.

#### 2.0.2 TORLESSE - DEFINITION AND USAGE

The name 'Torlesse', first used in a geological context by Haast (1865), was revived by Suggate (1961) who proposed the name Torlesse Group for a heterogeneous assortment of structurally complex, poorly fossiliferous, relatively quartz-rich, flysch-like, non-schistose rocks of the New Zealand Geosyncline forming the ranges of the South Island of New Zealand. Previously these rocks had been classified as "Undifferentiated Jurassic - Triassic - Permian" (Willett, 1948), "Alpine Facies" (Wellman, 1952, 1956), or "Undifferentiated greywackes" (Grindley et al., 1959). Stevens (1963) extended the application of the name Torlesse to comparable rocks in the main ranges in the North Island where it is now applied to lithologically and structurally similar rocks. Warren (1967) raised the rank to Super-group as suggested earlier by Campbell & Coombs (1966).

The development of an appropriate and widely accepted hierarchical nomenclature for the rocks of the Rangitata Orogen has in recent years been the centre of considerable controversy. Consequently, it is here proposed to use the



long-established and much used name "Torlesse" at an informal level to refer to the rocks and terrane where Late Triassic - Late Jurassic aged rocks occur within the study area.

### 2.0.3 LOCAL STUDIES OF TORLESSE ROCKS

Despite scattered lithological and petrological descriptions (Webby, 1959; Reed, 1957b), very little information on the structural position of the Torlesse or the distribution of rock types within it is known in the North Island. In only a few instances has any attempt been made to unravel the lithological and structural relationships of the southern Ruahine Range and northern Tararua Range (Sporli & Barter, 1973; Zutelija, 1974; Sporli & Bell, 1976; Munday, 1977). These studies and current work have shown that by mapping small areas it is possible to determine windows into the structural history and local stratigraphic succession despite the reputation these rocks have of being a "difficult" monotonous sequence.

Superficially the rocks of the study area are lithologically uniform, mostly interbedded grey sandstones and siltstones with dark argillites, which are highly jointed, complexly folded and faulted, highly indurated and are of low metamorphic rank (prehnite-pumpellyite facies of Coombs et al., 1959). Massive (unbedded) very thick units of sandstone or argillite are much less common. Detrital conglomerates, limestones, cherts and a volcanic association are rare.

Locally the rocks are sparsely fossiliferous, so that a number of Mesozoic stages are apparently absent or poorly represented by the fossil record. However, with the compilation of known fossil localities in Torlesse rocks by Campbell & Warren (1965) and Speden (1976), it is apparent that fossils of Triassic and Jurassic age predominate in the local area. The overall distribution of fossil localities appears to define distinct faunal zones (Speden, 1976) with Triassic fossil-yielding rocks lying to the west of Jurassic fossil-yielding rocks.

A number of recent studies indicate the presence of melange units within the Torlesse (Bradshaw, 1973; Sporli & Bell, 1976; Feary & Pessagno, 1980). Recent world-wide interest in melange terranes and their relationship to, and understanding of, plate tectonics, has led to a resurgence of interest in the Torlesse in the last decade.

### 2.0.4 USE OF THE TERM 'GREYWACKE'

Within New Zealand the term greywacke has been used in one sense to refer to

successions of rocks with certain characteristic features of composition, lithological alternation and sedimentary structures (Grant-Taylor, 1964), and in a second sense to indicate a type of sandstone made up of a wide range of grain sizes, with a fine-grained detrital and usually recrystallised matrix with a mixed mineral and rock-fragment composition (Reed, 1957b). The term greywacke has been used loosely in a third sense, to distinguish the older rocks of New Zealand (e.g. greywacke bedrock) from Cretaceous and Cenozoic cover beds here giving a connotation of induration (Stevens & Speden, 1978). Greywacke nomenclature is discussed in detail by Reed (1957b).

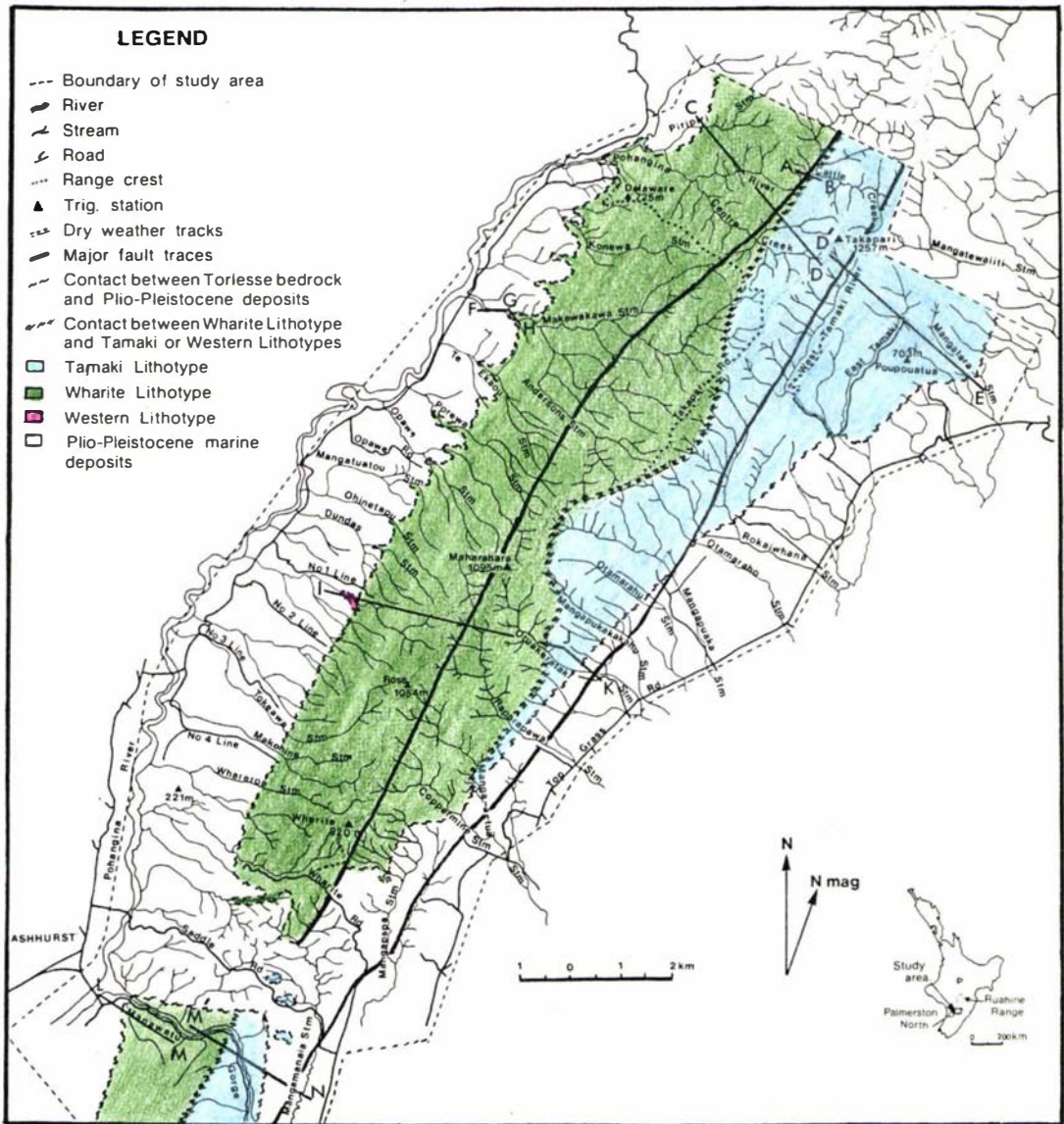
To avoid uncertainties and ambiguities it is proposed here to use the term "greywacke" as indicated in the second sense outlined above. All the sandstones comprising the bedrock within the study area are thus greywackes. While it is apparent that many greywackes occur in flysch-like successions and they are very similar to flysch sandstones (*sensu stricto* Dzulyński & Walton, 1965), there is one major compositional difference. This is the high proportion of volcanic rock fragments and volcanic minerals within the sandstones which precludes them from being classified as *sensu stricto* flysch sandstones (Dzulyński & Walton, 1965).

## 2.1 LOCAL STRATIGRAPHY AND LITHOLOGY

### 2.1.1 INTRODUCTION

From analysis of the field data it has been established that the Late Mesozoic rocks of the southern Ruahine Range may be grouped into three lithotypes (Fig. 2.2). From east to west, the lithotypes are referred to as: (1) the Tamaki Lithotype; (2) the Wharite Lithotype; and (3) the Western Lithotype. The outcrop pattern indicates that each of the lithotypes is linear in outline (though of variable thickness), and each lithotype maintains a consistent stratigraphic position relative to the other lithotypes. The surface outcrop of each of the lithotypes lies sub-parallel to the northeast axial trend of the southern Ruahine Range and strata comprising each lithotype strike predominantly between northeast and northwest and regularly dip at high angles towards the east.

The Tamaki and Western Lithotypes are structurally very similar in that each consists of a relatively undeformed sequence of predominantly graded sandstone, siltstone and argillite lithologies in regularly alternating bedded units of varying thickness and in which the bedded units have retained their original stratal continuity. Such a sequence of strata may



**FIGURE 2.2:** Distribution of Torlesse bedrock lithotypes in the southern Ruahine Range. Plio-Pleistocene marine deposits flank both sides of the Range and occur across the Manawatu Saddle (uncoloured within study area perimeter). Torlesse bedrock is exposed within inliers along the eastern side of Manawatu Saddle. Letters A-N mark lines of cross-section (see Map 1). Cross-section O-P (Map 1) lies south of the area shown on this map.

be referred to as comprising a stratified or coherent terrane. The strata closely resemble graded-bedded sequences commonly referred to as distal turbidites (see Chapter 3). Strata within each lithotype young towards the west so that much of the eastward-dipping and westward-younging strata are overturned.

The Tamaki Lithotype differs slightly in composition from the Western Lithotype. In the former lithotype, additional lithologies are present. These include pebbly mudstone, calcareous siltstone and intraformational conglomerate.

Outcrops of the Tamaki Lithotype to the east are separated from outcrops of the Western Lithotype to the west by extensive exposures of bedrock comprising the centrally located Wharite Lithotype. Strata comprising the Wharite Lithotype are lithologically and structurally very different from that of the Tamaki and Western Lithotypes.

The Wharite Lithotype consists of a strongly deformed succession of lens-shaped clasts or blocks of competent lithologies including sandstone, conglomerate, breccia, limestone, chert and volcanics set in a black, green or red coloured pervasively sheared argillaceous matrix. Sequences of regularly-bedded, graded and alternating strata resembling strata comprising the Tamaki and Western Lithotypes, are also present. The size of the lens-shaped clasts and blocks varies considerably from as small as 0.05m diameter to very large blocks up to 0.5 km in length. The clasts, blocks and bedded sequences are generally aligned within the all-encompassing matrix and impart a foliation on the bedrock that is sufficiently consistent over wide areas to be able to be accurately measured. The Wharite Lithotype therefore essentially comprises a broken or melange terrane within which stratal continuity has largely been destroyed. A direction of younging could not be established for the sequence of strata comprising Wharite Lithotype.

Strata of the Wharite Lithotype dip eastward beneath the Tamaki Lithotype. These two lithotypes are generally in conformable contact with each other but fault contacts have been observed at several localities. Strata comprising the Western Lithotype dip eastward beneath Wharite Lithotype. The contact between Wharite and Western Lithotypes is not faulted and is conformable.

Contacts between the Mesozoic bedrock comprising the core of the southern Ruahine Range and Plio-Pleistocene deposits that flank the Range are everywhere unconformable. Many but not all of these contacts are faulted (see Chapter 6).

Special care was taken in determining the younging direction of strata. Graded bedding, the nature of the contact between bedded units and small-scale sedimentary structures proved to be the most useful criteria.

For mapping purposes each of the three recognised lithotypes was subdivided into lithozones and associations (Tables 2.1, 2.2 and 2.3). The usage of informal stratigraphic nomenclature is preferred for this study. However, for clarity in the text it was found necessary when referring to the lithozones and associations to use capital letters e.g. Graded-Bedded Lithozone or Thin-Bedded Association.

The term lithozone is here defined as a rock unit representing a zone or succession of strata possessing common lithologic characteristics (from Wheeler et al., 1950, p 2364). The term 'association' (after Bradshaw, 1972) is used in a similar context but as a subunit of lithozone. The term association is used in preference to facies, lithofacies or lithotope because the environment of deposition is uncertain and the lateral passage of one association into another, though likely, cannot be proved (Dunbar & Rogers, 1957, p 137; Krumbein & Sloss, 1963, p 229-330).

### 2.1.2 TAMAKI LITHOTYPE

#### A. Distribution

The Tamaki Lithotype can be traced throughout the entire length of the study area (40 km) and is thickest in the north about the vicinity of the West Tamaki River and Mangatera Stream catchments. Here outcrops of Tamaki Lithotype comprise the foothills to the northeast of Poupouatua (U23/722172), hereafter referred to as the Mangatera foothills, and extend westward across the crest of the Range into the upper reaches of the Makawakawa and Pohangina Rivers. In this area, outcropping bedrock comprising the Tamaki Lithotype is no more than 8 km wide. Southward of Mangapukakakahu Stream, the Tamaki Lithotype thins rapidly and between Raparapawai Stream and Saddle Road it is buried beneath Plio-Pleistocene marine deposits though inliers of Tamaki Lithotype do occur in the vicinity of Saddle Road. The Tamaki Lithotype crops out again at the eastern end of the Manawatu Gorge where it is exposed over approximately 1.3 km width (Map 1).

#### B. Nature

The Tamaki Lithotype is a lithostratigraphic unit within which relatively undeformed beds of coherent lithological units can be successfully mapped. This lithotype characteristically comprises a regularly bedded sequence of

predominantly graded units of alternating, non-calcareous sandstone, siltstone and argillite interbedded with occasional thicker, massive (unbedded), graded or ungraded sandstones and rare thick argillaceous horizons that together bear all the characteristics of distal facies clastic sedimentary deposition. Most bedded sequences are laterally persistent across the width of exposed stream-bed outcrops within the confines of the steep narrow valleys of the Range. At some locations, where the sandstones attain great thickness, the alternation is less noticeable but it is nevertheless always present. Such strata in bush-cleared foothill areas are traceable on aerial photographs as prominent ridge-forming features many tens of metres wide and in excess of 0.5 km to 1.0 km long. The most striking feature of strata comprising the Tamaki Lithotype is the regularity of the alternating bedded units from which structural attitudes of strike and dip are readily obtained. The strata are predominantly eastward-dipping, westward-younging and hence are overturned.

Isolated areas of eastward-dipping and eastward-younging strata are found in the northeast of the study area (U23/732185) and at the eastern end of the Manawatu Gorge (T24/497944). For reference purposes, accessible exposures of strata comprising the Tamaki Lithotype are best exposed along road, rail and stream cuttings at the eastern end of the Manawatu Gorge between T24/492932 and T24/492950.

### C. Lithologic Components

There are seven lithologic components recognised in the Tamaki Lithotype. These comprise:

#### 1. Sandstone

Sandstone is the dominant lithologic component within the Tamaki Lithotype. It is well indurated, moderately sorted and light grey to green-grey in colour and contains abundant angular grains of quartz, feldspar and locally a predominance of volcanic rock fragments (see Chapter 5). Sandstones vary considerably in grain size from fine- to coarse-grained.\* Throughout the Tamaki Lithotype fine- to medium-grained sandstone beds predominate and make up a large percentage of stratal sequences in which the individual sandstone beds are either very thin-bedded (0.02-0.1m) or thin-bedded (0.1-0.3m). Medium- to coarse-grained sandstones make up much of the stratal sequences in which the individual sandstone beds are thick-bedded (0.3-2.0m), very thick-bedded (>2m) and where an occasional bed

---

\* Grain size parameters are those of Folk et al. (1970)

attains a thickness of up to 5m width.

Grading within individual sandstone beds is very conspicuous in very thin and thin beds but difficult to discern in thick and very thick beds. Grading is generally absent in sandstone beds of greater thickness than two metres.

Internal sedimentary structures are best preserved in the very thin and thin beds of fine- to medium-grained sandstone (see Chapter 3).

Jointing of sandstone beds is present everywhere irrespective of bed thickness but, like veining, it is well developed in some areas of the study area and poorly developed in others.

## 2. Argillite

Argillite is subordinate in volume to sandstone but is nonetheless a major lithologic constituent of the Tamaki Lithotype. The typical argillite consists of poorly sorted clastic grains embedded in a slightly recrystallised clayey matrix. Rock fragments are absent. In thin section they are seen to be siltstones rather than claystones. These argillites are very similar to those described from the Wellington district by Reed (1957b). The black colour of freshly exposed argillite is characteristic and is presumably due to its carbon content. Although flakes of carbonaceous material were observed, no distinctive organic fragments that could be identified as plant material were found. Perfectly formed pyrite cubes are also a feature of many argillaceous horizons. Argillite occurs as discrete beds between beds of sandstone and siltstone or as thin partings within beds of these lithologies. In general, beds of argillite vary in thickness from 0.02-0.3m and rarely exceed 0.5m thickness. Grading within argillite beds is imperceptible. Pervasive shearing is a common feature of all argillite deposits. Black graphitic surfaces develop where shearing is present. Physical and chemical weathering along shear fractures highlights the extensiveness of this shearing, reducing argillite outcrops to a crumbling, loose mass of very angular, sharp-edged chips that are easily removed from the outcrop by natural processes. Shearing often destroys internal sedimentary structures which are poorly preserved but sometimes micro-graded parallel laminations are present. Fine fissility (shale structure) is absent.

## 3. Siltstone

Volumetrically siltstone appears to be a less significant lithologic component of the Tamaki Lithotype than either sandstone or argillite as much

of the siltstone grades into adjacent beds of sandstone or argillite. Consequently, siltstone rarely forms beds of any considerable thickness and always forms thinner beds than does the sandstone. Siltstone resembles sandstone in colour, induration, sorting and seems to differ only in grain size which varies from fine to coarse siltstone grades. Siltstone is readily distinguishable from argillite on the basis of colour and induration, the latter being black and sheared. Sedimentary structures are very well preserved and jointing is well developed.

#### 4. Intraformational Conglomerate

Conglomerates form a minor lithologic component of the Tamaki Lithotype. They comprise a mixture of dominantly rounded and minor sub-angular pebbles\* measuring between 0.002-0.01m in diameter (Figs 2.3 and 2.4). The clasts are set in a fine- to coarse-grained sandstone matrix. Clasts of volcanic compositions predominate. Conglomerates are often interbedded with medium- to coarse-grained sandstones, the contacts always being abrupt and varying from a planar to an irregular undulating form. Small-scale grooves, gouged into the underlying sandstone bed to a depth of a few centimetres, are a characteristic contact feature. No internal sedimentary structures have been noted, however graded contacts with the sandstone beds have been observed. Bed thickness of conglomerates varies between 0.1-0.3m but larger units measuring several metres thickness and of unknown length are suspected. In cross-section they give the impression of being lenticular-shaped, channel-like deposits. Sometimes conglomerates grade laterally into sandstone. Their areal distribution is irregular and isolated.

#### 5. Chert

A single occurrence of red chert has been observed at T24/492944 (Map 1). In view of the intensely deformed nature of the strata adjacent to the outcropping chert and of the presence of a fault zone nearby, it is suspected that this chert has been in-faulted. The absence of chert elsewhere throughout the Tamaki Lithotype but its presence within nearby outcrops comprising the Wharite Lithotype would tend to favour this interpretation.

#### 6. Calcareous Siltstone

Calcareous siltstone forms a conspicuous but volumetrically insignificant lithologic component of the Tamaki Lithotype. The siltstone occurs as lenses within interbedded sequences of sandstone, siltstone and argillite

---

\* The term 'pebble' is used here to refer to constituent inclusions of all pebble sizes within conglomerates, irrespective of their roundness.





FIGURE 2.3: Small sized conglomerate pebbles within a fine- to medium-grained sandstone matrix. Rock samples Mte2 from Mangatera foothills area at locality U23/731182.



FIGURE 2.4: Coarser sized pebbles than in Figure 2.3 set within a medium-grained sandstone matrix. Note the rounded to subangular shape of the constituent pebbles. Rock sample Mte5 from Mangatera foothills area at locality U23/735188.

(Fig. 2.5). The lenses measure between 0.1 and 0.3m in width and show signs of soft sediment deformation, in the form of stretching along the line of strike. Petrographically the siltstones are of fine- to medium-grain size with a calcareous matrix. Internally they are light grey in colour but weather to a creamy-brown. Calcite veining is common. From chemical dissolution and thin section studies the calcareous siltstones appear to be fossiliferous. Outcrops of calcareous siltstone appear to be stratigraphically restricted but good exposures occur in the Manawatu Gorge at T24/495935.

## 7. Pebbly Mudstone

The term pebbly mudstone is used here as a descriptive name, without regard to the manner of origin, for a rock unit composed of dispersed pebbles in an argillaceous matrix. They occur as thin (0.1-0.3m) interbeds with sandstone and argillite within graded-bedded sequences of strata that dominate the Tamaki Lithotype. Pebbly mudstones consist of a black coloured argillaceous matrix within which occur conspicuous poorly-sorted, subrounded, non-oriented pebbles of small size (0.002 - 0.01m). These are identical in size to pebbles found in the intraformational conglomerates. Pebble composition consists of arenaceous material identical to the sandstone and siltstone beds between which the pebbly mudstone beds are interbedded, plus volcanic pebbles similar in composition to those found in the intraformational conglomerates. The proportion of matrix and pebbles is highly variable between outcrops but on average consist of 75% matrix and 25% pebble constituents. Internal sedimentary structures within beds of pebbly mudstone have not been seen. Pebbly mudstones are a very minor lithology within the Tamaki Lithotype.

### D. Mappable Lithozones within the Tamaki Lithotype

#### 1. Graded-bedded Lithozone

On the basis of the predominance of sequences of strata in which conspicuous grading, both within and between bedded lithologies is characteristic, the Tamaki Lithotype was mapped as a single lithozone - a Graded-Bedded Lithozone (Table 2.1, Map 1). Lithologies such as massive sandstone and argillite, pebbly mudstone, intraformational conglomerate and calcareous siltstone do not occur in beds of sufficient thickness to be mapped at 1:25 000 scale and therefore cannot be considered as separate lithozones.

Within the Tamaki Lithotype the Graded-Bedded Lithozone consists of



FIGURE 2.5: Lenses of calcareous siltstone (arrowed) within an interbedded sequence of sandstone, siltstone and argillite comprising the Tamaki Lithotype. Note the brown colour of the weathered outer surface. Locality T24/495935.

**TABLE 2.1:** Strata of the Tamaki Lithotype comprise a Graded-Bedded Lithozone. This Lithozone is subdivided into Associations on the basis of average outcrop thickness of individual beds. Lithologic components of each Association and relationships between Associations is shown.

Lithozone	Association	Lithologic components in order of dominance	Stratigraphic relationships with other Associations
Graded-Bedded	Very Thin-Bedded (0.02 - 0.1m)	Fine- to medium-grained Sandstone. Argillite. Siltstone. Very rare calcareous Siltstone, pebbly mudstone, and intraformational conglomerate.	Commonly interbedded with Thin-Bedded Association. Occasionally interbedded with Thick-Bedded Association. Rarely interbedded with Very Thick-Bedded Association.
	Thin-Bedded (0.1 - 0.3m)	Fine- to medium-grained Sandstone. Argillite. Siltstone. Common intraformational conglomerate and calcareous siltstone. Rare pebbly mudstone and chert.	Commonly interbedded with Very Thin-Bedded and Thick-Bedded Associations. Occasionally interbedded with Very Thick-Bedded Association.
	Thick-Bedded (0.3 - 2m)	Fine- to coarse-grained Sandstone. Siltstone. Argillite. Common Intraformational conglomerate.	Commonly interbedded with Thin-Bedded and Very Thick-Bedded Associations. Occasionally interbedded with Very Thin-Bedded Association.
	Very Thick-Bedded (2 - 5m)	Medium- to coarse-grained Sandstone. Siltstone. Argillite.	Commonly interbedded with Thick-Bedded Association. Occasionally interbedded with Thin-Bedded Association. Rarely interbedded with Very Thin-Bedded Association.

regularly-alternating, graded-bedded units of predominantly sandstone, siltstone and argillite lithologies together with minor interbeds of pebbly mudstone, intraformational conglomerate and calcareous siltstone. The minor lithologies occur only in locally restricted areas.

The characteristic feature of the Graded-Bedded Lithozone is that on an outcrop scale the thickness of individual beds can be remarkably consistent (Figs 2.6 and 2.7). In the field it is apparent that this Lithozone can be subdivided, on the basis of bed thickness of individual units, into four distinct associations:

- (i) Very Thin-Bedded Association;
- (ii) Thin-Bedded Association;
- (iii) Thick-Bedded Association;
- (iv) Very Thick-Bedded Association (Table 2.1).

However, frequent changes in thickness of individual beds often within distances too small to be shown at map scale (1:25 000), prohibit the mapping of associations. Furthermore, the gradation of one association into another made it difficult to define boundaries between them. Instead the average bed thickness at specific localities is indicated with the use of symbols. Similarly, isolated outcrops of lithologies including calcareous siltstone, pebbly mudstone, chert and intraformational conglomerate are indicated with the use of symbols (Map 1).

(a) Associations

(i) Very Thin-Bedded Association

A sequence of strata in which the individual beds (stratum) are predominantly between 0.02-0.1m thick but within which an occasional bed up to 1m thick may occur. Lithologies found as bedded units in this sequence include sandstone, siltstone and argillite with rare calcareous siltstone, pebbly mudstone and intraformational conglomerate. Argillite is usually of equal to subequal volume to sandstone.

Sequences of Very Thin-Bedded Association make up approximately 10% of outcrops comprising the Graded-Bedded Lithozone of the Tamaki Lithotype. This association is commonly found in conjunction with sequences of Thin-Bedded Association (Table 2.1).

An areally restricted outcrop of this association that differs from other exposures of the same association is exposed in road cuttings along the Delaware Ridge (T23/664174). Here the beds are in general finer grained



FIGURE 2.6: Strata comprising Very Thin-Bedded Association of the Tamaki Lithotype exposed on Delaware Ridge at locality T23/664174. Bedded units strike north-south, dip eastward (left) and young westward (right). Note the differences in weathering and fold deformation with Figure 2.7. Hammer is 0.28m long.



FIGURE 2.7: A representative example of the Thin-Bedded Association of the Tamaki Lithotype in Rokaiwhana Stream at locality T23/664157. Photo shows grey coloured sandstone and siltstone units alternating with black argillites. Strike is N 20 E and dip is vertical. Younging direction is to the west (right) and is indicated by the graded beds. Note also the pervasive shearing in the argillite units and the blocky fracture pattern of the sandstone and siltstone units at near right angles to bedding, but without displacement of any of the bedded units. Compass case is 0.09m wide.

than elsewhere in the study area and the intensity of folding is greater. The characteristic yellow-brown appearance of this outcrop contrasts with the usual grey and black colours of other outcrops. Although largely surficial and perhaps largely due to weathering (compare Figs 2.6 and 2.7), the difference in colour is in part the result of a high proportion of silt-sized material that give sandstone lithologies in this area a muddy appearance (Fig. 2.6). To the east and west of this locality are outcrops of the Thin-Bedded Association (Fig. 2.7).

(ii) Thin-Bedded Association

A sequence of strata in which the individual beds are predominantly between 0.1-0.3m thick but within which an occasional bed of between 1-3m thick may be found (Fig. 2.7). Lithologies include predominant sandstone and siltstone, subordinate argillite, minor conglomerate and calcareous siltstone and rare pebbly mudstone. Sequences of this type have a different appearance to those of the Very Thin-Bedded Association in that the argillite beds are clearly of lesser thickness than the interbedded sandstones. Here the argillites form beds 0.02-0.15m thick, that is, generally in the very thin-bedded range, between beds of sandstone 0.05-0.3m thick. Argillite beds of greater thickness than 0.3m are very rare.

Sequences of Thin-Bedded Association make up approximately 60% of outcrops comprising the Graded-Bedded Lithozone. This association occurs extensively throughout the area mapped as Tamaki Lithotype and is often found in association with sequences of either the Very Thin-Bedded Association or the Thick-Bedded Association (Table 2.1).

Accessible exposures of Thin-Bedded Association may be seen at the eastern end of the Manawatu Gorge either along the river banks or railway line between T24/494932 and T24/492950.

(iii) Thick-Bedded Association

A sequence of strata in which the individual beds of sandstone are predominantly 0.3-2m thick between which beds of argillite are either thin (0.01-0.3m) or occur as mere partings less than 0.01m thick. Also present are substantial thicknesses of graded sandstones and siltstones as amalgamated beds (Walker, 1966; Andrews et al., 1976) and thin beds (0.01-0.3m) of intraformational conglomerate. An occasional thick bed of argillite in excess of 0.5m may be present. Calcareous siltstones and pebbly mudstones are absent.

Sequences of Thick-Bedded Association make up approximately 25% of all exposures comprising the Graded-Bedded Lithozone. Sequences of Thick-Bedded Association often occur in association with sequences of either Thin-Bedded Association or Very Thick-Bedded Association (Table 2.1). This association occurs throughout the area mapped as Tamaki Lithotype and is best exposed in the Mangatera foothill area (U23/732185). Here, the thick beds of sandstone protrude on the farmed landscape as a series of parallel ridges traceable along the northeast strike of the strata for distances of up to 1 km in length.

(iv) Very Thick-Bedded Association

This Association comprises a sequence of strata of very limited extent (rarely in excess of 25m thickness) in which individual beds of predominantly sandstone composition exceed 2m thickness with a maximum observed thickness of 5m. Very rarely are beds of argillite of comparable thickness to the sandstone beds present, however, when observed they are seen to contain very thin (0.01-0.05m) interbeds of fine-grained sandstone or siltstone. These interbeds often pinch out along strike, rest on a scour base which at places can be irregular or planar and commonly have a gradational top. Slaty cleavage is a prominent feature of these very thick argillite beds. Pyrite nodules are often present which on weathering produce iron streaking. The very thick sandstone beds appear to be massive, that is, internally ungraded, however very thin discontinuous laminae or wisps of argillite may occur towards the top of the bed.

Calcareous siltstone, pebbly mudstone and intraformational conglomerate are not found in this Association. Sequences of Very Thick-Bedded Association make up approximately 5% of all outcrops comprising the Graded-Bedded Lithozone. They are most commonly found interbedded with sequences of Thick-Bedded Association (Table 2.1), however an exposure of Very Thick-Bedded Association can be seen in a tributary of Mangapuaka Stream at T23/623124 where it is found interbedded with a sequence of Thin-Bedded Association.

2.1.3 WHARITE LITHOTYPE

A. Distribution

Wharite Lithotype is exposed as a continuous linear stratigraphic unit of variable thickness, cropping out along the entire length of the study area. The total traceable outcrop length along strike exceeds 40 km. The maxi-



mum outcrop thickness of this Lithotype in the vicinity of the Makawakawa catchment is no more than 6.5 km thick. This Lithotype essentially comprises the entire western flank of the southern Ruahine Range and most of the eastern flank, extending from southward of Mangapukakakahu Stream to the southern boundary of the study area.

#### B. Nature

Wharite Lithotype consists of a mappable, internally fragmented and mixed rock body containing a variety of clastic, pelagic and volcanic blocks, commonly in a pervasively deformed matrix. The term 'melange' is used here to describe in a general sense such a rock body. 'Melange' is a useful descriptive term, alerting the reader to the possibility that such a body may not conform to classic principles of superposition and stratigraphic succession. This usage of the term grew from a Penrose Conference on melanges, convened in 1978 (Silver & Beutner, 1980).

"The term refers to rock mixtures formed by tectonic movements, sedimentary sliding, or any combination of such processes, with no mixing process excluded. It does not imply a particular mixing process" (Silver & Beutner, 1980). As the original stratal continuity has largely been destroyed in the Wharite Lithotype, bedding is often indistinct. The most prominent measurable feature is a marked alignment defined by: (1) Stretched but still intact beds and/or strings of isolated clasts comprised of competent lithologies set within an argillaceous matrix. Shape, spatial distribution and orientation of the clasts give rise to a planar fabric, which can be used as a mapping feature here referred to as foliation.\* Most of the clasts are elongated parallel to the regional strike of the strata. (2) Abundant surfaces of shear and dislocation within the matrix. These surfaces of shear and dislocation are subparallel to the planar fabric defined by the orientation of clasts of competent lithologies.

Systematic measurement of foliation attitudes at numerous localities was necessary to establish a broad structural pattern. Although linear and planar elements may be obvious and regular within a given outcrop, such features are traced to nearby exposures with great difficulty. The regional foliation pattern is generally consistent with the strike and dip of bedding in the adjacent Tamaki Lithotype. Exceptions to this occur on a

---

\* Foliation as used in structural geology is a general term for a planar arrangement of textural or structural features in any type of rock (Gary *et al.*, 1977).

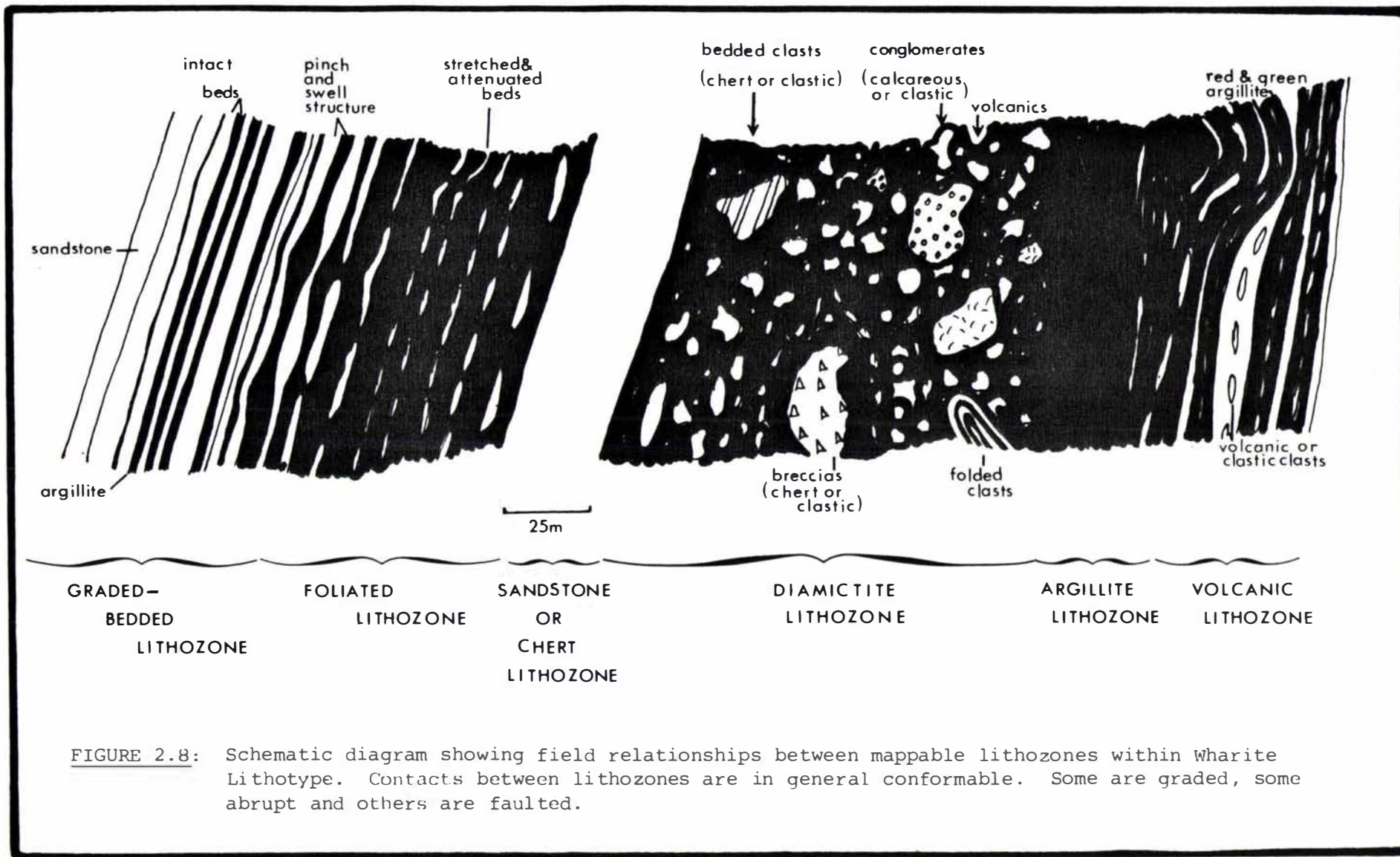
large scale where foliation attitudes show a marked but consistent change from the regional northeast, north and northwest strike to an almost east-west strike, at the Manawatu Gorge, in the vicinity of Maharahara copper-mine and in Piripiri catchment (Map 1). These deviations from the regional pattern are thought to be due to folding (see Chapter 7).

In view of the chaotic nature of this Lithotype no reliable measurement of younging direction could be established. For reference purposes the most accessible outcrops of Wharite Lithotype are exposed in road cuttings along much of the length of the Manawatu Gorge road. The Wharite Lithotype is approximately 4 km wide at this point. Here, exposures offer a good cross-sectional view of the lithologies comprising Wharite Lithotype from which the structural attitudes of foliation are readily apparent.

### C. Preview

A brief preview is here deemed necessary in order to explain a number of difficulties concerning the organisation of the following text. These difficulties stem from the diversity of lithological components and the very wide range of clast sizes present. Clast composition and size are features used to differentiate rock units into mappable lithozones.

Where a clast is of sufficient outcrop dimension to be mapped at 1:25 000 scale, and is distinctive and easily recognisable throughout Wharite Lithotype, it has been mapped as a lithozone. In each case the clast is differentiated from the surrounding argillaceous matrix of which it is an integral part. It was intended that by selectively mapping these distinctive lithologies their outcrop pattern would reveal a number of marker horizons, the amount of displacement of which could indicate the intensity of deformation and disintegration of the Wharite Lithotype as a whole. Lithozones defined in this way include Sandstone Lithozone, Chert Lithozone, Argillite Lithozone and Volcanic Lithozone (Fig. 2.8). However, the majority of clasts throughout the study area are of smaller than mappable-size and must therefore be included within a map unit that in outcrop shows some distinctive and easily recognisable feature. The distinguishing feature of such outcrops is the organisation of clasts within the rock unit. That is, the clasts are not differentiated from the encompassing matrix but are together mapped as a lithozone. Examples of lithozones defined in this way include Foliated Lithozones and Diamictite Lithozones (Fig. 2.8). Foliated Lithozones are rock units in which the clasts are aligned within an argillaceous matrix to form a planar fabric of consistent and measurable attitude to constitute foliation. Diamictite Lithozones are rock



units in which the clasts are randomly distributed throughout the encompassing matrix.

The Graded-Bedded Lithozone consists of an undeformed sequence of regularly bedded alternating sandstone, siltstone and argillite lithologies similar to those comprising Tamaki Lithotype.

Many of the lithologies described in this section are only found as 'float' boulders within stream channels thus their association with other lithologies is not known and the lithozone from which they were eroded cannot be established. These lithologies include boulders of andesite, dolerite, laminated chert, calcareous conglomerate and calcareous breccia. Still other lithologies only occur as small-sized *in situ* clast constituents and do not in themselves form sizeable outcrops that can be mapped at 1:25 000 scale. However, their location is indicated with the use of symbols (Map 1).

It is therefore considered practical to indicate at this point (*i.e.* under Lithologic Components) the lithozone(s) with which each lithology is associated in the field. This simplifies the following description and discussion of the lithozones themselves and eliminates the need to list in full the clast components of each lithozone.

#### D. Lithologic Components

##### 1. Black Argillite

Black argillite consists predominantly of silt and clay sized particles but locally may contain a minor sand component. Argillite occurs either as interbeds of uniform thickness between beds of competent lithologies, in which case it is very similar to the argillite comprising interbeds within the Tamaki Lithotype; or as an all-encompassing matrix around clasts of competent lithologies. Argillite is well indurated but in the majority of cases is highly pervasively sheared. Weathering commonly emphasises the discrete shear surfaces within argillite. Some shear surfaces have a lustrous appearance due to the presence of graphite. Sedimentary structures including parallel and cross-lamination are sometimes preserved but have in general been obliterated by shearing. Argillite in outcrop is a distinct dark blue-black colour with dull lustre.

Argillite content varies considerably from one lithozone to another. Argillite Lithozones comprise 100% argillite. Argillite content within Diamictite Lithozones can range from 90% to less than 10% by volume depending upon clast content. Foliated Lithozones show considerable variation

in argillite content. Although generally subordinate in volume to the competent lithologies, the argillite content of Foliated Lithozones can be as high as 70%. Foliated Lithozones contain a higher percentage of argillite than Graded-Bedded Lithozones. Graded-Bedded Lithozones contain approximately 30-50% argillaceous material as interbeds, the amount present at any one locality being dependent upon bed thickness and frequency of bedding. Other lithozones apart from Volcanic Lithozones contain insignificant proportions of argillaceous material. The red and green argillite component comprising Volcanic Lithozones is described under Volcanic Lithologies.

Argillite as interbeds and as matrix together comprise up to 40% of the total volume of the Wharite Lithotype.

## 2. Competent Lithologies

Competent lithologies within Wharite Lithotype comprise sandstone and siltstone with well preserved clastic textures; sandstone conglomerate and breccia; calcareous siltstone, calcareous conglomerate; volcanic materials including pillow lava; and rare dolerite and andesite; a variety of coloured chert and chert breccia and a very rare micritic limestone. The heterogeneous distribution of these lithologies throughout Wharite Lithotype is very apparent in the field.

The competent lithologies have been subdivided on the basis of composition. The subdivisions, listed in order of volumetric importance are:

- (a) Clastic Lithologies;
- (b) Volcanic Lithologies;
- (c) Chert Lithologies; and
- (d) Calcareous Lithologies.

Although relative proportions are difficult to estimate, probably more than 95% of the lithologies are clastic in origin, 4% are volcanic and siliceous materials and less than 1% calcareous siltstones and limestones.

### (a) Clastic Lithologies

#### (i) Bedded Clasts

These consist of sequences of interbedded sandstone, siltstone and argillite typically fine- to medium-grained, and poorly sorted. They are lithologically similar to strata comprising the Tamaki Lithotype. Argil-

lite interbeds are always subordinate in volume to the sandstone. Bed thicknesses range from 0.02-0.1m (very thin-bedded) to 0.1-0.3m (thin-bedded). Individual beds of thicker dimensions were not observed. Where outcrops exceeded greater than 25m width the sequence was mapped as a Graded-Bedded Lithozone, consisting of either a Very Thin-Bedded or Thin-Bedded Association. Some bedded sequences showed signs of internal sedimentary structures such as cross-laminations and grading. However, rarely could they be used to determine younging direction with any degree of confidence. Soft sediment deformation features within these clasts are either folds or pinch-and-swell structures (see Chapter 7).

(ii) Sandstone and Siltstone Clasts

Clasts of sandstone or siltstone together constitute the most abundant lithologies comprising the Wharite Lithotype. Compositionally, the sandstone and siltstone lithologies within Wharite Lithotype do not appear to be significantly different to those sandstone and siltstone lithologies comprising Tamaki Lithotype (see Chapter 5).

Clasts of sandstone vary in size from less than 0.01m in diameter to enormous rock units of more than 50m in outcrop width. Sandstone clasts in excess of 25m thick constitute a mappable unit in this study and are named Sandstone Lithozones. Siltstone clasts of these dimensions are not present. Sandstone and siltstone clasts of lesser diameter constitute components of Foliated and Diamictite Lithozones.

Very occasionally sandstone lithologies contain near spherical 'cannon-ball' boulders of calcareous siltstone. The boulders measure approximately 0.1-0.3m in diameter, are of a finer grain size (fine-grained) than the sandstone (medium-grained) in which they are embedded, and superficially weather to a distinct creamy brown colour. Sometimes pyrite nodules are found as inclusions in the sandstone within which the calcareous 'cannon-ball' boulders are embedded. These lithologies have not been found at *in situ* outcrops but only occur as remnant 'float' material in river beds.

(iii) Conglomerates

There is a wide variety of conglomerate present in the Wharite Lithotype including those described from the Tamaki Lithotype. None of the conglomerates contain inclusions of larger than the maximum pebble size (0.064m). Pebbles are predominantly of rounded to subangular shape and are comprised essentially of clastic, volcanic and chert lithologies (Figs 2.9, 2.10 and 2.11). Constituent pebbles vary in size from 0.001-0.03m in diameter.



FIGURE 2.9: Pebble-dominated conglomerate containing predominantly clastic and volcanic lithologies set within a sandstone matrix. The majority of pebbles are subrounded to rounded. Rock sample TE1 from Te Ekaou catchment at locality T23/590163.

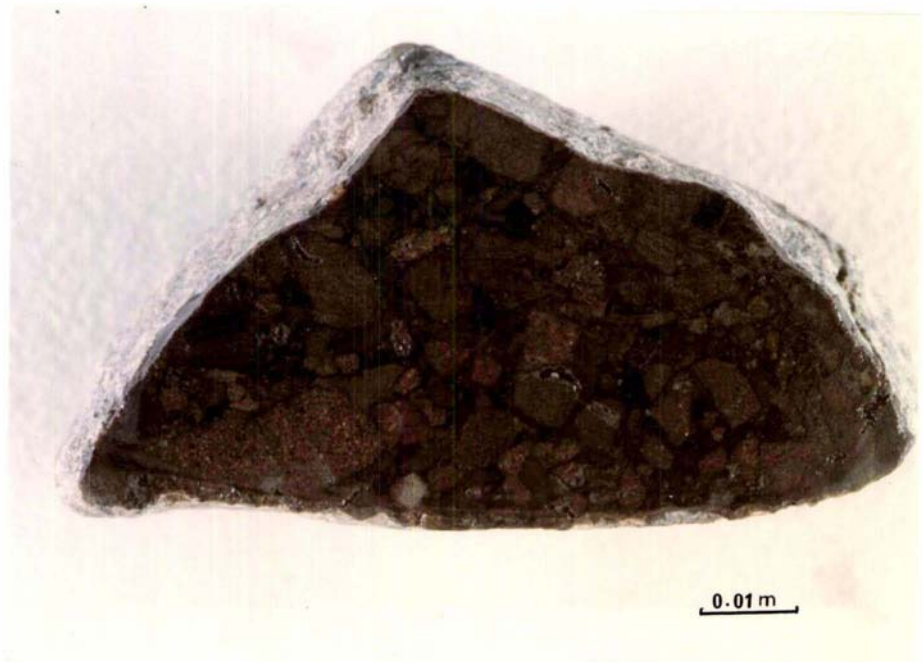


FIGURE 2.10: Pebble-dominated conglomerate containing clastic and volcanic lithologies set within a muddy siltstone matrix. Pebbles are sub-angular to rounded in outline. Rock samples Or6 from south branch Oruakeretaki at locality T23/602063.



FIGURE 2.11: Conglomerate comprising predominantly muddy siltstone matrix within which pebbles of clastic and volcanic lithologies are randomly scattered. A wide range of pebble sizes and shapes is present. Rock sample Crl from Cross Road Stream at locality T24/488928.



FIGURE 2.12: Conglomerate consisting of rounded to subangular, light coloured, fine-coarse grained sandstone and siltstone pebbles set within a darker sandy matrix. Occasional dark pebbles of argillite are also present. The conglomerate is well indurated. Rock sample Kol from Konewa catchment at locality T23/608208.



The average pebble size is approximately 0.005m in diameter. Pebble content of conglomerates varies between 10% and 90% of the total volume. Conglomerate matrix may consist of argillaceous materials (Figs 2.10 and 2.11) or sandstone (Fig. 2.9). All the conglomerates are well indurated. None of them were found as mappable rock units but instead comprise portions of the Diamictite and Foliated Lithozones. A rare type of conglomerate with distinctive outcrop characteristics is restricted to and forms a minor component of the Wharite Lithotype. This conglomerate consists of numerous light grey coloured pebbles of sandstone composition, set within a dark coloured sandy matrix (Fig. 2.12). The pebbles vary in size from 0.001-0.01m in diameter. Surficial weathering of the clasts produces a white coloured exterior. This conglomerate has been found as clasts ranging in size from less than 0.05m to 10m thickness within Foliated and Diamictite Lithozones but has not been found as outcrops of sufficient dimensions to form a mappable unit at a 1:25 000 scale. Small outcrops of this conglomerate occur at T23/608208 and T23/590088.

(iv) Autoclastic Sandstone Breccia

These consist of irregularly shaped angular fragments\* of clastic lithologies set within an argillaceous matrix. The fragments are sometimes arranged more or less parallel to each other and signs of 'flow' around them is common. Fragment size ranges from 0.001-0.01m in diameter in hand specimens (Fig. 2.13) but some of larger sizes are common. Autoclastic breccias are well indurated. They occur within and are part of Foliated Lithozones. These autoclastic breccias differ significantly from fault breccia in this area in that the latter is intensely quartz or calcite veined and carbonate cemented. An autoclastic breccia from the study area (Fig. 2.13) resembles autoclastic breccias described from the Wellington area by Reed (1957b). A rock sampled from the same locality as sample MG2 in the Manawatu Gorge was referred to by Zutelija (1974) as a mylonite.

A second type of autoclastic breccia consists of stretched and attenuated sandstone fragments within an argillaceous matrix that shows signs of flowage (Fig. 2.14). Fragments are generally elongate in shape and angular in outline. Individual fragments vary between 0.02-0.2m in width. These autoclastic breccias are clearly the result of fragmentation of very thin-bedded strata. They occur as *in situ* outcrops but not of sufficient size to form a mappable unit. Such an outcrop can be found in the North Oruakeretaki catchment at locality T23/590087.

---

\* The term 'fragment' is used to imply angularity of rock particles within breccias as opposed to the term 'pebble' which implies roundness of clasts within conglomerates.



FIGURE 2.13: An autoclastic breccia comprising angular chips of sandstone with signs of internal quartz veining, set within an argillaceous matrix. A very wide range of chip sizes is present. Rock sample MG2 from Manawatu Gorge at locality T24/490951. A sample from the same locality is referred to by Zutelija (1974) as a mylonite.



FIGURE 2.14: An autoclastic breccia consisting of stretched and attenuated thin beds of sandstone interbedded with argillite. Flowage of the interbedded argillaceous material during soft sediment deformation resulted in the fragmentation of the sandstone beds into small, angular and isolated or aligned 'trains' or clasts. Photograph taken in North Ormakeretaki catchment at locality T23/590087.  
For scale, the compass case is 0.09m wide.

(b) Volcanic Lithologies

Volumetrically, volcanics are the most abundant lithology of the subordinate rock types. They are widespread, occurring as clasts within Diamictite Lithozones, as interbeds with clastic sediments and/or as clast components within Foliated Lithozones. They also occur as rock units of mappable size constituting Volcanic Lithozones. These lithologies are restricted to the Wharite Lithotype.

(i) Isolated Clasts

The clast lithologies include dolerite (Fig. 2.15) andesite and vesicular basalt (Fig. 2.16). Most of the clasts with basaltic texture are red, black or green in colour. They occur as single isolated or clusters of clasts varying in size from a few centimetres to several metres in diameter. In general the volcanic clasts are subrounded to rounded in shape but angular volcanic clasts are also present. They are encompassed within a black, red or green argillaceous matrix. Individually the clasts are not of sufficient dimensions to be of a mappable scale and are included as constituents of Diamictite Lithozones and Foliated Lithozones.

(ii) Red and Green Argillite

Unpredictable in location, thin beds of predominantly red coloured argillite occur as interbeds within Foliated Lithozones. These interbeds on average range from 0.1-5m thickness and are generally traceable for up to 10m. Green argillites are also present but are less common than the red argillites. Some contacts between interbeds of coloured argillite appear sharp due to the colour differences but are otherwise conformable. Other contacts where intermixing of the red and/or green argillites with the black argillite has occurred are obviously gradational.

All the argillites are typically carbonate-poor, non-tuffaceous pelagic sediments. The presence of slaty cleavage has destroyed most of the original internal sedimentary structures. However, some exposures show very faint plane parallel to slightly curvy, thin (0.005m) laminae of alternating silt and clay size particles.

Some of the red and green argillite beds contain clasts of clastic and/or volcanic lithologies (Fig. 2.17), whilst other beds are devoid of clasts. Clast sizes vary between a few millimetres to 2m in diameter. At some outcrops, intermixing of the coloured argillaceous materials has destroyed bedding and produced a structureless mass of irregular thickness. These



FIGURE 2.15: A slabbed sample of ?diorite containing large feldspar phenocrysts set within a dark fine-grained mafic matrix. Rock sample Tkl found as float boulder in the lower reaches of Tokeawa Stream bed.

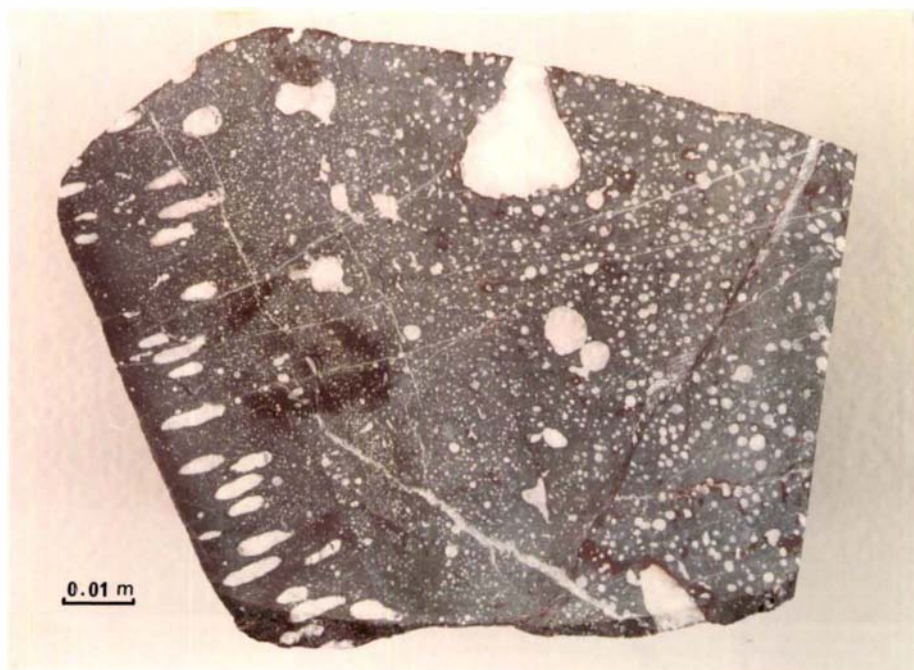


FIGURE 2.16: A slabbed sample of vesicular basalt containing amygdules of calcite. Note the wide range in shape and size of the vesicles. Rock sample was found as float boulder in the lower reaches of Makawakawa River catchment.



FIGURE 2.17: Interbedded red and green argillites together with clasts of spilite (sp), chert (ct), and sandstone (sd), lithologies. In the background is a Diamictite Lithozone dominated by black argillaceous matrix within which there are no chertose or volcanic lithologies. Sequence occurs in the Pohangina River catchment at locality T23/661235. *Field pack is 0.60m high.*

outcrops appear to be of limited lateral extent and tend to pinch out abruptly. Where outcrops of red and green argillite constitute a zone of greater than 25m width and within which they make up a substantial proportion of the lithology they have been mapped as a Volcanic Lithozone (Fig. 2.17).

(iii) Pillow Lava

Several outcrops of pillow lava structure have been found within the Manawatu Gorge, the better exposures being at T24/472954 and T24/486950. The strongly weathered pillows are of red-purple colouration and measure approximately 0.25-1m in diameter. They appear ellipsoid in shape, having a flat irregular base and a smooth rounded concave outline. At locality T24/486950 the outcrop is internally conformable and coherent with each pillow occurring *in situ*. The pillows indicate that the sequence is overturned and thus are consistent with the generally inferred westward younging direction of the Wharite Lithotype. Compositionally the pillows are basaltic and very vesicular, containing amygdules filled with calcite (Fig. 2.16). Outcrops of pillow lava have been mapped as Volcanic Lithozones. Other volcanic compositions including dolerite and andesite have not been found as *in situ* strata.

(c) Chert Lithologies

(i) Non-laminated Cherts

Apart from one isolated outcrop of chert within the Tamaki Lithotype, which is considered to have been in-faulted, chert can be considered to be restricted to outcrops within Wharite Lithotype.

A wide variety of non-laminated cherts have been found in the study area. A common variety is orange-pink in colour, is highly sheared internally and crumbles readily when extracted from outcrop. This chert is commonly found as thin (0.02-0.1m) beds within argillaceous units that comprise part of Foliated Lithozones. Rarely do these thin chert beds form continuous undisrupted units. More commonly the thin chert beds have been fragmented into small clasts that are arranged in quasistratiform strings along a prominent foliation. Repeated strings of clasts give the impression of disrupted bedding as each clast is identical in composition and colour.

Other chert varieties including cream and pink mottled, uniform grey and bright red (Fig. 2.18), have only been found as isolated clasts within Diamictite Lithozones. All of the cherts are highly indurated, though



FIGURE 2.18: A variety of coloured chert lithologies found as thin discontinuous lenses within Foliated Lithozones or as discrete clasts within Diamictite Lithozones.



FIGURE 2.19: A clast of laminated, blue-green chert. Internally the chert is very sheared and calcite veining is prominent. This clast was found as a float boulder in the Manga-a-tua catchment at locality T23/572040.  
*For scale, the geological hammer is 0.28m long.*

intensively veined. Some of the chert varieties contain poorly preserved radiolaria (see Chapter 4) whilst others are barren. In the study area cherts are sometimes but not exclusively found in association with outcrops of pillow lava.

(ii) Laminated Cherts

Two large clasts of laminated chert, one measuring approximately 2m square, the other 4m square, were found in the Manga-a-tua and Makawakawa catchments, respectively. Both blocks are identical in that they consist of very thin laminae measuring 0.01-0.05m thickness. The chert is a translucent green colour (Fig. 2.19), is internally fractured and calcite veining is prominent. The laminae are flexured, suggestive of deformation shortly after deposition, whilst the chert was still in a gel-like condition. Open shears, joints and tectonic partings are characteristic. Laminated cherts of this variety have not been found *in situ* but are thought to comprise one of the clast lithologies within Diamictite Lithozones.

Thinly laminated (0.01-0.3m) alternations of pink and red chert frequently occur in association with spilitic lithologies and together comprise rock units up to 50m thickness. These rock units have therefore been mapped as Volcanic Lithozones. At Maharahara these cherts are associated with an ore body rich in copper sulphide. Samples of copper ore from this mine (Fig. 2.20) show typical green efflorescence of copper carbonate (malachite).

(iii) Chert Breccia

A single boulder of indurated chert breccia has been found in Makohine Stream as part of the bedload. The predominantly white and cream coloured fragments are very angular, vary between 0.01-0.05m in diameter and are cemented by a microcrystalline siliceous cement (Fig. 2.21).

(iv) Autoclastic Chert Breccias

These consist of small (<0.01-0.03m) fragments of white and cream chert set within an indurated argillaceous matrix (Fig. 2.22). Whilst most outcrops of autoclastic chert breccia are too small to map, others are relatively extensive and have been mapped as Chert Lithozones.

(d) Calcareous Lithologies

(i) Micritic Limestone

One white, micritic, fossiliferous, indurated limestone boulder has been





FIGURE 2.20: Sample of copper ore from Maharahara Coppermine within Coppermine catchment showing green efflorescence of copper carbonate (malachite). Sample collected by D W Toy. Sample location unknown.



FIGURE 2.21: Chert breccia, consisting of angular coloured fragments of chert set in a microcrystalline siliceous cement, was found in Makohine catchment at locality T23/498050. For scale, the compass case is 0.09m wide.



FIGURE 2.22:

Autoclastic chert breccia comprising angular, white coloured fragments of chert set within an indurated argillaceous matrix. Signs of flowage of the matrix and subsequent alignment of chert fragments can be seen at the bottom of the photograph. Photograph taken in Pohangina catchment at locality T23/686230. For scale, compass case is 0.09m wide.

extracted from the matrix of a Diamictite Lithozone in the Pohangina River. In view of its greater age (see Chapter 4), relative to the rest of the sequence within which it was found, it is interpreted to be an allochthonous lithology.

(ii) Calcareous Siltstone

Calcareous siltstone interbedded with argillite forms a minor component of Foliated Lithozones. Here once-intact bedded units of calcareous siltstone have been pulled apart along bedding into discrete clasts or "trains" of clasts that define a foliation. Calcareous siltstone also occurs within Diamictite Lithozones as small, isolated and rounded clasts. The average clast size is between 0.01-0.03m in diameter. Rarely do clasts exceed 0.5m diameter. Calcareous siltstone clasts have a characteristic weathered brown exterior and light grey interior. Calcite veining is common. These calcareous siltstone clasts are identical in composition and thickness to conformable calcareous siltstone lenses found within the Thin-Bedded Association of the Tamaki Lithotype, exposed within the Manawatu Gorge at T24/495935. Calcareous siltstones have not been found as undisrupted bedded units anywhere in the study area.

(iii) Calcareous Conglomerate

This lithology has only been found as boulders within stream bedload materials (Fig. 2.23). Each boulder consists of well rounded, spherical to ovoid shaped calcareous siltstone pebbles cemented together by a calcareous sandstone matrix. The pebbles are of uniform size, averaging approximately 0.02-0.1m in diameter. The exterior surfaces of the pebbles weather to a distinctive brown colour. These conglomerates are fossiliferous (see Chapter 4). Pyrite nodules are often associated with these conglomerates (Fig. 2.23). This lithology is restricted to the Wharite Lithotype.

E. Mappable Lithozones Within the Wharite Lithotype

1. Introduction

The Wharite Lithotype is essentially a tectono-stratigraphic unit within which mappable lithozones are defined either on the degree and style of internal organisation, or on the basis of lithology. There are seven recognisable lithozones. Listed in order of dominance these are:  
 (1) Foliated Lithozones; (2) Sandstone Lithozones; (3) Volcanic Lithozones; (4) Diamictite Lithozones; (5) Graded-Bedded Lithozones;



FIGURE 2.23: Calcareous conglomerate containing rounded pebbles with brown weathered exterior set in a calcareous sandstone matrix. Rust coloured streaks are the result of weathering of pyrite nodules. Sample was found in Mangapapa catchment at locality T23/537109. *Hammer is 0.28m long.*

(6) Chert Lithozones; and (7) Argillite Lithozones (Table 2.2).

Six of these lithozones are only found in the Wharite Lithotype, with the Graded-Bedded Lithozone being common to all three lithotypes mapped in the study area (Map 1).

Three of the mapped lithozones are thought to represent rock units that have been deformed differentially. These lithozones can be ranked on the basis of the degree of fragmentation of the competent lithologies within each lithozone. Graded-Bedded Lithozones within which deformation of the bedded units has been slight to moderate display slight pinch-and-swell structure and in some cases soft-sediment folding. Foliated Lithozones characteristically show evidence of more intense deformation than is evident in the Graded-Bedded Lithozones. The more pronounced style of deformation ranges from a stretching of bedded units to complete fragmentation of once-intact bedded units, into 'trains' of isolated clasts arranged in linear fashion. This linear arrangement of clasts defines a measurable foliation. Rock units mapped as Foliated Lithozones reflect a wide range of deformation styles that are thought to represent local variations in the intensity of deformation ranging from moderate to strong (see Chapter 7). Diamictite Lithozones may represent the end product of strong to very strong deformation of rock units to the stage where all signs of bedding have been destroyed, foliation is no longer evident (perhaps as a result of rotation of the clasts) and the clasts are characteristically randomly oriented and scattered throughout the rock unit.

All gradations exist between Graded-Bedded and Foliated Lithozones and between Foliated and Diamictite Lithozones.

The following discussion of these three lithozones is in the order of ranking based on the degree of internal fragmentation. An alternative origin for Diamictite Lithozones is also discussed. The remaining four lithozones, defined on the basis of lithology, show little or no sign of post-depositional deformation at an outcrop scale. This is largely because of their great thickness, high induration (particularly the Sandstone, Chert and Volcanic Lithozones) and in the case of Argillite Lithozones the general absence of other lithologies within this lithozone to highlight the style and intensity of deformation. These latter lithozones are discussed in turn.

(a) Graded-Bedded Lithozones

These consist of regularly interbedded graded units of sandstone, silt-

Table 2.2: Strata of the Wharite Lithotype are differentiated into seven distinct Lithozones. The Graded-Bedded Lithozone is further subdivided into Associations on the basis of average outcrop thickness of individual beds. Lithologic components of each Lithozone are ranked in order of dominance. Stratigraphic relationships between Lithozones is also indicated.

Lithozone	Association	Lithologic components in order of dominance	Stratigraphic relationships with other Lithozones
Graded-Bedded	Very Thin-Bedded (0.02 - 0.1m)	Fine- to medium-grained Sandstone. Black Argillite. Siltstone.	Predominantly found in juxtaposition with Foliated Lithozones and occasionally with Argillite Lithozones.
	Thin-Bedded (0.1 - 0.3m)	Fine- to medium-grained Sandstone. Black Argillite. Siltstone.	
Foliated		Sandstone and Siltstone. Black Argillite. Chert. Calcareous Siltstone. Volcanic Argillite (red and green). Sandstone Conglomerate and Breccia.	Found in juxtaposition with all other Lithozones.
Diamictite		Argillite. Sandstone and Siltstone. Chert. Volcanic Lithologies (Basalt, Andesite). Limestone.	Found in juxtaposition with all other Lithozones.
Sandstone		Sandstone.	Found in juxtaposition with Foliated and Diamictite Lithozones.
Chert		Chert. Minor volcanics.	Found in juxtaposition with Diamictite and Foliated Lithozones.
Volcanic		Basalt. Volcanic Argillites. Black Argillite with competent clastics.	Found in juxtaposition with Diamictite and Foliated Lithozones.
Argillite		Black Argillite. Chert. Calcareous Siltstone. Siltstone and fine-grained Sandstone.	Found in juxtaposition with Diamictite, and Foliated Lithozones.

stone and argillite very similar to the sequences of strata comprising the entire Tamaki and Western Lithotypes. As previously described, the thickness of individual beds is usually remarkably consistent at outcrop scale and can be used as a basis to subdivide these sequences into Associations. Only the Very Thin-Bedded and Thin-Bedded Associations have been recognised in Graded-Bedded Lithozones within the Wharite Lithotype (Table 2.2). Their occurrence within Wharite Lithotype is not as rare as is indicated on Map 1, as many outcrops are of insufficient width to be mapped at 1:25 000 scale. The lateral extent of these Lithozones is unknown but because they cannot be traced from one catchment to another they are unlikely to extend more than 0.5 km in length.

Although internal sedimentary structures and grading are often preserved, limited exposure makes the direction of younging difficult to discern. A consistent direction of younging could not be established. The strata within these Lithozones is sometimes traceable along a consistent strike direction that parallels the foliation direction in adjacent outcrops mapped as Foliated Lithozones. This is, however, dependent upon the intensity of deformation present at each outcrop. A gradation of deformational intensities is present. These range from: (1) beds of competent lithologies that show slight thickness variations; to (2) those that display distinct pinch-and-swell features; to (3) beds that are strongly stretched but maintain traceable bedding horizons; and (4) beds that are pulled apart parallel to bedding and fragmented into discrete tabular shaped clasts separated from one another by argillaceous matrix. The tabular shape and thickness of the stretched clasts is largely controlled by enclosing bedding planes and the length of the clasts is probably determined by the intensity of jointing. The ends of the clasts may be sharp and angular, rounded or pinched (Table 2.3). The stretching of beds is often accompanied by folding the style of which strongly suggests that some of the deformation was syndepositional (see Chapter 7).

There appears to be a direct correlation between bed thickness and intensity of deformation. The thinner beds comprising the Very Thin-Bedded Association appear to show greater deformation than bedded units comprising the Thin-Bedded Association. With increased deformation the argillaceous interbeds have been tectonically thinned as a result of mobilisation of this material into the gaps between the clasts of competent lithologies. In the field, Graded-Bedded Lithozones are predominantly found in juxtaposition with Foliated Lithozones and occasionally with Argillite Lithozones (Table 2.2).

**Table 2.3:** Diagnostic features at outcrop scale of three major Lithozones comprising the Wharite Lithotype.

	Graded-Bedded Lithozone	Foliated Lithozone	Diamictite Lithozone
Organisation	Varies from bedded sequences displaying stretched but intact units with pinch-and-swell features to rare boundinage structure and very rare aligned clasts.	Clasts arranged in 'trains' that constitute foliation with consistent measurable dip and strike.	Random clast orientations with no signs of internal organisation such as bedding or foliation.
Composition	Bedded sequences of sandstone, siltstone and argillite.	Clast compositions include clastic, volcanic, chertzose, and calcareous lithologies. Matrix is predominantly clastic but occasionally volcanic argillite is present.	Clast compositions include clastic, volcanic, chertzose and calcareous lithologies. Matrix is clastic argillite.
Clast and Bed Shape	Beds are tabular or elongate with angular, pinched or rounded ends.	Clasts and stretched beds are elliptical in shape. Some have pinched ends, others are blunt and angular.	Clasts are near spherical or equant and commonly lens-shaped.
Bed Thickness	Bed thickness averages 0.05 - 0.3m with occasional thick beds of sandstone measuring 1 - 2m thick.	Most common bed sizes range between 0.05 - 1.0m with frequent larger beds measuring greater than 1m in diameter.	Not applicable.
Clast Size	Clast size determined by bed thickness and spacing of joints.	Clasts of all sizes. Clast size is dictated by the thickness of the original bedding as listed above.	Generally comprise clasts of small size range between 0.02 - 1.0m but rarely may include clast sizes up to 10m in diameter.
Clast Roundness	Angular.	Angular to subrounded.	Larger clasts are predominantly subrounded to rounded. Smaller clast sizes are generally subrounded to very angular. Very small clasts are very angular.



(b) Foliated Lithozones

The term Foliated Lithozone is used here to denote those sequences consisting essentially of black argillaceous material in which sandstone (Fig. 2.24), chert and calcareous siltstones occur either as rare bedded units or more predominantly as clasts arranged along distinct planes as 'trains of clasts' resembling a stretched stratification. In these sequences the 'trains of clasts' maintain a clearly recognisable consistent strike and dip through a substantial stratigraphic thickness. Such an alignment of clasts constitutes a foliation (Fig. 2.24). Occasionally thin interbeds of red and/or green argillaceous material parallel foliation. Clast dimensions within argillite-dominated Foliated Lithozones range from 0.05-1m thickness. Some Foliated Lithozones consist of sequences of strata that are sandstone - dominated within which the dimensions of individual clasts of sandstone generally exceed 1m thickness.

Not all the strata within Foliated Lithozones are disrupted. In many places, sharp contacts exist between disrupted beds and undisrupted beds.

Indeed, most disrupted beds appear to be in stratigraphic units that are sandwiched between undisturbed beds. Contrast in degree of deformation is especially evident between thick sandstone-dominated sequences and thin bedded argillite-dominated sequences, however, in many places the thickness of bedding does not seem to have controlled deformation. The Foliated Lithozones are therefore a composite of both undisrupted and disrupted sequences ranging in thickness from less than 1m and involving one or two beds to over 100m and involving many beds.

The characteristic structural style of Foliated Lithozones is predominantly a product of deformation resulting in fragmentation of once-intact bedded sequences of strata. Conceptually the intensity of deformation witnessed in Foliated Lithozones is intermediate between that seen in deformed sequences of Graded-Bedded Lithozones and Diamictite Lithozones with all gradations being present.

Although gradations between deformed Graded-Bedded Lithozones and Foliated Lithozones exist, it is not difficult to distinguish them in the field. They differ in that the argillaceous content of Foliated Lithozones in general appears to be much greater, despite the presence of a greater number of thick interbeds of competent lithologies, than is present within Graded-Bedded Lithozones. Furthermore, clast composition in the Foliated Lithozones is more varied and may include lithologies of chertose, calcareous and volcanic compositions (Table 2.3). Clast shape also differs in



FIGURE 2.24: Foliated Lithozone within which once-bedded sandstone units have been pulled apart along strike, during deformation, into isolated lenses. Strike of relict bedding is here referred to as foliation. Photograph taken in Coppermine catchment at locality T23/545048. *For scale, the width of the compass case is 0.09m.*

that clasts within Graded-Bedded Lithozones tend to be tabular in shape with angular edges whereas those comprising Foliated Lithozones are commonly angular to subrounded and elliptical in shape (Table 2.3), presumably due to much greater stretching attendant with increased deformation. In the field Foliated Lithozones are found in juxtaposition with all other lithozones (Table 2.2).

(c) Diamictite Lithozones

The term diamictite is here used to denote a non-sorted or poorly sorted, non-calcareous, terrigenous sedimentary rock that contains a wide range of particle sizes, such as a rock unit with sand and/or larger particles in a muddy matrix (Gary et al., 1977). The most important characteristic of the diamictite deposits in the study area is the lack of any obvious sign of sorting or internal fabric such as bedding or foliation of the contained clasts (Figs 2.25 and 2.26). Most of the material comprising the diamictites is of similar lithological composition to the rock sequences with which it is interbedded. However, a few clast lithologies within the diamictite are of known allochthonous origin (see Chapter 4) but truly exotic clasts are absent.

A wide variety of clast sizes and shapes is characteristic of diamictites. Very small (0.001-0.005m) fragments of competent lithologies are in general very angular in shape and may have been derived from comminution of larger clasts during deposition or later cataclasis. Clasts of average size (0.05-1m) are irregularly spherical to elongate and vary in roundness from very angular to subrounded (Table 2.3). Near spherical yet poorly rounded clasts are most dominant. Clasts of this size range may have been derived from either subaerial erosion or cataclasis. Large clasts (1-10m) are most commonly near spherical and subrounded. Clasts measuring between 0.05-10m generally have smooth surfaces that are coated with a thin layer of polished scaly matrix. Polished surfaces may indicate that these clasts have been rotated during deformation.

On the basis of the clast :matrix ratio, and size, shape and composition of clasts a wide variety of diamictite types were recognised in the field.

Some diamictites are dominated by clasts between 0.01-0.1m in diameter with an occasional larger clast up to 0.2m diameter. In these instances the clast composition is predominantly sandstone but at one locality a rare deposit of diamictite consisting predominantly of clasts of chertzose composition was found (Fig. 2.25). Diamictites in which the clast size-range is small characteristically contain clasts that are either angular to very



FIGURE 2.25: Diamictite which contains very angular chert clasts of small size range within a sheared argillaceous matrix. Note the random distribution of clasts. Outcrop occurs in Manga-a-tua catchment at locality T23/557054, Hammer is 0.28m long.



FIGURE 2.26: Diamictite containing clasts of varying sizes and compositions, within a sheared argillaceous matrix. The clasts of sandstone (sd) and spilite (sp) are randomly arranged throughout the outcrop. Outcrop occurs in the Makawakawa catchment at locality T23/590189. Largest spilite boulder (right of photograph) is 4m in diameter.

angular in shape (Fig. 2.25) or are rounded to subrounded, but were not found to contain mixtures of both angular and rounded clasts. The equant shape of the clasts in these diamictites is very characteristic.

Other diamictites characteristically contain clasts that are generally within the 0.1-1m diameter size range, with an occasional larger clast measuring between 1-10m in diameter. Compositionally these deposits are diverse and usually contain a mixture of volcanic, chertose, calcareous and clastic rock types. The smaller clasts tend to be more angular than the larger clasts (Fig. 2.26 and Table 2.3).

Variations in the clast : matrix ratio are also very obvious in outcrop. Some diamictites contain very few clasts of competent lithologies and are therefore essentially thick units of argillite. Where the clast content of such outcrops is less than 5% the deposit was mapped as an Argillite Lithozone. Diamictites may contain few or a large number of clasts that can comprise up to 50% of the deposit. A wide variety of diamictite deposits with intermediary percentages (5-50%) of clast constituents are present in the study area.

Because of the large variations in the above characteristic features of diamictites it was not practical to classify and map each type of diamictite. All the diamictite outcrops therefore have been mapped as a single lithozone. It is not clear whether the thick Diamictite Lithozones represent accumulation during one or several successive episodes. The absence of depositional breaks within these deposits suggests that accumulation was not episodic. No redeposited diamictites have been recognised. In the field, Diamictite Lithozones are found in juxtaposition with all other lithozones (Table 2.2).

The origin of diamictites in the study area may be the result of two distinct and quite separate processes: (1) by extreme fragmentation of Foliated Lithozones with subsequent rotation and mixing of the broken fragments (see Chapter 7); or (b) by sedimentary depositional processes associated with submarine debris flows (see Chapter 5). The final product of both processes is a rock unit consisting of predominantly randomly oriented clasts set within a ductile dark argillaceous matrix. However, some diamictites, within which the clasts are not completely randomly distributed, show a faint foliation. These foliated diamictites thus resemble Foliated Lithozones. The foliation, as defined by the alignment of clasts, may be due to: (1) if extreme fragmentation of a Foliated Lithozone has been incomplete, mixing of the broken fragments may not have occurred - foliation in

this case is defined by the relict bedding; or (2) compaction after deposition of a debris flow deposit.

As foliated diamictites appear so very similar to strongly fragmented Foliated Lithozones (and grade into them) criteria were established to distinguish them.

(i) Distinction between Foliated Diamictite Lithozones and Strongly Fragmented Foliated Lithozones

While a foliated diamictite of debris flow origin is likely to have a more varied range of clast sizes than a strongly fragmented Foliated Lithozone, this criterion alone is not sufficiently reliable to distinguish the two lithozones. The latter tend to contain clasts of uniform size but this is dependent on the bedding thickness and regularity of bedding in a succession from which the clasts were derived. The most useful distinguishing field criterion is the composition of the contained clasts. If clasts of mixed lithologies lie along the same foliation plane the deposit is considered to have been deposited by a debris flow with the foliation being superimposed during compaction. These deposits have been classified as diamictites. Clast-rich diamictites are more likely to show a faint foliation in response to compaction than clast-poor diamictites. Conversely if clasts of mixed lithologies are segregated and are aligned along separate foliation planes, the deposit is likely to have originated as a result of incomplete fragmentation of a Foliated Lithozone. This foliation is likely to be due to the preservation of vestiges of bedding. Unfortunately, this criterion cannot be applied when deposits contain clasts of a single lithological type. Clast shape and roundness are not considered to be reliable criterion. Clasts produced by fragmentation are generally elongate or equant depending upon the spacing of joints. The clasts generally have sharp edges and may have either pinched or blunt ends. Those deposited by debris flows are likely to be near spherical in shape with rounded edges but become flattened and lens-shaped during deformation (see Chapter 7). Unfortunately, clasts in either Foliated or Diamictite Lithozones are not always of a distinctive shape but instead a wide range of clast shapes may occur in either Lithozone.

(d) Sandstone Lithozones

These consist of thick (>25m width), often highly jointed sequences of predominantly sandstone composition. Several sets of joints are usually present at any one outcrop but jointing in one direction usually predominates.

Outcrops of these units often stand out on valley slopes and ridges as resistant blocks or slabs. In river channels they often form sites of waterfalls or gorges. Where these thick, resistant Sandstone Lithozones strike across river channels they result in deviation of the river around the obstacle. Sandstone Lithozones cannot be traced as continuous units between catchments and consequently are not thought to exceed more than about 0.5 km in length. Although evidence of extensional deformation at outcrop scale is often absent it appears likely that dislocation of these once continuous sandstone units into very large blocks has occurred.

Many of the contacts between Sandstone Lithozones and adjacent lithozones are abrupt but are thought to be conformable. Occasionally, shearing along this contact is evident. The thickness of these sandstone units is generally many times the thickness of the thickest sandstone units present within the Tamaki Lithotype. In the field, Sandstone Lithozones are found in juxtaposition with Diamictite and Foliated Lithozones (Table 2.2).

(e) Chert Lithozones

Although an abundant constituent of Wharite Lithotype, chert rarely occurs in units of sufficient thickness to be mapped at 1:25 000 scale. Exceptions occur in Pohangina catchment at localities T23/686230 and T23/687232 (Map 1) where Chert Lithozones, comprising essentially chert breccia and other minor lithologies, occur in juxtaposition with outcropping Volcanic Lithozones.

(f) Volcanic Lithozones

Three outcrops of pillow lava of mappable size are known in the study area, two of which crop out in road cuttings along the Manawatu Gorge road at T24/472954 and T24/486950. The third outcrop occurs in Pohangina catchment at T23/686230. The distribution of pillow lava is thought to be widespread because pillow boulders have been found as clast constituents within Diamictite Lithozones and as float material in streams throughout the study area. There is no evidence of sills, dykes or other shallow volcanic intrusives in the study area. Thick outcrops of red and green argillite are included within Volcanic Lithozones.

A thick belt of copper sulphide bearing rocks associated with chert and volcanics has been mapped as part of the Volcanic Lithozone. Because of its distinctive colour this lithozone can be used as a stratigraphic marker bed. Its width is extremely variable because it comprises many discontinuous units, some of which peter out along strike. Each unit may be between

10-250m thick and is commonly interbedded with equally thick units of clastic composition. Volcanic Lithozones are found in juxtaposition with Foliated and Diamictite Lithozones (Table 2.2). Both sheared and conformable contacts with adjacent lithozones have been observed.

(g) Argillite Lithozones

These lithozones are very rare because most of the outcrops of thick black argillaceous material either contain clasts or thin interbeds of clastic, chertose or calcareous lithologies. Where outcrops of argillite contain less than 5% of competent lithologies as clasts or interbeds the unit is mapped as an Argillite Lithozone (Fig. 2.27). Where greater than 5% of competent lithologies is present as clasts that are randomly distributed throughout the rock body the outcrop is mapped as Diamictite Lithozone. Where the clasts are aligned and form a distinctive foliation, the outcrop is mapped as a Foliated Lithozone. In the field outcrops of Argillite Lithozones may grade into Diamictite or Foliated Lithozones (Table 2.2).

2.2.4 WESTERN LITHOTYPE

A. Distribution

This Lithotype comprises the westernmost exposure of Torlesse rocks in the study area and is restricted to small areas lying to the west of the Wharite Lithotype. The largest exposure occurs in the lower reaches of No. 1 Line catchment between T23/534096 and T23/540094 (Map 1). The lateral extent of this Lithotype within the study area is unknown because it is buried beneath overlying Plio-Pleistocene marine deposits.

B. Nature

The Western Lithotype is an informal lithostratigraphic unit consisting of a sequence of interbedded sandstone, siltstone and argillite. The bedded units vary in thickness from very thin-bedded (0.02-0.1m) to thick-bedded (0.3-2m) but overall thin-bedded units (0.01-0.3m) predominate. Beds of sandstone or argillite of greater than 2m thickness are absent (Table 2.4).

Graded bedding and primary sedimentary structures are abundant. Parts of this Lithotype are undeformed whilst other parts show signs of soft-sediment deformation including stretching of bedded units, boudinage structure and open folding. The strike of the strata is consistently between northwest and northeast and dip angles are everywhere very steep. Eastward dipping, westward younging strata predominate, indicating that they have been over-





FIGURE 2.27: An outcrop of argillite that is essentially devoid of clasts and interbeds of competent lithologies and has been mapped as an Argillite Lithozone. Weathering along numerous cleavage surfaces produces a rough surface texture on outcrops of exposed argillite. Location of outcrop is in No. 4 Line catchment at T23/506046. *Compass case is 0.09m wide.*

**Table 2.4:** Strata of the Western Lithotype comprise a Graded-Bedded Lithozone. This Lithozone is subdivided into Associations on the basis of average outcrop thickness of individual beds. Lithologic components of each Association and relationship between Associations is shown.

Lithozone	Association	Lithologic components in order of dominance	Stratigraphic relationships with other Associations
Graded-Bedded	Very Thin-Bedded (0.02 - 0.1m)	Fine- to medium-grained Sandstone. Argillite. Siltstone.	Commonly interbedded with Thin-Bedded Association. Occasionally interbedded with Thick-Bedded Association.
	Thin-Bedded (0.1 - 0.3m)	Fine- to medium-grained sandstone. Argillite. Siltstone.	Commonly interbedded with both Very Thin-Bedded Association and with Thick-Bedded Association.
	Thick-Bedded (0.3 - 2m)	Fine- to medium-grained sandstone. Siltstone. Argillite.	Commonly interbedded with Thin-Bedded Association. Occasionally interbedded with Very Thin-Bedded Association.

turned, In many respects the character of this Lithozone is very similar to the Graded-Bedded Lithozone of the Tamaki Lithotype.

### C. Lithologic Components

The Western Lithotype comprises three lithologies; sandstone, siltstone and argillite (Table 2.4). Their textural and compositional features are similar to those described from the Tamaki Lithotype.

There are, however, two noticeable differences: (1) there is less argillaceous material as interbeds between the sandstones and siltstones so that outcrops appear to be dominated by grey sandstone and siltstone lithologies; and (2) there are no intercalated beds of calcareous siltstone, pebbly mudstone or intraformational conglomerate present.

### D. Mappable Lithozones Within the Western Lithotype

Strata comprising this Lithotype are mapped as one unit - a Graded-Bedded Lithozone, that may be subdivided into three associations on the basis of bed thickness in a similar manner to mapping of the Tamaki Lithotype. These associations are: (1) Very Thin-Bedded Association; (2) Thin-Bedded Association; and (3) Thick-Bedded Association (Table 2.4).

The characteristic features of each association are very similar to those of the same association comprising the Tamaki Lithotype.

The lithotypic status of the Western Lithotype is questionable because it is of limited areal extent. Thus there is a possibility that outcrops of Western Lithotype represent large blocks of Graded-Bedded Lithozone constituting part of the Wharite Lithotype. This possibility is supported by the presence of bedrock outcrops of similar appearance to those comprising Wharite Lithotype further to the west of outcropping Western Lithotype. These outcrops occur in Porewa, Konewa and Pohangina catchments. On the other hand, evidence to support the likelihood that the Western Lithotype is part of a laterally more extensive "coherent terrane" includes the presence of a substantial thickness of similarly "bedded lithologies" immediately to the north of the study area (Munday, 1977). These "bedded lithologies", in the vicinity of Oroua River catchment lie to the west of a zone of melange. This melange may confidently be correlated with the Wharite Lithotype (see Chapter 4).

C H A P T E R    3

---

SEDIMENTARY STRUCTURES AND PALEOENVIRONMENTAL ANALYSIS

CONTENTS

	<u>page</u>
3.0 SEDIMENTARY STRUCTURES ... ..	76
3.0.1 INTRODUCTION ... ..	76
3.0.2 INTERNAL STRUCTURES ... ..	77
A. Grading ... ..	77
B. Lamination ... ..	80
C. Convolute Lamination ... ..	83
D. Flaser Bedding ... ..	84
E. Flame Structure ... ..	85
F. Cross-Lamination ... ..	85
G. Disrupted Bedding ... ..	85
3.0.3 EXTERNAL STRUCTURES ... ..	87
A. Sole Markings ... ..	87
1. Load Casts ... ..	87
2. Longitudinal Ridges and Furrows ... ..	88
B. Surface Markings ... ..	88
1. Small-scale Ripples ... ..	88
3.0.4 TRACE FOSSILS ... ..	88
3.0.5 TRANSPORTATION AND DEPOSITIONAL PROCESSES ... ..	89
A. Sediment Gravity Flows ... ..	89
1. Turbidity Current ... ..	89
2. Grain Flow ... ..	91
3. Fluidised Sediment Flow ... ..	93
4. Debris Flow ... ..	94
B. Ocean Bottom Currents ... ..	96

C. Discussion	...	...	...	...	...	...	97
3.1 PALEOENVIRONMENTAL ANALYSIS	...	...	...	...	...	...	99
3.1.1 DEPTH OF DEPOSITION	...	...	...	...	...	...	99
3.1.2 PROXIMITY OF SOURCE OF DEPOSITIONAL ENVIRONMENT	...	...	...	...	...	...	102
3.2 DEPOSITIONAL ENVIRONMENT	...	...	...	...	...	...	103

CHAPTER 3SEDIMENTARY STRUCTURES AND PALEOENVIRONMENTAL ANALYSIS3.0 SEDIMENTARY STRUCTURES3.0.1 INTRODUCTION

The structures described in this section are those formed within beds which can be seen in cross-section. Of these perhaps the most obvious are grading and lamination. These are usually very well preserved in sandstone and siltstone lithologies. Described with internal structures are some external features, such as ripples, which are included here because of their direct association with internal structures. Convolute lamination and disrupted bedding of load deformation origin are also discussed. An occurrence of a trace fossil is documented. Sedimentary structures occur throughout the study area but are best preserved in undeformed strata comprising the regularly bedded Graded Lithozones. Because of subsequent episodes of ductile and brittle deformation (see Chapter 7) sedimentary structures, though present, are less well preserved in strata comprising Foliated Lithozones. These structures are very scarce within Sandstone and Argillite Lithozones. Consequently the majority of sedimentary structures described here are from outcrops comprising the Tamaki and Western Lithotypes with fewer examples from outcrops comprising the Wharite Lithotype.

The interpretative value of sedimentary structures in this area is severely limited by poor outcrop exposure. Few are of value as environmental indicators as most of the examples were not found *in situ*. Whilst observation and interpretation of small-scale internal sedimentary structures in the field is difficult, the use of slabbed samples proved invaluable. Many of the features described in this section are from slabbed samples.

Ancient sediments showing a regular alternation of graded coarse- and fine-beds through a substantial stratigraphic thickness are thought to be typical of deposits of turbidity currents, for which the terms greywackes, redeposited beds, flysch and turbidites have been used. As the origin of these beds is still controversial the non-committal terms of "flysch-like" (Kuenen, 1964) and "flysch-type" (Kuenen, 1967) have been proposed.

"Flysch-type" is defined as deposits of alternating coarse- and fine-beds showing characteristics of "turbidites", such as graded bedding, and internal sedimentary structures fitting Bouma's (1962) "turbidite facies model". "Flysch-like" is defined as alternating sequences, reaching thicknesses of geosynclinal magnitude but lacking typical "turbidite" characteristics (Van der Lingen, 1969). Many of the sedimentary structures described from this area are characteristic of "turbidites" for which the term "flysch-type" deposit is here used.

### 3.0.2 INTERNAL STRUCTURES

#### A. Grading

Grading constitutes the gradual reduction, in a progressively upward direction within an individual stratification unit, of the upper particle size limit (Gary et al., 1977). Grading was observed predominantly in regularly interbedded sequences of alternating sandstone, siltstone and argillite comprising Graded Bedded Lithozones within all three Lithotypes. Grading within beds of sandstone comprising Sandstone Lithozones is often imperceptible. Grading within argillite beds comprising Argillite Lithozones is best seen in slabbed rock samples. Grading was the basis for determining most younging directions in the study area; reverse grading was not observed. It is now generally accepted that graded bedding is perhaps the most characteristic feature of turbidite deposition. Graded beds are deposited from a waning current and may range in thickness from one centimetre or less to one or more metres (Pettijohn, 1975).

Bouma (1962) systematised many of the sedimentary structures known to be associated with turbidity currents (*sensu stricto*). All of the structures contained within the Bouma sequence as described by Bouma (1962) have been observed both in the field and in slabbed rock samples. However, single beds displaying the entire Bouma sequence (Ta-e) were not found (Fig. 3.1). Incomplete Bouma sequences display both top and bottom 'truncation'. Where top truncation has occurred, the sequence consists of repetitions of sandstone and argillite beds, (Ta, Te) or sequences of graded sandstone (Ta) with thin intervening argillite (Te). In each case the basal (Ta) unit comprises sandstone that is often massive and ungraded in its lower part but becomes progressively more graded towards the top. A sharp bedding plane contact usually separates this basal unit from the overlying argillite (Te) unit. The sharpness of this contact between the two lithologies is highlighted by the colour difference between these materials. The same sequence has been observed in slabbed rock samples (Fig. 3.2 and

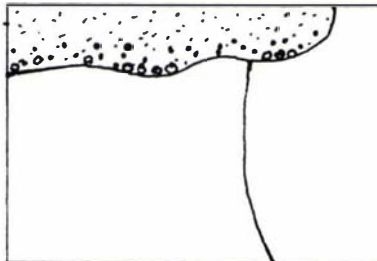
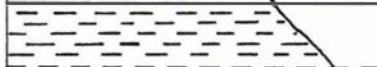
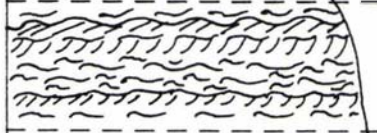

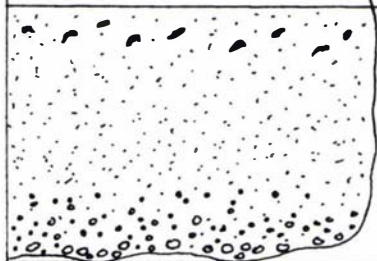
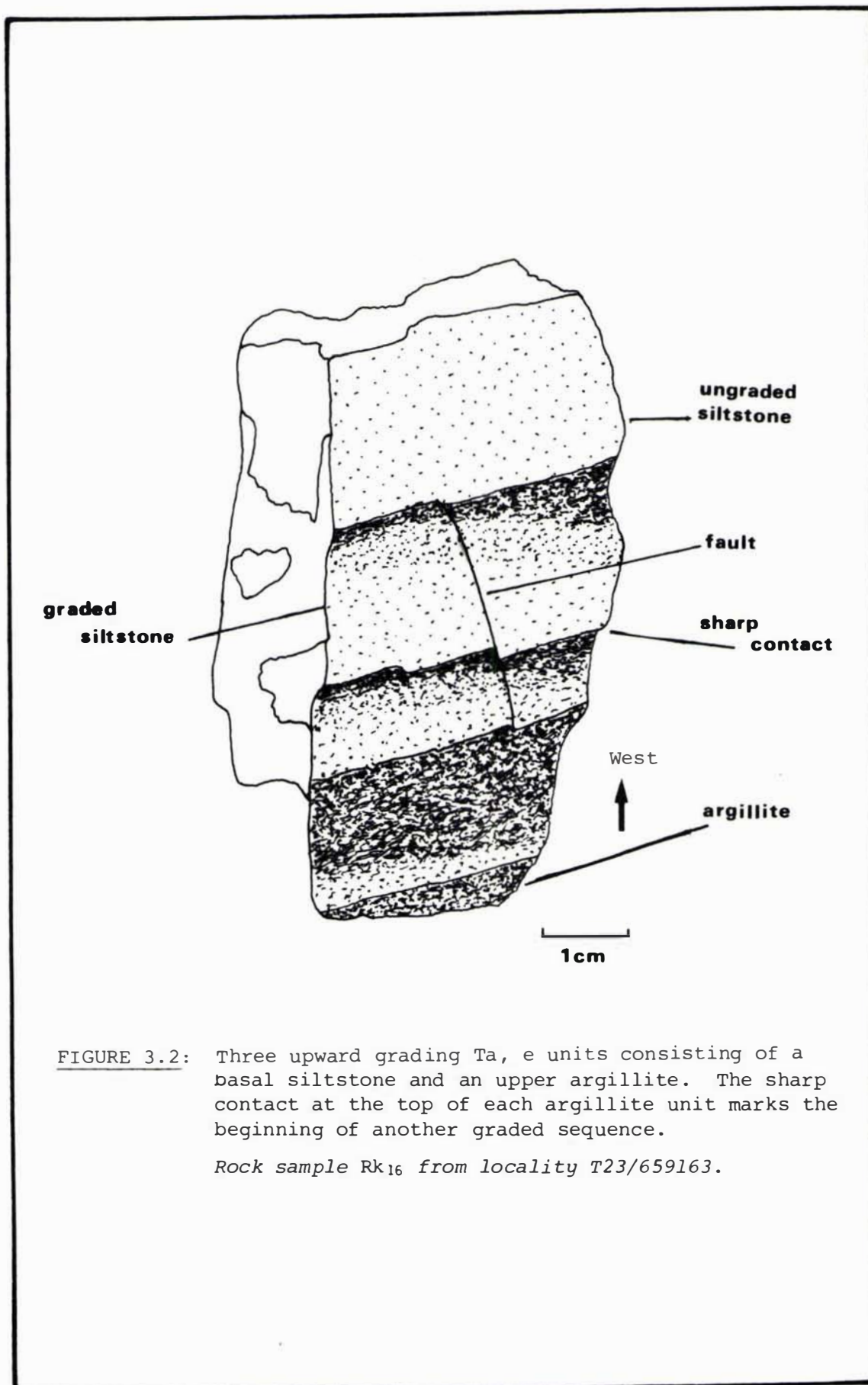
	Grain size	Bouma (1962) divisions	Interpretation
	↑ argillite ↓	Te Pelite	Pelagic settling or fine-grained low density turbidity current deposition
	↑	Td Upper parallel laminae	
	↑ silt ↓	Tc Ripples, wavy or convoluted laminae	Lower part of lower flow regime
		Tb Plane parallel laminae	Upper flow regime plane bed
	↑ sand ↓	Ta Rip-up clasts. Massive, graded. Sole mark.	Upper flow regime. Rapid deposition and quick bed

FIGURE 3.1: Ideal sequence of structures in a turbidite bed (the Bouma sequence), from Bouma (1962) and Blatt et al. (1972).





**FIGURE 3.2:** Three upward grading Ta, e units consisting of a basal siltstone and an upper argillite. The sharp contact at the top of each argillite unit marks the beginning of another graded sequence.

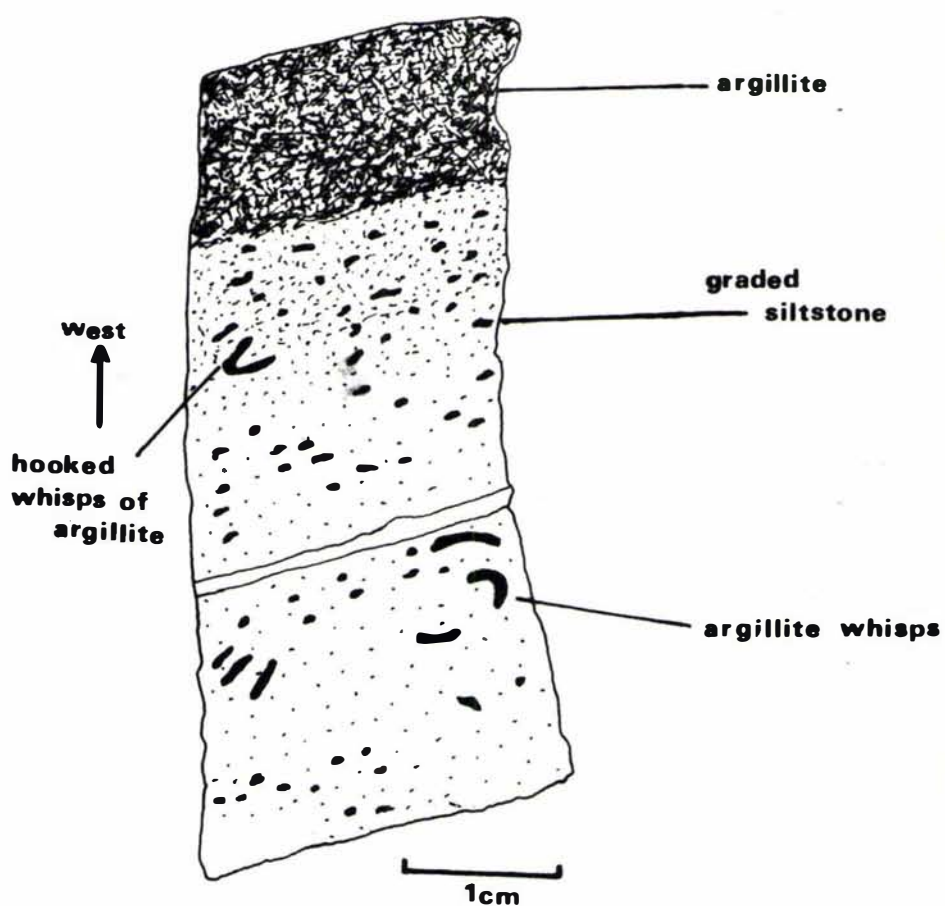
*Rock sample Rk<sub>16</sub> from locality T23/659163.*

3.3) where graded siltstone is overlain and is in sharp contact with argillite. Repetitions of Ta, Te units in the field do not comprise a substantial stratigraphic thickness because this sequence is usually interrupted by an occasional very thick (2-5m) and ungraded sandstone bed every 10m or so. Alternatively, the argillite (Te) unit is reduced in thickness to a very thin, sometimes discontinuous bed or to a mere parting between successive graded sandstone (Ta) units. This suggests that amalgamation of genetically separate units may have occurred through the erosion of interbeds as was proposed by Walker (1966). Such a mechanism could account for sequences of recurrent graded sandstone and siltstone that are essentially devoid of argillite. However, Angelucci *et al.* (1967) consider amalgamation to be an unlikely explanation and prefer "closely subsequent current pulses" as a more likely cause. Another feature of these Ta, Te sequences is the presence of rip-up argillite clasts distributed throughout the Ta unit. In slabbed samples these clasts were seen to be hook-shaped (Fig. 3.3). This is interpreted to indicate that the argillite bed was disrupted while in a soft-sediment condition. Erosion of these argillite interbeds is likely to have occurred during the early stages of turbidity current activity when the current is presumably strongest.

Where bottom truncation has occurred, sequences most commonly consist of Tb-e, Tb-d or Td-e units. This is interpreted by Walker (1965) as late stage deposition after the basal Ta units have been deposited elsewhere. Sedimentary structures characteristic of the Tb-e units are deposited in a low flow régime during the waning stages of turbidity current activity. Micro-grading between parallel laminations characteristic of deposition in the Tb or Td units has been observed in thin section.

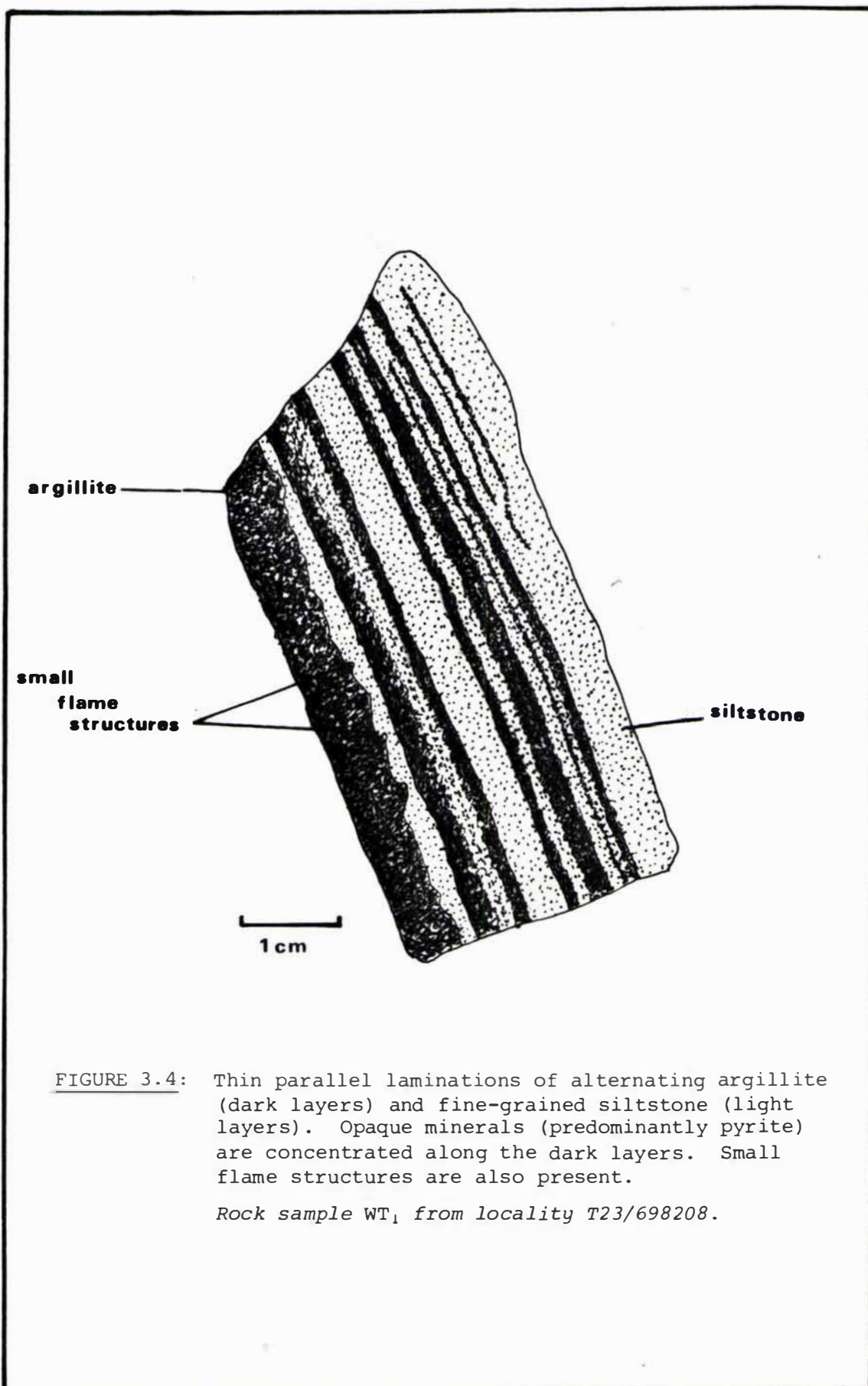
#### B. Lamination

Parallel and ripple lamination in the study area occur in close association with sequences of strata where graded bedding is a prominent feature. Lamination (Fig. 3.4) is best preserved in the very thin-bedded (0.02-0.1m) and thin-bedded (0.1-0.3m) sequences but has also been noted as thin, faint and often discontinuous laminae near bedding plane contacts of thick-bedded (0.3-2m) units of otherwise structureless sandstone. In most cases laminae are 0.5-1 mm thick and have been traced along outcrops for distances of up to 3m. The observed thickness of the interval of lamination ranges from between 0.05-1m. Lamination in graded sequences is in places associated with small-scale current bedding. Most laminations in this area are the result of grain size differences and are highlighted where argillaceous



**FIGURE 3.3:** Slabbed rock sample of *in situ* siltstone containing whisps of argillite. The siltstone grades westward into an overlying bed of argillite. The presence of hook-shaped argillite whisps indicate that the argillaceous material was eroded from an underlying bed while in a soft-sediment condition.

*Rock sample ET<sub>2</sub> from locality U23/709169.*



**FIGURE 3.4:** Thin parallel laminations of alternating argillite (dark layers) and fine-grained siltstone (light layers). Opaque minerals (predominantly pyrite) are concentrated along the dark layers. Small flame structures are also present.

*Rock sample WT<sub>1</sub> from locality T23/698208.*

material is interlaminated with siltstone. Mineral concentration particularly of mica and opaque oxides and/or carbonaceous material sometimes enhances the colour contrast between laminae (Fig. 3.4). In all cases examined, the beds do not part readily along these laminations. The origin of laminations in this area is thought to be due to variations in the rate of supply or deposition of materials with some traction along the water-sediment interface taking place during the latter stages of deposition to produce local sorting.

### C. Convolute Lamination

Convolute lamination was only found in sequences where regularly interbedded units of sandstone, siltstone and argillite of between 0.02-0.1m thickness (very thin-bedded) and 0.1-0.3m thickness (thin-bedded) were graded. Beds of convolute lamination are thus considered to correspond with the Tc interval of the Bouma sequence (Fig. 3.1). Because of poor outcrop exposure beds of convolute lamination could not be traced for more than 3m distance. Nearly all examples of convolute lamination occurred in beds of less than 0.1m thickness. Within these beds the convolutions only involved those laminations within the bed and not the bed itself. Individual laminations are traceable from fold to fold although many folds either die out towards the top and bottom of the bed or are truncated by overlying parallel laminations of the Td unit.

"The classical concept of the origin of convolute lamination in flysch-type beds, as developed by Kuenen (1953) and Ten Haaf (1956) is as follows: firstly, current ripples or other ripple-like corrugations form. In flowing over these ripples the turbidity current induces suction on the crests and pressure in the troughs, forming convolutions by hydroplastic deformation" (Van der Lingen, 1969). Since the original theory of Kuenen and Ten Haaf many other modes of origin of convolute lamination have been proposed. Current drag has been the common explanation of convolute lamination in flysch-type deposits (Ballance, 1964). Loading has been thought to produce certain types of convolute lamination (Dzulynski & Walton, 1965), in that these structures appear to result from preconsolidation deformation or from deformation during deposition of highly mobile or plastic sediments, e.g. formation of subaqueous slumping, gliding or sliding. Various authors have considered that liquefaction and the resulting quick condition play an important part in the formation of convolute lamination (Kingma, 1958b; Williams, 1960). Liquefaction originates in cohesionless sediments when the pore-water pressure increases to a

value at which the shearing strength approaches zero. When the shearing strength equals zero, the sediment behaves like a liquid. Pore-water overpressure can be caused by shock (earthquakes), differential loading or differences in ground-water level within and without the sedimentation basin (Graff-Petersen, 1967). Van der Lingen (1969) considers that liquefaction is the primary cause of most if not all deformation structures within the 'Tc unit' of Bouma (1962), with loading and current drag playing subordinate roles. However, Kuenen (1953) does not accept that liquefaction plays a role in the formation of convolute lamination. He envisages that sediment, deposited as ripples, is in a highly fluid, hydroplastic, quicksand condition from which convolutions develop as a result of extrusion of water through compaction. Observations of convolute lamination in the study area produced no new information on the cause of this structure.

#### D. Flaser Bedding

All the transitions from wavy bedding through flaser bedding to lenticular bedding (Reineck & Wanderlich, 1968) are present in the study area. However, most outcrops tend to be dominated by flaser bedding. Flaser bedding characteristically forms within beds of up to 2m thickness that comprise medium- to fine-grained sandstone and siltstone. These beds display continuous sedimentary deposition throughout their thickness. The flasers are very thin (0.01-0.5m), are laterally discontinuous and are irregularly distributed throughout the flaser bedded unit. Flaser bedding appears to be geographically restricted in occurrence in this area. It has been found within four adjacent tributary catchments of Rokaiwhana Stream at approximately the same stratigraphic level. At localities T23/653146, T23/656150, T23/659154 and T23/661162 flaser bedded units are interbedded with graded sequences of either very thin-bedded (0.02-0.1m) or thin-bedded (0.1-0.3m) strata.

The origin of flaser beds is associated with small-scale current ripples. Current ripples are most readily envisaged as forming in shallow water (Friedman & Sanders, 1978) but they also occur in deep water due to the action of unidirectional ocean bottom currents. Turbidity currents also produce ripples. During deceleration of such a current, sand, silt and clay falling from suspension may be reworked on the bed into ripples (Collinson & Thompson, 1982). The associated formation of wavy, flaser or lenticular beds with ripples is dependent upon the amount and rate of supply and deposition of the sediment.

### E. Flame Structure

Flame structure (Walton, 1956) is poorly preserved in outcrop in this area. Where observed they occur in accompaniment of load casts. Flame structure observed in slabbed samples appears to be the result of current drag across laminae of argillaceous composition (Fig. 3.4). Flame structure resulting from load deformation was observed to occur at the base of graded sandstone (Ta) units whilst flame structure as a result of current drag occurred in either Tb or Td laminated units of fine-grained siltstone and argillite composition. Evidence for flame structure resulting from horizontal slip or drag (Gary *et al.*, 1977) or water expulsion (Dott & Howard, 1962) was not found in this area.

### F. Cross-Lamination

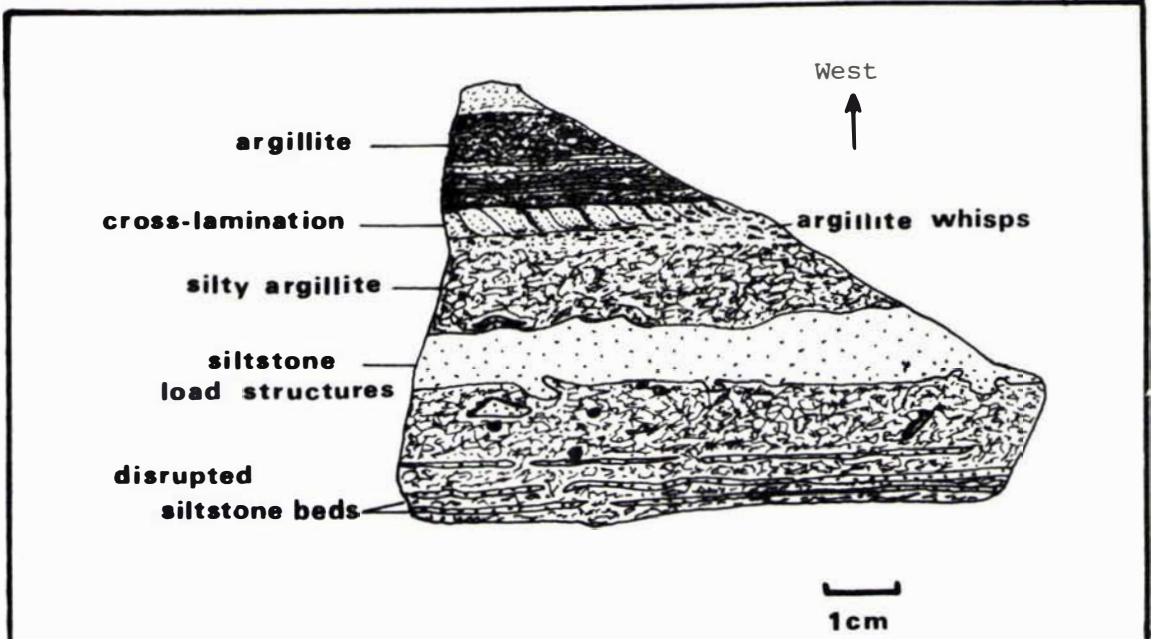
This is defined as small-scale cross-stratification characterised by fore-set beds, less than 0.01m in thickness that are inclined to the general bedding (McKee & Weir, 1953). They are mostly a result of deposition from migrating small-current and wave ripples (Reineck & Singh, 1975). Cross-laminations occur most commonly in fine-grained sandstone and siltstone beds where bed thickness varies from between very thin (0.02-0.1m) to thin (0.1-0.3m). Truncated cross-laminations were used to indicate superposition (Fig. 3.5).

### G. Disrupted Bedding

Three forms of disrupted bedding have been recorded in this area. The first involves disruption of a thin bed of siltstone by the injection of argillaceous material into the bed of siltstone (Fig. 3.6). This may have been the result of loading due to rapid emplacement of the siltstone, thereby causing the underlying clay to liquefy and inject the overlying siltstone. An external shock such as an earthquake may also cause this.

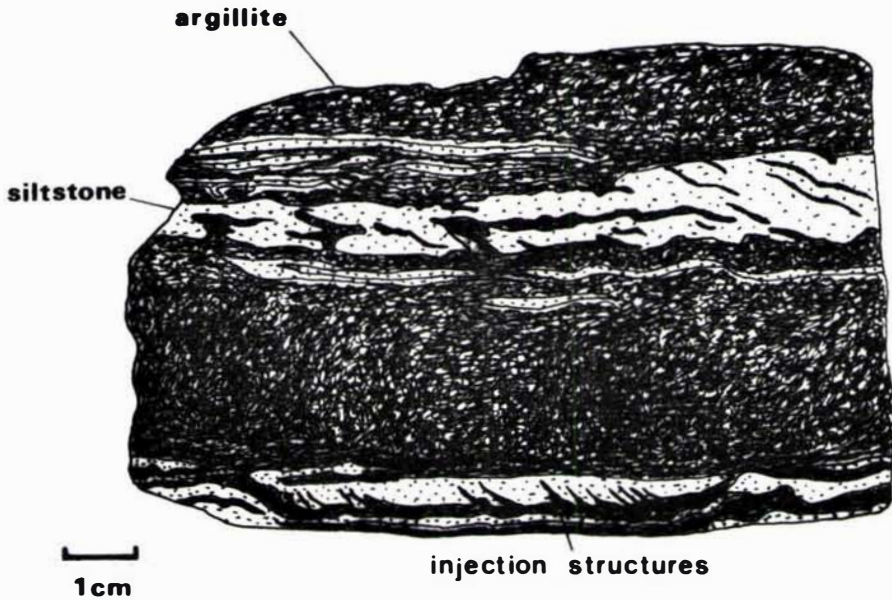
The second involves the extensional pulling-apart of very thin beds of competent material accompanied by flowage of liquefied argillite (Fig. 3.5). Disruption in this case may be the result of loading through compaction of interbedded materials of different competency. Both types of disrupted bedding are considered to represent syndepositional deformation, the bedded materials being in an unconsolidated condition. Syndepositional deformation is indicated by the presence of rounded and often hook-shaped terminations of disrupted beds (Fig. 3.5).

The third type of disrupted bedding involves the disaggregation of a thin



**FIGURE 3.5:** A variety of internal sedimentary structures including disrupted beds, load structure, argillite whisps and truncated cross-lamination.

*Drawn from slabbed sample.*



**FIGURE 3.6:** Disrupted siltstone horizons interbedded within an argillaceous medium. The lenses of argillaceous material within the siltstone horizons are possibly injection structures as a result of syndepositional deformation.

*Drawn from slabbed sample.*



bed of argillite into numerous angular clasts that remain concentrated along a well defined horizon within a thick sequence of sandstone. The angularity of the clasts indicates that disruption of the argillite bed was post-depositional. Post-depositional loading by compaction in the sandstone and consequent upwards ejection of water may have caused *in situ* disruption of overlying argillite beds in these instances. Alternatively, fluidisation of the surrounding sandstone could also result in disruption of the bedded argillite. These clasts are distinctly different to those referred to earlier as rip-up clasts for which syn-depositional erosion of soft sediment by turbidity currents was proposed. Rip-up clasts are, in general, scattered throughout a thin bed comprising silt-sized material that forms part of the Bouma (1962) Ta-e sequence of intervals as a result of turbidity current deposition. In contrast, clasts of argillite indicative of post-depositional disruption of an argillite bed are usually concentrated along a well defined horizon within a thick bed of sand-sized material. There are no internal sedimentary structures visible in these beds although rare grading may sometimes be visible. Such beds are here considered to be of either grain flow (Stauffer, 1967) or fluidised sediment flow (Middleton, 1970) origin (see Depositional Processes).

### 3.0.3 EXTERNAL STRUCTURES

Structures that form on bedding plane surfaces are of two types. Sole markings (Kuenen, 1957) occur on the basal surface of beds of sandstone interbedded with argillite and surface markings (Van der Lingen, 1969) are found on the top surface of sandstone beds.

#### A. Sole Markings

##### 1. Load Casts

Small-scale load casts were seen in slabbed rock samples (Fig. 3.5). In the field, load casts reached dimensions of 0.15m diameter and 0.05m depth as seen in cross-section. Load casts were rarely seen on bedding plane surfaces because steeply dipping strata in this area afford little opportunity for large areas of these surfaces to be exposed. Load casts were found in association with thick-bedded (0.3-2m) stratal sequences.

The mechanism of formation is gravity acting on beds which were unstable due to their high porosity and lack of compaction and coherence and to differences in density between the beds. Load structures in this area appear to have been initiated by unequal loading related to the sedimentation process. That is, when a thick sand layer is rapidly deposited on

a layer of clay, it will be denser than the clay and if both sediments are weak it will tend to sink into the clay by loading (Collinson & Thompson, 1982).

## 2. Longitudinal Ridges and Furrows

These have been found at one locality only (U23/733184). Their preservation on the basal surface of a thick bed of sandstone indicates that the sequence at this locality is eastward younging. The ridges and furrows are spaced at 0.05-0.1m intervals and are between 0.01-0.03m deep (high).

The asymmetrical shape of these ridges and furrows, their even spacing, constant north-south orientation of straight and continuous crest lines and their parallelism along 2-3m of outcrop length is suggestive of surface wave activity or of a current origin. Conclusive evidence of their genesis and paleocurrent direction is absent. An east-west paleocurrent orientation at right angles to the longitudinal ridges and furrows is inferred.

### B. Surface Markings

#### 1. Small-scale Ripples

Examples of small-scale ripples were not found *in situ* and have therefore not been used to determine paleocurrent flow direction. In profile these ripples are strongly asymmetrical. In plan they have short curved crests and closely resemble photographs in Friedman & Sanders (1978, p 551) of small-scale ripples that have been described as linguoid (Allen, 1966, p157).

The ripples are found in rows that form across the line of flow, the ripples in each row being offset in relation to those in front. Such small-scale asymmetrical ripples may form under turbulent or laminar flow conditions but their formation is restricted to constant current flow (Allen, 1966, p 184). The lowest velocity capable of producing small-scale ripples in fine sand is about 20 cm/sec (Reineck & Singh, 1975).

#### 3.0.4 TRACE FOSSILS

A series of worm burrows were found *in situ* at T23/665173 within a silty argillaceous sequence of the Very Thin-Bedded Association in the Tamaki Lithotype. Burrows at right angles to bedding are circular in cross-section whilst burrows parallel or inclined to bedding are elliptical in cross-section. Burrows vary in diameter from 0.01-0.05m. These trace fossils are of no paleoenvironmental significance.

### 3.0.5. TRANSPORTATION AND DEPOSITIONAL PROCESSES

Subaqueous sediment transport and deposition is currently considered to be the result of either sediment gravity flows or ocean bottom currents.

#### A. Sediment Gravity Flows

Four types of sediment gravity flow have been proposed by Middleton & Hampton (1973) but only one type (turbidity currents) has previously been demonstrated to be an effective mechanism for moving coarse sediment into deep water. The four individual sediment gravity flow types are distinguished on the basis of how grains are supported above the bed: (1) turbidity currents, in which the sediment is supported mainly by the upward component of fluid turbulence; (2) grain flows, in which the sediment is supported by direct grain-to-grain interactions; (3) fluidised sediment flows, in which the sediment is supported by the upward flow of fluid escaping from between the grains as the grains are settled out by gravity; and (4) debris flows, in which the larger grains are supported by a 'matrix', that is, by a mixture of interstitial fluid and fine sediment. It is probably realistic to accept that in most real sediment gravity flows, more than one form of grain support will be important. Furthermore, other mechanisms such as traction (by dragging or rolling of particles on the bottom) or saltation (by hydraulic lift forces and drag) may operate during the last stages of deposition and produce or modify some of the textures and structures observed in the sediment bed that is finally deposited from the flow.

The merits of each sediment gravity flow mechanism is here assessed in view of the preserved sedimentological evidence in the study area.

#### 1. Turbidity Current

The most common depositional process generally attributed for considerable thicknesses of alternating sandstone, siltstone and argillite, is high density turbidity currents (Bouma, 1962; Kuenen, 1964). In the oceans, most turbidity currents appear to be surges that are initiated by some event (generally catastrophic in nature) and move downslope away from their source. Three common and well documented mechanisms that can result in the emplacement of sediment in suspension to create a turbidity current include: (1) a river in flood; (2) storm waves generated during a hurricane acting on continental shelf deposits; and

(3) subaqueous slope failure. Turbidity currents may be divided into three main parts: the head, the body and the tail (Middleton & Hampton, 1973). From flume experiments it has been determined that as a turbidity current moves downslope erosion occurs at the head, whilst deposition takes place from the body or tail of the same current. Rapid deposition from suspension may be expected in proximal regions due to waning turbulence in the source area, rapid flattening of the slope, or by the spreading out of the current as it moves onto the basin floor. In most cases there should be rapid sedimentation with little traction because sediment is buried almost as soon as it is deposited. The lower part of a turbidite bed should therefore be massive or show only poorly developed faint lamination and poor scour marks. In more distal regions, there may be a relatively extended period of scouring by the head of the flow, followed by relatively slow deposition from the body and tail of the flow. Under these circumstances one expects the sole of the bed to have well developed scour marks, (e.g. flutes) and the bed itself to display traction structures such as lamination and cross-lamination. If deposition is slow enough, more extended traction takes place with the formation of typical "upper flow régime" plane lamination or ripple cross-lamination. Generally, the Bouma sequence (Fig. 3.1) indicates both a decreasing flow intensity (or flow regime) and a decreasing rate of deposition from suspension and increasing importance of traction as one goes from the bottom to the top of the bed (Middleton & Hampton, 1973). Obviously, if within the current, great eddies or secondary flow systems are present, this simple picture of gradual decrease in speed may shift back and forth within a wide range. However, despite such variations, the inevitable overall progression is from fast to slow (Friedman & Sanders, 1978). Some of the last materials to settle from suspension are fine-grained silts and clays. Considerable thicknesses of clay may accumulate, the differences in bed thickness simply represent varying time periods between successive inputs of arenaceous material. Such a process, without interruption, explains the presence of rare massive argillite beds. However, most argillite units contain very thin laminations and interbeds of fine-grained siltstone that can either be explained as a result of differences in the settling rate of silt and clay particles from suspension or the sorting of the uppermost argillite unit by traction currents to remove the clay fraction and thus leave the remaining siltstone fraction as a concentrate. The discontinuous and thin nature of these interbeds

and laminations may favour the latter process. In view of the high silt content of most of the argillites it seems likely that very little of the argillaceous material is of truly pelagic origin.

The deposits resulting from deposition by turbidity currents consist of alternating sequences of sandstone, siltstone and argillite of varying thickness and regularity. Whilst it is realised that not all such alternating sequences are necessarily of turbidity current origin it is clear from field evidence that many of the features such as rhythmically layered, alternating thin beds of sandstone, siltstone and argillite; sandstone beds with sharp bases grading upward into argillite; the sequence of intervals: massive, plane laminated, cross-laminated or convoluted, and again plane laminated; and sole markings are diagnostic features of an idealised turbidite sequence (Bouma, 1962) best explained at present by the turbidity current model. These features are characteristic of each of the Associations comprising Graded-Bedded Lithozones within the Tamaki (Table 2.1), Western (Table 2.4) and Wharite (Table 2.2) Lithotypes. However, in order to explain other internal sedimentary features found in sequences of Very Thick-Bedded Association within the Tamaki Lithotype and in massive units of sandstone comprising Sandstone Lithozones within Wharite Lithotype, a secondary process referred to as grain flow (Middleton & Hampton, 1973; Feary, 1979) acting in association with turbidity currents has been suggested.

## 2. Grain Flow

Deposition from grain flows is fundamentally by mass emplacement and the resultant deposits have been described as massive and ungraded but with diffuse parallel lamination and dish structure (Wentworth, 1967) in some beds. Grain flow beds are generally thick and sharply bounded. Soles of the beds are either flat and featureless or they have one or more load deformed marks. Stauffer (1967) suggested that grain flows are further characterised by the absence of traction current or turbidity current features, such as erosional sole markings (e.g. flute casts), convolute lamination, cross-lamination, ripple marks and current scours.

Positive identification of grain flow deposits is still problematical, for large-scale grain flows described by Stauffer (1967) have been reinterpreted by others as normal proximal turbidites. Furthermore, all features proposed to be characteristic of grain flows probably can

be produced by other transport processes. Many of the very thick-bedded and massive sandstone units in the study area contain features described as being characteristic of grain flow origin, but it is unlikely that any of these beds could be reinterpreted as 'proximal turbidites' in view of their intimate association with an essentially 'distal turbidite' facies. It therefore seems likely that grain flows may be a companion to some turbidity currents (Sanders, 1965). Sanders envisaged sediment gravity flows to consist of two parts: an upper turbidity current with grains supported by turbulence, and a lower, faster moving grain flow with grains supported by dispersive pressure. However these grain flows maintain dispersive pressure, the evidence from the sediments indicates that they can travel faster than an accompanying turbidity current. When the two move together, the grain flow acts as a frictionless basal carpet for the turbidity current. Within the fast-travelling basal flow, the coarsest particles move to the front. After they have come to rest, the finer particles catch up and may out-distance them. Proof that this differential movement has occurred is shown by horizontal as well as vertical grading, and by the deposition in any small depression on the ocean floor of coarser sediments than is found elsewhere nearby. Where both a grain flow and a turbidity current travelled together and both deposited their loads in close succession, the material dropped by the grain flow underlies the turbidite (Friedman & Sanders, 1978). A variation on the same theme postulates that as grain flow processes have very limited ability to transport coarse sediment for significant distances over moderate slopes (Lowe, 1976) it seems unlikely that such a process could transport fine-grained conglomerate as a grain flow. The logical conclusion, therefore, is to assume that either turbidity currents or debris flows transport conglomerate pebbles together with finer grained detritus to the site of deposition where a final stage of grain flow took place during deposition. These processes account for the occurrence of fine- to medium-grained sandstone with fine-grained conglomerates as basal members of turbidite beds.

With such high-energy conditions it is conceivable that flows may become turbulent so that a continuum may exist between grain flows and turbidity currents. Thus some flows may be combinations of the two types to give rise to successions of strata that are in part turbidite-like and in part grain flow-like. Such an interaction between these two processes may explain the frequent occurrence of an abnormally thick bed of ungraded sandstone within an otherwise graded thin-bedded

sequence that contains most features characteristic of turbidite-deposition.

### 3. Fluidised Sediment Flow

Sands subject to liquefaction are those that are loosely packed or that have textural properties that are favourable to breakdown of the fabric. Once the fabric is destroyed, the grains no longer form a rigid framework to the deposit, but must be supported at least in part by the pore fluids. So long as grains are supported by the pore fluid, the sand has little strength and behaves like a fluid. Thus liquefied or fluidised sand can flow rapidly down relatively gentle slopes of 3-10° (Middleton, 1970). The main problem with fluidisation as a mechanism of sediment transport is that the excess pore pressures are rapidly dissipated by loss of pore fluids. The real significance of fluidisation, however, is its combined occurrence with other support mechanisms. Grain flows in particular can be expected to be aided by fluidisation effects, because during flow the grains, by necessity, are in a relatively dispersed state, but deposition involves consolidation with consequent upward expulsion of pore water. The upward fluid drag is a fluidisation effect, helping to support grains, and thereby prolonging the life of a flow. The "fluidisation effect" may even be felt after flow ceases, if deposition is rapid enough to trap excess pore water which is eventually expelled by consolidation. Upward drag may not be strong enough to fluidise the bed completely in these instances, but it might mobilise enough grains to affect textures and structures significantly. In particular such a process is thought to be the primary cause of convolute lamination (Kuenen, 1953; Kingma, 1958b) and a major factor in the disruption of some argillite beds.

Argillite horizons have in places been disrupted by the intrusion of clastic material as is demonstrated by the presence of angular clasts of argillite, within a clastic matrix. In some of the thicker sandstone horizons such disrupted argillites can still be recognised as distinctive layers. Finlow-Bates (1970) has suggested that some of the thick sandstone units within which concentrations of argillite clasts occur at distinct levels may have originated as sequences of alternating sandstone and argillite and that movement of the sand by fluidisation has disrupted the argillites to such an extent that the clastic material of the sandstone beds has merged completely to form

an apparently continuous sedimentary unit. In view of the coherent nature of the angular argillite clasts, it is thought that disruption by fluidisation occurred some time after deposition of the sand. Water expulsion from the sand may have been caused either by sediment compaction or occurred as a result of earthquake vibration. 'Dish structure' as named by Wentworth (1967) and described by Stauffer (1967), may possibly result from consolidation of a fluidised bed (Middleton & Hampton, 1976). Dish structure consists of a series of concave-upward laminations found most typically in massive to faintly laminated, fine- to medium-grained sandstone beds. The dishes are typically about 0.04-0.05m wide and 0.001-0.002m deep. They are typically flatter near the bottom and grade upward into tightly curved dishes. Although *in situ* examples of these structures are not widespread in the study area they were observed rarely within massive sandstone units of the Tamaki Lithotype and more abundantly within massive sandstone units of the Wharite Lithotype. Also observed within these units of sandstone were sandstone sills, dykes and injection phenomena of probable fluidisation origin.

#### 4. Debris Flow

Subaqueous debris flows have recently received consideration as a major transporter of ocean sediments (Hampton, 1970; Fisher, 1971). Hampton in particular has emphasised the possible importance of debris flow activity in the ocean. Debris flows account for the presence of rather uncommon muddy, coarse-grained marine conglomerates such as pebbly mudstones (Crowell, 1957; Peterson, 1965). Although several origins for pebbly mudstones are possible, particular attention is here paid to slumping in association with turbidity-current deposition as the most likely mechanism to account for the association of pebbly mudstones with turbidite sequences in the study area.

No slump or flow will take place unless certain conditions prevail, and the character of the slump or flow will depend largely on the relative interplay of these conditions. The process pictured here is dependent upon: (1) the existence of turbidity currents that bring gravel to the site of deposition; (2) the presence of an underlayer of soft clay; and (3) sufficient bottom inclination so that with instability the mixture of clay and pebbles moves downslope. Debris flows can move at relatively low speeds down slopes with a gradient as low as 1 in 100 (Middleton & Hampton, 1973). It is envisaged that



within a basin turbulent density currents may from time to time deposit gravel. If the gravel is deposited upon a sandy and already somewhat indurated bed it will form a stable layer.

Localized grain flow processes may take place during this phase of deposition to produce conglomerates. If, however, gravel were deposited on a soft, water-saturated clay surface, and the layer of gravel attained a bulk density greater than that of the underlying clay, instability would result in the formation of gravel lobes which are seen at places as load casts (Crowell, 1957). If the contrast in bulk densities were great, the bottom slope were sufficiently steep and the underlying clay layer were thick enough, instability could result in the movement of clay and gravel downslope together. As the mass gathered speed it would churn, mix and disperse pebbles throughout the clay. If relatively fluid, such a flow would deposit a thin, uniform layer of fine-grained pebbles set within a black argillaceous matrix. This deposit would comprise a pebbly mudstone and may form part of a thick sequence of alternating sandstone and argillite of turbidity current origin. On the other hand, if the mixed mass were viscous, it would move relatively slowly and probably plough into the substratum to produce obvious slump overfold structures. No structures of this nature have been found in the study area.

The thin and sparse development of pebbly mudstones within sequences of Very Thin-Bedded and Thin-Bedded Associations of the Tamaki Lithotype is consistent with the idea that they comprise part of a distal facies that was essentially deposited by turbidity current, having originated by slumping and sliding, in the source area, possibly as a result of tectonic activity, earthquakes or spontaneous liquefaction of thick piles of unconsolidated sediment (Hampton, 1972). Slumping may also result from increased rates of deposition during flood periods on unstable slopes (Stanley, 1969). The absence of slump structures and thicker pebbly mudstone horizons with larger clast sizes is also consistent with such an interpretation. Presumably these pebbly mudstones would be associated with sediments deposited closer to the origin of slumping and would therefore comprise sequences that may be likened to a proximal turbidite facies.

Diamictite Lithozones (see Chapter 2) within the Wharite Lithotype are considered to be the result of debris flow activity. These deposits contain subrounded clasts of widely varying sizes and lithologies

that are randomly distributed throughout an argillaceous matrix. The absence of internal slump structure or sorting suggest that the debris flows were relatively fluid. Similarly the absence of slump structures in adjacent strata suggest that emplacement was rapid.

It has been demonstrated that sandy debris flows should be common in the ocean and that sandy submarine debris flow deposits can be low in clay content similar to sands emplaced by other gravity sediment flow processes (Hampton, 1970). Such a process may explain the great thickness of some of the massive sandstone units (Sandstone Lithozones) within Wharite Lithotype, that are many times thicker than other sandstone units considered to have been deposited by turbidity currents and associated depositional gravity flow processes.

#### B. Ocean Bottom Currents

At the time the turbidity current hypothesis was initially formulated, bottom currents in deep ocean environments were not known to exist. However, bottom currents are now an attractive alternative explanation for problematic flysch-type deposits since their existence has not only been demonstrated by direct measurement but also by analysis of photographs of the sea floor. Oceanographic research has revealed the existence of strong bottom currents in the oceans (Hollister & Heezen, 1966). Current features such as ripples, current lineations, and scour marks have been photographed at depths greater than 5000m. Current velocities up to 40 cm/sec have been measured (Hollister & Heezen, 1966). These velocities are considered to be high enough to transport all grain sizes found in deep-sea sediments. These currents can receive their sediment load from alluvial flood debris and from material transported from submarine canyons by creep and slump.

Arguments concerning a turbidity-current versus bottom-current origin for ancient "turbidites" largely stem from the comparison between ancient flysch-type deposits widely interpreted as being the result of turbidity current deposition with recent deep-sea sediments which are believed to be turbidites. Criticism is twofold: first, that deep-sea sediments are not turbidites; and second, that ancient flysch-type deposits do not resemble Recent deep-sea sediments.

Evidence against a turbidite origin for Recent deep-sea sediments has been marshalled by Van der Lingen (1969). He points out that the

deep-sea sand and silt bodies are generally lenticular and discontinuous; the percentage of matrix varies greatly and clean, well-sorted sands may occur; a single type of sedimentary structure commonly occurs throughout a whole bed; grading is far less common than in ancient flysch-type sediments and typical "turbidite facies model" sequences are rare. All of these features may indicate bottom traction current activity. The overall appearance of these Recent sediments would tend to indicate that they are not as similar to ancient flysch-type deposits as some authors have suggested.

Evidence against a turbidite origin for ancient flysch-type rocks is that they often show features that one would not expect to find in a turbidite deposit, notably that they were laid down by currents which were not slope-controlled as one would expect to find in gravity-controlled turbidites. Scott (1966) found gravity-controlled slumps which had moved at right angles to paleocurrent direction. In this context it is interesting to note that Recent ocean bottom currents are not always slope controlled and often show a tendency to flow parallel to bathymetric contours (Klein, 1967). As an attractive compromise, it seems possible that some of the material deposited by ocean bottom currents comes from an upslope source, the sediment being displaced downslope by gravity and then coming under the bottom currents' influence. The continuity and direction of their flow would depend largely on the sea-floor morphology and the hydrographic setting of the environment of deposition.

There are, however, certain features of ancient flysch-type deposits which make an ocean bottom current origin less likely. Difficult to explain by bottom current deposition is the common uniform thickness and great lateral extent of flysch-type beds. With local exceptions, these beds have a constant thickness. Although it is seldom possible to trace beds from one outcrop to another in this area, predominantly because of lack of marker beds, in some areas overseas beds have been traced over distances of up to 100 km (Kuenen, 1967).

### C. Discussion

In conclusion, the considerable thickness of alternating very thin-, thin- and thick-bedded, graded units of sandstone, siltstone and argillite is considered to have been transported and deposited principally by turbidity currents. Variations in bedding thicknesses probably represent varying sized flow and time periods between

successive inputs of detritus. The sedimentary characteristics of the thick to massive ungraded or very poorly graded, moderately well sorted sandstone beds are considered to be consistent with deposition by non-turbulent grain flow processes that predominated during the final stages of deposition. However, transportation of this material to the site of deposition was probably achieved by turbidity current processes.

The beds and lenses of fine-grained conglomerate, most commonly found at the base of thick and massive medium-grained sandstone units, were almost certainly transported and deposited by the same mechanisms. In view of the poor capability of grain-flow processes to transport sediment any great distance, transportation of the coarser materials to the site of deposition may also have been by turbidity currents and/or sandy debris flows. At the site of deposition, grain-flow and traction processes probably operated during the final phase of deposition.

The thin poorly developed horizons of pebbly mudstone are thought to have originated as debris flows that developed into turbidity currents which were capable of transporting fine pebbles. These pebbles were then deposited upon an argillaceous bed into which they were incorporated at the site of deposition. Pebbly mudstones are unlikely to have been emplaced by debris flow activity because of their thin development, lack of erosive contacts at their bases and the absence of pebbles of larger size.

In view of the predominance of: (1) very thin-, thin- and thick-bedded regularly alternating sequences of graded beds with preserved internal sedimentary structures; (2) the poor development of very-thick and thick-bedded massive sequences of sandstone; (3) the poor development of thin beds of fine-grained conglomerate and total absence of coarse-grained conglomerates; and (4) the scarcity of thinly developed fine-grained pebbly mudstones and total absence of coarse-grained pebbly mudstone deposits, it is interpreted that the flysch-type sequences (Graded Bedded Lithozones) comprising each of the three Lithotypes in this area are distal facies deposits essentially emplaced by turbidity currents and modified by other sediment gravity flow processes. The absence of bioclastic limestone, the paucity of primary calcareous matrix, the sparseness of fossils and the textural immaturity of the arenites are also consistent with such a process. The willingness of most geologists to accept these, when found together, as convincing

evidence for turbidity current deposition is based on voluminous accumulated data from ancient deposits, modern environments and laboratory experiments (e.g. Walker, 1973).

Turbidity current deposition was periodically interrupted during the deposition of massive units of ungraded sandstone (Sandstone Lithozone) by grain flow or sandy debris flow activity and deposition of unsorted, argillite-dominated, debris flow deposits (Diamictite Lithozones).

### 3.1 PALEOENVIRONMENTAL ANALYSIS

The Torlesse has for a long time been considered by many authors to be the deep-water geosynclinal facies of the New Zealand Geosyncline. It is widely accepted that most of the sediments, regardless of their processes of deposition, accumulated in an environment generally unfavourable for bottom dwelling organisms and so usually contain few traces of life. Only rare incursions of shelf faunas are found amongst the sparse fossil assemblages that are preserved (Stevens & Speden, 1978). The textures of the sediments, the presence of primary sedimentary structures and the preservation of an occasional fossil indicate deposition may have occurred in a wide range of paleoenvironments from terrestrial to bathyal. Paleoenvironmental analysis is essentially concerned with determining: (1) the depth of deposition; and (2) proximity of the depositional environment to a source area. This discussion examines several lines of evidence available from: (1) internal and external sedimentary structures; to (2) composition of the sediments; and (3) fossil evidence that collectively may provide indications of the depth of deposition. Other lines of evidence such as: (4) textural and compositional features of detrital grains; and (5) bedding characteristics, stratigraphic thickness and lateral extent of the lithotypes help establish distance from source area.

#### 3.1.1 DEPTH OF DEPOSITION

Flysch-type deposits are generally regarded as deep-water sediments (bathyal and abyssal) by those authors accepting the turbidity current hypothesis (Kuenen, 1964; De Raaf, 1964). However, not all flysch-type sequences are of deep-water origin (Mangin, 1962). Unfortunately, very few objective depth indicators occur in flysch-type deposits within the study area. This discussion is thus limited to a small number of criteria that may help define environmental elements of the deposition area.

The sedimentary structures described from the study area are of little use

in determining depth of depositional environment because they form under many conditions and under water of almost any depth whenever a current moves across a sand surface. In deep water environments their formation is thought to be related to the presence of strong ocean bottom currents. Whether these currents were produced by downslope mass movement (debris flows, grain flows) or turbidity currents remains difficult to determine. The presence of these sedimentary structures within a turbidite sequence is not considered to be sufficient evidence to assume a turbidity current origin because they are also known to occur in non-turbidite strata (Pryor & Barr, 1968). Nor is such an association indicative of deep-water deposition because turbidites are simply a facies that may occur at the foot of a continental slope, within the basins of a continental borderland, in a prodelta environment, or even on some types of flood plain (Andrews *et al.*, 1974). With the use of other lines of evidence such as the absence of wave ripples, beach lithologies, bioherms, large-scale cross-bedding, channel features and thick deposits of well sorted sand it can be established that deposition occurred at depths below wave base.

Black argillites have been considered to accumulate in deep-water environments and are of pelagic origin (Stanley, 1969). However, the presence of a substantial siltstone content within argillaceous interbeds in the study area suggests that the argillites were derived and deposited under similar conditions to the siltstones. The poor sorting, the angularity of clastic grains, the abundance of unstable constituents and association with sandstone interbeds implies deposition of silt and clay together. Such a process is adequately explained by settling from suspension as outlined by the turbidity current model. It cannot be demonstrated that the argillaceous materials are pelagic in origin or that they accumulated in the hadal or lower abyssal zones.

The preservation of carbonaceous material and authigenic or biogenic development of pyrite cubes within argillaceous interbeds and massive argillite units could be interpreted as indicative of organic reducing conditions. Reduction may, however, take place in either shallow or deep-water and paleoenvironmental interpretations based on the presence of pyrite is therefore inconclusive. Also, much of the pyrite present in this area is likely to be of diagenetic origin.

The presence of chert in common association with coarse clastic deposits considered to be of shallow water origin has been used as an argument to

claim that some cherts may be shallow-water sediments (Davis, 1918; Taliaferro, 1943). However, the realisation of the role of turbidity currents in bringing coarse terrigenous material far out onto the ocean floor led to a reassessment of this hypothesis. The presence of intercalations of radiolarian chert within turbidite-like successions is considered to be one of the clearest lines of evidence for deep-water deposition (Reed, 1957b). It is thought that much of the radiolarian ooze on the present ocean bottom is not the result of settling from a planktonic biota composed solely of siliceous organisms but rather due to planktonic communities that include both calcareous (*e.g. Globigerina*) and siliceous forms. When the resulting sea-floor sediment is predominantly siliceous it is because most calcareous tests have been destroyed by solution at depth (Riedel, 1959). Radiolarian ooze forms only at depths sufficient for calcareous tests to be dissolved, that is, below the calcite compensation depth, thus leaving radiolarians to accumulate (Fagan, 1962). This depth is largely controlled by temperature and in the Pacific region is thought to range from 4200-4500m (Kennett, 1982).

Rhythmically bedded chert and clastics have been found within flysch-type strata at only one locality (T24/492944). Here, a 20m thick unit of chert occurs within regularly bedded clastic lithologies that are locally siliceous and comprise part of the Tamaki Lithotype. Calcareous siltstone lenses also comprise this flysch-type sequence so the presence of carbonate in close proximity to chert requires explanation. This may be due to: (1) the chert and interbedded clastics being deposited at depths greater than the calcite compensation level, the carbonate thus being of diagenetic origin; or (2) the calcareous siltstone lenses are of primary origin. This second alternative would mean much of the strata comprising the Tamaki Lithotype was deposited at depths less than the calcite compensation level and that in all probability the chert has been tectonically interleaved into the Tamaki Lithotype. The chert is very sheared and the adjacent clastic strata show strong signs of tectonic deformation atypical of that seen elsewhere within the Tamaki Lithotype. This sequence also lies along the strike of a Late Quaternary fault breccia zone. It is thus interpreted that at this locality the chert has been infaulted into the otherwise coherent-bedded Tamaki Lithotype. This view is consistent with the non-siliceous nature of the Tamaki Lithotype elsewhere in the study area. The calcareous siltstone lenses are therefore of primary origin and the sequence was probably deposited at depths of less than the calcite compensation level.

Unidentified trace fossils are present at only one location (see Sedimentary Structures). The enigmatic scarcity of a fauna and bioturbation may be taken as evidence of a high rate of deposition (at almost any depth) or deposition at very great depths where animal life is absent. Unless more reliable depth indicators can be found, no depth conclusions can be based on fossil evidence.

### 3.1.2 PROXIMITY OF SOURCE TO DEPOSITIONAL ENVIRONMENT

The composition and texture of clastic lithologies indicate that much of the sand and silt fraction has been derived from a mixed volcanic-plutonic terrane (see Chapter 5). The grains have suffered little chemical alteration or physical abrasion. The angular shape and fresh appearance of the grains probably indicate rapid or short transportation from source area and poor sorting implies rapid deposition. Conversely, the roundness of pebbles within pebbly mudstones and intraformational conglomerates indicate substantial pebble abrasion prior to transportation to the area of deposition. As mentioned previously, the turbidity current hypothesis in association with other sediment gravity flow mechanisms best explains how these materials may be transported and deposited together.

To preserve a thick flysch-type sequence, the most likely environment is one that is consistently deep and quiet (Walker, 1976). The sediments accumulated to a substantial thickness within part of a depositional structure of geosynclinal dimensions.

According to the general hypothesis of turbidity current formation, turbidites should be spread over huge distances on the basin floor. In this case, it should be possible to trace individual stratum over great distances. Outcrops in the study area are in most cases cross-sectional views of near-vertical dipping strata exposed within narrow stream channels. Lateral continuity of individual stratum has been traced for distances of between 100-300m. Greater lateral continuity of strata is suspected as rarely were beds seen to be of lenticular shape.

In conclusion, the strata have more of the features that characterise distal turbidites (Walker, 1967) than proximal turbidites in which the poor development of intraformational conglomerates and pebbly mudstones is particularly significant. From the above evidence, it is suggested that the Torlesse comprising the southern Ruahine Range was deposited in a marine environment with a transportational connective route to land but seaward of a continental slope or rise paleoenvironment in water of an



unspecified depth but at least below wave-base.

### 3.2 DEPOSITIONAL ENVIRONMENT

Extensive areas of fine-grained pelagic and hemipelagic sedimentation together with sediment gravity-flow deposits similar to those documented from the study area form a large proportion of submarine fan, continental rise and slope sequences. However, one of the most distinctive differences between submarine fan and continental rise and slope sediments is reflected in the instability of slopes. Disruption and reorientation of sediment into slides and chaotically deformed masses is usually very common on slopes. In contrast, the frequency and scale of these features on submarine fans and rises are usually relatively minor (Cook *et al.*, 1982). The absence of slump features as well as the absence of features characteristic of continental rise and upper fan environments such as submarine canyons and levee bordered valleys favour the interpretation that sequences of strata within the study area were most likely deposited in close proximity to the middle fan, lower fan and basin plain regions of the model. However, because the dimensions of the submarine fan in this area are unknown it is equally probable that sequences of strata characteristic of the study area represent overbank or levee deposits between widely spaced channels in the upper fan region where channels only form a small percentage of the fan surface (Howell & Normack, 1982).

Within the study area, strata comprising the Very Thick-Bedded Association consists of fine- to medium-grained sandstone in thick, laterally continuous, massive and often composite bed sequences. Minor scour and rare small-scale channel features are also present. Clasts of argillite occur along distinctive horizons through predominantly ungraded sandstone beds though faint parallel laminations, dish structure and grading may also be present. Strata comprising the Very Thick-Bedded Association are commonly interbedded with Thick-Bedded Association in which case all gradations of characteristics of each Association occur, rendering it difficult or arbitrary to subdivide the unit. Both Associations are interbedded with Thin-Bedded Association (see Table 2.1). The Very Thick-Bedded Associations may occur in a channelised setting, particularly but not exclusively on the inner and middle fan. These very thick beds reflect grain flow processes and when they are transitional to beds of the Thin-Bedded Association fluxo-turbidity currents are suggested (Carter, 1975; Middleton & Hampton, 1976).

Strata comprising the Thick-Bedded Association are fine- to medium-grained sandstones commonly interbedded with thin layers of argillite. The sand-

stone beds are classical turbidites of Bouma (1962) and are of uniform thickness for considerable lateral distances. Normal grading is common and rare sole marks occur along sharp basal surfaces. Thin layers of fine-grained intraformational conglomerate characteristically occur at the base of these sandstone beds. Top and bottom truncation of the Bouma intervals is common. Typically these sequences consist of repetitions of the Ta-e divisions suggesting that they were deposited close to their source (proximal) (Walker, 1981). The Thick-Bedded Association is generally associated with upper parts of channel-fill sequences and with such non-channelised settings as middle fan fringe, outer fan or even basin plain (Howell & Normack, 1982). These sandstone beds are primarily deposited by turbidity currents (Kuenen & Migliorini, 1950; Middleton, 1967).

The Thin-Bedded- and Very Thin-Bedded Associations consist of thin interbeds of sandstone and argillite with sandstone beds being tabular and persisting laterally for considerable distances. Each sandstone bed is typically graded and displays the upper parts of the Bouma Sequence. Where the basal Ta sandstone bed is preserved it is generally less than 0.3m thick. The Thin-Bedded Association dominates the stratigraphic sequence mapped as Graded-Bedded Lithozone. This Association is transitional with strata comprising thinner sequences of Very Thin-Bedded Association and the Thick-Bedded Association with which it is interbedded.

Thin-Bedded- and Very Thin-Bedded Associations are regarded as traditional "distal turbidites" though such thin-bedded turbidites actually occur in nearly all parts of a submarine fan as well as on the basin plain. These Associations in general represent deposition by low-density turbulent flows (Howell & Normack, 1982). Parts of these Associations, however, are characterised by a variety of internal-bedding characteristics including flaser, wavy and discontinuous bedding, massive sand, and graded sand. Such features are thought to represent high-concentration gravity and traction flow processes typical of overbank or levee deposits that are most likely to occur in channelised environments of a submarine fan.

The very high proportion of argillite comprising debris flow deposits (Diamictite Lithozones) suggests that their source area was a site of extensive fine-grained argillite and silt sedimentation. Such areas include the continental rise. Because continental slopes are especially susceptible to mass movement, a high percentage of material on the slope may be allochthonous. For example, up to 40-50% of some ancient slope sequences consist of mass transport deposits (Cook & Taylor, 1977). If so, the

presence of allochthonous boulders, within Diamictite Lithozones, some of which have been identified as being of shallow water origin (see Chapter 4), can be explained in terms of debris flow activity resulting from slump movements on the continental slope or continental rise.

C H A P T E R    4

---

PALAEONTOLOGY

CONTENTS

	<u>page</u>
4.0 INTRODUCTION    ...    ...    ...    ...    ...    ...    ...    ...    ...	106
4.1 LIMESTONE BLOCK (T23/f7530)    ...    ...    ...    ...    ...    ...	106
4.2 RETROCERAMUS SPECIMENS (T23/f3)    ...    ...    ...    ...    ...	108
4.3 FOSSILIFEROUS CALCAREOUS CONGLOMERATES    ...    ...    ...    ...	110
4.4 RADIOLARIAN CHERT    ...    ...    ...    ...    ...    ...    ...    ...	110
4.5 FOSSILIFEROUS CALCAREOUS SILTSTONE    ...    ...    ...    ...    ...	110
4.6 DISCUSSION    ...    ...    ...    ...    ...    ...    ...    ...	110
4.7 FAUNAL ZONES AND LOCAL CORRELATION    ...    ...    ...    ...    ...	114

## C H A P T E R    4

### PALAEONTOLOGY

#### 4.0 INTRODUCTION

In 1975 a fossiliferous block of indurated micritic limestone (T23/f7530) was discovered in the Pohangina River valley by Dr M J Shepherd (Department of Geography, Massey University, Palmerston North). This locality, T23/660235, was revisited in 1978 and the entire limestone block weighing 33.5 kg collected. The bulk of the block is lodged with the Department of Geology, University of Auckland. The remainder of the material is held in the Department of Soil Science, Massey University (Table 4.1). Fauna extracted from the limestone have been submitted to the New Zealand Geological Survey, Lower Hutt, for identification. The key faunal elements have been identified by H J Campbell (macrofauna), J E Simes (conodonts) and C P Strong (foraminifera) (Appendix IIIa). Their preliminary findings and the significance of key fossils is presented briefly in Appendix IIIb.

At a second locality (T23/644142) two specimens identified by G R Stevens (pers com) as *Retroceramus (Retroceramus) haasti* (Hochstetter) were found at T23/f3\* by the author in 1978. These specimens were found *in situ* within argillite. They are lodged in the Massey University Reference Collection (Table 4.1).

At a number of other localities throughout the southern Ruahine Range boulders of fossiliferous conglomerate have been found only as loose bedload material within stream channels. Radiolarian chert is also present in the study area. All of these fossils have been found in lithologies comprising Wharite Lithotype. As shown in Chapter 2, Wharite Lithotype is considered to be a melange.

Fossiliferous, calcareous siltstone occurs as concretionary lenses or as thin interbeds in both the Wharite and Tamaki Lithotypes.

#### 4.1 LIMESTONE BLOCK (T23/f7530)

This block was found *in situ* on the left bank of Pohangina River approxi-

---

\* Fossil locality number within the New Zealand Fossil Record File of the Geological Society of New Zealand based on the NZMS 260 metric map series.

TABLE 4.1: Fossil record dates from study area.

N.Z. fossil record number	M.U. reference collection number	Metric grid reference	New Zealand stage	International stage	International period	Fossil	Collector
T23/f7530	MU 3	T23/660235	Oretian- Otamitan	Early Norian	Late Triassic	Fossiliferous block of limestone	M J Shepherd
T23/f3	MU 1 & 2	T23/644142	Ohauan	Middle Kimmeridgian	Late Jurassic	* <i>Retroceramus (Retroceramus)</i> <i>haasti</i> (Hochstetter)	M Marden

\* Identification by G R Stevens

mately 2.3 km upstream from the junction with Piripiri Stream tributary. It occurred 1m above normal river level and 4-6m from the edge of the active river channel. In outcrop the limestone block was conspicuous by its lighter grey-white colour contrasting against the black argillaceous matrix. This outcrop forms part of a Diamictite Lithozone (see Chapter 2) within which other clasts are predominantly of sandstone lithologies with minor chert. The clasts show no overall preferred orientation but the long axis of the limestone block was near vertical. No other fragments of fossiliferous limestone were found either at this locality or elsewhere throughout the southern Ruahine Range.

Acid extraction of fossils produced a particularly diverse fauna which include foraminifera, brachiopods, gastropods, bivalves, ammonoid fragments, crinoid and echinoid elements, ostracods (Appendix IIIa) and conodonts (Appendices IIIb and IIIc). Comments on the identification, interpretation and significance of the fauna appear in Appendix IIIb and are based upon palaeontological work in progress at New Zealand Geological Survey.

The age of this limestone block is Oretian which has been correlated with the Early Norian of the world Triassic (Appendix IIIb). The considerable age difference between this limestone block and other dated fossils (see below) from this area suggest that this limestone is allochthonous.

#### 4.2 RETROCERAMUS SPECIMENS (T23/f3)

Two incomplete moulds of *Retroceramus* (*Retroceramus*) *haasti* (Hochstetter) (Fig. 4.1) were found embedded *in situ* within an argillite outcrop at T23/644142. This outcrop occurs at stream level on the left bank of the southernmost tributary of Rokaiwhana catchment within a very steep-sided gorge approximately 1.4 km from the junction of this tributary with Rokaiwhana Stream. The argillite is massive, indurated and devoid of recognisable bedding features. There are no clasts of competent lithologies embedded within the argillite. Fault plane shear surfaces are particularly well developed in the vicinity of the fossil locality. The relationship of this fossil-bearing lithology within Wharite Lithotype is, however, not clear. It may be part of a large faulted block or, alternatively, part of the matrix comprising Wharite Lithotype. An autochthonous origin for the fossils is favoured but cannot be firmly established.

These *Retroceramus* specimens are of Ohauan age (Stevens, pers com). This correlates with the Middle Kimmeridgian of the world Triassic.



FIGURE 4.1: Specimens of *Retroceramus* (*Retroceramus*) *haasti* (Hochstetter) (T23/f3) found within Rokaiwhana Catchment at T23/644142. Identification by G R Stevens.



#### 4.3 FOSSILIFEROUS CALCAREOUS CONGLOMERATES

Rounded boulders of calcareous conglomerate (Fig. 2.23) have been found as stream bedload but not in outcrop. They comprise well rounded sometimes elongate clasts of arenaceous and calcareous lithologies. The clasts are embedded in an arenaceous matrix that has a substantial carbonate content (see Chapter 5). The fossils are incorporated within the matrix.

Unidentified macrofossil fragments are suspected. Microfossils include foraminifera, and possible bryozoans (Fig. 4.2). The fossils have only been seen in thin section as acid extraction failed to produce a single specimen. Identification of these fossils has not been attempted.

#### 4.4 RADIOLARIAN CHERT

Dark red, haematite stained cherts (jaspers of Reed, 1957b) contain poorly preserved radiolaria. Radiolarian chert has been found at locality T24/492944. The radiolaria are seen in thin section as spherical casts.

Many have a solid outer ring structure of radiating needles of chalcedony. Central portions of the radiolaria consist of cryptocrystalline quartz (Fig. 4.3). Other cherts from this area contain spherical objects that have similarly been replaced by radiating needles of chalcedony. It is, however, uncertain whether these are pseudomorphs of radiolarian casts or are spherulites of chalcedony.

#### 4.5 FOSSILIFEROUS CALCAREOUS SILTSTONE

Calcareous siltstones contain unidentified spherical objects similar in appearance to radiolaria seen in cherts in this area. The fossils either have a solid outer ring structure with a core of infilling calcite in the form of either sparite or micrite (see petrological slide NRS1) or have a porous appearance (see petrological slide RK15, slide A). They occur at localities T24/484924, T23/512039, T23/566085 and T23/646145.

#### 4.6 DISCUSSION

Melange terranes within the Torlesse characteristically contain allochthonous blocks many of which are fossiliferous (Bradshaw, 1973; Munday, 1977; Feary & Pessagno, 1980).

The presence of allochthonous blocks indicates that mobilization and subsequent emplacement by either tectonic or sedimentary mechanisms has taken place. The absence of sheared margins separating the limestone

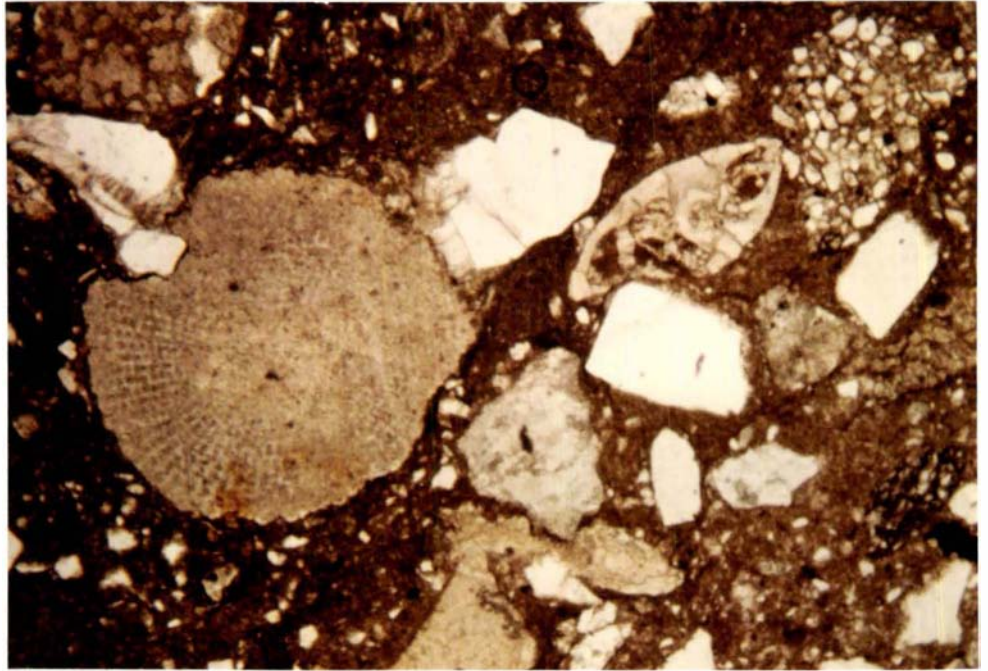


FIGURE 4.2: Fossiliferous calcareous conglomerate containing fragments of foraminifera, and possible bryozoan. Thin section view from rock sample Mtu<sub>1</sub> (Mangatuatou Stream) at locality T23/562113 x30, plain light.

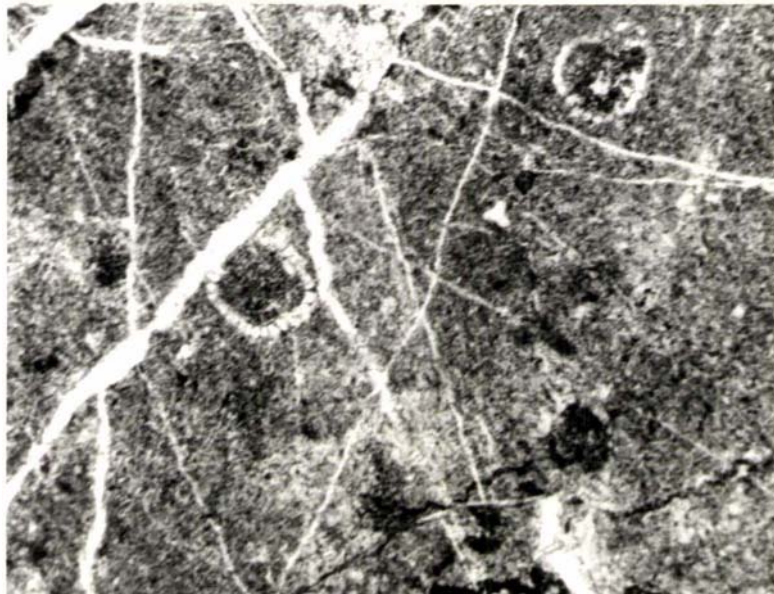


FIGURE 4.3: Radiolarian chert showing spherical radiolaria with double ring structure. The radiolaria have been replaced by chalcedony. Central portions of radiolaria consist of cryptocrystalline quartz. Thin section view of rock sample MG<sub>1</sub> (Manawatu Gorge) at locality T24/492944, x120, plain light.

block (T23/f7530) from the encompassing argillaceous matrix indicates the possibility of emplacement by subaqueous mass transport processes, the most likely of which is debris flow. On the other hand, the presence of numerous sheared surfaces between larger mappable units within the Wharite Lithotype tends to suggest that the lithology in which the limestone block is embedded has been tectonically emplaced. In addition the absence of sheared margins around the limestone block does not necessarily exclude tectonic emplacement.

In contrast, the fossils collected at T23/f3 are thought to be contemporaneous with the argillaceous matrix in which they are embedded. It cannot, however, be proven whether this massive unit has been tectonically emplaced or represents sedimentation at the time of melange formation. An autochthonous origin for the *Retroceramus* specimens is favoured.

The fossiliferous calcareous conglomerates are clearly allochthonous but are of unknown age. It is interpreted that they were indurated prior to emplacement within the melange having been eroded from an older terrane. This interpretation suggests that the fossils contained within the boulders are older than the time of melange formation as indicated by the presence of the fossil T23/f3 and therefore pre-date Late Jurassic time.

The radiolarian cherts are of diverse origins. Many of the larger blocks of chert are considered to be allochthonous whilst thin beds of chert interbedded within argillite clearly represent contemporaneous deposition. These cherts are considered to span a wide age range which on the basis of the ages of other contained fossils in the melange may range from between Late Triassic to Late Jurassic. At present radiolarian cherts within Torlesse bedrock are of little stratigraphic significance. They may, however, prove to be potentially useful to date the age of some of the source rocks associated with them in this melange terrane.

Fossiliferous calcareous siltstones in this area are at present undated and hence are of little stratigraphic use. However, the occurrence of fossils within calcareous siltstone lenses and interbeds, that clearly represent contemporaneous deposition with surrounding clastic lithologies, may provide a certain means of dating these lithologies. If so, the occurrence of fossiliferous calcareous siltstone, within clastic sequences comprising both the Wharite and Tanaki Lithotypes could be utilised to establish whether or not at least some of the strata comprising these lithologies is of a similar or different age.

The discovery of fossils of known age at localities T23/f7530 and T23/f3 within a melange comprising part of the Torlesse bedrock demonstrates the considerable age difference between allochthonous lithologies of Late Triassic (Oretian), Early Norian age and an essentially argillaceous matrix containing autochthonous macrofossils of (Ohauan) Middle Kimmeridgian age. This relationship is further exemplified by the presence of fossils of similar age found to the north of the study area. These include: (1) a belemnite (*Belemnopsis keari* Stevens) and a bivalve (*Pleuromya milleformis* Marwick) of Heterian age, found in a boulder in the Waipawa River catchment (on the east side of the Range) by Te Punga (1978); and (2) several species of *Monotis* of Early to Late Warepan age and specimens of the brachiopod (*Halorella ruahinensis* n. sp) of Otamitan age described from the Oroua River catchment (on the west side of the Range) by Milne & Campbell (1969). Munday (1977) located several additional sources of *Monotis* fossils in the Oroua River area and recognized that some occur within a melange terrane whilst others are from *in situ* outcrops of coherent terrane that lie to the west of the melange.

As pointed out by Hsu (1968) and Hsu & Ohrbom (1969) the assignment of a time-range of deposition to all rocks in a melange on the basis of the oldest and youngest fossils found in such a melange is incorrect. Age determinations from allochthonous blocks are clearly unsatisfactory for dating the age of emplacement of a melange terrane but do give: (1) a maximum age for the enclosing matrix if the exotic blocks were emplaced by sedimentary processes; or (2) a maximum age to the melange formation if the blocks were emplaced tectonically.

From fossil occurrences described here it can be said that melange formation has involved rocks of Late Triassic age (Late Karnian - Early Norian) to Late Jurassic age (Middle Kimmeridgian). At best it can only be assumed that melange formation may have continued until at least Late Jurassic time or younger, yet predates metamorphism of the Torlesse in this region, as both the matrix and clastic blocks show equivalent low grade metamorphism.

Until such time that more age determinations from this and other melange terranes are available it would be premature at this stage to suggest a more precise age for melange formation in this area.

#### 4.7 FAUNAL ZONES AND LOCAL CORRELATION

Strata comprising the Torlesse have been divided into faunal zones on the basis of the age of fossil assemblages. The lower half of the North Island comprises three major faunal zones, the distribution of which indicates regional younging towards the east. The oldest Torlessia zone lies to the west of a central Monotis zone, to the east of which lies a Late Jurassic zone (Fig. 3; in Speden, 1976).

The Tararua and Ruahine Ranges are included in the Monotis zone on the basis of Monotis fossils (in Milne & Campbell, 1969) from two widely separated localities. These occur to the south of this study area at Otaki Forks (S26) and to the north of this study area within Oroua River catchment (S22, T22). In recent years Speden's (1976) zonal interpretation has been complicated by: (1) the discovery of a melange in the Oroua River area; and (2) the discovery of Late Jurassic fossils from the Ruahine Range. The implications and significance of these finds are now discussed in relation to the current interpretation of the distribution of the Monotis zone in the southern Ruahine Range.

In the Oroua River area, 10 km to the north of the study area is a zone of melange that is here considered to be the same melange mapped in this study as the Wharite Lithotype.

Some authors consider that each of the localities at which Monotis specimens were found within Oroua River catchment, occur within melange (Grant-Mackie, 1975) and are hence allochthonous in origin. However, Munday (1977) suggests that at least three of the Monotis localities within this catchment occur *in situ* within a 'bedded series' that lies to the west of the melange. Of these three localities the two easternmost ones occur in close proximity to the melange and show signs of tectonic deformation. The third locality lies further to the west and is relatively undeformed. Munday (1977) argues that the Monotis specimens collected from localities adjacent to the melange occur in lenses that represent a former bed which has been broken and sheared by tectonic movement but is essentially *in situ*. If Munday's interpretation is correct, the strata comprising the 'bedded series' then represents part of an *in situ* westward younging Triassic terrane of Warepan age (Munday, 1977). A shallow water depositional environment for the Monotis specimens within this terrane is then of considerable significance and the existence of a Monotis zone in this area can be verified.

Should the alternative interpretation be correct then the Monotis zone may require revision.

The recent discoveries of fossils of Late Jurassic (Heterian-Ohauan) age in Rokaiwhana catchment (this study) and Waipawa catchment (Te Punga, 1978), both of which occur embedded in an argillaceous matrix clearly indicates that some of the argillaceous component in these areas is of Late Jurassic age. If it is assumed that these fossils are autochthonous it is then highly probable that the Late Jurassic zone (zone 5 of Speden, 1976) is more extensive than was previously thought and, in fact, comprises much of the southern Ruahine Range. This faunal zone would then incorporate not only the melange (Wharite Lithotype) but also the bedded unfossiliferous stratal sequences eastward of the melange, *i.e.* Tamaki Lithotype of this area. Stratigraphic correlation of these Lithotypes with identical 'belts' of unfossiliferous strata to the northeast of the study area in the Moorcocks Stream - Tukituki River area (Pohangina Melange and Kashmir Belt, respectively, of Sporli & Bell, 1976) together with the presence of a belemnite of Heterian age within Waipawa River catchment (Te Punga, 1978) are suggestive of a Late Jurassic zone in these areas also. This faunal zone may also incorporate locality N150/f483 (of Heterian-Ohauan age) in the Waewaepa Range (eastward of the Tararua-Ruahine Range) (see Fig. 1; in Speden, 1976). This Late Jurassic zone is dominated by Heterian to Ohauan aged fossils.

If it is accepted that melange formation continued until at least Late Jurassic age then the presence of melange within the northern Tararua Range as identified in this study would indicate that some of this Range is also part of the Late Jurassic zone of Speden (1976). Melange has been traced for 12 km southward of the study area to Pahiatua Track. Still further southward the presence of volcanic and associated lithologies (including limestone) similar to those found in the southern Ruahine Range where they are restricted to melange terrane is suggestive of the presence of a melange here also. A limestone boulder (S26/f12) from the Tauherenikau River 130 km to the southwest of the Pohangina River locality may have been eroded out of a melange in this area. The distribution of these lithologies in the Tararua Range appears to be confined predominantly to the eastern side of the Range but a 4m wide melange zone has been reported in the Otaki Forks area (Rattenbury, 1982). It is not considered likely that this melange is the same melange that has been traced in this study from the Moorcocks Stream-Tukituki River south-

wards to the Pahiatua Track. The presence of autoclastic breccia (Reed, 1957a, 1957b) in the Rimutaka Range, may also represent melange, though not necessarily the same melange that occurs in the southern Ruahine Range.

The full areal extent of melange in the Tararua and Rimutaka Ranges will not be realised until detailed stratigraphic mapping of these Ranges has been undertaken. If it can be shown by fossiliferous evidence, that melange terrane in these Ranges is of a similar age to that in the southern Ruahine Range, then the extent of the Late Jurassic zone will require updating. On present evidence it appears that much of the southern Ruahine Range should be incorporated within the Late Jurassic zone of Speden (1976). Also, it is apparent that the extent of the Monotis zone requires redefining and may need to be restricted to localised areas where Monotis specimens can be considered to be autochthonous. On the basis of the present known distribution of Monotis specimens that are considered to represent biocoenoses, it is suggested that the Monotis zone be confined to the Otaki Forks area and perhaps include at least one locality in the Oroua River area.

The inferred presence of a shallow-water depositional environment for Monotis in these areas is, however, incompatible with the favoured deep-water interpretation for sediments comprising much of the Torlesse both elsewhere throughout New Zealand and in the southern Ruahine Range (see Chapter 3). This problem remains unsolved.

C H A P T E R    5

PETROGRAPHY

CONTENTS

	<u>page</u>
5.0 INTRODUCTION ... ..	117
5.1 SANDSTONE AND SILTSTONE ... ..	117
5.1.1 MINERALOGY ... ..	118
A. Quartz ... ..	118
B. Feldspar ... ..	119
C. Rock Fragments .. ...	119
D. Biotite and Muscovite ... ..	120
E. Chlorite ... ..	121
F. Metamorphic Accessories ... ..	121
G. Detrital Accessories ... ..	121
H. Matrix ... ..	122
I. Classification .. ...	122
5.2 ARGILLITE ... ..	122
5.3 CONGLOMERATE ... ..	123
5.4 AUTOCLASTIC BRECCIA ... ..	125
5.5 VOLCANIC LITHOLOGIES .. ...	125
5.5.1 MINERALOGY ... ..	126
5.5.2 DEFORMATION ... ..	128
5.5.3 MAJOR AND TRACE ELEMENT ANALYSES OF VOLCANIC LITHOLOGIES ... ..	129
A. Introduction ... ..	129
B. Chemical Variations .. ...	129
C. Conclusions ... ..	137
5.6 CHERT .. ...	137
5.7 CALCAREOUS LITHOLOGIES ... ..	138
5.7.1 MICRITIC LIMESTONE (BIOMICRITE) ... ..	138
5.7.2 CALCAREOUS SILTSTONE ... ..	138
5.7.3 CALCAREOUS CONGLOMERATE .. ...	139
5.8 PROVENANCE .. ...	139



CHAPTER 5PETROGRAPHY5.0 INTRODUCTION

The results of this study are based on the examination of approximately 200 petrological slides representative of most of the lithologies present in the study area (see Chapter 2). Specimen numbers are prefixed by letters that denote the catchment from which each was collected (Appendix IVa). Collection sites of most of these specimens are shown on a map (Appendix IVb). Rock samples and petrological slides are lodged in the Department of Soil Science Reference Collection, Massey University, Palmerston North. The Reference Collection (MU) numbers for specimens in Appendix IVb are listed in Appendix VII .

5.1 SANDSTONE AND SILTSTONE

Grain size is based on the Wentworth (1922) size classes. Samples from this area fall into grain size classes ranging from medium sand to very fine silt. The dominant size classes occur between medium and fine sand. All samples are dark- to light-grey or green-grey when fresh and lighter in colour when weathered.

The most characteristic micro-textural feature is the degree of sorting which is generally poor but can be described as moderately good in some samples. The poor sorting is attributed to the presence of intraclastic grains of predominantly quartz and feldspar, together with abundant rock fragments, embedded in a fine-grained matrix. The coarser grained lithologies are more poorly sorted than the finer grained lithologies. In the latter, better sorting is often associated with grading and lamination, e.g. Po<sub>7</sub>, Rk<sub>16</sub> (Fig. 3.2), WT<sub>1</sub> (Fig. 3.4) and Rk<sub>18</sub>. Another textural feature is the marked angularity of the clastic grains, varying between subangular to angular. However, a very small proportion of particles, particularly the heavy mineral detrital grains, are subrounded. Such rocks have been described as micro-breccias by Reed (1957b, p 13). In contrast to clastic grains, rock fragments tend to be rounded to subangular. Ductile deformation has produced local mortar texture, e.g. Or<sub>7</sub>, Rk<sub>13</sub>, Co<sub>10</sub>. Structures of sedimentary origin include load casts, flame structure and the presence of rip-up clasts, (see Figs 3.2-3.6). Microfaulting is evident in Slide MkD<sub>8</sub>.

A detailed point-count analysis was not attempted as it was considered to be beyond the scope of this study. Instead, compositional percentages are based upon microscopic examination of approximately 75 petrological slides for each of which the compositional constituents were estimated within two different fields of view and averaged. These estimates, though essentially subjective, are believed to be within the correct order of magnitude as they do not differ markedly from point-count analyses of Torlesse rocks elsewhere in the southern half of the North Island (see Reed, 1957b; Zutelija, 1974; Munday, 1977; Rowe, 1980; and Rattenbury, 1982).

Compositionally the sandstones and siltstones are essentially similar in that all the major components are present in both lithologies and they differ only in their relative proportions. The clastic grains are composed mostly of quartz, feldspar and mica. Clastic quartz forms between 15% to 35%, feldspar forms approximately 30% and the micas form less than 5% of most of the sandstone and siltstones in this area. Accessory clastic grains approximate 1% of the total rock composition. Rock fragments are the most variable component (10-60%) and are largely responsible for the textural appearance of these rocks. Sedimentary and volcanic rock fragments predominate, while granitic and metamorphic rock fragments are subordinate. Matrix content varies from between 10% and 25%.

#### 5.1.1 MINERALOGY

##### A. Quartz

Clastic quartz in general comprises between 15-35% of the total composition and averages around 25-30%. Quartz grains are angular to well rounded. The smaller grains tend to be more angular than larger grains. However, fracturing of grains of all sizes produces angular grains of medium sand to very fine silt grade. Grain size is highly variable and ranges from a maximum of around 1 mm diameter, e.g. Mg<sub>3</sub>, Rk<sub>4</sub> and Dn<sub>1</sub> to a minimum discernible size of less than 0.03 mm.

Almost all of the quartz is monocrystalline, clear and strained. Grains displaying undulose extinction show slightly biaxial interference figures. Varieties of quartz include polycrystalline (excluding chert) and wavy (quartz with undulose extinction) and non-wavy monocrystalline quartz. Distinction between strained quartz and non-twinned feldspar, in the absence of feldspar staining techniques, proved difficult. Quartz recrystallisation is indicated by patches of intimately packed, adjacent quartz grains, overgrowths and healed fractures. Recrystallised quartz predominantly occurs as vein and shear infilling, examples of which are found

in most slides.

Inclusions are common and include sericite, opaques and epidote minerals. Inclusions commonly form straight or curved rows across quartz grains, e.g. Rk<sub>4</sub> and Dn<sub>1</sub>. A number of grains show embayments of calcite and sericite which indicate corrosion of the quartz grain or replacement of the calcite and/or sericite.

#### B. Feldspar

The average feldspar content is between 25% and 35% but ranges between 15% and 40%. Individual grains range in size from greater than 1 mm e.g. MkD<sub>7</sub> and Dn<sub>1</sub> to less than 0.1 mm and are variably shaped from angular, subrounded, irregular to rectangular crystal form.

Plagioclase predominates over minor K-feldspar. Plagioclase composition as estimated by the Michel-Lévy method was less than An<sub>20</sub>. Detrital plagioclase displays both carlsbad and carlsbad-albite twinning but authigenic albite is generally clear, unzoned and untwinned. Plagioclase grains commonly show signs of albitisation and saussuritisation, e.g. Pr<sub>3</sub>. Alteration products include calcite, opaques, sericite and epidote group minerals. Alteration and replacement is evident along grain boundaries, twin planes or cleavage planes. Complete replacement of entire grains is common. Deformation twins, often bent, kinked and offset, are common, as is undulose extinction.

K-feldspar occurs as clear microcline (sections not showing twinning), twinned microcline or untwinned orthoclase. Microcline twinning, e.g. Pr<sub>3</sub> and Ou<sub>2</sub>, perthitic strings, e.g. Pr<sub>3</sub> and Mg<sub>3</sub>, chessboard texture, micrographic intergrowths and myrmekite, e.g. Et<sub>3</sub>, Dn<sub>1</sub> and Pr<sub>3</sub> are apparent.

#### C. Rock Fragments

Rock fragments were divided into three categories: sedimentary, metamorphic and plutonic, and volcanic.

Sedimentary rock fragments are mainly siltstones and argillites though coarser-grained rock fragments of medium sandstone size are present in some sandstones. Rock fragments are subrounded to rounded and are of variable size, generally less than 4 mm, e.g. Dn<sub>1</sub>. Argillite rock fragments of large size may be the result of post-depositional deformation resulting in the flattening and elongation of argillite fragments around rigid grains, thereby assuming the appearance of patches of matrix. Siltstone rock fragments have a higher argillaceous content than sandstone

rock fragments. Siltstone and sandstone rock fragments were distinguished from the host rock by subtle differences in texture including matrix content, sorting, packing, boundary continuity and opacity. The sedimentary rock fragments are of similar mineralogical composition to the host rocks and are probably largely intraformational.

Metamorphic and plutonic rock fragments were difficult to recognise. In particular, metamorphic fragments that may be described as phyllites or sericite schists are not dissimilar in composition or texture to very fine siltstones and argillites from this area. The strong alignment of micaceous constituent minerals is a feature of both supposed metamorphic rock fragments, e.g. MkD<sub>7</sub> and Pr<sub>3</sub> and some very fine siltstones, e.g. Or<sub>4</sub>. Metamorphic rock fragments rarely exceed 1 mm length, are characteristically elongate and are subangular.

Plutonic rock fragments are subrounded to rounded and are an inconspicuous component within sedimentary lithologies in this area.

Volcanic rock fragments are of two types - intermediate and basic. Texturally and compositionally they are identical to those described as lithologic components of the Wharite Lithotype. These rock fragments display trachytic to pilotaxitic and hyalopilitic texture. The acid rock fragments are considered to have been derived from essentially rhyolitic and andesite lavas. The highly altered basic igneous rock fragments are considered to be of essentially basaltic lava composition. Volcanic rock fragments are generally rounded to subrounded and vary in size from less than 0.1 mm to 1.5 mm, e.g. Mte<sub>6</sub> and Mte<sub>7</sub>. The main alteration processes affecting volcanic rock fragments include chloritisation, zeolitisation and concentrations of authigenic opaques, predominantly pyrite. Lithologies rich in volcanic rock fragment content also tend to contain a high percentage of chert fragments. Consequently, chert fragments are included in the volcanic rock fragment category.

Rock fragment content is particularly abundant in the coarser-grained sandstone lithologies but diminishes rapidly with decreasing grain size of the host rock.

#### D. Biotite and Muscovite

Biotite is the predominant ferromagnesian mineral. Normal brown pleochroism is shown by most grains. However, reddish brown and green pleochroic varieties (due to chlorite replacement) are also present, e.g. Pr<sub>3</sub>. Muscovite accompanies biotite, though is far less plentiful. Grains vary in

size from around 1 mm length, e.g. Pr<sub>3</sub> to minute oriented grains less than 0.05 mm long, e.g. Or<sub>4</sub>. Most grains are strained, kinked and have waxy extinction, e.g. Co<sub>8</sub>. Biotite and muscovite comprise less than 5% of the total rock composition of lithologies from this area.

#### E. Chlorite

Chlorite content can be as high as 15%, much of which occurs in the form of interstitial matrix of authigenic origin. It occurs as a replacement product after biotite, e.g. Co<sub>8</sub>, or as inclusions, e.g. ET<sub>3</sub>.

#### F. Metamorphic Accessories

Calcite is the most obvious and most abundant secondary replacement mineral, completely enveloping volcanic rock fragments and feldspar, e.g. Ou<sub>2</sub> and Pr<sub>3</sub>, replacing zeolite and actively corroding quartz boundaries. Calcite occurs as a vein mineral predominantly in association with quartz and sericite, e.g. Mg<sub>3</sub> and Rp<sub>12</sub>. Calcite crystallisation is, in general, the last recognisable mineral phase.

Quartz recrystallisation forms veins or irregular patches of either micro-crystalline quartz (chert-like) or mosaics of anhedral grains, e.g. Mka<sub>1</sub>, Mkd<sub>9</sub> and Or<sub>13</sub>.

Epidote minerals most frequently result from alteration of plagioclase or volcanic rock fragments. They often occur adjacent to, or within, zones of quartz or quartz-calcite filled veins and in zones of deformation.

Opagues are principally pyrite, which occurs as irregular patches in the groundmass, e.g. Co<sub>8</sub> or as inclusions in plagioclase, e.g. Ou<sub>2</sub>. Staining by opaque oxides is frequently concentrated along the margins of veins, zones of shear, e.g. Mkd<sub>8</sub> around the margins of rock fragments, e.g. ET<sub>3</sub> and as concentrations along sedimentary laminations, e.g. WT<sub>1</sub>. Opagues appear to occur in greatest concentrations in the finer grained lithologies and in particular are most prolific in argillaceous lithologies.

The presence of prehnite and pumpellyite, though well documented as occurring in Torlesse rocks in the Wellington area (Reed, 1957b; Rowe, 1980), was not established with confidence in this area.

#### G. Detrital Accessories

These include amphiboles, apatite, sphene, zircon, epidote, clinozoisite and augite, e.g. Mte<sub>7</sub> and Rk<sub>9</sub>. These accessory minerals appear to be most abundant in the coarse-grained lithologies that have a high volcanic rock fragment content.

## H. Matrix

The matrix includes all material, authigenic or detrital, less than 0.02 mm in size (after Reed, 1957b) that occurs interstitially. Matrix minerals include chlorite, sericite, calcite, feldspar, metallic opaques (pyrite with some leucoxene), non-opaque heavy minerals (?haematite/limonite) and carbonaceous material. Matrix content is high, variable, and in general increases with: (1) decreasing size of clastic grains; (2) the degree of alteration of clastic grains and rock fragments; and (3) where ductile deformation has affected the rock. In the latter case the matrix content may be as high as 40-50%, e.g. Or<sub>7</sub>.

## I. Classification

Sandstone and siltstone lithologies examined from this area are predominantly lithic feldsarenites (Folk *et al.*, 1970). Volcanic rock fragments (including chert) are particularly abundant in some lithologies, e.g. Rk<sub>9</sub>, ET<sub>3</sub>, Mte<sub>6</sub> and Mte<sub>7</sub>. These volcarenites are, however, restricted to the northeast of the study area where they occur in association with conglomerates rich in pebbles of volcanic composition (see Section 5.8).

Fine-grained lithologies tend towards a feldsarenite composition. This is thought to be due to a reduction in the rock fragment content as a consequence of their mechanical weakness and chemical instability.

A diverse range of sandstone and siltstone lithologies occur in each of the three mapped lithotypes in this area. This diversity is predominantly textural, being governed in the main by rock fragment abundance and composition. However, as the rock fragments, detrital grains and secondary minerals are mineralogically identical it is concluded that the sandstone and siltstone lithologies within each lithotype have been derived from a common source.

### 5.2 ARGILLITE

Although argillites are a very common lithology in the study area, they were not studied in detail as their small grain size makes mineral identification difficult. In thin section, black argillites are seen to be very fine siltstones but differ from other siltstones in this area in that they contain a substantial clay content. The dominant grain size lies between 0.06mm and 0.004 mm. The typical argillite is black to dark grey in colour and is well indurated. Sedimentary features include micro-grading, e.g. ET<sub>2</sub> (slide B) and fine-bedding. Bedding is also indicated by a preferred

alignment of either mica flakes, *e.g.* ET<sub>2</sub> (slide A), or matrix-poor siltstone clasts, *e.g.* ET<sub>2</sub> (slide A) or matrix-rich mudstone clasts, *e.g.* ET<sub>2</sub> (slide B) and WT<sub>2</sub>. The most important micro-textural feature of the argillites is the poor sorting of clastic grains, mainly angular quartz, twinned feldspar, biotite and muscovite lamellae (often bent), embedded in a recrystallised clayey matrix, *e.g.* WT<sub>2</sub>. The matrix consists of predominantly accessory minerals including calcite, epidote, sericite, illites, carbonaceous material and opaques. The argillites thus show on a finer scale the micro-texture and mineral content typical of interbedded siltstones and sandstones.

Interbedded red and green argillite have a similar fine-grained micro-texture and contain a mineral assemblage comparable to that of the black coloured argillite, *e.g.* Rp<sub>17</sub>. Direct evidence of bedding is absent, however, a strong preferred orientation of elongate mica flakes, together with haematite concentration within distinct zones may represent a crude stratification, *e.g.* Rp<sub>17</sub>. Some of the haematite staining is due to remobilisation as it is concentrated along micro-fractures that cross-cut this stratification, *e.g.* Wh<sub>1</sub> (slide B). The green colouration of argillites may be due to an increased chlorite content.

Micro-fracturing, *e.g.* Wh<sub>1</sub> (slide B) and mineralised veins and fractures containing mosaic quartz, suggest that red and green argillites have been subjected to several phases of deformation.

In outcrop, red and green argillites encompass clasts of competent lithologies including clastics, volcanics and cherts. A fragment of chert is seen in sample Wh<sub>1</sub> (slide B).

### 5.3 CONGLOMERATE

Four types of conglomerate have been recognised on the basis of textural differences. The first type consists of numerous pebbles set within an argillite dominated matrix, *e.g.* Or<sub>2</sub> and Rk<sub>6</sub>. The pebbles appear to 'float' within the matrix as if the matrix has flowed around them. The second type consists of sparse, isolated pebbles embedded within a silt-sized matrix that has a high component of fine-grained argillaceous material, *e.g.* CR<sub>1</sub> (Fig. 2.11) and Mp<sub>1</sub>. The third type consists of pebbles set within a relatively argillite-free matrix of sand or silt size, *e.g.* Mte<sub>2</sub> (Fig. 2.3), Mh<sub>1</sub>, Mte<sub>3</sub>, Op<sub>3</sub>, ET<sub>1</sub>, Mte<sub>4</sub> and Mte<sub>8</sub>. The fourth type consists almost totally of pebbles with little intervening matrix, *e.g.* Po<sub>2</sub> and Ko<sub>1</sub>.

In all cases the pebbles are subangular to rounded and in thin section can be up to 1 cm across, *e.g.* Op<sub>3</sub>. The pebbles comprise an assortment of sandstone and siltstone (of coarse-fine grain sizes), argillite, carbonate (*e.g.* Op<sub>3</sub>) chert and igneous lithologies (*e.g.* Mte<sub>3</sub>). Each of these pebble lithologies is of similar composition and texture to those already described as major lithological components of the mappable lithozones and are not described further. Pebbles of granitic and metamorphic origin occur in minor amounts, the former containing strongly perthitic k-feldspars, *e.g.* Op<sub>3</sub> and ET<sub>1</sub>.

The conglomerates from the Tamaki Lithotype contain pebbles of similar composition to the rock fragment constituents of adjacent sandstones. It is interpreted that the bulk of the sediment comprising the Tamaki Lithotype was derived from the same source and is thought to be largely of intraformational origin. There are no apparent mineralogical differences between the pebble constituents of these conglomerates and those from the Wharite Lithotype. As many conglomerates from the Wharite Lithotype have only been found as clast constituents within Diamictite Lithozones, for which a debris flow origin has been proposed (see Chapters 3 and 7), it is probable that they are allochthonous. However, because these conglomerates do not contain pebble lithologies 'exotic' to the Torlesse terrane, it is considered likely that they are largely of intraformational origin.

Conglomerates were not found in strata mapped as the Western Lithotype.

Two important observations concerning conglomerates of the Tamaki and Wharite Lithotypes have been made. First, conglomerates found in the Tamaki Lithotype typically contain a very high percentage of pebbles of volcanic origin. The greatest concentration of volcanic-rich conglomerate beds occur in the Mangatera foothill and East Tamaki River area. The surrounding sandstones and siltstones in this same area similarly contain a very high percentage of volcanic rock fragments. Westward of these localities, but still within the Tamaki Lithotype, these conglomerates occur as thinner beds in fewer localities and contain a lesser proportion of volcanic pebble constituents. At these latter localities the volcanic rock fragment content within the surrounding sandstones and siltstones also reflect a similar trend. This westward (in the direction of younging) decline in volcanic pebble content may simply reflect a reduction in volcanic sediment supply from the source area or increased supply of non-volcanic sediment from other source areas.

Second, ductile deformation appears to have affected many of the conglomer-



ates from the Wharite Lithotype particularly where mobilisation of the argillaceous matrix with fragmentation and rotation of pebbles of competent lithologies has apparently occurred. In contrast, there is little sign of ductile deformation having occurred within conglomerates comprising a sandy matrix. Evidence of such deformation is rare in conglomerates from the Tamaki Lithotype.

#### 5.4 AUTOCLASTIC BRECCIA

Episodes of both ductile and brittle deformation (see Chapter 7) have affected many lithologies in this area including cherts, clastics, volcanics and conglomerates, the characteristic features of which can be recognised both in the field (see Figs 2.13, 2.14 and 2.22) and on a microscopic scale. Autoclastic breccias from this area are characterised by the predominance of an argillaceous matrix in which angular fragments of various rock types are distributed.

On a microscopic scale a typical example Rp<sub>1</sub> (slide A) consists of angular fragments of chert, volcanics and sandstone, the long axes of which are aligned in one direction. The surrounding argillaceous matrix appears to 'flow' around the fragments. In other samples only fragments of one lithology occur, the most common examples of which are either arenites or chert.

In thin section most of the rock fragments have been recrystallised. Abundant patches of mosaics of secondary quartz and calcite occur throughout the argillaceous matrix. Chlorite and/or sericite is a common constituent in the argillaceous matrix, within patches of secondary mineralisation and within recrystallised rock fragments. Episodes of vein formation preserved within rock fragments (particularly cherts) indicate that they have been reworked (see Section 5.8). Calcite and quartz are the dominant vein minerals but there is no discernible difference in composition between pre- and post-deformation veins.

#### 5.5 VOLCANIC LITHOLOGIES

Texturally and compositionally the volcanic rocks sampled from this area may collectively be referred to as spilites. The altered nature of these rocks makes classification difficult. However, the majority are thought to be of basaltic composition, e.g. Mk<sub>4</sub>, (slide A), No. 1(1) and Mk<sub>1</sub>. Fewer examples of ?dioritic/gabbroic composition, e.g. Mh<sub>5</sub>, Rk<sub>2</sub>, trachytic composition, e.g. Mk<sub>3</sub> and andesitic composition, e.g. Mk<sub>5</sub> have also been found.

In outcrop the most easily identified volcanic rock is that showing pillow structure, the individual pillows measuring 0.25m - 1m in diameter. The pillows may be red or green coloured, the former variety predominating in this area. Lava has not been found as stratiform layers or as cross-cutting dykes but most commonly occurs as isolated blocks embedded within either volcanic or clastic argillite, the blocks being found only within stratal sequences comprising Wharite Lithotype. The following descriptive account of volcanic rocks from this area is based upon samples found both in outcrop and as 'float' material comprising bedload in stream channels.

The predominant texture varies from intersertal, *e.g.* Rp<sub>20</sub> to sub-ophitic, *e.g.* MG<sub>5</sub>. Other features include tracytic texture, *e.g.* Mk<sub>3</sub> and fluidic texture where bent laths of plagioclase with undulose extinction are aligned around the rim of vesicles, *e.g.* Mh<sub>3</sub>, Mk<sub>2</sub>. Plagioclase laths in a variolitic texture occur in a few samples, *e.g.* MG<sub>3</sub> and No. 2(4). One of the most apparent features is the presence of amygdules with diameters varying from 0.2 mm to 3 mm. The most abundant infillings, in order of dominance, include calcite, chlorite, zeolite, quartz and opaque oxides of iron. Combinations of minerals in vesicles include chlorite with calcite, *e.g.* MkA<sub>2</sub>, Tk<sub>1</sub>, calcite with opaque oxides of iron, *e.g.* Mh<sub>3</sub> and chlorite, calcite and opaques, *e.g.* MG<sub>5</sub> where chlorite forms a halo around the opaques.

The groundmass of most of these samples comprises a dense network of irregularly interwoven plagioclase laths to form a felted texture, *e.g.* Mk<sub>1</sub> and Mk<sub>2</sub>. The interstices between mineral grains in some slides comprise devitrified glass, *e.g.* Mk<sub>4</sub> (slide A) and in others comprise chlorite heavily charged with opaque oxides, *e.g.* Mk<sub>6</sub>. Interstices in the majority of slides comprise combinations of chlorite, opaque oxides, calcite and sporadic patches of quartz and epidote.

#### 5.5.1 MINERALOGY

Mineralogically the volcanic rocks are not diverse and contain predominantly albite-oligoclase, augite, chlorite, opaque oxides, calcite, epidote, illites, quartz and zeolites in variable proportions.

Albite is the most important member of the mineral association in these rocks. It occurs as phenocrysts (up to 5 mm length, *e.g.* Mk<sub>5</sub>) and as microlites (ca 0.04 mm length) in the groundmass, *e.g.* Rp<sub>20</sub>. Both phenocrysts and microlites of albite contain a great diversity of other minerals as inclusions. In particular, phenocrysts of large size contain inclusions of chlorite, calcite, sericite, opaque oxides and epidote. Sometimes only

the outline of the phenocrysts is observed, the area of primary plagioclase being filled with a fine-grained aggregate of these minerals, e.g. Mk<sub>5</sub> and No. 1(1). In extreme cases the plagioclase phenocrysts remain only as pseudomorphs, e.g. Mk<sub>5</sub>. Secondary recrystallisation of plagioclase has taken place in some rocks and is indicated by the presence of microlites with indistinct outline, e.g. No. 1(1), Rp<sub>20</sub> and Rp<sub>2</sub> (slide B) and as clear patches of twinned albite that are devoid of inclusions, e.g. Rp<sub>2</sub> (slide B). Recrystallisation also provides an alternative explanation for the presence of a thin rim of plagioclase surrounding phenocrysts that contain large areas of secondary minerals as inclusions, e.g. No. 1(1). The cloudy appearance of large phenocrysts may in some cases be due to saussuritisation, sericitisation or albitisation, e.g. Mk<sub>3</sub>.

Both albite and carlsbad twinning has been observed in microlites and phenocrysts, e.g. Pw<sub>1</sub> and CR<sub>2</sub>. Some of the large phenocrysts may have at one time been zoned, however, due to the presence of inclusions, clear examples of zoning were not seen in volcanic rocks from the study area. Deformation lamellae occur in some phenocrysts, e.g. Mk<sub>3</sub>.

Pyroxenes occur as large phenocrysts (up to 2 mm in length), e.g. Mk<sub>4</sub> (slide A) or more predominantly as short stumpy granular crystals (0.2 mm in diameter), e.g. Tk<sub>1</sub>. Pyroxenes are absent from many slides but where present are undergoing replacement by chlorite and/or calcite, e.g. Mk<sub>4</sub> (slide A). Where pyroxene is relatively fresh, augite has been identified, e.g. CR<sub>2</sub>. A sub-ophitic relationship with albite is evident in MG<sub>5</sub>.

Chlorite appears as a major constituent in most slides. It is mostly found diffused as fine-grained mesostasis between albite laths but also occurs as secondary minerals after pyroxene and opaques or as amygdules. It is also found as inclusions within plagioclase and as veinlets with albite, quartz or calcite. Spherulites of chlorite occur in Op<sub>1</sub> and No. 1(5). Chlorite is represented by at least four optically distinguishable varieties, often co-existing with each other and showing different textures. Amorphous, fibrous and crystalline textures have been recognised. Some pale green chlorites are almost isotropic, e.g. CR<sub>2</sub>, MkA<sub>2</sub> and Rp<sub>20</sub> whereas another variety of chlorite is strongly pleochroic and shows characteristic anomalous berlins blue interference colour, e.g. Rp<sub>8</sub>. Some chlorites are a deep emerald green colour, e.g. MG<sub>5</sub>, whilst others with a higher iron content are green-brown in colour, e.g. Tk<sub>1</sub>.

Calcite is a conspicuous mineral in most slides as a constituent of the ground mass, as inclusions in albite, e.g. Mk<sub>5</sub> and pyroxene, e.g. Mk<sub>4</sub>

(slide A), as amygdules, e.g. Mk<sub>4</sub> (slide A) and Mk<sub>1</sub>, and as veinlets, e.g. No. 1(5). Some calcite filled vesicles show dog-tooth texture, e.g. Mk<sub>1</sub> or patterns of concentric infilling separated by thin zones of concentrated opaques, e.g. Mk<sub>5</sub>.

Opagues. The opaque minerals haematite, rutile, pyrite and leucoxene are present. Opagues occur in many forms. Haematite occurs disseminated throughout and as an integral part of the groundmass where it occupies interstitial areas, e.g. CR<sub>2</sub> or blankets large areas as a dense concentrate, e.g. MkA<sub>2</sub> and Mk<sub>4</sub> (slide A). Haematite imparts a characteristic black or red colour on these rocks. Pyrite occurs as single euhedral cubic grains or as an irregularly shaped clump of grains, e.g. Op<sub>1</sub> and No. 1(1). These may occur in the groundmass, within vesicles or within phenocrysts of albite or pyroxene. Leucoxene occurs in Rk<sub>10</sub>. Opagues in the form of slender needle-like growths, e.g. No. 1(5) and Mh<sub>3</sub>, arranged either in trellis pattern (?sagenite webs) or at right angles to the margins of albite laths, may be rutile. Opagues occur along fractures, around rims of vesicles, e.g. Rp<sub>20</sub> and Mh<sub>3</sub> and in zones of deformation, e.g. No. 1(5).

Epidote and clinozoisite occur in Rk<sub>2</sub> as intergrowths. Clinozoisite shows a characteristic blue tinge on rotating the stage. Much of the epidote is at an advanced stage of alteration and forms irregularly shaped brown patches that are often associated with large areas of chlorite, mafics, or in zones of deformation, e.g. No. 2(4).

#### Accessory Minerals

Quartz occurs as vein infilling or in large irregular patches as crystal mosaics, e.g. Rp<sub>2</sub> (slide A), MG<sub>3</sub>, Rk<sub>10</sub>, and Mk<sub>3</sub>. Quartz is more common in rocks that have been strongly recrystallised, e.g. Rp<sub>19</sub> and MkD<sub>4</sub>.

Green Amphibole occurs in slide Rk<sub>11</sub>. The crystal grains contain inclusions of cubic opaques, circular patches of quartz and irregular patches of calcite.

#### 5.5.2 DEFORMATION

Ductile deformation in many cases produces 'mortar-like' texture in which a muddy fine-grained matrix separates clasts of the host rock. Often rotation of the clasts and flowage of the matrix appears to have occurred, e.g. Rp<sub>7</sub>. Zones of deformation are heavily stained with opaques, e.g. Rp<sub>7</sub>.

Episodes of brittle deformation are indicated by the presence of mineral

recrystallisation, fracturing and veining. Quartz, calcite and chlorite are the prominent metamorphic minerals, e.g. Rp<sub>19</sub> and No. 1(5).

### 5.5.3 MAJOR AND TRACE ELEMENT ANALYSES OF VOLCANIC LITHOLOGIES

#### A. Introduction

In recent years, geochemical analyses have been used as discriminants of magma types and for identifying the original tectonic setting of metamorphosed basic volcanic rocks, particularly in those cases where this cannot be unambiguously deduced from the geology. The method, pioneered by Pearce & Cann (1971, 1973) compares chemical element concentrations in a rock of unknown eruptive setting with their concentration in present day volcanic rocks of known tectonic settings.

Twenty three volcanic rock samples collected from the study area were chosen for major and trace element analyses. Fifteen of these samples are from outcrop localities and eight were found comprising stream bed-load material. All of these samples are from catchments draining Torlesse bedrock lithologies mapped in this study as Wharite Lithotype.

Major and trace element analyses were carried out by Dr B Roser, Victoria University, Wellington. These analyses are presented in Appendix IVc and sample localities are presented in Appendix IVb. Details of analytical methods (x-ray fluorescence) and instrumental conditions used in major and trace element analysis are outlined in Roser (1983).

#### B. Chemical Variations

Volcanic rocks from the study area (Torlesse terrane) have been subjected to alteration processes, the effects of which have been mobilisation and redistribution of many of the major elements (Roser, 1983). The main agent of elemental mobilisation and redistribution is low temperature seafloor alteration (halmyrolysis). Hydrothermal alteration may also contribute to elemental redistribution in some cases, especially where volcanic lithologies occur in association with mineralisation.

The effects of this elemental mobilisation and redistribution, along with regional metamorphism, is the almost total mineralogical reconstitution of lithologies of essentially basaltic composition for which the terms spilitic lava (Reed, 1957b) and metabasites (Roser, 1983) have been used.

Most major elements (e.g. K, Ca, Mg, Na, Si and, to a lesser extent, Fe

and Al) are mobile in rocks affected by the above processes (e.g. Cann, 1969; Pearce, 1975). Consequently, variation diagrams of mobile elements show no systematic variations with SiO<sub>2</sub> because mobility of these elements, together with SiO<sub>2</sub> mobilisation, obscures original trends produced during magmatic processes. In diagrammatic form, elemental mobility and redistribution is indicated by scatter (Fig. 5.1)\*.

Trace elements have been used successfully as discriminants of magma type and tectonic setting. In basaltic systems, trace elements such as Rb, K, Ba, Sr, Th, Zr, Pb, Ti, P, Nb and Y behave as incompatible elements during magmatic processes such as crystal fractionation or partial melting, and so will reflect the composition of the parental magma (Saunders et al., 1979). Of these elements Rb, K, Ba, Sr Pb and perhaps Th are prone to redistribution as a result of alteration. On the other hand Ti, P, Y, Zr and Nb have been shown to be resistant to alteration processes (Cann, 1970; Coish, 1977). The relative stability of these elements may be established by plotting their concentration against Zr, which varies systematically with igneous processes such as fractional crystallisation (Coish, 1977). Coherent trends against Zr reflect these processes, whilst scatter indicates that elemental mobilisation has occurred (Wood et al., 1976). Volcanic rocks from the southern Ruahine Range show systematic increases in TiO<sub>2</sub>, P<sub>2</sub>O<sub>5</sub>, Y and Nb with increasing Zr content (Fig. 5.2). This indicates that these elements are immobile with respect to each other, and it can therefore be inferred that the elemental contents of these rocks represent original magmatic abundances.

Magma types have been differentiated on the basis of alteration-resistant elements such as Ti, P, Y, Nb and Zr. Pearce & Cann (1973) have shown that Y/Nb can be used as a parameter to differentiate between alkaline and tholeiitic magma types even in highly altered or metamorphosed basalts. A Y/Nb ratio for tholeiitic rocks is greater than 2, for alkaline rocks is less than 1 and for transitional rocks lies between 1 and 2. On this basis, eleven of the volcanic rocks from the study area are tholeiitic, nine are transitional and three are alkaline.

The relationships of alteration-resistant elements Ti, Zr and Y have also been used to identify the tectonic setting of basaltic volcanics (Pearce & Cann, 1973).

---

\* These variation diagrams have been designed for rocks of basaltic composition. Trachytes from the study area are therefore not included, e.g. sample Mk<sub>3</sub>.

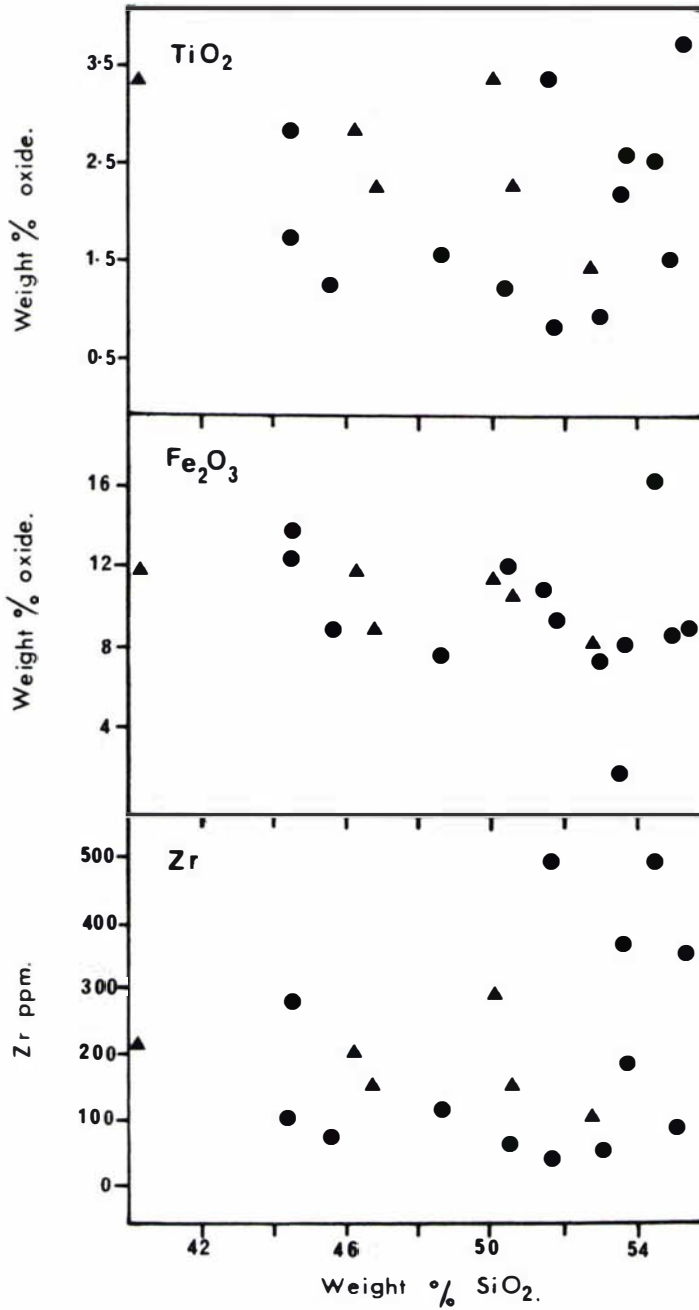
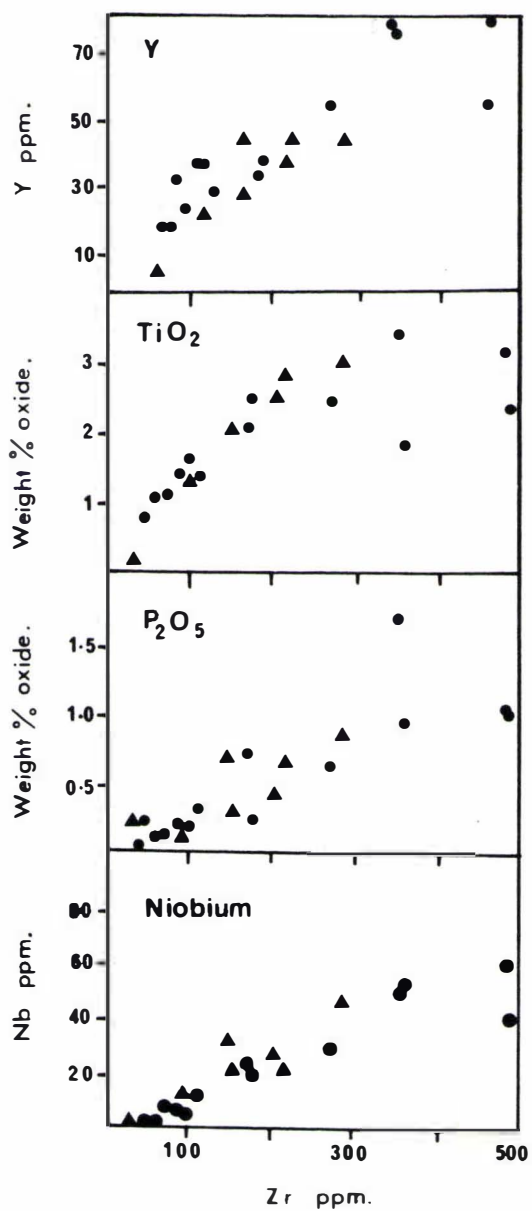


FIGURE 5.1: SiO<sub>2</sub> variation diagram for volcanic samples from the southern Ruahine Range. Dots represent outcrop samples, triangles represent float samples. Note the absence of coherent trends.



**FIGURE 5.2:** Zr variation diagram for volcanic samples from the southern Ruahine Range. Dots represent outcrop samples, triangles represent float samples. Note the systematic increase in major and trace element content with increasing Zr content.



This is achieved by using a Ti-Zr-Y discrimination diagram, developed by Pearce & Cann (1973), which allows visual discrimination between four magma types - intraplate basalts, ocean floor basalts, island arc low-potassium tholeiites, and calc-alkali basalts. A Ti-Zr-Y plot for volcanic rocks from the study area (Fig. 5.3) shows that whilst two samples are clearly of intraplate origin (field D) most fall into the ocean floor basalt field (field B). The fields of low-potassium tholeiites and calc-alkali basalts, however, overlap that of ocean-floor basalts on the Ti-Zr-Y discriminant plot. To clearly separate these, other discriminant plots are required (see Pearce & Cann, 1973). However, for the purposes of this study it is sufficient to illustrate that the samples from the study area are either of ocean-floor or intraplate basalt composition with none of the samples falling within fields A or C (Fig. 5.3).

Ocean floor basalts can also be separated from island-arc basalts using Ti-Cr relations (Pearce, 1975) and  $N_1$  content (Pearce, 1975). Both discriminant methods demonstrate the ocean floor basalt character of these samples. In general, ocean floor basalts are predominantly of basaltic composition and although differentiated rocks in the series basalt-andesite-rhyolite do occur (Aumento, 1969), they are very rare. Ocean floor basalts are generally tholeiitic, but transitional and alkalic varieties occur in some areas, such as the mid-Atlantic Ridge at  $45^{\circ}\text{N}$  (Muir & Tilley, 1964).

A further discriminant plot, the Zr/Y-Zr plot of Pearce & Norry (1979) clearly demonstrates that the volcanic samples from the study area are chemically similar to ocean-floor basalts of both mid-ocean ridge and intraplate nature (Fig. 5.4). Most basalts erupted in an intraplate setting can be identified by their Zr/Y ratios (Pearce & Cann, 1973) of which those with the highest Zr/Y ratios are alkalic (Fig. 5.4) in composition (Pearce & Norry, 1979). Samples of tholeiitic composition within the intraplate field suggest that intraplate basalts are not exclusively alkaline in nature (Roser, 1983). On the basis of major and trace element analyses of 81 metabasites, Roser (1983) concluded that there is no definite evidence for an arc setting, with the samples he analysed being more or less evenly split between mid-ocean ridge and intraplate settings. Confirmatory evidence of the absence of island arc basalts in this area is shown diagrammatically in Figure 5.5 where arc tholeiites are clearly distinguishable from mid-ocean ridge basalts (MORB) on the basis of Ti/V ratios. Arc tholeiites have Ti/V ratios of less than or equal to 20 whereas mid-ocean ridge basalts have Ti/V ratios of between 20 and 50 (Shervais, 1982). However, Ti/V ratios of individual samples are not as diagnostic of tectonic setting as are trends defined by suites

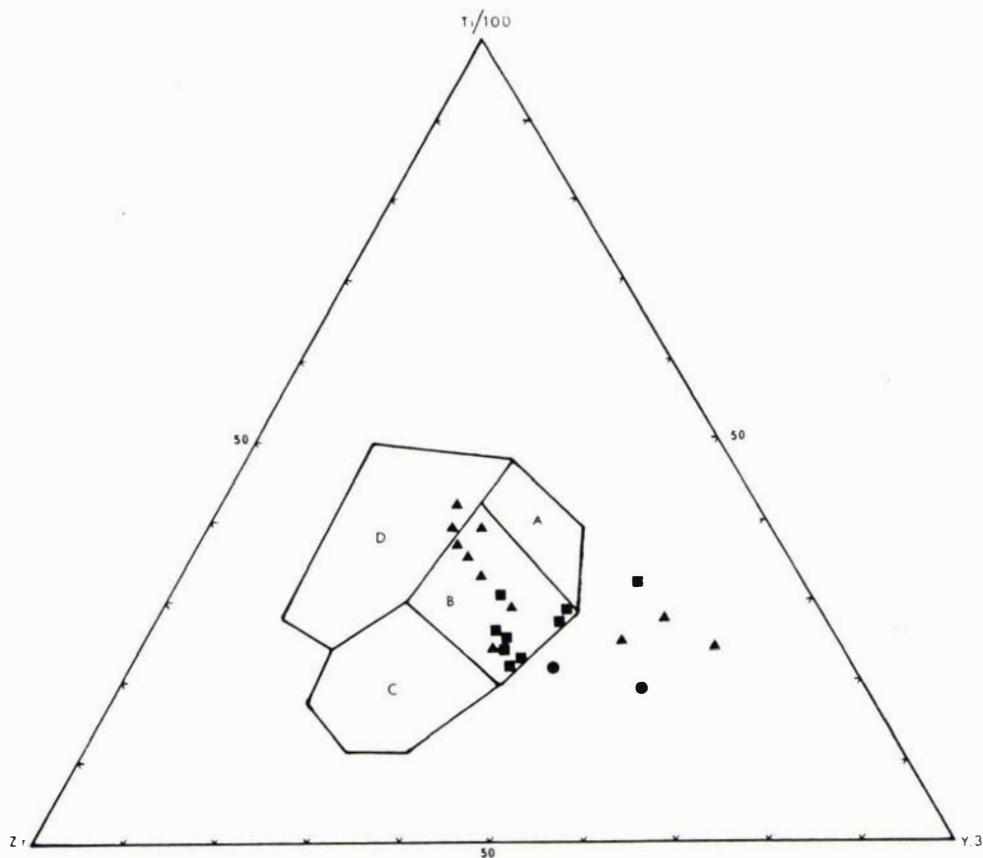


FIGURE 5.3: Ti-Zr-Y discriminant plot, after Pearce & Cann (1973). Fields A and B = low-potassium tholeiites, Field B = ocean-floor basalts, Fields B and C = calc-alkaline basalts and Field D = intraplate basalts. Dots represent alkalic samples, squares represent transitional samples and triangles represent tholeiitic samples.

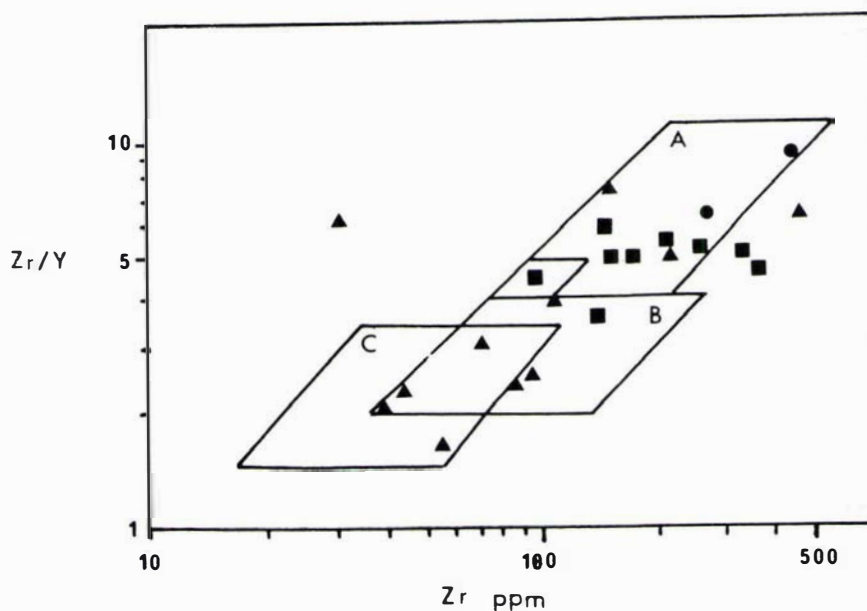


FIGURE 5.4: Zr/Y-Zr discriminant plot of Pearce & Norry (1979). Field A = intraplate, Field B = mid-ocean ridge basalts, Field C = island arc basalts. Dots represent alkalic samples, squares represent transitional samples and triangles represent tholeiitic samples.

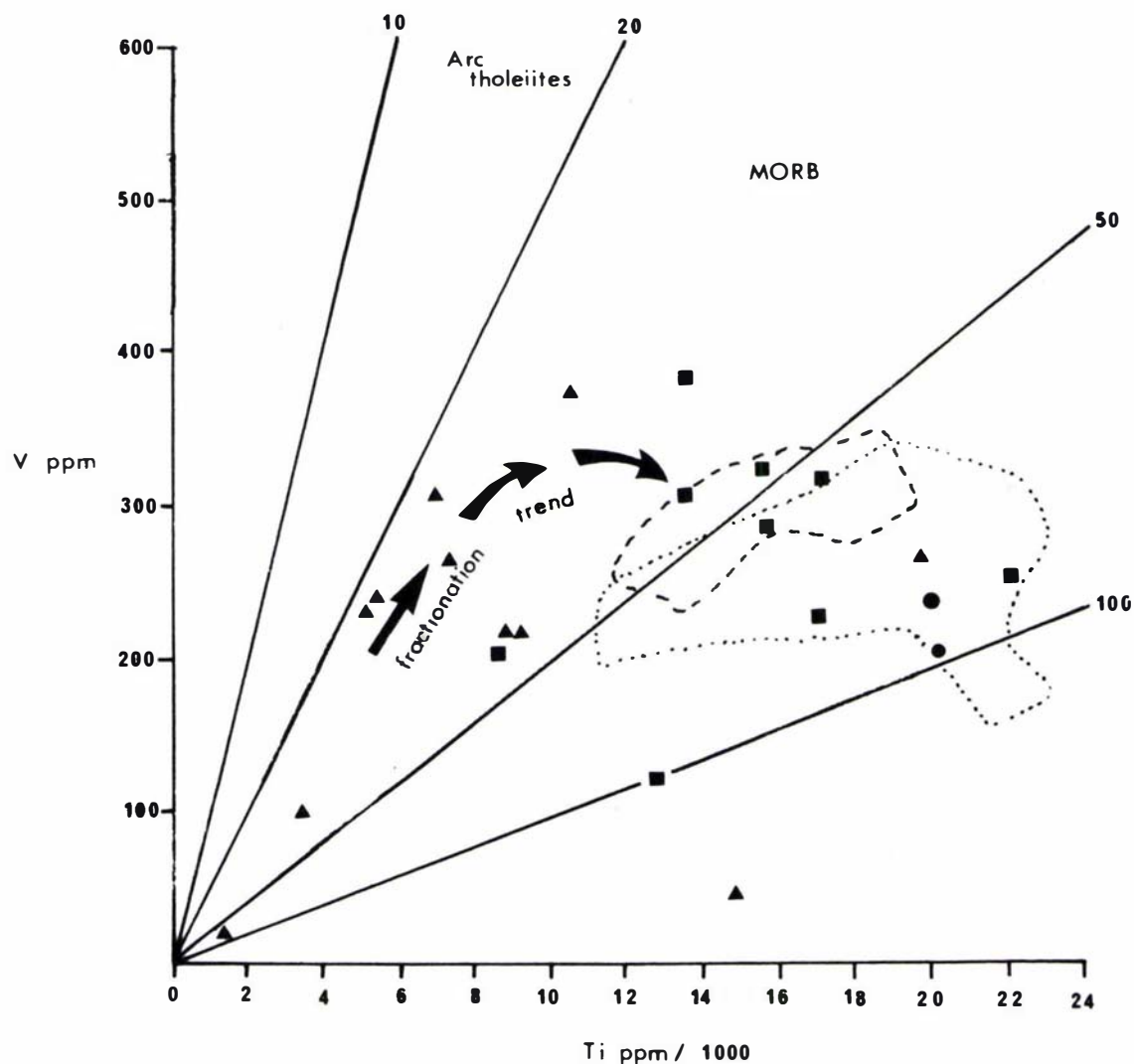


FIGURE 5.5: Ti-V plots of volcanic rocks from the southern Ruahine Range, after Shervais (1982). Dashed and dotted lines enclose fields given by Shervais (1982) for Hawaiian tholeiites and alkali basalts, respectively. Trend lines 10, 20, 50 and 100 are Ti/V ratios. Dots represent alkalic samples, squares represent transitional samples and triangles represent tholeiitic samples.

of related samples that exhibit a range in Ti and V abundances as a result of fractionation. During fractionation, MORB type magma evolves into magmas that have Ti/V ratios the same or greater than the primary MORB. Samples of these magmas define a hypothetical path of fractionation that initially parallels the Ti/V = 20 trend line to then curve across the constant Ti/V ratio line at low angles (Shervais, 1982). This trend is thought to represent fractionation of a MORB type magma from an essentially tholeiitic to an alkalic composition. Such a trend is thought to be characteristic of mid-ocean ridge basalts (Shervais, 1982). Though only poorly defined, due to the small number of samples analysed, samples from the study area show such a trend (Fig. 5.5). The larger number of samples analysed by Roser (1983) has enabled him to establish, with greater confidence, a similar trend for samples from the Torlesse, Waipapa and Haast Schist terranes.

Sporli (1978) suggested that the volcanic rocks of the Torlesse terrane represent tectonic slices of ocean crust and alkalic intraplate seamount volcanics. This suggestion is supported by the chemistry of samples from the southern Ruahine Range (Torlesse terrane) and by those of Roser (1983) from the Torlesse, Waipapa and Haast Schist terranes. The volcanic lithologies are thought to have been incorporated within greywacke sediments in an accretionary prism at a subduction margin (see Chapter 7).

The more silicic samples analysed in this study (trachytes and andesites) may represent tectonically included fragments of more differentiated oceanic volcanics, for example, a differentiated series of lavas ranging from basalt to quartz trachyte has been described from the intraplate volcano - Réunion Island (Gillot & Nativel, 1982), and benmoreites and rhyolites occur on Bouvet Island on the mid-Atlantic Ridge (Le Roex & Erlank, 1982). This interpretation should be viewed with caution however, as many of the volcanic samples from the southern Ruahine Range were not found *in situ* but instead occur as isolated clasts within diamictites. It is therefore equally likely that the more silicic samples formed at a different tectonic setting to that at which the basaltic samples formed. Thus the mixed assemblage of volcanic rocks in this area may represent erosion products from more than one volcanic terrane. However, in view of the absence of volcanic lithologies 'exotic' to the Torlesse terrane in the southern Ruahine Range, the former interpretation is preferred.

### C. Conclusions

Major and trace element analyses of volcanic lithologies from the southern Ruahine Range have been used to determine magma type and to define tectonic setting. Of the samples analysed, eleven are tholeiitic, nine transitional and three alkaline. These samples are similar chemically to oceanic basalts, the majority of which are considered to have been erupted in a mid-ocean ridge setting with the minority of samples appearing to have chemical affinities characteristic of an intraplate setting. None of the samples appear to have been derived from an island arc setting.

#### 5.6 CHERT

Red coloured cherts are heavily stained with haematite, e.g. Wh<sub>3</sub>. Other cherts of white, cream, pink and green colouration appear to derive their colour from the presence of admixtures of haematite, chloritic minerals and carbonate, e.g. No. 1(2). Grey coloured cherts show varying fields of microcrystalline to cryptocrystalline sized aggregates of quartz. Several episodes of veining have been recognised. An early set of veins containing quartz have been offset by a subsequent set of chlorite veins. Both of these sets of veins have in turn been offset by a later set of quartz veins, e.g. MG<sub>1</sub>.

Quartz veins characteristically contain euhedral crystals arranged in a mosaic. Other veins consist of fibrous silica (chalcedony) arranged at right angles to the walls of the vein, e.g. Rp<sub>18</sub>. Still other veins contain microcrystalline quartz, e.g. MG<sub>1</sub>. Some veins have very sharp margins, e.g. MG<sub>1</sub> but others have gradational or diffuse edges, suggesting that the mineral veins were growing at the expense of the host rock, e.g. Rp<sub>18</sub>. Chlorite showing anomalous blue interference colours is sometimes present in quartz veins, e.g. MG<sub>1</sub> as are ?prehnite needles, e.g. Rp<sub>18</sub>. Carbonate (calcite) replacement of quartz in veins is the latest recognised phase of mineralisation. Calcite replacement of the chert groundmass is a common feature and appears to be best developed in those cherts associated with copper bearing ores, e.g. Co<sub>4</sub>.

Pyrite occurs as disseminated grains throughout the groundmass in some cherts, e.g. MG<sub>1</sub>. Haematite occurs either as a vein mineral, e.g. No. 1(2) or is finely scattered throughout the iron stained groundmass, e.g. MG<sub>1</sub> and Wh<sub>3</sub>. Differing concentrations of haematite define a crude parallel layering in sample No. 1(2) that may represent a primary depositional feature.

Poorly preserved radiolarian casts occur in sample MG<sub>1</sub>. In other samples, spherical objects replaced by radiating needles of chalcedony may represent pseudomorphs of radiolarian casts, e.g. No. 1(2), or spherulites of silica.

## 5.7 CALCAREOUS LITHOLOGIES

### 5.7.1 MICRITIC LIMESTONE (BIOMICRITE) (T23/f7530)

This limestone (Po<sub>5</sub>) consists of a micritic groundmass and numerous fragments of a diverse microfauna (see Chapter 4). Rock fragments include both clastic and basic volcanic lithologies. Secondary minerals include patches of mosaic quartz and sparry calcite together with disseminated specks of opaques (pyrite). Traces of prehnite are present, thereby indicating that this allochthonous block of limestone of Late Triassic age has not been subjected to metamorphism of a higher grade than the surrounding clastic sediments of Late Jurassic age within which it is embedded.

### 5.7.2 CALCAREOUS SILTSTONES

The majority of lithologies of calcareous composition are replaced siltstones. Replacement has occurred to varying stages, ranging from almost complete replacement by micrite, e.g. No. 1(4) or microspar, e.g. MG<sub>4</sub> to partial replacement, e.g. Rk<sub>15</sub> (slide A), Mh<sub>4</sub> and MG<sub>6</sub>.

Detrital grains of feldspar, quartz, mica and heavy minerals are common constituents. Carbonaceous or argillaceous material is present in sample MG<sub>6</sub>. Disseminated iron oxide (pyrite) is a common constituent, e.g. Rk<sub>15</sub> (slide A), and NRS<sub>3</sub> (slide B). Haematite occurs either as a concentrate along vein or shear margins, e.g. No. 1(6) or as a light reddish stain throughout the groundmass, e.g. MG<sub>4</sub>. Cross-cutting veins or pods of sparry calcite and mosaic quartz, e.g. Op<sub>2</sub> and No. 1(6) are of secondary origin. Offset veins indicate that several episodes of veining have occurred, e.g. Wh<sub>4</sub>.

Microfossils occur in samples Rk<sub>15</sub>, NRS<sub>1</sub>, Mh<sub>2</sub> and NRS<sub>3a</sub> and <sub>3b</sub>. Some have a double-ring structure of which the outer ring may be solid, e.g. NRS<sub>1</sub> or the outer ring may be porous, e.g. Rk<sub>15</sub> (slide). The central portion consists of a structureless infilling of calcite. Others have been wholly replaced by either sparry calcite or micrite. They range in size from 0.05-0.4 mm in diameter and have tentatively been identified as radiolarian and possibly some foraminifera. Primary sedimentary structures such as discontinuous laminae are present in sample Wh<sub>4</sub>. Spherulitic texture was observed in sample Mp<sub>2</sub>. Cone-in-cone structure comprising fibrous calcite

was observed in sample Un<sub>2</sub> (slides A and B). Riedel shears as sites of secondary quartz crystallisation are present in sample No. 1(4).

### 5.7.3 CALCAREOUS CONGLOMERATE

The large buff-coloured calcareous pebbles so obvious in the field (Fig. 2.23) are either almost pure micrite or calcareous siltstones, e.g. Mtu<sub>1</sub>, Rk<sub>1</sub> and Rk<sub>3</sub>. These pebbles are embedded in sandstone matrix comprising rock fragments, heavy minerals and detrital grains. Rock fragments include chert, clastics and fine-grained volcanics. Detrital grains include quartz, feldspar and micas. The matrix has in places been replaced by secondary calcite. Calcite replacement of detrital quartz and particularly feldspar is evident. Pyrite is a minor but obvious constituent of these conglomerates, e.g. Rk<sub>3</sub> and is seen in outcrop as pyrite nodules (Fig. 2.23). Microfossils (see Chapter 4) have been found within the matrix of samples Mtu<sub>1</sub> and Rk<sub>1</sub> (slide A). The large calcareous clasts appear to be unfossiliferous. However, indistinct spherical casts similar to those seen in calcareous siltstone lithologies elsewhere and tentatively identified as microfossils are present in sample Mtu<sub>1</sub> (slide B). Macrofossil fragments also appear to be present within the matrix of these calcareous conglomerates, e.g. Mtu<sub>1</sub> (slide B) and Rk<sub>1</sub> (slide A).

### 5.8 PROVENANCE

Sandstones and siltstones examined from each of the three lithotypes are texturally and compositionally similar, the constituents of which are thought to have been derived from a common source. Compositional and textural immaturity of the sandstones and siltstones and the enormous volume of the Torlesse indicate a substantial continental source. The high quartz and feldspar content, the presence of perthitic and myrmekitic textures in some grains and moderate mica content suggest that the bulk of the mineral constituents was derived from a quartzofeldspathic plutonic provenance.

In general, sedimentary rock fragments predominate, volcanic (including chert) and carbonate rock fragments are abundant while metamorphic and plutonic rock fragments occur only in minor amounts. The predominance of sedimentary and volcanic rock fragments indicate a mixed source. The rarity of plutonic rock fragments in sandstone as compared to the abundance of plutonic grains may be explained if plutonic rocks had been broken down to their constituent grains by weathering and transport before reaching the site of deposition, or if the plutonic grains were reworked from older Torlesse rocks.

Conglomerate pebbles also indicate a mixed source, the composition of the constituents being of similar proportions to the lithic rock fragment content in sandstones and siltstones. However, plutonic and metamorphic pebbles are more conspicuous in conglomerates than in sandstones with many showing strongly perthitic k-feldspar, e.g. Op<sub>3</sub> and ET<sub>1</sub>.

An anomalously high concentration of volcanic rock fragments within sandstones and of volcanic pebbles within conglomerates occurs in the Mangatera foothill and East Tamaki River areas. This may be explained by fluctuations in the rate of supply of detritus from the mixed source areas. The high proportion of volcanic lithologies is also suggestive of rapid or short transport and/or rapid deposition before breakdown of the volcanics to their constituent grains can occur. Well-rounded conglomerate pebbles of quartzofeldspathic sandstone and argillite are suggestive of reworking. These and other pebble constituents (particularly volcanic and chert) contain mineralised cracks and veins not present in the host rock, thereby indicating that they were derived from an older terrane that had been buried and indurated prior to uplift and erosion. Many conglomerates of post-Permian age, elsewhere in New Zealand, are also believed to have been derived by cannibalistic reworking of older Torlesse rocks (Andrews *et al.*, 1976; Smale, 1978; MacKinnon, 1980). Quantitative evidence for reworking is given by MacKinnon (1980) who showed that most sandstone clasts comprising conglomerates are indistinguishable from coeval or older Torlesse rocks.

Volcanic rock fragments in sandstones and siltstones and volcanic pebbles in conglomerates are identical in composition to lavas found in the study area. Chemical analyses of the latter indicate that they are of mid-ocean ridge (ocean plate boundary) and intraplate (ocean plate) origins (see Section 5.5.3). These lavas of essentially basaltic composition and associated cherts are likely to be older than the proposed Late Jurassic age of deposition of the bulk of the sandstone, siltstone and argillite within which they are incorporated (see Chapter 4). An indication of the likely age difference between these materials is provided by Feary & Pessagno (1980). They dated radiolaria from chert within Early Cretaceous Torlesse rocks of the North Island as being of Early Jurassic age, that is, about 50M years older than the fossils in the surrounding greywacke sediments.

Provenance of the limestone block at T23/f7530 and of calcareous conglomerate boulders is unknown. Both are fossiliferous and clearly of shallow water origin, yet occur within unfossiliferous sediments of deep marine



origin. The known Late Triassic age of the limestone block (see Chapter 4) indicates that it is allochthonous. Thus a similar origin and age is proposed for the undated, fossiliferous calcareous conglomerates. Carbonate pebbles of similar lithology occur within clastic conglomerates indicating that the former are also likely to have formed part of the Torlesse source terrane. These allochthonous lithologies are of the same metamorphic grade as the sequences within which they are now contained, thus indicating that the source terrane had not been subjected to metamorphism of greater than the prehnite-pumpellyite grade.

It is not known which, if any, of the lithologies described above occurred together in the same source terrane(s). The diversity of lithologies now comprising the lithotypes within the study area indicates that they were derived from mixed source terranes. The age of these former source terranes is largely unknown but at least some of the lithological components were eroded from a terrane comprising Late Triassic aged limestones.

C H A P T E R    6

LATE QUATERNARY TECTONICS

CONTENTS

	<u>page</u>
6.0 PREVIOUS WORK AND CONTINUING INVESTIGATIONS ... ..	142
6.1 FIELD METHODS ... ..	142
6.2 NAMING OF FAULTS ... ..	145
6.3 CLASSIFICATION OF FAULT ACTIVITY ... ..	145
6.4 FAULT TRACE DATA ... ..	147
6.5 HISTORIC DISPLACEMENT ... ..	148
6.6 DESCRIPTION OF ACTIVE FAULTS ... ..	148
6.6.1 WELLINGTON FAULT ... ..	148
A. Vertical Displacement ... ..	149
B. Horizontal Displacement ... ..	151
C. Dating and Correlation of Fault Displaced Late Quaternary Alluvial Terrace Surfaces ... ..	153
1. Terraces displaced by the late Quaternary trace of Wellington Fault .. ...	156
2. Interpretation ... ..	159
D. Parallel Traces ... ..	161
E. Tilted Wedge ... ..	162
F. Tilted Terrace Surface ... ..	164
6.6.2 SPLAY FAULTS ... ..	164
A. Mangarawa Fault ... ..	165
B. Beagley Road Fault ... ..	165





## CHAPTER 6

### LATE QUATERNARY TECTONICS

#### 6.0 PREVIOUS WORK AND CONTINUING INVESTIGATION

Many early geologists made mention, and realised the significance, of major fault lines bordering the flanks of the northern Tararua Range and southern Ruahine Range in the vicinity of the Manawatu Gorge, (e.g. Thomson, 1914; Ongley & Williamson, 1931a). Firth & Feldmeyer (1943) and Ower (1943) were first to prepare geological maps of this area upon which faults are shown. These were later incorporated on the maps of Dannevirke Subdivision by Lillie (1953). The most recent geological map of this area is at 1 : 250 000 and portrays the faults known to be active or inactive (Kingma, 1962). A number of unpublished theses contain additional information on the faults in the vicinity of the Manawatu Gorge. Theses by Rich (1959), Piyasin (1966), Grammer (1971), Carter (1963) and Zutelija (1974) are most useful.

To monitor secular and earthshift deformation in this region, the New Zealand Geological Survey has installed a survey pattern across the Wellington Fault immediately to the north of Woodville (Blick, 1976; 1977).

#### 6.1 FIELD METHODS

The fault traces shown in the mapped area (Fig. 6.1) are based upon aerial photograph interpretation and extensive field mapping during which details of features not clearly visible on the photographs were plotted and field measurements made. Extensive field reconnaissance was necessary because much of the area is heavily bush clad, so many geomorphic features associated with fault activity are masked by vegetation. In such areas linear features, though suspected of being faults, are initially mapped as lineations because of the lack of evidence supportive of fault activity in the field. However, in most instances the major lineations visible on low altitude aerial photographs and Landsat images can be verified in the field by the location of fault planes with or without gouge, and/or fault crush zones. Eastward and westward flowing streams draining perpendicular to the strike of the major northeast trending faults provide the major ex-

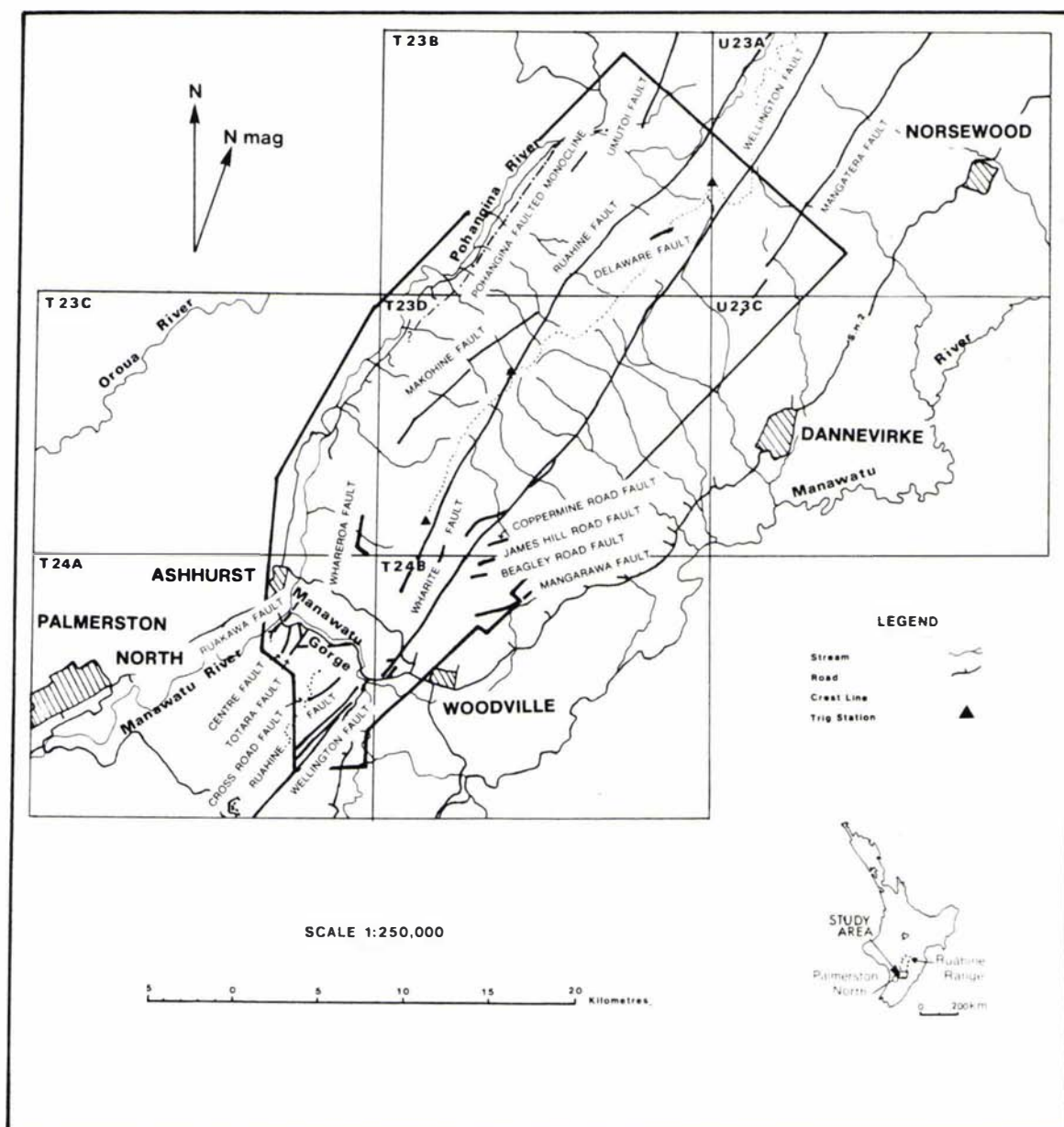


FIGURE 6.1: Reference map of the mapped region (heavy outline), showing map-sheet boundaries, major faults (solid line) and faulted monocline (dot-dash line).

posures supportive of faulting.

All traces that demonstrate positive evidence of Late Quaternary faulting are shown on Map 4. Measurements of lateral displacements were made by pacing. Vertical measurements were recorded where possible but on slopes lateral offset commonly precluded accurate determination of vertical displacement. Similarly, vertical displacement on slopes commonly precluded accurate determination of lateral offset so only scarp heights could be noted in such cases.

Those features that may be explained by other causes such as gravity movements have been shown using a different symbol. These include slumps, ridge-top scarps (gravity fault traces of Beck, 1968), ridge-top benches and ridge-top depressions (Tabor, 1971) that invariably parallel topographical 'highs'. They are likely to have been triggered by earthquakes but are not in themselves of tectonic origin. A relationship between major fault zones and the incidence of large-scale slump movements in this area is clearly established (Marden, 1981 and Chapter 10).

Topographical features of tectonic origin that do not in themselves show positive evidence of Late Quaternary faulting but together define traceable fault traces are shown with the use of symbols (Appendix Va, Abbreviations - Tectonic Data). These traces have been mapped in this way because the absence of measureable displacements of Late Quaternary age in the vicinity of the traces precludes determination of the age of the last period of fault movement. Such traces are nonetheless considered to be active (see Classification of Fault Activity). Where the sense of vertical movement is known for these features of tectonic origin the symbols used to denote them are placed on the upthrown side.

Steeply inclined bedding plane faults and low-angle thrusts within Torlesse bedrock are indicated on Map 4 with strike and dip symbols.

In the west of the mapped area features of tectonic origin are poorly preserved within Plio-Pleistocene marine deposits that flank the southern Ruahine Range. Here many large-scale gravity movements, although possibly triggered by earthquake shaking, cannot be shown to be aligned along known Late Quaternary fault traces. Their presence, however, may be related to a monoclinial structure that parallels the major tectonic fault traces in this area.

Faults of pre-Late Quaternary age are predominantly contact faults be-

tween Torlesse bedrock and the overlying Plio-Pleistocene marine deposits. Rejuvenation of movement along most of these contacts is often difficult to establish because of the absence of Quaternary surface features in the vicinity of the contact faults. However, Late Quaternary displacement along contact faults can be demonstrated at several localities in this area, indicating that these faults may be rejuvenated. This evidence is justification for including all contact faults on the Late Quaternary map (Map 4). It should be noted that the unconformable contact between Torlesse bedrock and younger sediments is not everywhere a fault contact.

## 6.2 NAMING OF FAULTS

As a result of the numerous studies involving faulting in the local area a number of major fault traces have been renamed many times. For those faults with traces largely confined to the local area, an established name proposed by a previous author has been adopted. However, there is one exception. The trace of Wellington Fault has been delineated from Wellington to the Manawatu Gorge and northwards on to Lake Waikaremoana as a continuous trace (Lensen, 1958). Within the local area, near Kahuki (T24A/470890), the Wellington Fault trace splinters into two traces, the northern extensions of which are referred to as the Ruahine and Mohaka Faults (Kingma, 1962). The name Ruahine Fault has been adopted for the westernmost fault trace. However, the name Wellington Fault (Wellman, 1948) has been chosen in preference to Mohaka Fault. The tectonic significance and regional extent of this trace, along which Late Quaternary movements are evident throughout its length is the justification for the use of the name Wellington Fault in the mapped area. Newly discovered fault traces have been assigned names largely derived from the local area.

## 6.3 CLASSIFICATION OF FAULT ACTIVITY

The classification of active faults is that described in detail by Officers of the Geological Survey (1979). The dating of movements on a fault is based upon the age of the deposit or surface displaced by the fault trace. Where the age of the reference surface is not accurately known, the history of fault movements becomes particularly difficult to relate to an absolute time scale. Fortunately, during the course of this study a number of radiocarbon dates (Appendix Vb) have been obtained from displaced reference deposits in the vicinity of the Wellington Fault. These dates indicate the approximate age of



the displaced surface but do not indicate when displacement occurred. This allows for only average rates of fault displacement to be calculated.

In the mapped area the Wellington Fault has repeatedly displaced alluvial terrace surfaces of pre-Ratan, Ratan (30-40 000 years B.P.), (Milne, 1973a), Ohakean (10 000 to 25 000 years B.P.) and Holocene (<5 000 years B.P.) age. Throughout the length of this Fault, fresh displacement features are common and it has therefore been classified as a Class I Active Fault. The James Hill Road Fault displaces an alluvial terrace surface of Ratan age. Repeated movement is suspected, however a lack of evidence for movement in the last 5000 years indicates that it is a Class II Active Fault. The Mangarawa Fault displaces surfaces of pre-Ratan and Ratan ages. Repeated movement can be demonstrated. Movement along this Fault has not occurred in the last 5000 years, therefore it has been classified as a Class II Active Fault. Coppermine Road Fault displaces alluvial surfaces of Ratan and Ohakean age. As the youngest of the displaced surfaces is not thought to be as young as 5000 years B.P. and because more than one movement cannot be demonstrated, this Fault has been classified as a Class II Active Fault. Beagley Road Fault displaces marine deposits of Plio-Pleistocene age only. The timing of displacement is unknown but because the strike and physiographic expression of this fault is similar to those above and because it lies in close proximity to them, Beagley Road Fault is also classified as a Class II Active Fault.

The Makohine, Whareroa, Umutoi, Centre, Mangatera and Ruahine (in south) Faults are contact faults separating Torlesse bedrock from Plio-Pleistocene marine deposits. The absence of geomorphic features suggestive of recent fault displacement is interpreted as indicating they have not been active during the last 5000 years, nor is evidence of movement over the 5 000 - 50 000 year period preserved. Only one period of movement can be demonstrated and this may have taken place during the 50 000 - 500 000 year period. However, because the Late Quaternary trace of Wellington Fault coincides with the contact between Torlesse bedrock and Plio-Pleistocene marine deposits at several localities, and because Wharite Fault is a contact fault showing clear signs of Late Quaternary displacement, it is considered that all contact faults in the mapped area may be 'Potentially Active Faults'. Supportive evidence includes similar strike and physiographic expression between contact and active faults.

The Ruahine Fault, by virtue of its location within the Ruahine Range, is very poorly preserved. Severe erosion within upper catchments has largely removed fault displaced physiographic features along it, so most of the evidence for locating this fault is based on outcrops of fault gouge within Torlesse bedrock. Absence of fault displaced surfaces of known age preclude any classification of activity of the Ruahine Fault. As mentioned above, this fault is in part a contact fault, displacement along which may have taken place during the 50 000-500 000 year period. As with other contact faults in this area, some of which show definite signs of Late Quaternary displacement, the Ruahine Fault is considered to be a 'Potentially Active Fault'.

The classification of those faults that displace exhumed surfaces of marine planation carved into Torlesse bedrock is uncertain. Good preservation of features of tectonic origin such as are seen along traces of the Totara, Cross Road and Delaware Faults suggest that at least one period of fault displacement has taken place as recently as Late Quaternary time. It is not considered likely that these fault traces have been exhumed. At present these faults are classified as Late Quaternary fault traces. Repeated movement cannot be proven on these faults so a classification of activity cannot be presented.

Te Punga (1957) identified several large-scale active structures referred to as 'live anticlines' lying to the west of and parallel to the Ruahine Range. Within the mapped area Plio-Pleistocene marine deposits have been upwarped into a monoclinial structure that has in places been faulted without forming a discrete surface trace. The Pohangina Faulted Monocline is a structure along which continued uplift could result in further fault displacement. Such features are classified as 'Potentially Active Faults'.

The majority of fault planes shown on Map 4 coincide with bedding or foliation strike within Torlesse bedrock. These fault planes are considered likely surfaces for potential future movements either along the same plane or along parallel planes and therefore are considered to be in an 'Active Bedding Fault Area'.

#### 6.4 FAULT TRACE DATA

Each locality where data have been recorded is identified by a three-digit number following the relevant NZMS 260 quarter sheet number. This data point number is plotted on the upthrown side of the fault.

The data (Appendix Va) have been stored in a retrieval system as part of a wider programme.

Horizontal and vertical offsets of data points listed in Appendix Va are, in general, the components of net offset across the fault of a correlatable feature. Where two or more traces of the fault are present the net offset is usually the algebraic sum of the offsets on each trace. Where only one component of the offset (either vertical or horizontal) is listed, post-faulting modification of the feature such as river erosion, may have occurred. In cases where modification has decreased the amount of apparent offset (for example, cutting back of a terrace riser), the measurement listed is a minimum for offset of the feature. A vertical offset for a terrace riser by convention, refers to the surface at the top of the riser.

The scarcity of displacement data along all but the Class I and II faults in the mapped area does not permit horizontal or vertical displacement rates, or periodicity of movement to be calculated.

## 6.5 HISTORIC DISPLACEMENT

No fault displacements within historic times (since c. 1870 AD) have been recorded on faults in the mapped area. However, in 1931 during the Hawkes Bay earthquake (100 km to the northeast) there was considerable ground displacement and mass movement (Henderson, 1933) some of which occurred in parts of the northern Ruahine Range (Conly, 1980). Similarly the Wairarapa earthquake (70 km to the southeast) in 1942 was also accompanied by local ground displacement and mass movement (Ongley, 1943a, 1943b).

## 6.6 DESCRIPTION OF ACTIVE FAULTS

### 6.6.1 WELLINGTON FAULT

The Wellington Fault demarcates the eastern margin of the southern Ruahine and northern Tararua Ranges over much of their length. The Late Quaternary trace of Wellington Fault consists of an almost unbroken lineament of fault features that can be readily traced throughout the length of the mapped area, a distance of 45 km.

In the far north of the mapped area the trace solely displaces Torlesse bedrock and delineates the base of the Range. It separates the main axis of the Range to the west from the Mangatera foothills to the east.

The main channels of the Rokaiwhana Stream, West Tamaki River and the upper reaches of Cattle Creek drain along the trace for considerable distances. Here the surface trace of Late Quaternary fault movement coincides with earlier displacements which resulted in considerable vertical movement to form the Range.

Further to the south, the trace in part coincides with the contact between marine deposits of Plio-Pleistocene age to the east and Torlesse bedrock to the west. In the far south of the mapped area the trace displaces marine deposits of Plio-Pleistocene age and Late Quaternary fluvial terraces within drainage channels of major eastward draining streams. Here the expression of the latest movement on this fault consists of a near continuous principal trace which in places bifurcates into short discontinuous traces to the west of, and parallel to, the principal trace (see Parallel Traces). In addition, Late Quaternary fault displacement, possibly associated with movements along the Wellington Fault, has involved creation of splay faults lying to the east of this trace. These splay faults include Mangarawa, Beagley Road, James Hill Road and Coppermine Road Faults. Splay faults to the west of the principal trace of Wellington Fault include Delaware Fault and an unnamed fault at T24B/207 (Inset B).

#### A. Vertical Displacement

Measurement of the true vertical component of fault displacement is restricted to a few localities only. This is because in most instances post-displacement aggradation and/or erosion have modified the true value of displacement for a reference surface. The amount of Late Quaternary vertical displacement along the trace of Wellington Fault has not been uniform because in some localities older surfaces are displaced by lesser amounts than surfaces of younger age. For example, a surface of ?Porewan age at T23D/653-654 has been displaced by 0.5m whereas most surfaces of Ohakean and even Holocene age have been displaced by equal or greater amounts (see Dating and Correlation of Fault Displaced Late Quaternary Alluvial Terrace Surfaces). Also surfaces of similar age have been displaced by varying amounts. For example, the greatest amount of measured vertical displacement is of a surface of ?Porewan age. At T24B/238 this surface has been vertically displaced by about 10m whilst at T23D/645-647 it has only been displaced 0.5m to 2.0m. It therefore seems likely that either reversals in the direction of vertical displacement have occurred or vertical displacements have been differential along the length of Wellington Fault.

The upthrown side along the Wellington Fault changes repeatedly, the changes in some cases being associated with small changes in strike (compare T24A/026 with 032, Inset E, and T23D/694 with 695, Inset A). In general, New Zealand's faults are not entirely reverse, transcurrent, or normal in character, but are hybrids resulting from shear under either tension or compression (Lensen, 1976). The changes in upthrown side (Lensen, 1964; 1968a) imply that the angle between the strike of the dominantly transcurrent fault and the PHS (Principal Horizontal Shortening) direction is close to the critical angle at which a small change in the strike of the fault results in a change from the reverse to a normal component and *vice versa* (Lensen, 1962; Lensen & Otway, 1971). An easterly swing in strike is associated with a change in upthrown side from the southeast to the northwest. Similar changes of upthrown side with changing strike have been demonstrated along faults in Marlborough (Lensen, 1962) and along other sections of Wellington Fault (Lensen, 1969). Changing upthrown side with time but without changes in strike has been demonstrated by Lensen (1964; 1968b, 1969) for faults with a strike close to that of a purely transcurrent fault. In all cases reversals occurred in post-glacial time and imply either a small dextral change in PHS direction or a small sinistral rotation of the eastern part of New Zealand (Lensen, 1976).

During the period of rapid uplift of the Ruahine and Tararua Ranges it is considered likely that the vertical component of uplift was largely controlled by faults bordering the flanks of these Ranges. In particular, much of this vertical uplift took place along the steep eastern flank of these Ranges and would therefore have been controlled by the Wellington Fault. During this period of uplift the western side of Wellington Fault was upthrown relative to the eastern side. Present day evidence along the Late Quaternary trace of Wellington Fault indicates a change in upthrown side to the east of the trace. Much of the evidence for an upthrown eastern side is preserved in Plio-Pleistocene marine deposits and Torlesse bedrock. Fault displaced alluvial terrace surfaces of Ohakean and Holocene ages are equally upthrown either to the east or to the west sides of the trace. Although exceptions are to be found, it appears that the latest phase of uplift is to the east of the Wellington Fault trace.

Repeated vertical uplift during Late Quaternary times can be demonstrated at T23D/691a (Inset A) and T24B/205a (Inset B) where older scarps have been rejuvenated by more recent movements along the same trace. At both

localities the rejuvenated scarps display small amounts of vertical uplift of 1m and 0.5m, respectively. At the latter locality the rejuvenated scarp has been partially modified by man. Elsewhere, rejuvenated movement along existing traces has resulted in scarp collapse, for example at T24B/229 (Inset C). Evidence of repeated vertical uplift in earlier Quaternary times is preserved in the form of truncated spurs in Torlesse bedrock along the faulted eastern flank of the Range (see Truncated Spurs).

#### B. Horizontal Displacement

The most common evidence for horizontal displacement in this area is in the form of shutter ridges, where the ridge is displaced across the path of a drainage channel and results in offsetting the channel. All the shutter ridges in this area involve dextral displacement of either Plio-Pleistocene marine deposits or Torlesse bedrock. Amounts of shutter ridge displacement involving marine strata vary from a maximum range of 80-90m (T23D/638 and T23B/244) to a minimum range of between 20-30m (T24B/254 and T23D/642). Displaced shutter ridges in Torlesse bedrock can be seen at localities T23D/780, 781 and T23B/296 in Rokaiwhana Stream catchment. At each of these localities horizontal offsets of approximately 250m have been measured from aerial photographs. These are minimum values of offset since the leading end of the ridges have been reduced in length by subsequent fluvial erosion. At T24B/201a a spur comprising limestone of Nukumaruan age has been horizontally displaced by 20m. At T24B/218 and T24B/224 streams have been offset by 20m and 35m, respectively, by dextral transcurrent movement. The most important displacement occurs where a terrace riser of Porewan age has been offset at T23D/726 (Inset I). Here there is a total dextral transcurrent displacement of 150m (Fig. 6.2). The most recent evidence for horizontal displacement is in the form of offset stream channels upon alluvial terrace surfaces, the best of which are preserved at T24B/232 (Inset C). Here a terrace surface on the up-thrown western side of Wellington Fault is traversed by two abandoned shallow channels approximately 9m apart. The distance between the two channels may represent an episode of horizontal displacement during which the northernmost channel was abandoned and the southernmost channel formed. On the downthrown eastern side of the fault a single terrace edge approximately 40m to the south of the channels is here correlated with the northernmost channel. This displacement of 40m is a minimum value as subsequent fluvial erosion has removed evidence of

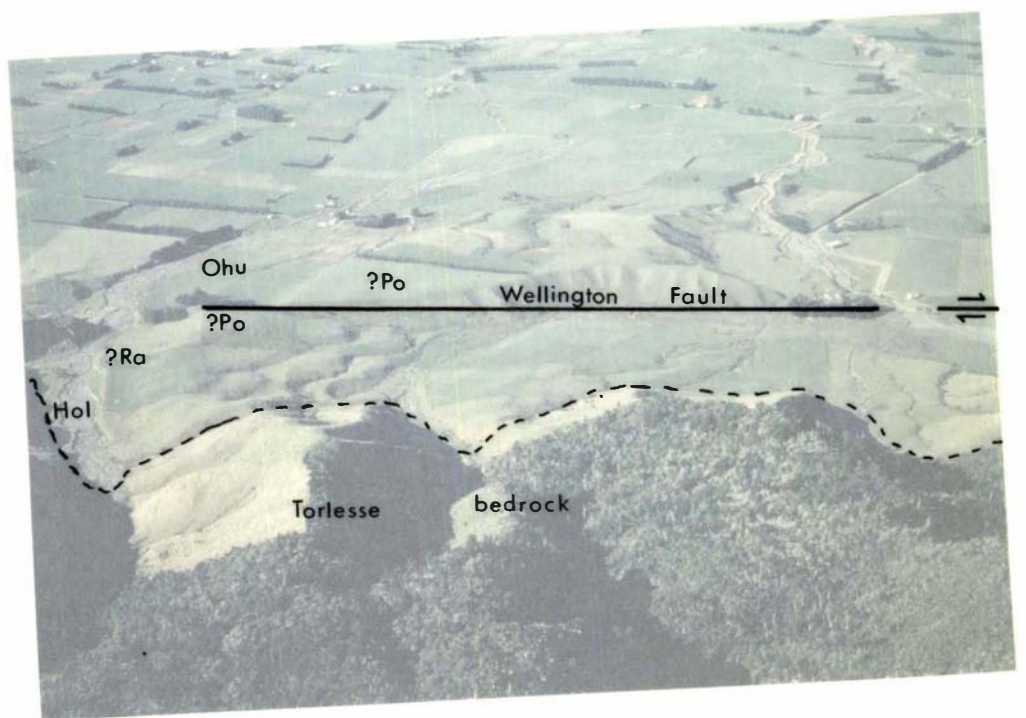


FIGURE 6.2: Dextral transcurrent displacement of high level terrace surface of ?Porewan age on Wellington Fault trace. Horizontal displacement of terrace riser is approximately 150m (see Inset I). View looking eastwards. Stream at left of photograph is Mangapukakakahu Stream. (photo : V E Neall)

both channels on the downthrown side.

C. Dating and Correlation of Fault Displaced Late Quaternary Alluvial Terrace Surfaces

Most of the rivers and streams in this area display suites of terraces formed by oscillations in climate, coupled with orogenic uplift during the Late Pleistocene. Successive episodes of colder, drier climate resulted in formation of aggradational terraces. These alternated with episodes of warmer, wetter climate to produce degradational terraces.

Much of the previous research dealing with correlation of aggradational terrace surfaces in this region has been carried out in the Rangitikei (Te Punga, 1952; Milne, 1973a, 1973b; Cowie & Milne, 1973) and lower Manawatu (Fair, 1968) River valleys, to the west of the southern Ruahine Range. Small-scale studies only, for example Rhea (1968) and Kaewyana (1980) have been carried out in the upper Manawatu River and tributary streams to the east of the Range.

This study is largely concerned with terrace sets that have been fault displaced within Late Quaternary times so it was considered impractical to set up a new set of stratigraphic names specifically in the study area. Unfortunately, river terrace sets on the east side of the Range cannot be directly traced through the Manawatu Gorge to be correlated with those on the west side of the Range. This, together with the absence of radiocarbon dating of terrace surfaces in the lower Manawatu Valley, makes it difficult to use the stratigraphy of Fair (1968). Instead, correlation with the terrace sets of the Rangitikei River has been facilitated by using radiocarbon dated surfaces, comparative thickness of loess, terrace surface morphology, height separation of terraces and the presence or absence of the Aokautere Ash. The c. 20 000 year-old Aokautere Ash marker bed (Kawakawa Tephra, of Vucetich & Howarth, 1976) was originally described and named by Cowie (1964a) in the Manawatu district. It occurs within sediments that Cowie (1964b) demonstrated to be loess derived from river flood plains. Cowie showed the loess to have been accumulating while the rivers were aggrading during the last stadial of the Otiran (Last) Glacial. Loess deposition continued until shortly after aggradation culminated in the formation of the Ohakea Terrace (Te Punga, 1952; Milne, 1973a, 1973b) and Holocene river down-cutting began. Loess containing Aokautere Ash is found on terrace and rolling hill country older than the Ohakea terrace (Milne, 1973a) and is accordingly called Ohakea loess (Cowie & Milne, 1973). In Rangitikei



River valley the base of Ohakea loess is radiocarbon dated (NZ 3188A) at  $25\ 500 \pm 800$  years B.P. (new  $t_{1/2}$  life is  $26\ 300 \pm 800$  years B.P. (NZ3188B) and the top is dated (NZ 3165A) at  $9480 \pm 100$  years B.P. (new  $t_{1/2}$  life is  $9760 \pm 110$  years B.P. (NZ 4165B)) (Milne & Smalley, 1979), consistent with the position of the Aokautere Ash in the lower third of the loess. Aokautere Ash has been found during the course of this study upon alluvial terrace surfaces within the mapped area at T24B/541971, T24B/545977 and T24B/560967 and to the east of Woodville at T24B/547918, T24B/547924, T24B/547927 and T24B/551949.

A stratigraphic sequence (Table 6.1) based upon lithostratigraphic units comprising alluvial terrace deposits and overlying loessial cover beds of distinctive character has enabled subdivision of the late Quaternary into chronostratigraphic units. The names given to each lithostratigraphic deposit and the equivalent time period (substage) during which deposition occurred have been adopted from the stratigraphy set up by Milne (1973a, 1973b) for the Rangitikei River valley.

The presence of a thick (1.5 - 2m) loessial cover containing the Aokautere Ash was used to distinguish terrace surfaces of pre-Ohakean age from terraces of Ohakean age or younger. The terrace surfaces upon which the Aokautere Ash was found are considered to be the youngest of the pre-Ohakean surfaces and are here correlated with Ratan aged surfaces in the Rangitikei River valley. Higher level surfaces of pre-Ratan age in many instances have been stripped of their loess cover and have therefore been fitted into the stratigraphic sequence on the basis of vertical separation from surfaces of known age. Although of uncertain age these surfaces are either Porewan or pre-Porewan in age and are referred to as Porewan and upper Pleistocene surfaces, respectively.

The last major phase of aggradation is represented by the Ohakean terrace set of which three river terrace subsets have been recognised. Loess cover upon these surfaces is generally less than 30 cm thick and is devoid of volcanic ash horizons. The age of these terraces is thought to span between 18 000 years B.P. through to approximately 10 000 years B.P. The precise dating of the two youngest of the three terrace surfaces of Ohakean age recognised in the study area has been obtained by radiocarbon dating.

The end of the Ohakean Substage was heralded by a period of river down-cutting here referred to as the Holocene, during which numerous flights of localised, discontinuous and often unmatched terrace levels were in-

Era	NZ series	New Zealand stages	Southwestern North Island substages	Dated horizons age B.P. (years x 10 <sup>3</sup> )	River terrace sets	Ballantrae research station		Mangapapa River valley		Other catchments
Upper Quaternary	HAWERA	Aranuian	Holocene	Undifferentiated				Hol.		Hol.
			Ohakean	* 10	Ohakea	Oh <sub>3</sub>	Oh <sub>3</sub>	b	Ohu	
				* 13		Oh <sub>2</sub>				a
				* 13.3		Oh <sub>1</sub>	Oh <sub>2</sub>			
				↓ 20				Oh <sub>1</sub>		
		25								
		Apitian								
		Ratan		Rata			Ra		Ra <sub>2</sub>	
		Orouan							Ra <sub>1</sub>	
		Porewan		Porewa			?Po		?Po	
Surfaces other than Porewan		Upper Pleistocene			?P1		?P1			

TABLE 6.1: Upper Quaternary stratigraphy of the Upper Manawatu district immediately to the east of the southern Ruahine Range between Woodville and Ruaroa.

\* Radiocarbon dated surfaces (see Appendix Vb)

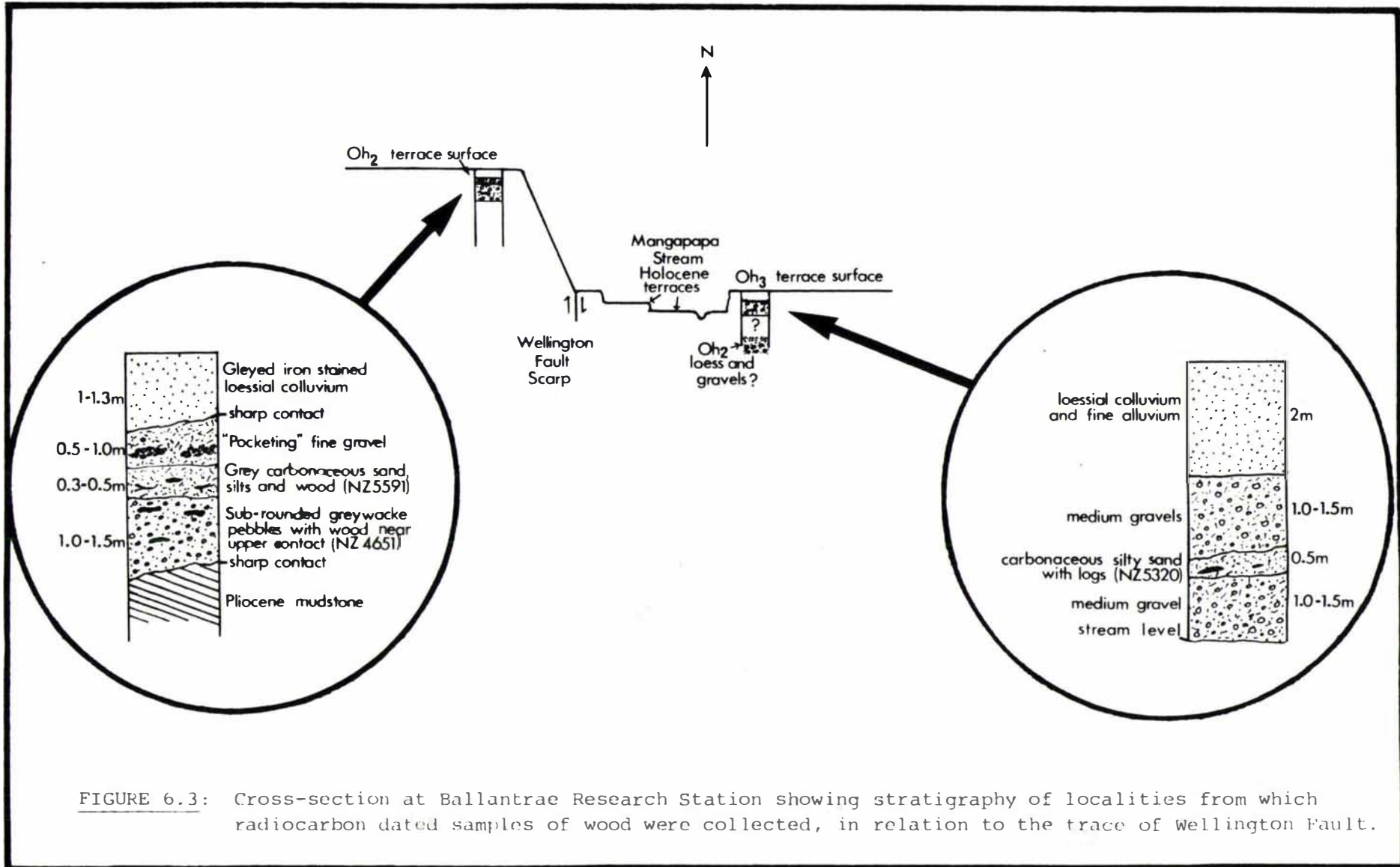
↓ Aokautere Ash

cised below the level of the youngest Ohakean surface. These younger terraces are devoid of loess cover and are of a stony character.

### 1. Terraces Displaced by the Late Quaternary Trace of Wellington Fault

Near Ballantrae Research Station approximately 2 km to the northwest of Woodville, the trace of Wellington Fault forms a prominent, steep, east-facing scarp that is upthrown on the northwest side. The fault displaces Plio-Pleistocene marine deposits overlain by a 1-2m thick veneer of alluvial terrace gravels and loess. The stratigraphy of the gravel veneer is exposed on the upthrown western side of the fault in a road cutting at T24B/517946. Here it comprises a lowermost unit of sub-rounded greywacke pebbles within which fragments of wood occur near its upper contact with an overlying thin unit of grey carbonaceous sandy silts. This latter unit also contains wood fragments and is overlain by a unit of "pocketing" fine gravel. The topmost unit is gleyed iron stained loessial colluvium (Fig. 6.3). Wood sampled from the basal part of the lowermost gravel, between 2.0m and 2.8m depth below the ground surface, has been dated (NZ 4651A) at  $12\ 900 \pm 200$  years B.P. (new  $t_{1/2}$  is  $13\ 300 \pm 200$  years B.P. (NZ 4651B)). Also from this locality, samples of wood from the thin horizon of grey carbonaceous sandy silt at about 1.5m depth below the ground surface have been dated (NZ 5591A) at  $12\ 650 \pm 150$  years B.P. (new  $t_{1/2}$  is  $13\ 000 \pm 150$  years (NZ 5591B)) (Appendix Vb). These radiocarbon results give an age for the younger of two terrace surfaces of Ohakean age, found on the upthrown western side of the Wellington Fault trace at Ballantrae. The younger surface is denoted with the symbol Oh<sub>2</sub> and the older with the symbol Oh<sub>1</sub>.

On the downthrown eastern side of the fault a gravel veneer of unknown thickness and of similar appearance to that on the upthrown side is exposed in a stream bank face at T24B/517945. Here the veneer consists of a unit of medium-sized gravel within which is a thin unit of carbonaceous silty sand containing fragments of wood. Loessial colluvium and fine alluvium overlie the gravels. Here a wood sample from the unit of carbonaceous silty sands at about 3m depth below the ground surface has been dated (NZ 5320A) at  $10\ 350 \pm 100$  years B.P. (new  $t_{1/2}$  is  $10\ 650 \pm 150$  years B.P. (NZ 5320B)) (Appendix Vb). This dated terrace surface is thus the younger of the Ohakean surfaces on the downthrown side of the Fault at Ballantrae (Fig. 6.3).



The present channel of Mangamanaia Stream is incised below the level of the Oh<sub>3</sub> surface. The flights of terraces of Holocene age have not been differentiated and are denoted by the symbol Hol.

At a distance of 4.25 km northward of Ballantrae the trace of Wellington Fault displaces a second sequence of alluvial terrace surfaces within Mangapapa River valley. There are no radiocarbon dates available in this area. However, the presence of Aokautere Ash at two localities dates two terrace surfaces as being of Ratan age and enables them to be used as surfaces of reference with which to compare terraces of unknown age. The oldest surface in this catchment is represented by two remnant surfaces, one on either side of the Wellington Fault trace at T24b/545982 and T24B/946985. Alluvial gravels underlie these surfaces but the poor exposure of cover beds makes it difficult to determine the age of this surface. It is here considered that the surface is of Porewan age and that most of the once thick loess cover has been removed by the strong winds that frequent the area. Two surfaces of Ratan age, both on the downthrown eastern side of the fault trace also flank Mangapapa valley and Aokautere Ash has been found on both of them at localities T24B/541971 and T24B/545977. There are no surfaces of equivalent age on the upthrown western side of the fault within the immediate vicinity of the trace. The centre of Mangapapa valley is filled with aggradational gravels of Ohakean age that comprise at least three terrace subsets (Table 6.1). The alluvial gravel veneer on each surface rarely exceeds 4m thickness and is capped with a thin layer of loess less than 30 cm thick. Just as at Ballantrae, surfaces of Oh<sub>1</sub> and Oh<sub>2</sub> age are only found on the upthrown side of the Wellington Fault trace. In contrast to Ballantrae, surfaces of Oh<sub>3</sub> age in Mangapapa valley, though poorly preserved, are present on the upthrown side of the Wellington Fault trace. Two terraces of Oh<sub>3</sub> aggradation have been recognised, the younger surface is denoted with the symbol Oh<sub>3</sub>b and the older with the symbol Oh<sub>3</sub>a (Table 6.1). On the downthrown eastern side of Wellington Fault trace an extensive surface of Oh<sub>3</sub> age stretches from the base of the fault scarp in Mangapapa valley downstream to Ballantrae. The remainder of terrace surfaces below the level of Oh<sub>3</sub> are classified as Holocene in age (Hol).

The significance of these two localities lies in the interpretation of the dated terrace surfaces with respect to fault displacement.

## 2. Interpretation

Terrace surfaces of pre-Ohakean age are not present at the Ballantrae site. The oldest of the Ohakean surfaces there ( $Oh_1$ ) is only preserved on the upthrown western side of Wellington Fault trace and is fault truncated at T24B/208 (Inset B). A meander loop incised to a depth of 2-4m below the level of  $Oh_1$  at T24B/208 (Inset B) is interpreted as representing the  $Oh_2$  phase of aggradation. This surface also is only preserved on the upthrown side of the Wellington Fault, remnants of which occur at the Ballantrae site and at T24B/206 (Inset B).

The timing of fault displacement of both the  $Oh_1$  and  $Oh_2$  terrace surfaces must postdate the cutting of the meander loop as the loop is seen to be truncated by the trace of Wellington Fault. The total amount of vertical fault displacement at this locality since  $Oh_2$  times exceeds the height of the present scarp at T24B/208 (16 metres) since neither the  $Oh_1$  surface nor the truncated section of the meander loop ( $Oh_2$  surface) is preserved on the downthrown eastern side of the fault trace. It is here interpreted that surfaces of  $Oh_1$  and  $Oh_2$  age downfaulted on the east side of Wellington Fault were subsequently buried during the  $Oh_3$  phase of aggradation. Evidence from radiocarbon dating indicates that the  $Oh_2$  phase of aggradation at Ballantrae ceased about  $13\ 300 \pm 200$  years B.P. (NZ 4651).

The second locality at Ballantrae (T24B/517945) from which a radiocarbon date was obtained indicates that gravel aggradation upon the  $Oh_3$  terrace surface continued until around  $10\ 650 \pm 150$  years B.P. (NZ 5320). From the absence of the  $Oh_1$  and  $Oh_2$  surfaces on the downthrown side of the fault it is interpreted that they have been buried beneath the  $Oh_3$  surface. From this interpretation the 12 metres of vertical displacement measured between the radiocarbon dated locality at T24B/517946 and the downthrown side of the fault at this point is a measure of the minimum amount of fault displacement that has taken place. A true value of vertical displacement will only be attained by locating the downthrown and buried wood-containing gravels and silts beneath the  $Oh_3$  surface (Fig. 6.3). Rejuvenation along the Wellington Fault trace has resulted in small amounts of uplift measuring between 0.5 - 1m at locality T24B/205a and in scarp collapse at the southern end of the trace at T24B/206 (Inset B) but the age of this displacement is uncertain. The presence of two alluvial fans of Holocene age, the ground surfaces of which have been displaced by fault scarps at T24B/214 and 215 and T24B/205a (Inset B)

indicates that movement on Wellington Fault at these localities post-dated deposition of the Oh<sub>3</sub> terrace surfaces and occurred within Holocene time.

A splay fault at T24B/207 displaces the ground surface of Oh<sub>2</sub> age vertically, by between 6.7m (northeast end) and 2m (southwest end), and another at T24B/209 displaces the ground surface of Oh<sub>1</sub> age vertically by 1m (Inset B). The splay fault at T24B/207 does not extend at its northern end across the Wellington Fault trace. Movement on this splay fault may have offset the Wellington Fault trace by approximately 30m dextrally, but the Mangamanaia Stream has removed all evidence at the critical point where the offset is thought to occur (Inset B). Alternatively, the splay extends only to the southwest of Wellington Fault trace, is sympathetic to the main fault and has not offset it dextrally.

Within Mangapapa valley the Porewan terrace has been displaced approximately 10m vertically by Wellington Fault trace at T24B/545982 (Inset C). The two oldest Ohakean terraces (Oh<sub>1</sub> and Oh<sub>2</sub>) are truncated by the Wellington Fault (Inset C). The most extensive surface is that of Oh<sub>2</sub>. A poorly defined fault trace strikes parallel to and approximately 90m to the west of the principal trace, displacing the Oh<sub>2</sub> ground surface vertically by between 20 cm at its northern end to 2m at its southern end. This trace at its northern end does not displace the Oh<sub>3</sub> ground surface and therefore predates this episode of aggradation. Thus displacement along this fault trace must have coincided with movements along the principal trace of Wellington Fault at the end of the Oh<sub>2</sub> phase of aggradation. As at Ballantrae, it is postulated that aggradation of the Oh<sub>2</sub> surface on the upthrown western side of Wellington Fault trace within Mangapapa valley ceased as a result of fault displacement at around 13 000 years B.P. Incised below the level of the Oh<sub>2</sub> surface and only on the upthrown side of the fault trace are two Oh<sub>3</sub> terrace levels, here termed Oh<sub>3a</sub> (oldest) and Oh<sub>3b</sub> (youngest) (Table 6.1 and Inset C). With movement on the upthrown side of the fault, Mangapapa Stream initially became incised within the Oh<sub>2</sub> terrace to then regrade to a new aggradational level forming the Oh<sub>3a</sub> surface. Further fault movement at this locality led to a second localised Oh<sub>3b</sub> surface comprising a terrace on the upthrown side and a fan on the downthrown side of the scarp (Inset C). During the deposition of Oh<sub>3b</sub> fault displacement continued. This increasingly resulted in the accumulation of bedload as a fan-shaped deposit extending downstream from the fault and along the scarp face thus reducing the offset height of

the fault scarp. The total amount of vertical displacement along the Wellington Fault trace at this locality is therefore uncertain because of modification by both stream erosion and deposition at the base of the scarp. Evidence suggests that a vertical displacement of 7m (measured near T24B/230) preceded the formation of the Oh<sub>3a</sub> and Oh<sub>3b</sub> surfaces. Further displacement resulted in: (a) collapse of the main scarp at T24B/229 (Inset C); (b) formation of a 2m scarplet across the Oh<sub>3b</sub> surface at T24B/230; and (c) an increase in the height of the scarp at T24B/231 to give a true value of vertical displacement of 2m. The timing of this latter phase of displacement is thought to have been within Holocene times.

The Oh<sub>3a</sub> surface is not well preserved upstream (on the upthrown western side) of the fault scarp in Mangapapa valley. This contrasts with the extensiveness of this surface downstream (downthrown eastern side) of the Fault. Here the Oh<sub>3a</sub> surface can be traced from Mangapapa valley to Ballantrae and suggests that the Oh<sub>3</sub> surface represents continued deposition upon the downfaulted Oh<sub>2</sub> surface. Evidence from Ballantrae indicates that this phase of deposition continued until at least 10,650 ± 150 years B.P. based on NZ 5320B. This correlates well with the timing of a major erosion phase further north in the southern Ruahine Range, dated (NZ 4314A) at 11 800 ± 150 years B.P. (new t<sub>1/2</sub> life, 12 150 ± 150 years B.P. (NZ 4314B) (Hubbard & Neall, 1980) (Appendix Vb, see Chapter 11).

At the onset of Holocene times, Mangapapa Stream abandoned sediment deposition on the Oh<sub>3b</sub> surface as a result of further downcutting to form lower degradational terraces.

#### D. Parallel Traces

At a number of localities along Wellington Fault there occur remnants of other traces that trend parallel to but at varying distances from the principal trace. For example, a trace between localities T24B/201 to 201c lies approximately 250m to the east of the principal trace bounding a block of Nukumaruan limestone to the west from alluvium to the east. This 750m long trace tapers out to the north and south beneath terrace alluvium.

At locality T24B/226a and 226b there are two isolated traces 175m west of the principal trace of Wellington Fault. Although the northern extension of these traces is sketchy they are aligned with a poorly defined scarp lying 90m to the west of locality T24B/228 (Inset C). A



little further to the north, traces at T24B/261 to 263, T23D/608 to 614 and T23D/615 to 619 parallel the principal trace of Wellington Fault about 500m to the west. At locality T23D/620 a sharp change in the strike of the trace towards the northeast indicates that major bifurcation of the principal trace of Wellington Fault occurs just south of Manga-a-tua Stream. It is therefore probable that the area between the principal trace and the discontinuous traces to the west is a wedge that extends approximately 10 - 11 km southward of Manga-a-tua Stream. The location at which the westernmost trace joins the Wellington Fault at the southern end of the wedge is uncertain.

A third example is a parallel trace extending from locality T23D/696 to 707, a distance of around 2 km length. This trace lies about 200m to the east of the principal trace of Wellington Fault for much of its length but merges with the principal trace at T23D/707 (Inset A). The area between is a wedge comprising a graben at its northern end and a horst at its southern end. The traces do not seem to merge at their southern end but remain parallel to at least as far as Raparapawai Stream where all evidence of the easternmost trace is lost.

A fourth example of a parallel trace occurs between localities T23D/782 to 787. This 500m long trace lies parallel to and at about 350m to the west of the principal trace of Wellington Fault.

Parallel traces in many instances appear to result from bifurcation of the principal trace in response to compressional lateral displacement which in this area is dextral transcurrent.

#### E. Tilted Wedge

An example of a wedge may be seen on the trace of Wellington Fault approximately 1 km to the northwest of Kahuki (T24A/026 to 047, Inset E). Here the trace bifurcates at its southern end for a distance of 2 km along strike and merges again at its northern end. The maximum width of the wedge is approximately 125m at its midpoint (Fig. 6.4).

The wedge is traversed by Kahuki Stream, to the north of which the area between the two fault traces has been downfaulted to form a graben. The graben is occupied by a large pond and area of swamp. At the southern end of the graben the area between the fault traces is upwarped into a mound that prevents drainage of the swamp. To the south of Kahuki Stream the area between the fault traces is upfaulted into a horst, the horst

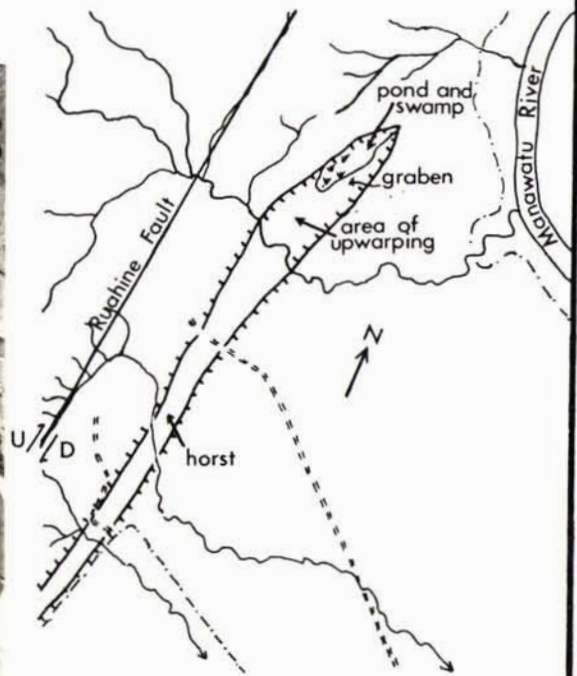
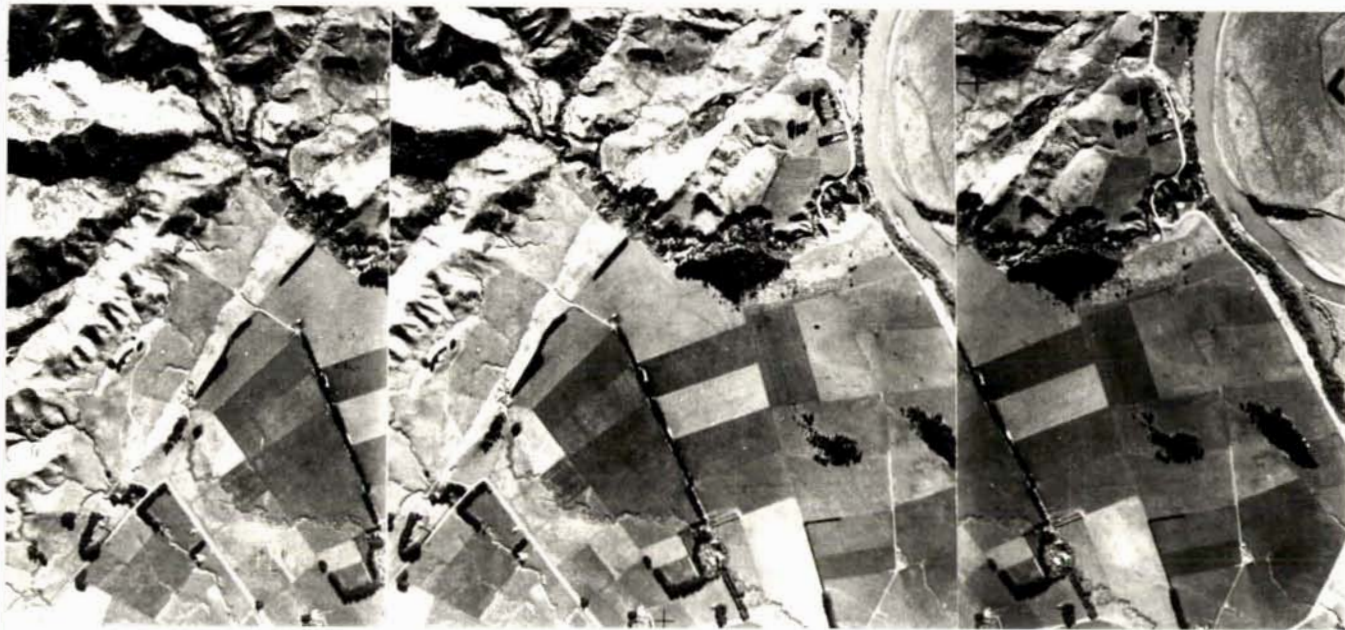


FIGURE 6.4: Stereoscopic pair showing a tilted wedge located at T24A/477899 on the trace of Wellington Fault. See Inset E (on map) for scale.

being bordered by scarps between 5 and 16 metres high. Where the easternmost fault trace crosses Kahuki Stream, marine deposits of Plio-Pleistocene age dip at  $30^{\circ}$  towards the east on the upthrown side of the fault. The dip of this strata steepens in an upstream direction to a maximum of  $60^{\circ}$  to the point where the westernmost trace crosses Kahuki Stream.

The wedge is thought to be tilted towards the northeast. Tilted wedges have been attributed to lateral displacements along bifurcating fault traces (Lensen, 1958b) which, along a relatively straight fault, can be regarded as indirect evidence of a transcurrent fault (Lensen, 1976).

#### F. Tilted Terrace Surface

Between Oruakeretaki Stream and Raparapawai Stream a terrace surface of Ratan age is cut by two parallel traces of the Wellington Fault (Inset A). The traces are approximately 175m apart. The surface of the terrace lying between the two traces is inclined about  $6^{\circ}$  to the east. The scarps at T23D/691a and T23D/702 indicate that displacement of the terrace during the latest phases of movement resulted in uplift to the east of each trace. It therefore seems probable that uplift to the east of the trace at T23D/691a and downthrow to the west of the trace at T23D/702 has resulted in a  $3^{\circ}$  increase in the surface tilt of the terrace between the two parallel traces of Wellington Fault.

As this tilted terrace is confined to the area between the two parallel fault traces it is likely that the fault traces bound a horst. This horst together with the graben formed between the traces at T23D/695 and T23D/707 may form part of a larger wedge structure that is tilted towards the north. A little to the north at locality T23D/706 an Ohakean terrace surface to the east of the fault traces is inclined at  $3^{\circ}$  towards the east. This surface together with others of Ohakean age to the east and west, such as T23D/695 and T23D/707 have not been tilted as a result of fault displacement. This tilting of the Ratan surface occurred prior to Ohakean time.

#### 6.6.2 SPLAY FAULTS

Four splay faults strike towards the northeast from the Late Quaternary trace of Wellington Fault. They displace Pleistocene marine strata and/or Late Quaternary alluvial terraces. Although none of these four traces can be shown to join the Wellington Fault, their sense, amount and timing of movements is thought to be similar. All show vertical uplift predominantly to the northwest.

### A. Mangarawa Fault

Striking 040-055°T east of north this fault displaces both alluvium and Pleistocene marine deposits along its 2.3 km length. Displacement has produced a scarp of variable height. A subdued scarp may to some extent be used as an indication of early fault movement but is here considered to be due mostly to recent cultivation practices. Several springs issue from the base of east facing scarps along the length of this fault.

The absence of displaced reference features precludes determination of the amount of horizontal displacement that has taken place along this fault. However, the presence of vertically displaced terrace surfaces of Ratan, Porewan and ?Pleistocene ages enables determination of rates of vertical displacement in Late Quaternary time (see Frequency and Rate of Fault Displacement on Active Faults).

At the southwestern end of the trace of T24B/284 an alluvial surface of Ratan age has been displaced vertically by 2 - 3.5 metres. Here the amount of displacement is variable because the scarp has been modified by recent drainage realignment work and is crossed by Pinfold Road at the point of steepening grade. Mangarawa Fault tapers out to the southwest within hill country comprised of Pleistocene deposits. At its northeastern end, Mangarawa Fault is seen to bound the eastern side of an upfaulted 'island' of marine strata at T24B/293 (Inset D) but does not displace the surrounding alluvial terrace surfaces of Ohakean age. Vertical displacement therefore preceded Ohakean time. Between these localities terrace surfaces of ?Porewan and ?Pleistocene ages have been vertically displaced by a similar amount. Eastward of T24B/292 (Inset D) the trace is thought to splinter, with the northwestern trace petering out at T24B/582978 whilst the southeastern trace lying approximately 250m to the northwest of Valley Road parallels Valley Road for a distance of approximately 1.75 km (outside the mapped area). This trace coincides with the lithological contact between deposits of Pleistocene age to the northwest and alluvial gravels of Ohakean age to the southeast.

### B. Beagley Road Fault

The second of the splay faults can be traced with confidence for approximately 1 km length to come within 200m, at its southwestern end (T24B/271), of the Late Quaternary trace of Wellington Fault. All trace of this fault is lost for 1.5 km distance northward of T24B/271. At T24B/282 this fault trace resumes along a strike of 050-060°T east of north

for 0.5 km. Beagley Road Fault cuts Pleistocene marine deposits throughout its length.

The absence of reference features along the trace precludes measurement of either vertical or horizontal displacements.

Subdued southeast facing scarps up to 6m high are characteristic of this trace. Here slope instability in the form of earth slumps is common. Springs characteristically issue from the base of the scarp. The southwestern section of this trace comprises a series of uphill-facing scarps each with 2m high southeast facing scarps. The differences in scarp heights along the trace indicate that at least two periods of fault displacement have taken place in Late Quaternary time but conclusive evidence is lacking.

#### C. James Hill Road Fault

At a strike of  $045^{\circ}\text{T}$  east of north this fault displaces Pleistocene marine deposits throughout much of its 1 km length. Southeast facing scarps up to 6m height with subdued outline are substantially eroded. At localities T24B/266 to 268 an alluvial surface of Ratan ( $\text{Ra}_2$ ) age has been displaced vertically by 2m. The amount of horizontal displacement cannot be discerned. The trace tapers out within marine deposits at both ends of its traceable length.

#### D. Coppermine Road Fault

The northernmost of the four splay faults strikes at  $060^{\circ}\text{T}$  east of north at its southwestern end, before swinging northward to between  $015^{\circ}\text{T}$  and  $040^{\circ}\text{T}$  east of north at its northeastern end. This trace, throughout much of its 2 km length, displaces Pleistocene marine deposits but at its northern end alluvial terrace surfaces of Manga-a-tua and Coppermine Streams are also displaced. A Ratan ( $\text{Ra}_2$ ) aged terrace is displaced 1-2m vertically at T23D/801 and 802. This terrace is the same surface that is displaced by both James Hill Road Fault at T24B/266 to 268 and Mangarawa Fault at T24B/284. An Ohakean aged terrace at T23D/803 to 805 is displaced a similar amount. This Ohakean surface is the same as that crossed but not displaced by Mangarawa Fault at T24B/293. Lower level surfaces of Holocene age on the left bank of Manga-a-tua Stream, to the northeast of locality T23D/805, are not displaced by Coppermine Road Fault and here the trace of the fault tapers out. The amount of horizontal displacement cannot be determined.

### 6.6.3 WHARITE FAULT

This is essentially a contact fault separating Torlesse bedrock on the uplifted western side from Plio-Pleistocene marine deposits on the down-thrown eastern side. However, a very thin veneer of Nukumaruan deposits on the upthrown side preserves evidence that fault displacement has taken place in Late Quaternary time. At T23D/601 and 602 streams have been diverted along the base of an uphill-facing scarp. A minimum vertical displacement of 1m at both localities indicates that the eastern side was upthrown during the latest phase of fault movement. Water seeps and considerable large-scale slope instability occur along this fault.

A northward extension of Wharite Fault beyond locality T23D/607 is uncertain because of lack of preservation in steep catchments. The geological contact north of T23D/607 swings to a northeasterly direction to cross two other tributaries of Mangapapa Stream. It is not known if this section of the geological contact is also faulted because the contact is not exposed. To the south, Wharite Fault can be traced to locality T24B/540996 where a high level terrace of Porewan or older age has been downthrown on the eastern side. A deep saddle across the narrowest part of the terrace marks the position of the fault trace. Further southward at T24B/538993 a ridge comprised of Torlesse bedrock has been dextrally offset across an eastward draining tributary of Mangapapa Stream. Here the shutter ridge and offset drainage channel indicate lateral displacement of approximately 150m. Signs of fault brecciation and deformation of bedrock lithologies are present within this stream channel just upstream of the shutter ridge. Still further southward the trace of Wharite Fault is thought to coincide with an offset ridge spur at T24B/543983. The corresponding ridge spur on the eastern side of the trace cannot be determined with confidence so the amount and sense of offset is unknown.

### 6.6.4 FREQUENCY AND RATE OF FAULT DISPLACEMENT ON ACTIVE FAULTS

#### A. Vertical Displacements

Observations of truncated bedrock spurs indicate that vertical fault displacements on active faults in this area have been recurrent and episodic. These episodes of vertical fault displacement have largely been responsible for much of the altitudinal difference between the

crest of the Range and the surrounding low lying plains. In the vicinity of West Tamaki River this altitudinal difference approximates to 500m, most of which is thought to have occurred since the marine transgression began in Waitotaran time. More specific evidence of vertical fault displacement consists of displaced alluvial surfaces. Where lower (younger) surfaces are displaced by lesser amounts than upper (older) ones, continued repeated vertical displacement can be measured. The net vertical displacement of surfaces of known age and the frequency of displacement are essential to the understanding and calculation of rates of fault movement. Vertical measurements of fault scarp heights only provide minimum values of displacement.

At Ballantrae, vertical fault displacement of the Oh<sub>1</sub> terrace surface (T24B/208) by Wellington Fault have been greater than the measured 18.9m high scarp at this locality. The Oh<sub>1</sub> surface post-dates the Aokautere Ash and is thought to have formed approximately 18 000 years B.P. This gives a minimum rate of vertical fault displacement of 1.05 mm/yr. Here also the Oh<sub>2</sub> surface has been vertically displaced by between 16m at locality T24B/208 (cut off meander loop) and 12m at locality T24B/206. The Oh<sub>2</sub> surface has been dated at approximately 13 000 years B.P. (NZ 5591). Thus minimum rates of vertical displacement of between 1.23 mm/yr and 0.92 mm/yr are interpreted.

In Mangapapa Stream catchment an alluvial surface of Oh<sub>2</sub> age shows a true vertical displacement of 6m (Inset C). A subsequent displacement of 2m at T24B/230 and T24B/231 may represent a single episode or two distinct episodes of fault displacement. This evidence suggests that between 8-10m of cumulative vertical fault displacement has taken place at T24B/228 since Oh<sub>2</sub> times. However, since the northeastern section of the fault scarp has been partially buried it seems likely that the total amount of vertical displacement either approximates or exceeds the height of the scarp at its southwestern end. It is therefore suggested that the total vertical displacement at this locality has been greater than 15m (Inset C). Assuming that the Oh<sub>2</sub> surface displaced at T24B/228 is of equivalent age to the 13 000 year old displaced Oh<sub>2</sub> surface at Ballantrae, the minimum rate of vertical fault displacement in Mangapapa River catchment approximates 1.15 mm/yr.

A terrace surface of stony appearance and devoid of loess is displaced by the trace of Wellington Fault at T24B/231. This surface is judged to be approximately 5000-6000 years old and has been vertically displaced by 2m. This is considered less than expected for the calculated minimum rate of vertical displacement so either: (a) the overall calculated rate is over-estimated; or (b) vertical displacement has been greater in Ohakean than in Holocene times; or (c) the terrace is considerably younger than the estimated age.

From evidence elsewhere along the trace of Wellington Fault it appears that much of the vertical component of faulting took place during pre-Ohakean and Ohakean times and that post-Ohakean displacements have been less frequent and of smaller separation. Post-Ohakean displacements have largely resulted in small scarps of between 0.5m to 1m high and/or collapse features on the older, higher and steeper scarp faces.

Major fault displacements in pre-Ohakean times coinciding with periods of extensive alluvial aggradation and subsequent stream incision, resulted in the abandonment of a high-level river channel between Manga-a-tua Stream and Mangarawa through which Manga-a-tua Stream once drained. The presence of Aokautere Ash within this abandoned channel indicates that a dramatic change in the course of the Manga-a-tua Stream occurred prior to 20 000 years B.P. and was followed by substantial stream incision in response to movement on Wellington Fault.

The Mangarawa Fault displaces surfaces of alluvial origin. The Ohakean terrace, although present at T24B/293 (Inset D), is not displaced by this fault. Only surfaces of Ratan and older ages are displaced. Successively older surfaces have been displaced by larger amounts than younger surfaces. The vertical displacement of the younger of two surfaces of Ratan ( $Ra_2$ ) age as measured at T24B/283 (Inset D) is 3.5m. The older surface of Ratan ( $Ra_1$ ) age as measured at T24B/286 and 287 has been displaced vertically by 7.2m. At locality T24B/291 a surface of probable Porewan (Po) age has been vertically displaced by 15.6m. A similar amount of displacement was measured on the oldest surface of Pleistocene (Pl) age at locality T24B/289).

Each of the above measurements are here regarded as true values of vertical displacement. At least three distinct periods of vertical displacement of approximately 3.5m (latest), 3.7m and 8.4m (oldest) have thus taken place along Mangarawa Fault to total the 15.6m vertical displacement of the oldest surfaces. As the assigning of an age to



each displaced surface is tentative, the following rates of vertical displacement are also tentative. The preservation of a fault scarp across the younger of the Ratan ( $Ra_2$ ) surfaces (dated in Rangitikei River valley at c. 30 000 years B.P.; Milne, 1973b) suggests a rate of vertical displacement of 0.12 mm/yr. The timing of earlier fault displacements is less certain. The displacement of the older Ratan ( $Ra_1$ ) surface (dated in Rangitikei River valley at c. 40 000 years B.P.; Milne, 1973b) gives a rate of vertical displacement of 0.18 mm/yr. As the Porewan and older Pleistocene surfaces have been displaced by similar amounts it is interpreted that a single episode of displacement, post-dated the formation of the Porewan surface. The age of the Porewan surface (dated in Rangitikei River valley at c. 70 000 years B.P.; Milne, 1973b) gives a rate of vertical displacement of 0.22 mm/yr. This displacement along Mangarawa Fault began in post Porewan time and gradually waned to cease before Ohakean time.

#### B. Horizontal Displacements

Horizontally displaced reference features particularly along the Wellington Fault demonstrate progressive dextral transcurrent movement during Quaternary times. In particular, differing amounts of horizontal offset of shutter ridges appear to indicate that displacement in older terrain has been greater than that in younger terrain. This may be either the result of progressive displacements with time or the result of different responses by various lithologies to fault deformation. It is possible that the denser, more brittle greywacke bedrock is displaced more readily and by greater amounts than the less dense marine deposits and alluvial terrace deposits which are prone to internal deformation with consequent smaller amounts of surface displacement.

The most common evidence of horizontal displacement is in the form of shutter ridges. Displaced shutter ridges involving Torlesse bedrock are offset between 250m on Wellington Fault to 150m on Wharite Fault. Displacements involving marine deposits of Plio-Pleistocene age are particularly well developed along the trace of Wellington Fault and range between 90m and 20m. As the age of these displacements is largely unknown a rate of displacement cannot be obtained.

A high level terrace surface of probable Porewan age at T23D/726) (Inset I) has been dextrally offset by 150m. This surface is considered to be around 70 000 years old (Milne, 1973b) giving a rate of horizontal displacement of approximately 2.14 mm/yr. The maximum possible rate of dis-

placement of this pre-Ohakean surface (>10 000 years B.P.) is 15 mm/yr. At T24/232 (Inset C) two abandoned stream channels 9m apart are preserved on the upthrown western side of the trace of Wellington Fault. The distance between the two channels may represent an episode of horizontal displacement during which the northernmost channel was abandoned and the southernmost channel formed. On the downthrown eastern side of the fault trace a single terrace riser approximately 40m to the south of the channel is correlated with the northernmost channel on the upthrown side. This horizontal displacement of 40m is a minimum value as subsequent fluvial erosion has removed evidence of both channels on the downthrown side. The age of this displaced surface is unlikely to be older than 6000 years B.P., which gives an average rate of horizontal displacement of around 6.66 mm/yr.

## 6.7 DESCRIPTION OF POTENTIALLY ACTIVE FAULTS

### 6.7.1 RUAHINE FAULT ZONE

The Ruahine Fault splits from the Late Quaternary trace of Wellington Fault approximately 5 kilometres south of Ballance bridge near Kahuki Stream (Inset E). Between Kahuki Stream and Centre Road, Ruahine Fault separates Torlesse bedrock on the western uplifted side from steep, east-dipping Pleistocene marine deposits on the downthrown eastern side. An extensive area of fault brecciated and gouged greywacke bedrock at T24A/476901 (Inset E), fault guided stream reaches and a marked topographical break in slope along this section of the Tararua Range front delineate the position of Ruahine Fault. North of the Manawatu Gorge and across the Manawatu Saddle, Ruahine Fault is without topographical expression. Consequently, interpretations as to its location through this area by previous authors varies greatly. Though highly probable, there is little evidence to support continuation of Ruahine Fault across the Manawatu Saddle as a contact fault separating a series of isolated greywacke 'windows' to the west from Pliocene deposits to the east. Alternatively, the trace of Ruahine Fault could be interpreted to extend down the Manawatu Gorge, from near the Ballance bridge to Te Apiti Stream. This latter interpretation takes the fault trace through Torlesse bedrock. Within Te Apiti Stream crushed bedrock and disrupted strata occur at T24B/501956 and may be evidence for the latter alternative. In the headwaters of Mangamanaia Stream the trace of Ruahine Fault once again separates Torlesse bedrock to the west from Pleistocene marine deposits to the east. Here, at T24B/521989, a high north-south striking bedrock bluff, approximately 2 km long, marks the position of the trace. From Wharite Road northwards the Ruahine Fault trace dis-

places Torlesse bedrock. Passing to the east of Wharite Trig. this trace is marked by a series of fault breccia zones within headwater tributaries of Mangapapa catchment. The trace is less well defined in Coppermine and Manga-a-tua catchments where extensive zones of fault brecciated bedrock occur throughout the length of each catchment. This suggests that the Ruahine Fault trace is but one of a swarm of traces within a more extensive Ruahine Fault Zone. Many of these secondary traces cannot be delineated for distances greater than 5 km, either because: (a) exposure is poor; or (b) the faults peter out. Secondary traces veer from the principal trace in a north to northeasterly direction, usually at a point where the strike of the principal trace changes direction. The principal trace of Ruahine Fault is well preserved within Raparapawai Stream catchment. Here evidence includes a series of low saddles across ridge crests and extensive areas of brecciated bedrock (up to 500m wide) in each tributary crossed by the trace. Subsidiary features such as slumps and ridge-top depressions are particularly well developed along this section of the trace (Map 4). North of Raparapawai catchment the principal trace of Ruahine Fault crosses the crest of the Range, via a low saddle at T23D/571089, to strike along the main stream bed of the upper reaches of Mangatuatou Stream. Within Raparapawai catchment a secondary trace splinters from the principal trace and strikes northward across the eastward-draining catchment of North Oruakeretaki Stream. This trace also crosses the crest of the Range, via a low saddle located between Maharahara and Mantanginui Trigs where it peters out within Opawe catchment. Extensive brecciation of bedrock lithologies within the upper reaches of Mangapuaka catchment indicates the presence of additional fault traces in this area, many of which lack topographical expression.

Immediately to the east of Maharahara Trig. at T23D/585106 there are two prominent sharply defined fault scarps of 50m and 75m length, respectively. Where a walking track crosses these scarps their heights have been measured at between 6-8m, uplift being to the northwest. The sharp definition and steep scarp faces of these faults is unusual in that erosion elsewhere in this deeply dissected mountainland has essentially destroyed much topographical evidence suggestive of Late Quaternary faulting. These scarps may therefore provide the most convincing evidence suggestive of fault displacement within the Ruahine Fault Zone during Late Quaternary time.

Northward of Maharahara Trig. the principal trace is well defined by an

alignment of saddles, fault guided stream reaches and to a lesser degree by eroded fault scarps that can be traced with difficulty across the headwater reaches of Opawe, Porewa and Te Ekaou Streams. A very distinct kink in Andersons Stream, where an extensive breccia zone is exposed at T23B/612156, marks the position of the trace. It then veers towards the northeast across the upper reaches of Makawakawa Stream where it can be seen to strongly influence the drainage pattern of small fault guided tributaries. Within one of these tributaries at T23B/641192 fault brecciated bedrock is exposed throughout its length. Here fluvial erosion of the softer brecciated rock has resulted in deep stream dissection, the banks of which show considerable slope instability. A very deep saddle across the ridge separating Makawakawa Stream catchment and Pohangina River catchment is traversed by Takapari Road at T23B/661208 where road cuttings afford excellent exposures of fault brecciated bedrock. Signs of fault brecciation along the strike of this trace can also be seen where it crosses Centre Creek at T23B/671215 and Cattle Creek at T23B/692234, the latter of which is some 350m wide. Northward of Cattle Creek the trace of Ruahine Fault is thought to approximate the main channel of the Pohangina River for a distance of approximately 15 km before passing across a low saddle, to the east of Otumore Trig., into Tukituki River catchment (north of the mapped area).

Two splay faults, Piripiri and Cross Road Faults, strike towards the southwest of the principal trace of Ruahine Fault for a limited distance before petering out. Further examples of splay faults may be represented by traceable but discontinuous alignments of near vertical bluffs, here mapped as scarps. One such scarp alignment traverses Te Ekaou and Porewa catchments whilst a second traverses Opawe and Mangatuatou catchments. A third scarp alignment across Ohinetapu, Dundas, No. 1 Line and No. 2 Line catchments appears to parallel the principal trace of Ruahine Fault. Rather than a splay from the Ruahine Fault, an alternative interpretation is that it represents a northward extension of Makohine Fault. If this interpretation is correct then Makohine Fault ceases to be a contact fault northward of No. 2 Line where the trace veers toward the northeast into the bedrock lithologies comprising the Range. All of the splay faults described are upfaulted on the eastern side, but as is the case with the principal trace of Ruahine Fault the timing of displacement is largely unknown.

As none of the traces within the Ruahine Fault Zone traverse alluvial surfaces of Late Quaternary age it is difficult to establish whether or

not this fault was active in Late Quaternary time. In the southern part of the mapped area the trace separates Plio-Pleistocene marine deposits from Torlesse bedrock and is thus a contact fault. Because other contact faults in the study area have moved at least once in the last half million years, some showing positive evidence of Late Quaternary fault movement, it is considered that the principal trace of Ruahine Fault should be mapped as being potentially active. The absence of surface expression of this trace across much of the Manawatu Saddle is interpreted as being a function of the thickness of the covering strata. Any permanent displacement in the underlying bedrock has probably been accommodated by plastic deformation rather than brittle faulting within the overlying Plio-Pleistocene cover strata.

#### 6.7.2 TOTARA FAULTS

The Totara Faults comprise three traces located at the northern tip of the Tararua Range approximately 1.2 km upstream from the western end of the Manawatu Gorge. The westernmost and centrally located traces separate, along the southern part of their length, upthrown Torlesse bedrock to the east from downthrown marine strata of Pleistocene age to the west. As with other contact faults, this section of the trace is marked by a steep bedrock bluff to the east of the trace. Fault breccia and gouge in Torlesse bedrock on the south side of the Manawatu Gorge may indicate that these two traces extend at least to the Gorge but there is little field evidence to suggest that they extend across the Gorge. Nevertheless, stream alignments along the strike of these traces on both sides of the Gorge may indicate that drainage has been influenced by these faults. The easternmost trace displaces Torlesse bedrock throughout its length. A series of fault breccia zones, exposed along that part of the trace that parallels the south bank of the centre part of the Manawatu Gorge, have been measured as dipping at  $73^{\circ}$  towards the southeast. The dip and strike of these breccia zones approximates the foliation of the bedrock at these localities. Elsewhere along this trace features of fault origin are poorly preserved and subdued in outline.

A thin covering of Pleistocene deposits on the upthrown eastern side of the Totara Faults has been vertically displaced but by an unknown amount. The absence of displaced reference features along any of the three traces precludes any determination of horizontal fault displacement.

A scarp at T24A/453943 is taken as evidence of rejuvenated movement along the westernmost trace within Late Quaternary times, with the sense

of vertical displacement being the same as those in the past. With the possibility of further movements taking place along this fault, it is considered likely that the westernmost of the Totara Faults is potentially active.

#### 6.7.3 CROSS ROAD FAULT

Throughout its 3 km length this fault displaces Torlesse bedrock. The main feature of Cross Road Fault is the subdued outline of the north-east-striking, 2-10m high, east-facing scarp which is delineated by a series of springs and swamps at its base. These springs and swamps give rise to drainage channels all of which begin at the base of the fault scarp. Several large-scale gravity collapse features are also located along the line of fault scarp at T24A/462917 and T24A/466918 (Inset E).

The fault is upthrown to the west. It cannot be demonstrated that the thin discontinuous veneer of marine strata in the vicinity of the scarp has been displaced thus the relative age of fault movement is unknown. The absence of displaced reference features is taken as an indication that Cross Road Fault has not been active during Late Quaternary times. However, the presence of free-flowing groundwater and fresh-looking gravity collapse features may indicate that fault movement has taken place in Pleistocene times. As the sense of displacement is similar to that of the Ruahine Fault it seems likely that Cross Road Fault may have been generated by movement along Ruahine Fault. It is therefore likely that the timing of movement is similar. With the absence of evidence for repeated fault displacement Cross Road Fault is classified as being potentially active.

#### 6.7.4 DELAWARE FAULT

This fault displaces Torlesse bedrock in an area where marine planation has presumably removed previously existing deposits of Plio-Pleistocene age once deposited upon an eroded bedrock surface. Marine strata have been located at 700m altitude in this area at T23B/625224 but nowhere have such deposits been found upon the extensive peneplaned surface of Delaware Ridge at approximately 1100m altitude.

The Delaware Fault has a strike of 050<sup>0</sup>T east of north and consists of an 8-10m high, northwest facing scarp that is upthrown on the southeast side. Impeded drainage on the downthrown northwest side has formed an

extensive area of swamp at the base of the scarp.

Zones of fault breccia and gouge within tributaries of the West Tamaki catchment, along the line of strike of Delaware Fault, indicate that it extends some considerable distance beyond the Delaware Ridge towards the trace of Wellington Fault. If the Delaware Fault represents a splaying of the Wellington Fault it is conceivable that it has moved in Late Quaternary times. The sharp straight outline and steep scarp face favour the interpretation that this fault is of recent origin as opposed to an exhumed origin.

#### 6.7.5 PIRIPIRI FAULT

Within the Upper Pohangina catchment (to the north of the mapped area) Piripiri Fault splays from the Ruahine Fault in a southwesterly direction towards Piripiri Stream catchment where it appears to peter out. The strike of the fault varies between  $025^{\circ}$ T east of north in Pohangina catchment to  $035^{\circ}$ T east of north in Piripiri catchment. Physiographical evidence for this fault is poorly preserved on account of deep valley dissection in this area. However, a series of fault saddles across catchment divides and fault-guided reaches of small tributary streams delineate the position of this fault. In the field, extensive areas of non-cemented, fault-crushed breccia along the strike of this fault provide confirmatory evidence. Secondary features include some of the largest slumps in the southern Ruahine Range. The sense and amount of either horizontal or vertical displacement along this fault is unknown and because of the absence of reference features of known age in this area the timing of fault displacement also remains unknown. It is assumed that movement along the Ruahine Fault was accompanied by movement of a similar sense along its splay fault, the Piripiri Fault.

#### 6.8 DESCRIPTION OF POTENTIALLY ACTIVE CONTACT FAULTS

All potentially active contact faults define the boundary between the high-altitude, deeply-dissected terrain of the Range from the low-altitude moderately-dissected piedmont. Each fault is delineated by a sharp break in slope that separates Torlesse bedrock from Plio-Pleistocene marine deposits. These faults parallel the major active faults in the region. The steep, high scarps of the contact faults indicate that considerable vertical displacement has taken place in Pleistocene time. There is no evidence preserved of horizontal displacement on contact faults. Horizontal and vertical movements along these faults in Late

Quaternary times cannot be demonstrated because no offset surfaces of this age were recognised. These faults are therefore considered to have been inactive during Late Quaternary time but are nonetheless likely to be sites of reactivated movement in the future. They have been classified as potentially active.

#### 6.8.1 WHAREROA FAULT

Whareroa Fault consists of a 1.5 km long, steep, west-facing, northwest-striking scarp separating Torlesse bedrock to the east from gently dipping Plio-Pleistocene marine deposits to the west. At its southern end, near Maungatukurangi Stream (T23C/492006), the scarp turns sharply to a N 115° E strike to then parallel the northern edge of the Manawatu Saddle for approximately 1 km distance. Fault brecciation is extensive and can be seen at T23C/499000 and T23C/491026. Ower (1943) observed the fault plane dipping at 80° E in the south branch of Whareroa Stream. This Fault is considered to be a reverse fault. Marine deposits to the west and south of this scarp have been dragged into moderate to steep attitudes as a result of uplift on this fault. Ower (1943) indicates that some of the strata adjacent to the Whareroa Fault were overturned to dip at 86° E but in this study strata close to the fault were observed to dip at 50° W. The angle of dip of the strata rapidly decreases over short distances to the west of the Fault.

#### 6.8.2 MAKOHINE FAULT

In the vicinity of No. 2 Line, Makohine Fault consists of a steep, 1.5 km long, west-facing, northeast-striking scarp separating Torlesse bedrock to the east from Plio-Pleistocene marine sediments to the west. Fault brecciation along this Fault can be seen where the trace crosses Te Awaoteatua Stream at T23D/515068. Here the fault plane dips at 46° E and is likely to be a reverse fault. Marine deposits adjacent to Makohine Fault are poorly exposed. Further westward the strata are seen to dip between 23° and 34° W. A southward extension of this Fault is thought to coincide with a fault breccia zone in Te Awaoteatua Stream at T23D/509062 and lithological contacts between Torlesse bedrock and Pleistocene marine deposits within Tokeawa Stream at T23D/505059 and Makohine Stream at T23C/500050. Signs of fault brecciation were not found at the latter two localities. A northward extension of this Fault to Ohinetapu Stream is thought to coincide with a linear series of steep, west-facing bedrock bluffs. This section of the Fault trace is not in contact with Pleistocene marine deposits.



### 6.8.3 UMUTOI FAULT

Umutoi Fault consists of a steep, 2 km long, west-facing, north-striking scarp separating Torlesse bedrock to the east from Plio-Pleistocene marine deposits to the west. This Fault forms an extensive breccia zone exposed at T23D/657251 in Piripiri Stream where the fault plane dips at  $85^{\circ}$  E, thrusting Torlesse bedrock westward over Plio-Pleistocene marine deposits. These marine deposits dip westward at approximately  $30^{\circ}$ .

### 6.8.4 CENTRE FAULT

Within the mapped area Centre Fault extends southward from the western end of Manawatu Gorge for a distance of 2.2 km along an approximate north-south strike. Here the presence of a fault is indicated by the local westward steepening of the dip of Plio-Pleistocene marine deposits to attitudes of  $35^{\circ}$  at T24A/455962 and  $42^{\circ}$  at T24A/449950. These deposits have been mapped by Ower (1943) and Feldmeyer *et al.* (1943) as dipping  $86^{\circ}$  eastward along the south bank of Manawatu River. South of the mapped area near Centre Creek (T24A/447933) Centre Fault coincides with the contact between Plio-Pleistocene marine deposits to the west and Torlesse bedrock to the east. The upthrown side is to the east but the amount of vertical displacement is unknown.

### 6.8.5 MANGATERA FAULT

In the northeast of the mapped area, Mangatera Fault separates uplifted Torlesse bedrock to the west from downthrown marine deposits of Pleistocene age to the east. At only one locality, U23A/736167, is there any sign of contact between greywacke bedrock and Pleistocene strata. Here massive mudstone with a band of limestone dipping southeastward at  $30^{\circ}$  adjoins the greywacke. This contact is suspected of being faulted but due to the paucity of exposure this was not able to be proven. Further westwards the line of Mangatera Fault is delineated by: (a) an uneven but marked topographical break in slope; and (b) exposures of fault brecciated greywacke bedrock containing uncemented gouge.

## 6.9 FAULTED MONOCLINES

### 6.9.1 RAUKAWA FAULT

Raukawa Fault is recorded as a high angle reverse fault (Rich, 1959) but was not located by the author. Evidence of this fault is an exposure of a fault plane within Pleistocene marine deposits in the southern

bank of the Manawatu River at c. T24A/451963. Here Rich (1959) recorded the fault plane as striking N 30° E and dipping 75° to 80° towards the east. The surface trace of this fault is masked by Holocene terrace alluvium that has not been displaced by the fault. According to Rich (1959) this fault can be traced for 5 km to the south of the Manawatu Gorge as a possible monoclinical flexure of steeply dipping beds within an area of otherwise low-dipping strata.

#### 6.9.2 POHANGINA FAULTED MONOCLINE

This Faulted Monocline can be traced without difficulty between Opawe Stream northward to the Pohangina River but with less certainty northward of this point and southward of Opawe Stream. Throughout its traceable length the monoclinical structure involves marine deposits of Plio-Pleistocene age. Low-dipping marine deposits gradually increase in dip westward to reach near vertical, or slightly overturned attitudes, at the Monocline. The best exposures occur in Makawakawa Stream at T23B/579193 and in Te Ekaou Stream at T23B/568181. Elsewhere the Faulted Monocline is represented by steeply dipping marine strata in the west lying in sharp contact with greywacke bedrock to the east. At these localities greywacke bedrock usually shows signs of intense faulting. This is evidenced by brecciated rock and gouge, e.g. in Porewa Stream at T23B/559163. North of Konewa Stream the Faulted Monocline takes a northeast bend to strike along the Pohangina River bed for 2.5 km where north-dipping marine strata on the north side of the river are in fault contact with brecciated greywacke bedrock on the south side of the river. At the junction of Te Anowhiro Stream the strike of the marine strata swings to the north again and a monoclinical structure is resumed. This section of the Faulted Monocline is thought to lie to the west of and parallel to Umotoi Fault for much of its length within the mapped area.

South of Opawe Stream the Pohangina Faulted Monocline, when extended along strike, coincides with areas of steeply dipping marine strata in Mangatuatou Stream. The massive (unbedded) nature of mudstone deposits in catchments south of Mangatuatou Stream make it difficult to determine the attitude of the strata and hence the position of the Faulted Monocline is uncertain. In view of the fact that this structure crosses numerous present day river terraces without displacing them led Carter (1963) to doubt Kingma's (1962) interpretation that the Pohangina Faulted Monocline has been recently active. Indeed, no evidence for Late Quaternary fault displacement along this structure could be found. It

is therefore considered to have been inactive during Late Quaternary times.

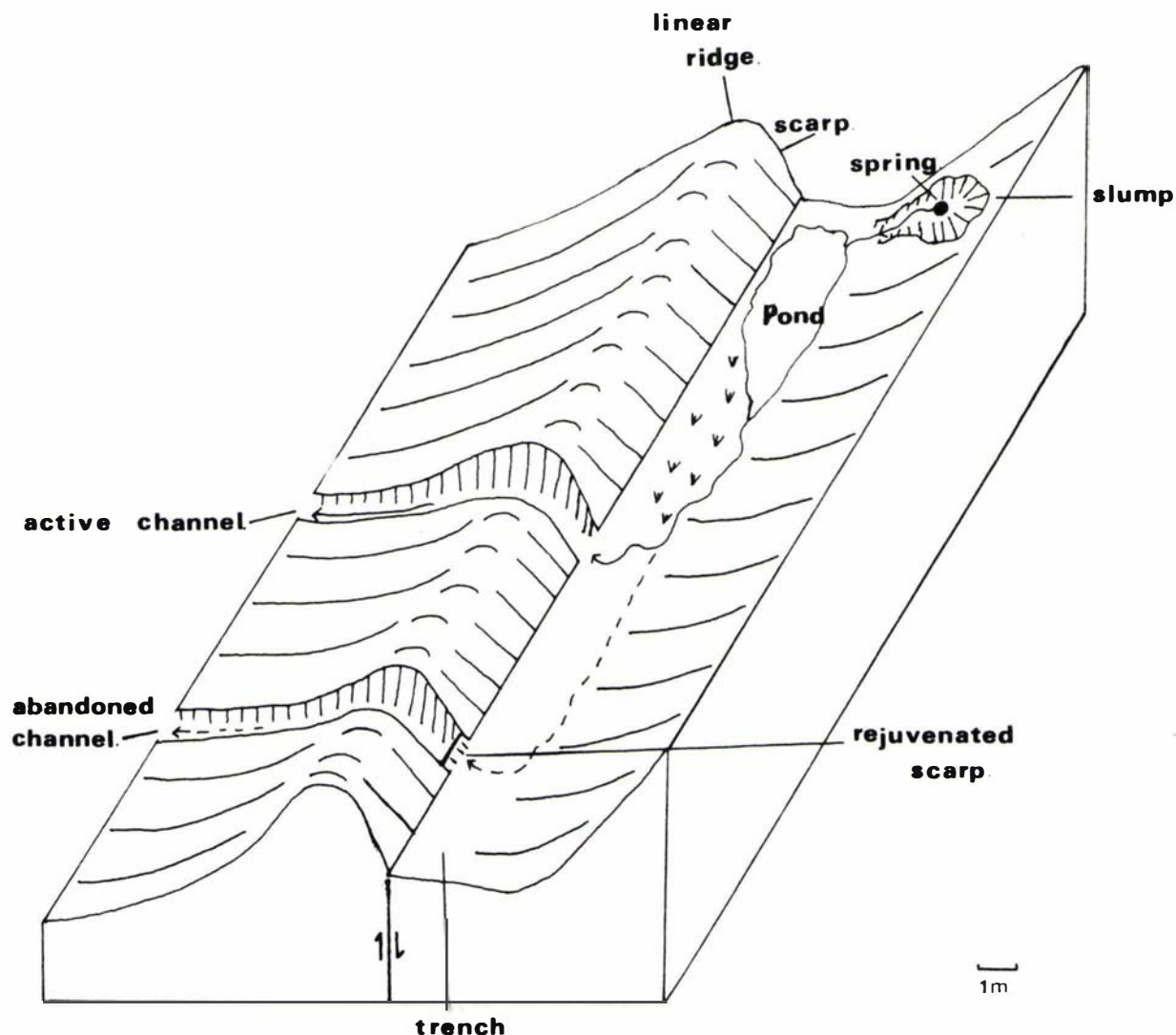
The Pohangina Faulted Monocline is tectonically analogous to a similar structure found to the south of the Manawatu Gorge lying between the west flank of Tararua Range and the Manawatu River. This monoclinical structure is faulted by Centre Fault and ?Raukawa Fault. North of the Manawatu Gorge the Monocline is thought to parallel the left bank of Pohangina River. Due to a lack of exposure it is not possible to prove if these two monoclinical structures are aligned and connected with each other.

## 6.10 SECONDARY FAULT FEATURES

### 6.10.1 UPHILL-FACING SCARPS

Uphill-facing scarps are one of the most common features of tectonic origin found along active fault traces in this area. They indicate that vertical fault displacement has offset the ground surface but signs of horizontal displacement are absent. The downhill side of the fault scarp is upthrown with the resultant moderately- to steeply-inclined scarp facing uphill (see Fig. 6.5). The steepness of the fault scarp is always greater than that of adjacent slopes. The dip direction of the faultplane is unknown and would require trenching to expose. Uphill-facing scarps are usually found on hillslopes comprising Plio-Pleistocene marine deposits and have not been found upon alluvial terrace surfaces. The direction of upthrown side as indicated by uphill-facing scarps often differs to that seen along lateral portions of the same fault trace where the trace displaces alluvial terrace surfaces.

Associated physiographical features include a round-topped, narrow (2-10m wide) and linear ridge on the downhill side of the fault scarp. On the uphill side and at the base of the fault scarp lies a trench that parallels the strike of the scarp (Fig. 6.5). The trench is variable in width (0.5m - 20m) and depth (0.5m - 10m) and often contains swamp and/or ponded water. Ponded water either originates within the trench as a result of upward percolation through fault gouge or along the fault plane, or emerges further uphill as springs and drains downslope into the trench. Fault gouge in the form of blue-grey pug has been sampled from such a trench at T23D/754. The trench, uphill-facing scarp and linear ridge are rarely of equal length at any one locality. Uphill-facing scarps vary in length from 2m to 400m in the mapped area.



**FIGURE 6.5:** Diagrammatic sketch illustrating features of tectonic origin commonly found along active fault traces. These include an uphill-facing fault scarp with a linear ridge on the downhill side and a linear trench on the uphill side of the scarp. Other commonly associated features of non-tectonic origin are also shown.

Where uphill-facing scarps parallel the slope face, the scarp is generally of even height throughout its length but where they climb upslope the depth of the trench shallows towards the top.

Recurring vertical displacement of slopes to form uphill-facing scarps can be demonstrated at T24B/237 and at T23D/755. At T24B/236 a fault scarp parallels the uphill-facing scarp at T24B/237 on its downslope side. This 8m high fault scarp faces downslope (towards the west) and marks the position of an earlier phase of vertical displacement at this site. At approximately 10m distance towards the east at T24B/237 the uphill-facing scarp with associated trench and ridge indicates a second more recent phase of vertical displacement. At T23D/755 an uphill-

facing scarp has been cut through, in several places, by antecedent drainage channels (Fig. 6.5). Rejuvenation of vertical displacement at this site has led to the abandonment of one of the drainage channels, the floor of which now lies some 0.5 - 1m higher than the present surface of the trench.

Where the trace of Wellington Fault crosses the ends of truncated bed-rock ridges such as at T23D/763 (Inset F), T23D/774 (Inset H) and T23D/767 (Inset G) numerous uphill-facing scarps occur within a narrow zone across the width of the spur. On Insets F, G and H only the scarps are shown, all of which strike towards the northeast along the approximate trace of Wellington Fault and all face uphill towards the northwest. Scarp heights rarely exceed 2m and all the trenches here are narrow, shallow and dry. Similar uphill-facing scarps occur as a series of four scarps in succession up a hillside in each of four locations (T24A/052-055) within 0.5 km of each other (see Inset E).

#### 6.10.2 FAULT PLANES, FAULT BRECCIA AND GOUGE (PUG)

##### A. Fault Planes

The fault planes of Active Faults are not exposed in this area. Numerous fault planes within breccia zones along Potentially Active Faults represent a phase of fault movement subsequent to that which resulted in extensive areas of brecciated bedrock. Exposures of fault planes along Potentially Active Contact faults occur along the western flank of the Range where fault planes separating Torlesse bedrock to the east from Plio-Pleistocene marine deposits to the west can be seen at T23B/657251 (Umutoi Fault) and at T23B/585192 (unnamed fault). The fault planes dip, respectively, at  $85^{\circ}$  and  $65^{\circ}$  towards the east. Ower (1943) records a reverse fault plane dipping at  $81^{\circ}$  towards the east at the point where Whareroa Fault crosses the south branch of Whareroa Stream. Along the eastern flank of the Range, Ower (1943) and Feldmeyer *et al.* (1943) mapped a fault contact within Coppermine Stream catchment separating Torlesse bedrock to the west from Plio-Pleistocene marine deposits to the east. The fault plane was mapped as dipping at  $75^{\circ}$  towards the west.

Within the mapped area the majority of active fault planes are bedding plane faults exposed in outcrops of Torlesse bedrock (Map 4). They coincide with bedding planes in the Tamaki and Western Lithotypes or contacts between rock units of differing composition in Wharite Lithotype.

The dominant strike direction is to the north-northeast parallel with the trend of major fault traces. However, secondary strike directions towards the north-northwest and east-west are also evident (see Chapter 7). The fault planes are generally steeply dipping, with the variability of dip and dip direction reflecting the pattern of folding and flexuring in the bedrock. Low-angle thrusts of variable strike, dip and dip direction are less common. Both high angle and thrust fault planes are generally but not always coated with soft, clay gouge of variable thickness (1-50 cm), evidence of slickensiding being rare. The dominant clay minerals are mica, kaolinite and chlorite. Less significant are vermiculite, mixed-layer clays and montmorillonite (Stephens, 1975).

#### B. Fault Breccia and Gouge

Fault breccia and gouge has been found in association with only two active faults - the Wellington and Wharite Faults. Within Torlesse bedrock cut by these Faults, zones of breccia and gouge occur at T24B/538993 (Wharite Fault) and at U23A/703203 and T23D/636107 (Wellington Fault).

Breccia and gouge occur within Plio-Pleistocene marine deposits on the Wellington Fault at T24B/543981 (Mangapapa Stream) and within Holocene alluvium at T23D/608055 (South Oruakeretaki Stream). Fault breccia and gouge can be found in association with all Potentially Active Faults and all Potentially Active Contact Faults. Breccia zones are unevenly distributed along the length of these fault traces and vary considerably in width. Some of the most extensive breccia zones occur along the Ruahine Fault Zone at T23B/692234 and T23B/613156. At T23D/564072 the breccia zone is approximately 300m wide but the width over which fault deformation can be recognised in the bedrock spans about 500m width. Within the zone of fault brecciation, breccia has been cemented with calcium carbonate and cut by veins of calcite. Where carbonate mineralisation is present, outcrops of fault breccia generally weather to a grey-white colour. Not all breccia zones are cemented or of this colouration. Some may be heavily iron stained, presumably as a result of ground water reaching the surface through the permeable breccia zone. Outside of the zone of brecciation, fault deformation is less intense and results in localised intense jointing, zeolite formation and a loosening of the bedrock constituents.

Mineralisation of fault breccia is assumed to indicate that the Ruahine Fault Zone coincides with a zone of early displacement at depth under conditions of confining pressure and circulating ground water. This displacement may represent faulting during the Rangitata Orogeny in Early Cretaceous times. Later displacements along this fault zone occurred within Early Quaternary and probable Late Quaternary times as part of the Kaikoura Orogeny. These latter displacements are thought to have taken place at shallower depths and resulted in the re-brecciation of the fault zone as well as the production of substantial quantities of non-cemented, soft, blue-grey fault gouge. The gouge forms as a coating or thin zone adjacent to the planes along which the most recent phase of fault displacement has taken place.

Fault planes, fault breccia and gouge zones have been recorded as sites of differential erosion by fluvial downcutting and/or mass movement within the southern Ruahine Range (see Marden, 1981).

### 6.10.3 MASS MOVEMENT FEATURES

#### A. Slumps

The steep, forest-clad slopes of the southern Ruahine Range are prone to erosion by large-scale mass movement, the most common type being slumping. The formation of classic ovate-shaped rock slumps, many of which exhibit backward rotation, frequently coincides with fault breccia zones. Such a relationship is well illustrated by the formation of numerous rock slump features along active traces of the Wellington and Ruahine Faults, particularly where they cross areas of deeply-dissected terrain within the Range (Map 4).

Similarly, earth slumps involving Plio-Pleistocene marine deposits occur along active fault and potentially active contact fault traces, the better examples of which occur in association with Wellington, Wharite and Umutoi Fault traces. Slumps also occur in association with the Pohangina Faulted Monocline. Factors that influence large-scale slump development within fault breccia zones are outlined in Chapter 10.

#### B. Ridge-top rents

Numerous examples of ridge-top scarps (gravity faults of Beck, 1968) ridge-top depressions (Tabor, 1971) and ridge-top benches, of gravitational origin, have been identified throughout the southern Ruahine

Range (see Chapter 10 and Appendix VI). These features are shown on Map 4 with a special symbol but are not included in the tabulated data.

#### 6.10.4 TILTED PLIO-PLEISTOCENE MARINE DEPOSITS

The amount of tilting of Plio-Pleistocene marine deposits due entirely to fault displacement is uncertain because marine strata flanking the Ranges have been tilted as a result of drag during tectonic uplift of the Ranges. Where marine strata are found to be in depositional contact with the underlying bedrock and the contact is not faulted, the attitude of the strata is generally between  $20^{\circ}$  to  $25^{\circ}$ . Tilting in these instances is due solely to localised tectonic uplift of the bedrock comprising the Ranges resulting in the up-dragging of the overlying marine strata.

Marine strata tilted to steeper attitudes have been found in association with: (a) active fault traces; (b) potentially active contact faults; and (c) faulted monoclinial structures.

In (a) marine strata tilted to an angle of  $60^{\circ}$  are found on the Late Quaternary trace of Wellington Fault at T24A/477899. Here the steeply dipping strata occur between two parallel fault traces that are part of a fault wedge. Within the wedge there has been additional upwarping or vertical fault displacement on one or both of the fault traces. To the east and within a short distance of these fault traces the dip of the strata lessens to  $30^{\circ}$ .

In (b) steeply tilted marine strata are often found on the downthrown side of potentially active contact faults. For example, strata adjacent to Whareroa Fault at T23C/492009 dip westward at an angle of  $50^{\circ}$ .

In (c) marine strata folded by the 'Pohangina Faulted Monocline' have been tilted to a near vertical and slightly overturned attitude in Makawakawa Stream at T23B/579193 and in Te Ekaou Stream at T23B/568181. South of the western end of the Manawatu Gorge a faulted monoclinial structure, to the west of Centre Fault, has resulted in marine strata dipping towards the west at angles of between  $35^{\circ}$  and  $42^{\circ}$ .

#### 6.10.5 SPRINGS

Many springs issue from the base of fault scarps, for example the line of closely spaced springs along Cross Road Fault (Inset E). In most instances soft and swampy ground is present at the base of these scarps



and in the case of springs issuing from scarps within marine strata, the fault scarp is prone to collapse. Where fault traces displace hillsides, emergent spring water is often dammed on the uphill side of the trace to form ponds or swamps, e.g. T23D/638 and 723. Numerous examples of slope instability can be attributed to springs emerging on hillsides. Springs also issue from zones of fault brecciation within Torlesse bedrock, particularly along the trace of the Ruahine Fault. Here groundwater is considered to contribute substantially to the instability of fault brecciated bedrock, failure of which generally results in large-scale mass movement features such as rock slumps (see Chapter 10).

#### 6.10.6 ZEOLITES

Outcrops of greywacke bedrock that lie adjacent to known fault zones often do not show some of the more obvious signs of fault deformation such as the presence of breccia or gouge. However, such outcrops are often "whitened" by the presence of a mineral that occurs either as a surficial coating or as a vein infilling. Thin section analyses of this mineral indicates the presence of the zeolite laumontite.

#### 6.10.7 TRUNCATED SPURS

The morphology of the east-facing, faulted range front contains evidence of recurrent episodes of Late Cenozoic vertical fault displacement along Wellington Fault. This evidence is preserved in the form of successive generations of truncated spurs cut into the Torlesse bedrock. Successive generations of truncated spurs are separated by narrow erosional remnant ridges.

A concept of the erosional modification of a fault scarp undergoing recurrent periods of movement separated by periods of stability has been developed by Hamblin (1976) in which he recognised that truncated spurs represent a series of discrete fault displacements over time. These displacements are separated by periods of quiescence too brief to leave a geomorphic record. Displacement of this type, in a geologic sense, is essentially continuous. However, periods of continuous displacement are separated by periods of quiescence during which little displacement occurs. During these periods of quiescence, erosion of the fault scarp causes the scarp to recede from the fault line to produce narrow remnant ridges preserved at the apices of truncated spurs. Also the slope angle of the spur face decreases and with time small

consequent streams develop on the truncated spurs.

These features are particularly well developed along Wellington Fault in the vicinity of Rokaiwhana Stream and West Tamaki River catchments. Of note in this area is: (1) the deep dissection of older truncated spurs by consequent streams; and (2) the steep scarp face of the most recent generation of truncated spurs. Other features noted in this area include: (3) fault displacement of some of the youngest generation of truncated spurs by the Late Quaternary trace of Wellington Fault; and (4) gravitational collapse of parts of these truncated spurs by slumping. Successive generations of truncated spurs indicate that vertical fault displacement along Wellington Fault in pre-Late Quaternary times has been recurrent and episodic. The number of episodes involved to produce 500m of vertical separation between the crest and the base of the Range in this area is uncertain.

#### 6.10.8 GAS PIPELINE

The Palmerston North - Takapau gas pipeline and a section of its southern extension to Pahiatua traverses active fault traces that are known to have moved within the last 500 000 years. As most of these faults have moved more than once and as repeated movements generally take place along the same fracture or fault trace, it is expected that future movements will also take place along these existing fault traces.

The gas pipeline between Palmerston North and Takapau crosses the Ruahine Fault at T24B/509971. As there is no surface trace of the fault at this locality the above location is an approximation only. Further eastward the gas pipeline crosses the trace of Wellington Fault at T24B/223 (T24B/534968) where part of an uphill-facing scarp has been destroyed. Immediately to the north of Beagley Road the gas pipeline trends across the northeasterly striking trace of Beagley Road Fault. Although no surface trace of this fault is present in the vicinity of the pipeline, an extension of the fault trace from locality T24B/282 along the strike of the trace would intersect the gas pipeline at approximately T24B/565992. The pipeline crosses James Hill Road Fault between localities T24B/264 and 265 (T24B/566998). To the north of Manga-a-tua Stream the pipeline follows the base of a low spur comprising marine deposits of Pleistocene age before swinging sharply northwards to parallel the south side of Top Grass Road. In doing so the pipeline crosses the northeastern extension of Coppermine Road Fault.

This Fault would be expected to intersect the pipeline at approximately T23D/583013. A little further to the north the pipeline follows a ridge crest where it passes to the east of but in close proximity to several large-scale mass movement features, one of which at T23D/589029 has a very obvious slump outline. Two other traces (marked tc) of unknown origin lie to the northwest of this slump. Near Foleys Road a branch pipeline heads southward to Pahiatua. This pipeline crosses the trace of Mangarawa Fault at locality T24B/283 (T24B/558966).

#### 6.11 IN CONCLUSION

There is evidence in this area to suggest that an early phase of faulting occurred at depth and under conditions of confining pressure and circulating ground water during the Rangitata Orogeny in Early Cretaceous times. Later uplift of the southern Ruahine Range during the Kaikoura Orogeny (Pliocene-Recent) was largely controlled by high-angle, northeast trending faults many of which have remained active well into Late Quaternary time. In some instances fault displacements in Late Quaternary time have coincided with the line of earlier fault movements but in other instances subsequent episodes of fault displacement have produced new traces. Still other faults show no evidence of movement in Late Quaternary times but are nonetheless considered to be potentially active.

The amount of vertical displacement along active faults in this area has not been uniform either along the length of the fault or through time. Greatest fault uplift has occurred along the eastern side of the Range on the Wellington Fault. Here Early Quaternary displacements have been largest in the northeast of the study area and least in the vicinity of the Manawatu Saddle. Much of the Late Quaternary vertical component of faulting has taken place during pre-Ohakean time but on some faults appears to have ceased prior to Ohakean time. Minimum rates of vertical fault displacement since Ohakean time approximate 1 mm/yr in this area. Post-Ohakean (Holocene) fault displacements have been less frequent and of smaller separation than pre-Ohakean and Ohakean displacements.

Horizontal displacements are of a dextral transcurrent nature. The amount of horizontal displacement that occurred in Early Quaternary times is largely unknown. However, displacement of shutter ridges by a maximum of approximately 250m has occurred in Quaternary time along Wellington Fault. In Late Quaternary times horizontal displacement of a pre-Ohakean terrace surface of uncertain age is indicative that 150 metres of dextral trans-

current fault displacement occurred prior to 10 000 years B.P. on Wellington Fault. The maximum possible rate of horizontal displacement of this surface is therefore 15 mm/yr.

There is no evidence to suggest that fault displacement has occurred within historic times in this area.

C H A P T E R    7

STRUCTURE AND DEFORMATION

CONTENTS

	<u>page</u>
7.0 STRUCTURE ... ..	190
7.0.1 FOLDS ... ..	190
A. Early Folds and Associated Structures ... ..	190
B. Isoclinal Folds . ... ..	191
C. Subhorizontal, Open, Asymmetric Folds ... ..	192
D. Steeply Plunging Open Folds ... ..	192
E. Sequence of Fold Deformation ... ..	196
F. Fold Orientation ... ..	197
7.0.2 FAULTS ... ..	198
7.0.3 JOINTS ... ..	198
7.1 DEFORMATION . ... ..	200
7.1.1 INTRODUCTION ... ..	200
7.1.2 DUCTILE DEFORMATION . ... ..	203
7.1.3 BRITTLE DEFORMATION . ... ..	204
7.1.4 DISCUSSION ... ..	206
A. Origin of Diamictites ... ..	206
B. Origin of Wharite Lithotype ... ..	107
C. Nature of the Contact Between Lithotypes . ... ..	213
D. Mechanism of Formation ... ..	216
E. Tectonics .. ... ..	218

CHAPTER 7STRUCTURE AND DEFORMATION7.0 STRUCTURE

The principal large-scale geological structure in the southern Ruahine Range comprises three Lithotypes of predominantly northeast-southwest striking bedrock lithologies. Strata are predominantly steeply eastward dipping and westward younging and hence are in the main overturned, although small areas of non-inverted eastward younging strata have been found in easternmost outcrops (Map 1 and cross-sections). These Lithotypes lie subparallel to the northeast trend of the Range. Each Lithotype occupies a consistent stratigraphic position throughout its outcrop length (40 km) but varies considerably in outcrop width. From east to west the Tamaki Lithotype, consisting of a relatively undeformed sequence of distal turbidites, lies to the east of and is overlain by the Wharite Lithotype. Wharite Lithotype comprises a complex sequence of predominantly clastic lithologies with minor volcanics that, in part, shows signs of intense deformation. The consistent stratigraphic position beneath and parallel to outcrops of the Tamaki Lithotype substantiates the informal lithostratigraphic status of the Wharite Lithotype but does not exclude its consideration as a tectonic unit, so is here referred to as a melange. Wharite Lithotype is in turn overlain by the westernmost unit, the Western Lithotype, which consists of a relatively undeformed turbidite sequence that in many respects is similar to that comprising the Tamaki Lithotype.

Contacts between Lithotypes are conformable but have in places been tectonically disrupted by faults that parallel the strike of the contact. To the east and west of the Range all contacts between Torlesse bedrock and Plio-Pleistocene deposits that flank the Range are unconformable. This contact is usually marked by an abrupt change in physiographic slope and is at many localities faulted (see Chapter 6).

7.0.1 FOLDSA. Early Folds and Associated Structures

Highly asymmetric folds with well developed axial plane cleavage and thickening of bedding in the hinge zone occur together with clastic dykes. These features formed when the sandstone beds were not completely con-

solidated and were therefore still in a mobile state. Their formation was syndepositional.

#### B. Isoclinal Folds

A large-scale, steeply plunging fold involving strata of the Tamaki Lithotype occurs near the eastern end of the Manawatu Gorge (Maps 1 and 2). Here the northeast-southwest striking axial plane trace of this fold approximates the river bed of the Manawatu River between localities T24/490930 to T24/492946. At T24/492946 the core of this north plunging fold appears to die out. The disappearance of this fold has been attributed to fault displacement (Zutelija, 1974). It is here considered likely that this fold has indeed been truncated by a fault (see Map 2), however, the sense and amount of fault displacement is unknown. To the east of the axial plane trace strata along the eastern limb of this fold dip steeply eastward, young eastward and are thus non-inverted. To the west of the axial plane trace strata also dip steeply eastward but young westward and are thus inverted. The dimensions of this fold are considerable, with a 1.5 km thick eastern limb and a 0.8 km thick western limb. The fold may be asymmetric with a thick eastern (non-inverted) limb and a thin western (inverted) limb, but this apparent asymmetry may be misleading because it is possible that the western limb has been truncated during or subsequent to emplacement of the overlying Wharite Lithotype.

Mesosopic folding within the core of this anticlinal structure is intense. In the majority of cases mesoscopic fold axes parallel the axial strike of the isoclinal fold. Most of the mesoscopic folds are considered to be parasitic and conjugate. Both mesoscopic and large-scale folding at this locality is further complicated by subsequent episodes of folding.

A second large-scale, steeply plunging isoclinal fold occurs in the northeast of the study area in the vicinity of the Rokaiwhana foothills, East Tamaki River and Mangatera foothills. Here a large-scale reversal in younging direction towards the east is thought to indicate that the easternmost exposures of Tamaki Lithotype form the eastern limb of one such fold. The direction of vergence of this fold is unknown, as is the position of its axial plane trace.

Isoclinal folds within Tamaki Lithotype are thought to represent the earliest recognisable major phase of folding in this area.

Within Wharite Lithotype steeply plunging isoclinal and subisoclinal folds with diverse axial trends have only been found on a small scale as isolated

hinge zones (Fig. 7. 1). These folds measure less than 1m across and the limbs are rarely traceable for more than 2-3m. They frequently occur in outcrops where no other sign of fold deformation is present. It is thought that these folds formed during the same early phase of fold deformation that affected the Tamaki Lithotype and are therefore of comparable age. These folds predate ductile deformation of the Wharite Lithotype.

No steeply plunging isoclinal folds have been recorded from strata comprising the Western Lithotype.

Isoclinal folds have also been recorded from Torlesse rocks in the Kaimanawa Ranges (Sporli & Barter, 1973), in the Tararua Range (Rattenbury, 1982) and in the Ruahine Range (Sporli & Bell, 1976). As yet it has not been established whether or not these structures have a common origin.

#### C. Subhorizontal, Open, Asymmetric Folds

These folds have only been identified at outcrop scale and are common to all three Lithotypes. In general, these folds plunge gently towards the north or south and axial planes are of gentle to moderate dip, predominantly towards the west. Fold axis measurements are mostly of this type of fold structure. In the main the strike of fold axes is towards the northeast (Fig. 7.2, diagram A), parallel to the strike of bedrock strata. However, significant numbers of these folds show diverse orientations of fold axes (Fig. 7.2, diagram A) and are presumably the result of subsequent episodes of folding.

The majority of these folds have long east-dipping limbs comprising inverted strata and short west dipping limbs comprising non-inverted strata. These folds vary in form from the most common shallow flexures (Fig. 7.3) to less common recumbent-like structures and to rare near-isoclinal folds with steeply dipping axial planes (Fig. 7.4, see also Fig. 2.6 in Chapter 2). Such folds are responsible for the frequent small-scale reversals in younging direction characteristic of Torlesse strata in this area. These folds post-date ductile deformation of the Wharite Lithotype.

#### D. Steeply Plunging Open Folds

These structures are considered to be responsible for most of the abnormal E-W and NW-SE stratal trends. Within the Tamaki Lithotype several S-shaped open folds occur in road exposures along Delaware Ridge at T23/674184 and T23/667175 (Map 3). Here strata comprising the Very Thin-Bedded Association predominantly strike NE-SW and dip steeply towards the east. The long limbs





FIGURE 7.1: Small-scale hinge zone of a steeply plunging isoclinal fold in Wharite Lithotype. Axial plane trace strikes north-south and limbs dip  $85^{\circ}$  eastward. Note the thickening of argillite beds in the hinge zone and two possible sets of brittle shear. An early set of extensional shears, normal to the sandstone bed (light colour), are preserved only in the sandstone, are without displacement and may have formed during the early phase of ductile deformation. The second set of shears displace both the sandstone and argillite beds and represent deformation during a later episode of brittle deformation. Locality T23/502025 in south Whareroa Stream.

*Geological hammer is 0.28m long.*

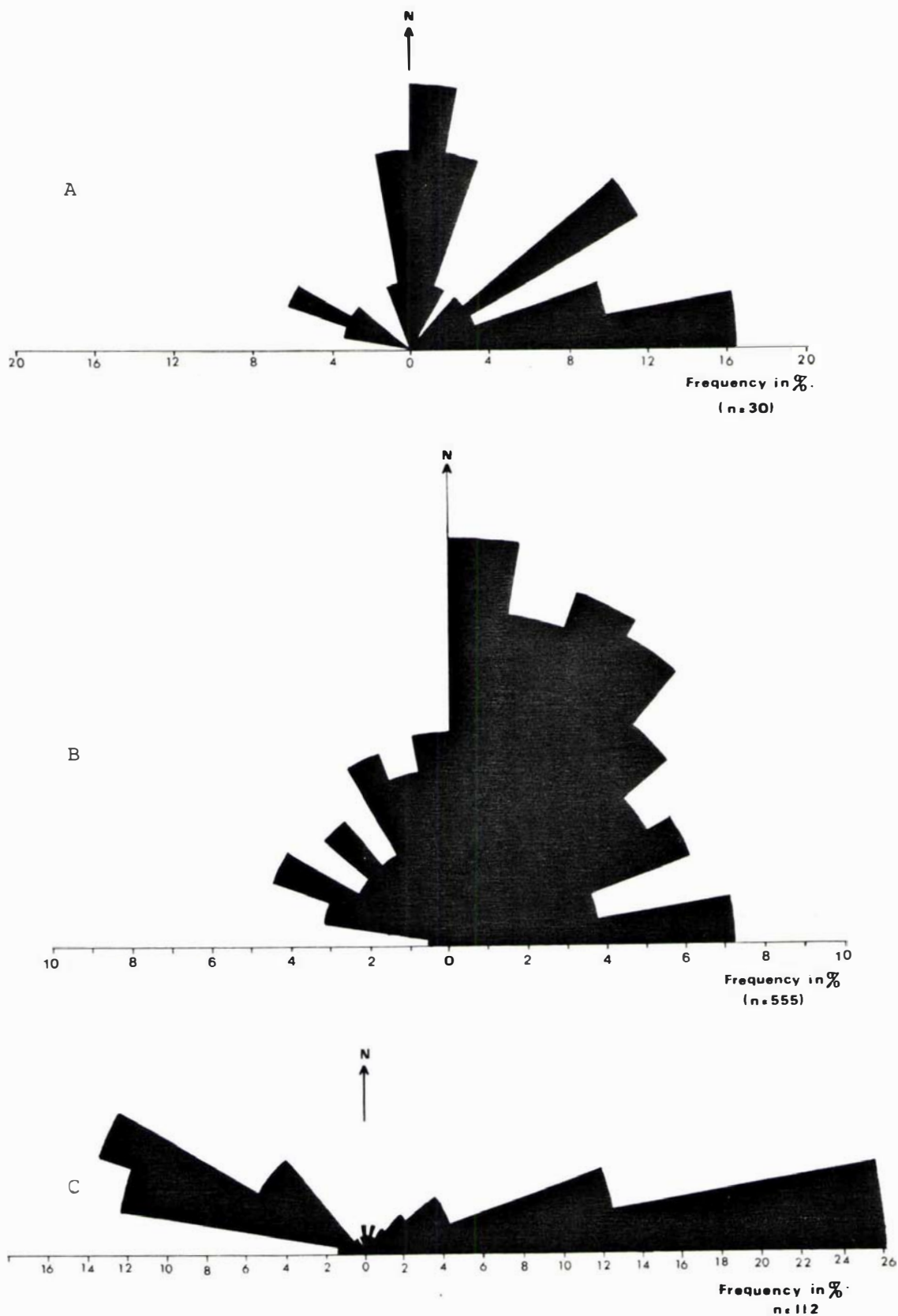


FIGURE 7.2: Rose diagrams showing orientation of fold axes (A), fault orientations (B) and joint orientations (C) measured with respect to north. All observations have been plotted in upper sector of polar graph sphere.



FIGURE 7.3: Subhorizontal, open flexure involving eastward-dipping, thin-bedded strata comprising Tamaki Lithotype. Fold axes plunge gently towards the southeast. The axial plane dips westward at approximately  $30^{\circ}$ . Distance from bottom left to top right of photograph is approximately 15m. Locality is within Cattle Creek at U23/700231.



FIGURE 7.4: Subhorizontal, near isoclinal fold comprising thin-bedded strata of the Tamaki Lithotype. Fold axis is north-south striking and near horizontal. West facing limb is thicker than east facing limb. Note the thickening of the hinge area comprising argillaceous materials. This fold is very localised and dies out towards the top left where the strata are thicker and predominantly of sandstone composition. Also note the four east-northeast striking, post-metamorphic faults (arrowed) that cut across and displace the competent sandstone beds. Locality is in Cattle Creek at T23/270232.  
*Geological hammer is 0.28m long.*

of these folds parallel this northeasterly strike trend whilst the short limbs are at near right angles to the long limbs. Their vergence is sinistral. The amplitude of these folds approximates 125m.

In the Manawatu Gorge the northerly striking axial plane of the isoclinal fold described previously has been refolded sinistrally about a steeply plunging open fold (Zutelija, 1974).

Within Wharite Lithotype several large-scale swings in the strike of bedrock foliation are thought to indicate the presence of both dextral and sinistral, steeply plunging, open folds. In particular, the near east-west trend of foliated strata in: (1) Piripiri catchment at T23/667250; (2) Pohangina catchment at T23/655235; (3) the combined upper catchment reaches of Coppermine, Makohine and Whareroa catchments; and (4) in the middle section of the Manawatu Gorge may represent this type of fold structure (Map 3).

Where these folds occur in the vicinity of the contact between the Tamaki and Wharite Lithotypes, the strike of the east-west aligned strata comprising Wharite Lithotype swings back to a northerly strike to parallel the strike of the contact, e.g. at localities T24/490950 (Manawatu Gorge) and T23/693234 (Cattle Creek).

The obvious swing in strike from northeast to northwest within Mangapukakakahu catchment may also represent a large-scale, steeply plunging, open fold (Map 3). Here parts of the contact between the Tamaki and Wharite Lithotypes are exposed. Strata comprising each lithotype parallels the strike of the contact which is therefore regarded as being conformable,

If this interpretation is correct it implies that this phase of folding involved already steeply dipping strata and that both lithotypes must have been in juxtaposition prior to folding. Also folding post-dated ductile deformation of the Wharite Lithotype because this episode of deformation does not cross-cut either these fold structures or the contact between the two lithotypes.

Steeply plunging open folds were not found in strata comprising the Western Lithotype.

#### E. Sequence of Fold Deformation

Three major post-lithification phases of folding have been recognised:

- (1) Isoclinal folds documented from the Tamaki Lithotype, together with isoclinal and subisoclinal folds documented from the Wharite Lithotype which are inferred to have been formed during the same phase of folding, are the earliest recognised in this area;
- (2) Subhorizontal, open asymmetric folds are common to all three Lithotypes and represent a second phase of folding which refolded both inverted and non-inverted limbs of phase one structures;
- (3) Steeply plunging open folds documented from both the Tamaki and Wharite Lithotypes refold structures formed during the two previous phases of folding and represent the latest recognised phase of folding in this area. Sporli & Bell (1976) observed that steeply plunging open fold structures were particularly well developed within the vicinity of faults and concluded that they are due to a relatively late faulting episode which probably had a pronounced strike-slip component. As both dextral and sinistral folds are present throughout the study area the predominant sense of shear is uncertain. There is little evidence to suggest the time of formation of steeply plunging open folds. They may have formed during the Kaikoura Orogeny (Pliocene-Recent), the Rangitata Orogeny (Late Mesozoic) or during some intermediate phase.

In concurrence with Sporli & Bell (1976) there is no evidence to indicate whether each of the fold phases described from the study area represent distinct events clearly separated in time or have been part of one gradually changing régime. There are no features in the study area which indicate when folding ceased, however, it is known that folding of Torlesse strata was accomplished prior to deposition of Waitotaran (Upper Pliocene) strata upon the plane of marine erosion in the Manawatu Saddle. West of Lake Waikaremoana, slightly deformed Late Cretaceous rocks lap onto steep-limbed, tight, northeast trending folds in the Torlesse (Grindley, 1960). It is therefore inferred that the tight folding and probably the initiation of the steep attitude of the axial planes predate the Late Cretaceous (Sporli & Bell, 1976). Neither the position of these folds in relation to higher order structures nor their relationship with these structures is known.

#### F. Fold Orientation

Fold axis orientation of the majority of folds in the study area is towards the northeast, north and northwest parallel to the strike of bedrock strata (Fig. 7.2, diagram A).

A lesser but significant number of folds of variable fold axis orientation

are the result of refolded earlier folds such as those which occur in axial regions of major northeast-southwest striking isoclinal folds.

### 7.0.2 FAULTS

Chapter 6 contains details of fault classification, the amount, sense and rate of fault displacement and many other aspects of faults and faulting.

Three distinctly different episodes of faulting have been recognised. An early episode of faulting is indicated by the presence of carbonate cemented fault breccia (Fig. 7.5), calcite veining and zeolite formation which are assumed to have formed at depth under conditions of confining pressure and circulating ground water. This episode of faulting is thought to have occurred in Early Cretaceous times during the Rangitata Orogeny.

A later episode of faulting, at shallower depths, has resulted in the re-brecciation of old fault zones to produce non-cemented fault gouge, and the initiation of high angle bedding plane faults which may or may not be coated with fault gouge. This episode of faulting is thought to have coincided with the onset of the Kaikoura Orogeny. The amounts of vertical and horizontal displacement along the major faults, e.g. Ruahine and Wellington Faults, is unknown but is likely to have been considerable whilst displacement along bedding plane faults has been minor and predominantly dip slip.

Fault plane and surface trace orientations produced during these two episodes of faulting are dominantly northeast- to southwest-striking (Fig. 7.2, diagram B).

The latest episode of faulting recognised in this area is represented by low-angle, non-mineralised, non-gouged thrusts that cross-cut bedrock strata and show a marked diversity of strike orientations, the dominant ones being east-northeast, west-northwest and east-west (Fig. 7.2, diagram B). Whether these fault orientations represent separate phases of faulting or are the result of post-faulting fold deformation is uncertain. Displacements along these faults rarely exceed 0.01m (Fig. 7.5).

### 7.0.3 JOINTS

Two types of joints have been recognised - mineralised and open. Both types of joint are most frequently associated with massive sandstone lithologies.

Mineralised joints were only found to occur along major faults. Here jointing is usually intense with the mineral infilling imparting a 'whitish'



FIGURE 7.5: Carbonate-cemented fault breccia (white colour) within a 30m wide fault zone. Rejuvenated fault movement, during Quaternary time, along a high angle fault plane has resulted in re-brecciation and formation of fault gouge. The fault plane strike is  $035^{\circ}$  and dip is  $76^{\circ}$  westward. Note that the bedrock within this fault zone has been completely milled to the extent that no fragment is larger than 0.02m in diameter. Location is T23/542032 in Coppermine Stream.

*Field pack is 0.6m high.*

colouration to the outcrop. Minerals include calcite, quartz and the zeolite laumontite. The intensity of jointing at these localities precluded measurement of joint orientations. The formation of these joints predates formation of the open joint sets with mineralisation probably coinciding with deformation during the Early Rangitata Orogeny.

Two sets of high angle open joints with variable dip direction predominate. They strike east-west and west-northwest to east-southeast, respectively (Fig. 7.2, diagram C). Their strike orientation is consistent throughout all three lithotypes. Open joint sets are a late deformation feature and may have accompanied episodes of folding or faulting.

## 7.1 DEFORMATION

### 7.1.1 INTRODUCTION

This section outlines syndepositional and post-depositional deformation features recognised predominantly in clastic strata comprising the southern Ruahine Range. The predepositional deformation histories of allochthonous rock types derived from older Torlesse terrane are largely unknown and are not considered here. The most common evidence of deformation is seen where uniform bedding is replaced by broken, irregular, or discontinuous bedding. As outlined in Chapter 2 a complete spectrum of degree of deformation is present from: (1) beds that show slight thickness variations (Fig. 7.6); to (2) beds that are pulled apart but maintain traceable bedding horizons defined as foliation (Fig. 2.24 in Chapter 2) and ultimately; to (3) beds that are pulled apart and appreciably disrupted and mixed so that bedding definition is lost (Fig. 7.7). These disrupted units are believed to represent the earliest phase of deformation, a phase that was essentially contemporaneous with deposition. This phase of deformation was characterised by soft-sediment extension of competent beds and ductile behaviour of argillaceous materials. Overall ductile behaviour during this phase of deformation was succeeded by the development of shear fractures during subsequent phases of brittle deformation.

The early phase of ductile deformation was largely restricted to the Wharite Lithotype, with strata comprising the structurally lowermost Tamaki Lithotype being only locally deformed immediately adjacent to the contact with Wharite Lithotype. The structurally uppermost Western Lithotype does not appear to have been affected by this phase of ductile formation. The features characteristic of brittle deformation are, however, common to all three lithotypes.





FIGURE 7.6: Thin beds showing slight thickness variations due to soft-sediment extension of competent sandstone beds and ductile behaviour of argillite beds. Beds strike at  $330^{\circ}$  and dip  $79^{\circ}$  westward. Locality T23/565153 in Porewa Stream.  
*Geological hammer is 0.28m long.*



FIGURE 7.7: Extremely disrupted and mixed clasts of sandstone encompassed by argillaceous matrix. The large central lens of sandstone shows pinch and swell structure, however bedding definition has essentially been lost with most clasts showing little or no alignment. Mineralised extension shears, preserved only in the sandstone clasts, and oriented normal to the long axis of the clasts, formed during the early phase of ductile deformation. Other shears, along which displacement has occurred, together with veins cross-cut both the argillaceous matrix and the clasts. These formed during a later phase of brittle deformation some of which were also mineralised. Note the presence of penetrative, sub-parallel anastomosing cleavage surfaces within the encompassing matrix immediately above the head of the geological hammer. These surfaces have been highlighted by weathering. Also note how small clasts of sandstone within the matrix have their long axes oriented parallel to surfaces of nearby larger clasts.

*Geological hammer is 0.28m long.*

### 7.1.2 DUCTILE DEFORMATION

The following descriptions of features of ductile deformation origin are from outcrops of strata comprising the Wharite Lithotype. These features on an outcrop scale are best displayed in Graded-Bedded, Foliated and Diamictite Lithozones, though on a map scale the Sandstone, Argillite, Volcanic and Chert Lithozones also show signs of ductile deformation.

The pronounced NE-SW aligned mesoscopic fabric, defined as foliation in Chapter 2, is recognised by: (1) a strong preferred orientation of lenticular clasts of competent lithologies (Fig. 2.24); and (2) penetrative, subparallel, anastomosing cleavage surfaces in the accompanying argillite that essentially parallel the clast foliation (Figs 7.7 and 7.8). On an outcrop scale, cleavage surfaces in the argillite conform closely to the outer surfaces of competent clasts. Thus where clasts display pinch-and-swell structures or have tapered ends, into and around which argillite flowed, cleavage surfaces diverge from their preferred NE-SW orientation. Even where individual cleavage surfaces are not visible in argillite, very small lenticular clasts of competent lithologies have their long axes oriented parallel to surfaces of nearby larger competent clasts (Fig. 7.7).

The fabric of Foliated Lithozones may reflect both tectonic flattening during deformation and the influence of the pronounced contrast in ductility between the competent clasts and the more ductile, relatively homogenous argillite in which they are immersed. The strong preferred orientation of the clasts suggests that they have been shortened normal to the foliation and extended parallel to it. Pinch-and-swell structure supports the interpretation that tectonic flattening has occurred (Cowan, 1978). However, experimental and theoretical studies of pinch-and-swell structure and boudinage by Ramberg (1955), Ramsay (1967) and Gay & Jaeger (1957) have shown that they also result from extension of relatively competent materials surrounded by a more ductile matrix. Extension appears to have occurred in all directions oriented approximately normal to foliation. The foliation in argillite parallels the plane of elongation of flattened competent inclusions and, hence, formed normal to the direction of maximum finite shortening.

Ductile deformation took place at relatively low temperatures and confining pressures during which mechanical processes of flow predominated to result in plastically and permanently deformed rocks. In thin section, however, it is clear that some rocks accommodated deformation by cataclastic flow. In particular, cherts and volcanic lithologies are partly or wholly brecciated. On an outcrop scale this deformation may have obliterated pre-

existing accumulations of pillow lava and also accounted for the local concentration of angular fragments of a competent lithology within the argillaceous matrix immediately adjacent to the margin of clasts of the same lithology. In contrast, most clasts of clastic lithologies show little evidence of cataclasis although narrow zones of mechanical granulation, less than 1 mm wide, were seen in thin section (see Chapter 5).

Macroscopic changes in clast shape apparently were accommodated principally by distributed intergranular movements and, to a lesser extent, by localised shear and extension fracturing. Extension fractures occur normal to the direction of clast elongation and are only preserved in the competent clast lithologies where they are seen to terminate at the clast-matrix boundary (Fig. 7.8). Most of these extension fractures occur as mineralised veins of calcite (Fig. 7.7). Macroscopic ductile behaviour of argillite is best illustrated where it has flowed around the edges and into necked regions of flattened and extended clasts. This behaviour resembles the patterns of flow of matrix in natural and experimental examples of pinch-and-swell structure and boudinage described by Ramberg (1955) and Ramsay (1967).

The pervasive nature of deformation and the initial ductility of sandstone beds indicates that the sediment pile was in a plastic state during the initial stage of ductile deformation. It is unlikely that this ductility was induced by elevated pressures and temperatures during metamorphism as the sandstones have retained their original detrital character and no significant recrystallisation other than veining has occurred. Early deformation of semi-lithified rock is indicated and was clearly pre- or syn-metamorphic because fractures and joints formed during this event are filled with metamorphic minerals.

This style of deformation is similar to that described elsewhere in Torlesse terrane by Bradshaw (1972), Sporli & Lillie (1974), Sporli *et al.* (1974) and MacKinnon (1980).

Early ductile deformation was superseded by several episodes of brittle deformation.

### 7.1.3 BRITTLE DEFORMATIONS

Early shear fractures are most easily recognised where they transect flattened clasts and beds of competent lithologies and are indistinct in argillite except where they have been subsequently filled with calcite (Fig. 7.7). These fractures are not as significant as the structures



FIGURE 7.8: Extensional shear fractures within lensed clasts of sandstone. The shear fractures lie at right angles to the long axes of the lensed clasts and terminate at the clast-matrix boundary. The wedge-shaped outline of some clasts suggests that detachment along compressional shear fractures may also have taken place. Penetrative anastomosing cleavage surfaces in the argillaceous matrix define a foliation that is parallel to the foliation defined by the alignment of sandstone clasts. Locality T23/565112 in Mangatuatou Stream.

*Geological hammer is 0.28m long.*

formed during ductile deformation because they are not penetrative on a mesoscopic scale and total displacements along them are comparatively minor. Offsets generally range from a few millimetres to several centimetres. The fractures are generally widespread and have widely divergent orientations. In general more than one set of fractures occur in an outcrop but their poor development and variable orientation preclude any detailed comprehensive analysis of their geometry. Although these shear fractures have only slightly modified the strong fabric developed during ductile deformation, one can visualise that an increase in both the intensity of fracturing and the amount of offset along fractures could promote the progressive disruption of originally interbedded lithologies to result in the formation of isolated lenticular-shaped clasts of competent lithologies within a matrix of sheared argillite.

Subsequent phases of brittle deformation occurred during episodes of Cenozoic and Quaternary faulting to produce: (1) high-angle faults which predominantly parallel steeply dipping bedding planes; (2) low-angle thrusts that cross-cut bedding plane attitude; (3) two prominent sets of open joints; and (4) resulted in the disruption of bedrock outcrops by loosening the sharp contact between clasts of competent lithologies and the encompassing argillaceous matrix (Fig. 7.9).

#### 7.1.4 DISCUSSION

In dealing with melange terrane one would like to determine whether the apparently chaotic nature and lithologic heterogeneity of: (1) the diamictites; and (2) the Wharite Lithotype as a whole are primary sedimentary features or the result of tectonic deformation.

##### A. Origin of Diamictites

In Chapter 2 (section 2.1.3E) it was suggested that diamictites may form either by extreme post-depositional fragmentation of bedded sequences or as primary sedimentary debris flow deposits. The predeformation and fabric of diamictites, in particular the rounded shape, diverse orientation and random dispersal of clasts (see Chapter 2) favours a sedimentary origin. The diamictites contain clasts floating in an argillaceous matrix. They are intimately associated with turbidity current deposits (see Chapter 3) and are contained within an assemblage composed entirely of marine rocks. These three factors are here interpreted to indicate that the diamictites originated as subaqueous debris flow deposits. The presence of an allochthonous block of limestone within a diamictite in this area may be used to

invoke processes of erosion of the limestone from an older terrane and its subsequent incorporation within a debris flow deposit. The absence of sheared margins separating the limestone block from the encompassing argillaceous matrix enhances the possibility of its emplacement by subaqueous mass transport processes. However, as was pointed out in Chapter 4 (section 4.6), the absence of sheared surfaces around the limestone block does not necessarily exclude tectonic emplacement because such surfaces may have been healed during metamorphism. The occurrence of this limestone as an isolated block and its absence as a coherent bed, suggests that it is not the result of the pulling apart of a bedded unit during ductile deformation. No explanation is offered to account for the absence of other blocks of this limestone from diamictites elsewhere in the study area but their presence to the north and south of the study area (see Chapter 4) may indicate the presence of other limestone-bearing diamictites in these areas. However, the derivation of the other limestone blocks has not yet been established. Nonetheless, it is considered that the widely spaced and isolated occurrence of this limestone is more readily explained in terms of discrete episodes of debris flow activity than by the tectonic pulling apart of a coherent bedded unit. Also, on an outcrop scale, no evidence from this area supports large-scale horizontal displacement by either ductile or brittle deformation of dislocated blocks over distances measured in kilometres. Overall, it is therefore favoured that diamictites in this area are of primary sedimentary origin.

Sedimentary processes including submarine sliding and downslope transport of argillite-rich and lithologically diverse debris flows probably resulted in the internally chaotic, non-bedded fabric of these diamictites. The lensing, rotation and weak development of aligned clasts in some diamictite deposits has therefore been superimposed during the subsequent episode of ductile deformation, whilst the internal fabric of most diamictites remained chaotic.

#### B. Origin of Wharite Lithotype

Lithologically, the bulk of sediments within Wharite Lithotype comprise flysch-type deposits of turbidity current origin (see Chapter 3). Whilst at some localities stratal sequences resemble the regularly alternating interbedded sandstones, siltstones and argillites (Graded-Bedded Lithozones) characteristic of the Tamaki and Western Lithotypes (see Chapter 2), the majority of flysch-type deposits within Wharite Lithotype consist of fewer alternations of interbedded lithologies, more variable bed thickness and a



FIGURE 7.9: Post-metamorphic, non-mineralised shear surfaces with partings up to 0.01m width across the fracture. Fractures cross-cut both the competent clasts and argillaceous matrix and frequently coincide with the contact between these materials. These shears formed during a late phase(s) of tectonic brittle deformation predominantly during episodes of faulting. These shears loosen the competent clasts resulting in a severe reduction of the overall strength of bedrock outcrops within Wharite Lithotype.

*Geological hammer is 0.28m long.*



wider variety of lithologies including red and green argillites. Where these flysch-type deposits are thin bedded, the sequence tends to be argillite-dominated and, conversely, where thick bedded, sequences tend to be sandstone-dominated. Ductile deformation of some of these deposits has in places resulted in sequences of foliated strata that exhibit a range of deformational forms (see 7.1.2). These disrupted sequences are interstratified with uniformly bedded sequences that show none of the effects of ductile deformation. In general, the argillite-dominated sequences tend to be the most severely deformed and the sandstone-dominated sequences the least deformed. However, in some places even the thickest sandstone beds show obvious signs of ductile deformation. These flysch-type sequences comprise the Foliated Lithozones. Although turbidite deposition predominated, it was periodically interrupted either by muddy debris flows comprising lithologically diverse pebble- to boulder-sized clasts (Diamictite Lithozones) or sandy debris flows (Sandstone Lithozones). It cannot be unequivocally demonstrated that these latter lithozones are in depositional contact with the flysch-type sequences or that they constitute part of a conformable sedimentary sequence. Nonetheless, as the structural attitude of these lithozones is fairly constant throughout Wharite Lithotype and as the contacts between these lithozones parallel both internal bedding (in Graded-Bedded Lithozones) and foliation (in Foliated Lithozones), it is tempting to consider such sharp contacts as depositional even though there may have been movement along them during ductile deformation.

The difficulty in interpreting the primary nature of contacts between all lithozones stems largely from the observation that these contacts occur within an argillaceous medium. The ductile nature of this medium is not conducive to the preservation of deformational forms typically associated with faulting. Instead, deformation of the argillite would tend to result in flowage and hence mask the true nature of the contact. It is suspected that mobilisation of argillite has occurred up to and during metamorphism, consequently many contacts of initial fault origin may have healed and now assume the appearance of a sharp but conformable depositional contact.

Perhaps the most significant and characteristic aspect of Wharite Lithotype is the complex interrelationship between the Volcanic Lithozones (and often associated Chert Lithozones) and the surrounding clastics. Volcanic Lithozones, particularly those comprised of massive volcanic and associated chert lithologies, seem to be stratigraphically restricted. Other Volcanic Lithozones comprising pillow lava accumulations and red and green argillite

horizons also occur in restricted stratigraphic lithozones but are more widespread than are the massive volcanics. All Volcanic Lithozones lie parallel to regional strike but it is not clear whether or not they are interlayered or interleaved with the surrounding clastics. All are entirely without connective dykes which suggests emplacement either by gravitational sliding or by tectonic interleaving.

The occurrence of volcanic and chert lithologies as clast constituents of pebble- to boulder-size within Diamictite Lithozones has been explained in terms of a subaqueous debris flow mechanism, thus providing a plausible explanation for the occurrence of larger blocks of these lithologies, of mappable size, within Wharite Lithotype. The alignment of Volcanic Lithozones that comprise massive volcanics and associated chert along the Ruahine Fault Zone which has been active during and/or since the Rangitata Orogeny may indicate that these volcanics have been infaulted into the flysch-type sequence along this surface of movement. Thus fault emplacement of the massive volcanics is suggested but not dictated by: (1) the partial alignment of these volcanics along a major fault zone that has been active since the Rangitata Orogeny; and (2) the high proportion of sheared contacts with clastic sediments. Evidence against fault emplacement includes: (1) conformable structural attitude with adjacent clastic sequences; (2) all contacts are not sheared but in places appear to be gradational in a sedimentological sense; and (3) not all outcrops of massive volcanics coincide with fault zones that have been active since the Rangitata Orogeny.

In conclusion, there is no unequivocal evidence to suggest whether these Volcanic Lithozones have been emplaced by either infaulting or gravitational sliding. It is here suggested that Volcanic Lithozones comprising massive volcanics and chert may have been emplaced as a sheet-like body of lithified rock by either mechanism. Shearing of the volcanic and chert lithologies off the seafloor and incorporation into an accretionary prism is favoured by Sporli & Bell (1976), Sporli (1978), Howell (1980) and Roser (1983).

Lines of evidence suggesting that these Volcanic Lithozones did not form contemporaneously with clastic sedimentation in the basin of deposition include:

- (1) Extrusion of submarine basalt would have to coincide with hiatuses in turbidite sedimentation;
- (2) Basalts and cherts are of probable, though unproven, older age than the surrounding clastic sediments;

- (3) Sheets of massive volcanics and cherts are without connective dykes;
- (4) There is no evidence of other lithologies characteristic of the Steinmann Trinity in this area; and
- (5) Massive volcanics and cherts have been subjected to more intense and a greater number of episodes of brittle deformation, than have the clastic lithologies, thereby suggesting that they were lithified prior to incorporation within the suite of clastic sediments.

Those Volcanic Lithozones that comprise: (1) red and green argillite as interbeds with alternating sandstone and black argillite; and/or (2) intact pillow lava accumulations that young in the same direction as the surrounding clastic sediments, suggests that they were deposited in the sedimentation basin. The absence of baked margins between the volcanics and surrounding clastic sediments does not necessarily negate such an interpretation as the exterior surface of the pillows may have cooled considerably prior to coming into contact with the clastic sediments. Although many of the contacts between these Volcanic Lithozones and the surrounding clastics are faulted, a mechanism of fault emplacement is discounted because: (1) most faulted contacts are clearly of Quaternary age and therefore post-date emplacement. None show signs of earlier movement; (2) not all contacts between these Volcanic Lithozones and the surrounding clastics are faulted; and (3) where the contact is not faulted, it appears to be gradational both in a sedimentological and a structural sense. These contacts are considered to be largely of primary depositional origin.

Pringle (1980) has described some unfaulted contacts between basalts and the greywacke suite from Torlesse and Haast Schist terranes of Otago and Canterbury. He interpreted these as distal flows, from intraplate volcanics nearing the subduction zone, that were coeval with turbidite sedimentation.

Cosedimentation of red and green argillites with clastic sediments is thought to indicate long hiatuses in turbidite sedimentation. The contacts between red and green argillites and the greywacke suite in both the study area and in Canterbury (Sporli et al., 1974; Sporli & Lillie, 1974), show hiatuses which were of sufficient duration to permit the volcanic argillites to oxidise.

Although active volcanism has not been described in modern depositional environments similar to that proposed for the Torlesse sediments, evidence from this area favours a syndepositional origin for Volcanic Lithozones

comprising both intact pillow lava structure and/or red and green argillite horizons. However, emplacement of large allochthonous rock bodies containing these lithologies by either a fault or gravitational mechanism cannot be overlooked. Slide masses of other than volcanic lithologies are also likely to be present. The most probable include large tabular blocks of massive sandstone comprising Sandstone Lithozones. They too are structurally conformable to the foliation in adjacent outcrops but they are usually terminated abruptly, seemingly truncated by the argillite.

In summary, a sedimentary origin has been attributed to the bulk of the Lithozones that comprise Wharite Lithotype. However, their formation implies tectonic instability in the area during deposition. Signs of tectonic instability include the irregularity in bed thickness and the irregularity in the frequency of alternate deposition of different lithologies. These features contrast markedly with the regularity of bedding thickness and frequent alternation of beds of different lithology so characteristic of the distal turbidite deposits comprising the Tamaki and Western Lithotypes. In addition, turbidite deposition was frequently accompanied by deposition of boulder-bearing argillaceous debris flow and sandy debris flow deposits resulting from large-scale slumping on the continental rise or slope. At times the level of tectonic instability declined sufficiently to permit a resumption of normal distal turbidite deposition. Periodically clastic sedimentation ceased altogether for sufficiently long periods of time to permit accumulation of thin (1-5 cm) beds of chert. A suggestion that volcanism in the vicinity of the depositional basin was contemporaneous with deposition is the presence of intact pillow lava accumulations and conformably interbedded red and green argillites the latter being of probable but unproven volcanic origin.

Tectonic sliding of some Volcanic, Chert and Sandstone Lithozones onto the sedimentary pile occurred contemporaneously with sedimentary deposition.

In conclusion, the sedimentological and structural analyses reported here are interpreted to indicate that the Wharite Lithotype is a proximal facies and the Tamaki Lithotype a distal facies. Furthermore, the Wharite Lithotype contains vari-sized allochthonous debris and hence constitutes an olistostrome. In addition, the Wharite Lithotype shows evidence of later deformation and tectonic remobilisation and hence also constitutes a melange. Thus it may be regarded as a tectonised olistostrome.

### C. Nature of the Contact Between Lithotypes

One of the most significant relationships observed in the study area is the nature of the contact between Wharite Lithotype and the structurally underlying Tamaki Lithotype.

The nature of this contact varies according to: (1) which of the identified lithozones comprising Wharite Lithotype lies immediately adjacent to the contact; and (2) whether or not the contact is faulted.

In all cases where strata comprising a Foliated Lithozone lie in contact with bedded strata (*i.e.* Graded-Bedded Lithozones) of the Tamaki Lithotype, the strike of the foliated strata to the west of the contact parallels the strike of bedded strata to the east of the contact. On approaching this contact from the east, *e.g.* at locality T23/675213, the bedded strata comprising the Tamaki Lithotype show a gradational westward increase in the intensity of deformation. A transition from non-deformed beds to mildly folded beds showing slight pinch-and-swell features occurs within a distance of between 2-5m from the contact. To the west of the contact strata comprising the Wharite Lithotype are strongly deformed and pulled apart to produce a foliation.

Where an Argillite Lithozone lies on contact with the underlying Tamaki Lithotype, *e.g.* at locality T23/661182, the bedded strata comprising the Tamaki Lithotype are undeformed whilst the argillite comprising the Argillite Lithozone shows a westward increase in the intensity of cleavage. Cleavage parallels the strike of bedded strata in the underlying Tamaki Lithotype.

At each of the above described localities the contact between the Wharite and Tamaki Lithotypes is interpreted as depositional. These contacts are not faulted and deformation is not penetrative for any great distance into strata comprising the underlying Tamaki Lithotype. This interpretation does not preclude the possibility that considerable movement occurred along this contact prior to or during metamorphism.

Sandstone, Volcanic, Chert and Diamictite Lithozones have not been found adjacent to the contact with strata comprising the Tamaki Lithotype in this area.

In places the contact between the Tamaki and Wharite Lithotypes is faulted and may be considered to be of two forms. The first display pre-metamorphism

fault movement and the second display post-metamorphism fault movement.

- (1) At locality T24/490951, the presence of autoclastic breccia (after Reed, 1957b), referred to as mylonite (Zutelija, 1974), indicates that pre-metamorphic movement occurred at the contact between Wharite and Tamaki Lithotypes. This contact may either represent a major tectonic break or a depositional contact that has been locally strongly disrupted during ductile deformation. The style of deformation seen at this locality is very similar to that witnessed throughout Wharite Lithotype.
- (2) At locality T23/650141, a Graded-Bedded Lithozone comprising Tamaki Lithotype occurs in sharp contact with a Foliated Lithozone comprising the Wharite Lithotype. Eastward of the contact the bedded strata of Tamaki Lithotype are undeformed even at the contact itself. Westward of the contact lensed sandstone clasts occur within a sheared argillaceous matrix. Both the foliated sandstone clasts and fracture cleavage in the matrix parallel the strike of bedded strata in the underlying Tamaki Lithotype. This contact is marked by a localised knife-sharp, steeply-dipping, bedding plane fault. The sharp outline of the fault and the absence of deformation of the uppermost beds of the Tamaki Lithotype indicate that fault displacement has occurred at this locality. The presence of soft clay-like gouge indicates that fault displacement was post-metamorphic.

At locality T23/694234, strata comprising both the Tamaki and Wharite Lithotypes are disrupted over a 300m wide zone. Within this zone the foliated strata comprising Wharite Lithotype parallels bedded strata comprising the Tamaki Lithotype. All the strata dip steeply towards the east. The structural attitude of the strata within this disrupted zone is the same as that both to the east and west of this zone. The contact between these two lithotypes occurs within this zone, disruption of which has been the result of Quaternary fault movement along the Ruahine Fault Zone. The strike of this steeply inclined fault zone parallels the strike of the strata and hence the contact between these two lithotypes. Fault disruption of the strata has made it difficult to locate the contact and impossible to determine the original nature of the contact. Nonetheless, it is considered that the parallelism of strata comprising both lithotypes across the contact and the lack of evidence of an early phase of fault displacement at this locality, is suggestive of a conformable contact of probable depositional origin.

The occurrence of high angle faults that display evidence only of Quaternary fault movement at the contact between the Wharite and Tamaki Lithotypes is considered to be largely coincidental. Where observed the contact between Wharite and Tamaki Lithotypes is interpreted to be of depositional origin because of: (1) the absence of penetrative deformation in the underlying Tamaki Lithotype; (2) foliation patterns in the Wharite Lithotype parallel bedding in the Tamaki Lithotype; (3) the contact is conformable with the structural attitude of the strata; (4) the Wharite Lithotype dips eastward beneath the Tamaki Lithotype; (5) the contact is not faulted at all localities; and (6) where faulted, the contact generally displays evidence of post-metamorphic fault disruption and/or displacement, there being little sign of earlier fault movements.

In summary, where local disruption of the uppermost strata of the Tamaki Lithotype has occurred at non-faulted localities along this contact, disruption was syndepositional and probably occurred as a result of rapid deposition of sediment by subaqueous mass transport processes. The presence of mylonite at the contact is suggestive of a major but localised tectonic break or may simply be the result of a local intensification of ductile deformation. Mobilisation of argillite prior to and during metamorphism suggests that at all localities the contact between these two Lithotypes is likely to have been subjected to some degree of tectonic deformation. Where post-metamorphic fault disruption and displacement has occurred along this contact it is in all cases considered to be coincidental. No evidence of nappe-structures of large-scale overthrusts occur along this contact.

The nature of the contact between the Wharite and Western Lithotypes is also interpreted as being depositional because: (1) there is an absence of penetrative deformation in the lowermost bedded strata of the overlying Western Lithotype; (2) bedding patterns in the Western Lithotype parallel the foliation in the underlying Wharite Lithotype; (3) the contact is conformable with the structural attitude of strata on either side of the contact; (4) the Western Lithotype dips eastward beneath the Wharite Lithotype; and (5) there is no evidence of an early phase of fault displacement along this contact.

Although all three Lithotypes are of regional extent and are broadly distinguished by differences in lithology, structure and deformation, they cannot be considered as discrete structural units in the sense of the "terrane concept" (Jones *et al.*, 1981) because: (1) the contacts between the Lithotypes are not everywhere faulted; (2) there is little direct

evidence suggestive of large displacement along the contact; (3) the Lithotypes are considered to be part of a continuous westward younging, overturned, stratigraphic sequence of Late Jurassic age; and (4) the Lithotypes have experienced the same metamorphic history.

However, should strata comprising the Western Lithotype be proven to form part of an extensive westward-lying terrane of Late Triassic age (see Chapter 4) then this contact can be considered a major tectonic break.

#### D. Mechanism of Deformation

An important question is whether deformation of the Wharite Lithotype is dominantly the result of processes near the sediment-water interface or of deeper tectonic origin. The absence of intense soft-sediment deformation features in the underlying Tamaki Lithotype indicates that the Wharite Lithotype was not emplaced into the basin of sedimentation as a single olistostromal unit. Consequently, deformation of the Wharite Lithotype itself is unlikely to be solely the result of gravitational sliding. However, as previously outlined, sliding may have been locally disruptive adjacent to some of the Volcanic and Chert Lithozones.

The absence of deformation in the overlying Western Lithotype could indicate that deformation of the Wharite Lithotype occurred prior to deposition of the Western Lithotype and therefore occurred at the sediment-water interface. Equally probable is that deformation of tectonic origin occurred at depth under an overburden and was confined to a linear zone such as a fault. The structures described in the preceding sections indicate that deformation of the Wharite Lithotype took place under confining pressures sufficiently high to permit ductile flow of the argillaceous matrix but not sufficiently high to prevent brittle fracturing of the competent lithologies. During early stages of deformation most of the clastic sediments may have been unlithified as rarely do they show any evidence of brecciation, whereas the massive volcanic and chert lithologies frequently show evidence of brecciation along their margins and in the necked regions between boudins, indicating they were lithified during deformation. The micritic limestone block was almost certainly completely lithified prior to deformation. The tectonism that is required to deform lithified blocks into lens-shaped clasts would be sufficient to cause similar effects in partly or completely lithified greywacke. Therefore, even though many clasts may once have been unlithified and initially deformed by surficial processes, it seems that their shapes can be explained equally well as resulting solely from tectonic deformation. The time lapse between deposition of a particular bed and its



deformation in a soft-sediment state does not necessarily indicate that it was contemporaneous or pene-contemporaneous with sedimentation. Neither does it necessarily imply deformation near the sediment-water interface. In some rapidly deposited clastic materials, lithification may take an extremely long time. For example, the Miocene sands of the Gulf Coast sedimentary province of Louisiana (Dickinson, 1953) occur at a depth of about 3300m and are still unconsolidated, so that deformation at the present time would produce structures with a style typical of deformation in soft sediment (Sporli & Barter, 1973).

As mentioned before, the style of deformation does not reflect milling, grinding or crushing. For the most part, large blocks are disaggregated into smaller clasts by boudinaging or fracturing. On an outcrop scale, separation between clasts is, in general, no greater than 1-2m and averages 0.1m. On a map scale, however, the inability to trace large blocks from one catchment to the next may indicate that displacements have been substantial and often exceeded 0.5 km. Separation of clasts at all scales recognised in the study area can be accommodated by both gravitational sliding and a tectonic mechanism.

A largely tectonic origin is inferred for most Torlesse rocks displaying similar styles and degree of deformation. This is suggested by both internal structural evidence including plastic deformation in the weaker materials and shearing, intense boudinage and disruption in the competent lithologies but also more convincingly by the gradational contacts between these areas and surrounding relatively intact rock sequences (MacKinnon, 1983). At some localities this gradation appears to be demonstrated by an increased proportion of stratified rock and a reduction of deformation to fewer and thinner zones. This tectonic deformation has been superimposed upon an earlier locally restricted deformation related to syndepositional gravitational sliding and to debris flow activity.

If the phase of steeply plunging open folding is mentally subtracted the contact between Wharite and Tamaki Lithotypes is seen to be a relatively straight, smooth boundary. As previously mentioned, the absence of penetrative deformation in the underlying Tamaki Lithotype and also the absence of any form of disconformity between the two lithotypes is suggested to be strong evidence against either gravitational emplacement along a slide plane or the telescoping along a low angle thrust fault of the Wharite Lithotype onto the Tamaki Lithotype. In addition, it is unlikely that strata comprising the Tamaki Lithotype is of greatly different age to that

comprising the Wharite Lithotype (see Chapter 4). For these reasons, it is considered that this contact is not a major tectonic break but is more probably a stratigraphic contact that has been subjected to differential deformation.

#### E. Tectonics

The Torlesse of the southern Ruahine Range has accumulated at a convergent plate margin. New Zealand lies across the boundary between the Indian Plate to the west and the Pacific Plate to the east. The Pacific Plate is subducted beneath the North Island as a shallow dipping thrust ( $12^{\circ}$ ), for some 250 km, before it abruptly descends into the asthenosphere at a dip of  $50^{\circ}$ . On the basis of sea-floor spreading rates (Minster *et al.*, 1974) and geodetic data (Walcott, 1978a), the Pacific Plate, comprising Cretaceous oceanic crust (Molnar & Atwater, 1978), is believed to approach the east coast of the North Island at a rate of 50 mm/yr. Since the Indian Plate boundary is inclined at  $50^{\circ}$  to the direction of Pacific Plate motion, the two plates converge obliquely.

At a convergent margin where there is active subduction, sea floor sediments are either subducted along with the oceanic crust or are scraped off and accreted to the base of the overriding plate or both. Evidence from both the North and South Islands where the presently accepted regional younging direction is towards the east, suggests that accretion has been the dominant process. With accretion of each new wedge, older wedges are thrust upward on reverse faults. If the most simple version of this process is assumed, the thrusts will form in sequence, with the earliest lying on the landward side and the youngest on the oceanward side. These thrusts are inferred to be sites of aseismic ductile deformation. Some of the deformation is probably facilitated by high pressures in liquids trapped in the argillite-rich matrix (Sporli & Bell, 1976). The Wharite Lithotype is here postulated to have formed in association with one such thrust fault.

In view of the absence of obvious structural discordance between the Wharite Lithotype and adjacent undeformed lithotypes (Western and Tamaki Lithotypes), it is inferred that this thrust zone was initiated at a very shallow angle of dip and that the sediments were deformed whilst in a near horizontal attitude. Ductile deformation, coincidental with asymmetric folding of the competent clastics, would initiate and facilitate the bulk rotation of the sheets around a subhorizontal axis until the bedding is at right angles to the subhorizontal direction of maximum shortening. At a later stage the thrusts and folds would cease to be active and could be

further rotated and possibly complexly refolded owing to increased underthrusting towards the west and accretion of additional sedimentary material. At relatively high levels in the sedimentary pile it is possible that sequences deformed in this way are rotated past the vertical to become completely overturned, as is the case in the southern Ruahine Range (Sporli & Bell, 1976). This would also explain the pattern of regional eastward younging of successive thrust sheets each of which is internally westward younging. Such a pattern cannot be explained in terms of a giant nappe.

Supportive evidence of imbrication and rotation of thrust sheets at continental subduction margins overseas has been summarised by Sporli & Bell (1976) in which they mention the following:

"Examples of such imbrication associated with subduction have been recorded from the landward side of the Aleutian trench (Grow, 1973, Fig. 6). The shear zones dip away from the trench and are spaced 5-10 km apart. Profiles on the inner side of the Nankai trough of Japan (Ingle *et al.*, 1973) show a gradual landward rotation of landward dipping thrust slices from a  $5^{\circ}$  dip near the trench to  $45^{\circ}$  dip 40 km away from the trench. Thickness of the thrust packets range from 800m to 2800m. A fossil example is recorded from the Cretaceous trench deposits of south eastern Alaska where Moore (1973) has recognised progressive landward rotation of asymmetric folds verging into the trench. Processes of this type may have caused the widespread steep attitudes in the Torlesse Supergroup of both islands (*sic*).

In examples of recent deformation at trenches, apparently undeformed sediment in the trench is separated from deformed material on the inner trench wall by the "tectonic front" (Carson *et al.*, 1974) which in many trenches migrates outward in discrete jumps governed by the decollement processes in the sequence undergoing subduction."

(p 444-445).

The Wharite Lithotype is only one of several units that display a similar deformational style, further examples of which include those described from the Kaweka Range (Crippen, 1977), Kaimanawa Range (Hegan, 1980), Tararua Range (Keller, 1954; Reed, 1957a; Rattenbury, 1982) and the Raukumara Range (Isaac, 1972; Feary, 1974).

In some of these areas, e.g. in the Kaweka Range (Feary, 1974) deformation has been related to tectonic sliding. Similarly, deformation of the Esk Head melange in north Canterbury (South Island) is possibly related to tectonic slides that occur in the area immediately to the north of this

melange (Bradshaw, 1972). However, as pointed out by Bradshaw, in some respects the differences in deformation style between melange and tectonic slides is one of intensity rather than kind (p 166).

Should strata comprising the Western Lithotype prove to be of Late Triassic age then Wharite Lithotype represents a melange separating two accreted thrust sheets with a sheet of Late Triassic age lying structurally above and to the west of a sheet of Late Jurassic age. The contact between Wharite and Western Lithotypes is then a major tectonic break of regional extent, the mapping of which is of considerable geotectonic significance to understanding the evolution of the New Zealand Geosyncline. The thickness of melange zones in the local area is known to be highly variable but other aspects of their geometry such as lateral continuity, structural relationships with adjacent coherent sequences and age remain unknown.

C H A P T E R 8

GEOLOGICAL HISTORY

CONTENTS

	<u>page</u>
8.0 INTRODUCTION ... ..	221
8.1 PRE-LATE CRETACEOUS GEOLOGICAL HISTORY OF THE TORLESSE ...	221
8.1.1 PROVENANCE ... ..	221
8.1.2 SEDIMENT TRANSPORT AND DEPOSITIONAL MECHANISMS ...	222
8.1.3 DEPOSITIONAL ENVIRONMENT . ... ..	223
8.1.4 AGE .. ... ..	224
8.1.5 LITHOSTRATIGRAPHY AND DEFORMATION .. ... ..	224
8.2 POST-LATE CRETACEOUS GEOLOGICAL HISTORY OF THE SOUTHERN RUAHINE RANGE ... ..	226
8.3 DEFORMED REMNANTS OF THE PRE-QUATERNARY EROSION SURFACE ..	228
8.4 ORIGIN OF THE MANAWATU GORGE AND A LOCAL ANALOGY ... ..	231
8.4.1 THE ANALOGY ... ..	233

## CHAPTER 8

### GEOLOGICAL HISTORY

#### 8.0 INTRODUCTION

This chapter is a synthesis of the major geological events that have been responsible for many of the characteristic features of rocks comprising the Torlesse terrane. Later episodes of Quaternary faulting are outlined together with an updated interpretation of the physiography of the southern Ruahine and northern Tararua Ranges and the formation of the Manawatu Gorge is presented.

#### 8.1 PRE-LATE CRETACEOUS GEOLOGICAL HISTORY OF THE TORLESSE

##### 8.1.1 PROVENANCE

Sediments comprising the Torlesse in the study area have been derived from a mixed volcano-plutonic source area which is thought to have lain to the south of New Zealand in the vicinity of the then position of Antarctica. The composition of clastic grains suggests that most of the mineral constituents were derived from a quartzofeldspathic plutonic provenance. Detrital grains of volcanic origin indicate derivation of a lesser component from a provenance comprising lavas of basaltic composition with minor rhyolitic and andesitic lavas. Sedimentary and volcanic rock fragments predominate. Metamorphic and plutonic rock fragments form an inconspicuous component. Sedimentary and volcanic lithologies in the conglomerates also indicate a mixed source. Both the volcanic fragments in the sandstones and the volcanic pebbles in the conglomerates are of similar composition and texture to the essentially massive volcanics and pillow lava basalts found to outcrop in this area. The presence of volcanic lithologies, both as rock fragments within sandstones and as pebbles within conglomerates, is suggestive of rapid deposition before breakdown to their constituent grains could occur. The pebbles contain mineralised cracks and veins not present in the encompassing matrix, indicating derivation from older sediments that had been buried and indurated prior to uplift and erosion. In addition, the well-rounded shape of the pebbles is suggestive of reworking. An allochthonous block of fossiliferous limestone together with blocks of calcareous conglomerates indicate derivation, at least in part, from a shallow water marine terrane.

It is not known if any of these diverse lithologies occurred together in

the same source terrane or if they were derived from mixed source terranes. As none of the lithologies are of greater metamorphic grade than the sequences within which they are now contained it is interpreted that the source terrane(s) had not been subjected to metamorphism of greater than prehnite-pumpellyite grade. In view of the absence in the study area of clasts that may be considered to be 'exotic' to the Torlesse, it follows that the reworked materials are largely of intraformational origin.

#### 8.1.2 SEDIMENT TRANSPORT AND DEPOSITIONAL MECHANISMS

Subaqueous sediment transport and deposition of the Torlesse is here considered to have been dominated by sediment gravity flow processes with ocean bottom currents operating in the latter stages of deposition to produce or modify some of the textures and structures observed. In view of the predominance of: (1) very thin-, thin- and thick-bedded regularly alternating sequences of graded beds with preserved internal sedimentary structures; (2) the restricted occurrence of very-thick and thick-bedded massive sequences of sandstone; (3) the poor development of thin beds of fine-grained conglomerates and absence of coarse-grained conglomerates; and (4) the scarcity of thinly developed fine-grained pebbly mudstone deposits, it is interpreted that the flysch-type sequences (Graded-Bedded Lithozones) comprising each of the three Lithotypes (Tamaki, Wharite and Western) are distal facies deposits essentially emplaced by turbidity currents and modified by other sediment gravity flow processes. The absence of bioclastic limestone, the paucity of primary calcareous matrix, the sparseness of fossils and the textural immaturity of the arenites are also consistent with such a process.

With the onset of precursory tectonic movements in Jurassic time that culminated in the main phase of the Rangitata Orogeny in the Early Cretaceous (Fleming, 1975), the source areas are likely to have become tectonically unstable. In these areas the triggering of mass movements produced sediment gravity flows. Signs of tectonic instability in the depositional basin are indicated by the irregularity in bed thickness and the irregularity in the frequency of alternate deposition of different lithologies that now comprise Wharite Lithotype. Here, turbidity current deposition of predominantly arenaceous materials (Foliated Lithozones) dominated but was periodically interrupted by deposition of massive units of ungraded sandstone (Sandstone Lithozones) by grain flow or sandy debris flow processes and deposition of unsorted argillite-dominated, boulder-bearing debris flow deposits (Diamictite Lithozones). Rarely the deposition of fine-grained argillaceous materials (Argillite Lithozones) occurred during a hiatus in the supply of coarser grained arenaceous materials.

Both the continental rise as a site of fine-grained argillite and silt sedimentation and the continental slope, as a site of extensive sediment accumulation that includes allochthonous debris, are considered likely source areas.

Radiolarian cherts occur either as thin beds within units of argillaceous material, representing biogenic accumulation during a hiatus in clastic sedimentation, or occur in association with volcanic lithologies. Sheet-like bodies of massive, altered oceanic basalt and pillow basalts often accompany the chert. Although unproven, it seems likely that these massive volcanics and associated cherts are older than the surrounding clastic sediments. An absence of connective dykes favours this interpretation, that these volcanics were emplaced as sheets onto a sedimentary pile by gravitational sliding during clastic sedimentation. Gravitational sliding of non-volcanic rock bodies is also considered likely but owing to the absence of fossils and distinctive discriminating petrological criteria it has not been possible to distinguish them from contemporaneous sediment accumulation.

Accumulations of intact pillow lava younging in the same direction as the surrounding clastic sediments strongly suggests contemporaneous volcanism. Red and green argillite horizons, of uncertain affinity, may be distal volcanogenic hemipelagic sediments that accumulated contemporaneously with clastic sedimentation.

Major and trace element analyses of volcanic lithologies indicate that they are chemically similar to oceanic basalts and the majority are considered to have been erupted in a mid-ocean ridge setting. A minority of samples appear to have chemical affinities with an intraplate setting. None of the samples are chemically consistent with derivation from an island arc.

### 8.1.3 DEPOSITIONAL ENVIRONMENT

Sediment deposition is here considered to have occurred in a deep-water environment of geosynclinal dimensions with a transportational connective route to land, but seaward of a continental slope or rise.

If the depositional environment comprises an extensive area of fine-grained pelagic and hemipelagic sedimentation together with gravity-flow deposits, then sedimentation on a marine fan is considered the most likely setting. The absence of slump structures as well as the absence of features characteristic of continental rise and upper fan environments (e.g. submarine canyons and levee bordered valleys) favour this interpretation. The sequence of strata within the study area are interpreted to have been most



likely deposited in close proximity to the middle and lower submarine fan and basin plain regions.

#### 8.1.4 AGE

Sedimentation, as indicated by the presence of autochthonous fossil specimens of *Retroceramus* (*Retroceramus*) *haasti* (Hochstetter), is thought to have occurred largely within Late Jurassic (Middle Kimmeridgian) time and probably continued into Early Cretaceous time, at least up until the onset of metamorphism of the Torlesse in this region. Sedimentation had definitely ceased prior to Late Cretaceous time as rotation of the strata to its present steep attitude predates Late Cretaceous sedimentation in adjoining regions.

Blocks of allochthonous origin include fossiliferous limestone and calcareous conglomerates of shallow water marine origin, the former of which has been dated as Late Triassic (Early Norian) in age. This indicates that the source terrane comprised, in part, rocks of Late Triassic age. Ages of radiolarian cherts and fossiliferous calcareous siltstones were not determined in this study.

#### 8.1.5 LITHOSTRATIGRAPHY AND DEFORMATION

Subdivision of the essentially sedimentary sequence into Lithotypes has been based on lithology and degree of stratal deformation. Boundaries between Lithotypes do not correspond with major tectonic breaks but rather reflect a change in the tempo of deposition and/or a change in the depositional process. This, in turn, is often reflected by either a change in lithology or differences in the internal structure of the rock body. The lithologic heterogeneity and, to a large extent, the structural organisation of the Wharite Lithotype can be explained in this way.

Tectonic instability is recorded by isoclinal folding of the uppermost strata (Tamaki Lithotype) in the depositional basin. This phase of folding is thought to predate the deposition of the lithologically diverse sediments that now comprise the Wharite Lithotype but is nonetheless part of the same fold phase represented by isoclinal and subisoclinal folds in the Wharite Lithotype. These folds may have been the result of local slumping or regional gravity sliding. This phase of folding, together with an increase in the tempo of sedimentation, is interpreted as indicating the onset of precursory tectonic movements to the Rangitata Orogeny. During the Rangitata Orogeny (Early Cretaceous) part of the sedimentary sequence (Wharite Lithotype) was severely deformed, deformation being predominantly ductile, accompanied by minor brittle deformation. Ductile deformation took place

at relatively low confining pressures and temperatures, during which mechanical processes of flow predominated, to result in plastically and permanently deformed rocks. However, this deformation occurred under conditions of confining pressure sufficient to deform already metamorphosed blocks of limestone, so it is considered likely that deformation took place under an overburden. As this overburden is likely to have been sediments that now comprise the Western Lithotype, which have not suffered ductile deformation, it is unlikely that tectonic flattening by the overburden was the mechanism resulting in this ductile deformation. Instead, a mechanism involving extension of relatively competent materials surrounded by a more ductile matrix is preferred. Extension appears to have occurred in all directions oriented normal to bedding to produce pinch-and-swell structure and eventual breakage. The individual clasts define a foliation. Foliation is observed as a strong preferred orientation of lenticular clasts of competent lithologies and by penetrative, subparallel, anastomosing cleavage surfaces in the surrounding argillaceous matrix. These cleavage surfaces lie approximately parallel to the margins of the competent clasts. Extension fractures formed during ductile deformation occur normal to the direction of clast orientation and are only preserved in the competent lithologies where they are mineralised. Brecciation also apparently occurred at this time and is seen on both a microscopic and outcrop scale. This brecciation indicates that the competent lithologies were lithified at the time of deformation. Cemented breccia, for example along the line of the Ruahine Fault, indicates that this fault was active during this early phase of deformation and that brecciation occurred at depth beneath an overburden. Ductile deformation predates metamorphism as the clasts of competent lithologies, the argillaceous matrix and the cementing minerals are all of the same metamorphic grade. It is assumed that the sedimentary pile was metamorphosed in a horizontal attitude prior to rotation around an approximately horizontal axis to attain its present steep attitude. The timing of both metamorphism and subsequent rotation in this area is uncertain but it does predate Late Cretaceous sedimentation. Rotation is possibly due to westward underthrusting at a convergent plate margin resulting in imbrication and westward rotation of thrust sheets, each of which is internally westward younging but forms part of a regionally eastward younging succession.

Brittle deformation occurred in conjunction with episodes of folding and faulting as a result of the second orogeny, the Kaikoura Orogeny, in Quaternary times. This orogeny is thought to have begun in the Pliocene

and active faulting indicates that it is continuing today. Brittle fracturing of the Torlesse bedrock during both the Rangitata and Kaikoura Orogenies is not as significant as the ductile deformation during the Rangitata Orogeny. This is because the brittle fractures are not penetrative on a mesoscopic scale and total displacements are comparatively minor. Brittle fractures transect both the competent and incompetent lithologies and are of variable orientation, having been reoriented during later episodes of folding. This is also true for open joints.

Two younger phases of post-isoclinal folding have been recorded. The earlier phase created subhorizontal, open, asymmetric folds which refold both inverted and non-inverted limbs of the earlier formed isoclinal folds. The later phase created steeply plunging open folds that refold all earlier structures. The age of folding is uncertain but most undoubtedly occurred during the rotation of the strata past the vertical to become completely overturned, however, some folding clearly post-dates the rotation.

## 8.2 POST-LATE CRETACEOUS GEOLOGICAL HISTORY OF THE SOUTHERN RUAHINE RANGE

The Torlesse bedrock comprising the Ruahine Ranges was raised above sea level during the Rangitata Orogeny in Early Cretaceous times (Fleming, 1975; Kingma, 1959). Subsequent peneplanation occurred between the Late Cretaceous and Paleocene when a marine transgression submerged the southern North Island (Kingma, 1959) and resulted in the Cretaceous strata in this area being totally stripped. Tertiary deposits within the study area are characteristically discontinuous and show marked lateral and vertical thickness variations. Unconformities are numerous and hence the sequence of Tertiary deposits is incomplete. Part of the incompleteness can doubtless be attributed to subaerial erosion during regressions, marine erosion, non-deposition or reworking of sediments during subsequent transgressions. The sequence is also apparently compressed due to low rates of sedimentation during periods of transgression. Local tectonic activity also influenced stratigraphic relationships.

The lowermost beds of Tertiary age belong to the Opoitian and Waitotaran (Upper Pliocene) stages and were deposited upon an almost horizontal eroded greywacke surface in shallow, current-scoured waters (Lillie, 1953). Waitotaran sediments contain greywacke pebbles probably derived from initial exposure of the Torlesse at the ancestral site of the future Ranges. The close of the Waitotaran was marked by widespread shallowing accompanied by uplift of the greywacke bedrock along the axis of the present-day Ranges. Uplift along this axis was differential, such that to the north and south of

the Manawatu Saddle emergent greywacke formed a region of low relief hill country, whilst between these emergent highs there formed a structural low - the "Manawatu Strait". This "Strait" connected the Dannevirke Depression on the east with possibly deeper water of the Wanganui Basin to the west of the emerging Range. Shallowing water conditions existed in the vicinity of this "Strait" during Early Nukumaruan times as is indicated by the presence of limestone on the eastern flank of the Ranges near the entrance to the Manawatu Gorge. On the western flank of the Range a considerable thickness of very coarse gravel poured into the shallow waters of the "Manawatu Strait" from the emergent parts of the Ranges. West of the Ranges there was marine sedimentation in the deeper water of the Wanganui Basin during most of the Nukumaruan time (Lillie, 1953). At the close of Nukumaruan time, siltstones, sandstones, lignites and coarse gravels were deposited intermittently. The Ruahine and Tararua Ranges were emergent and undergoing denudation. During the Late Nukumaruan and Early Castlecliffian times differential and possibly pivotal movement continued along the eastern flank of the Ranges which considerably raised the emergent greywacke to the north and south of the "Manawatu Strait" (Lillie, 1953).

By Middle Castlecliffian time, tectonic uplift forced the sea to retreat from the "Manawatu Strait" and withdraw from the flanks of the Ranges. To the east the Dannevirke Depression became emergent and the Manawatu River established its course across the slowly rising Range, making an initial incision into the greywacke bedrock.

The post-Castlecliffian effects of the Kaikoura Orogeny essentially accentuated earlier movements and brought the period of marine sedimentation to a close. The greywacke bedrock of the Ruahine and northern Tararua Ranges swelled upwards in a simple, broad, anticlinal, northeast trending flexure; arching the erosion surface and overlying Tertiary beds. Concomitant flexuring along east-west axes occurred to produce the structural sag at the site of the "Manawatu Strait". Here the erosion surface is seen to ascend both towards the south where it is preserved in the Tararua Range and towards the north across the southern flank of the Ruahine Range (immediately south of Wharite Trig.) before being destroyed by erosion further north. Covering strata were stripped from the higher parts of the Ranges leaving the marked summit accordance seen today both in the southern Ruahine Range and to the south in the Tararua Range (Wellman, 1948). The anticline was fractured on its eastern limb by faults which were initiated during Nukumaruan time, or earlier. The complete emergence of all the Pliocene sediments was followed by a long interval of erosion, resulting

in the present features of relief. The land surface left by the last major retreat of the sea has, in comparatively recent times, been considerably uplifted and dissected during successive episodes of intermittent regional uplift to produce steep sided ranges and a youthful, deeply incised valley physiography.

Within Quaternary time much of the uplift of the Ranges has been the result of vertical fault displacement along high angle, northeast striking faults that bound both the eastern and western flanks of the Ranges. In some instances, fault displacements in Quaternary times have coincided with the line of Early Cretaceous fault movements but in other instances subsequent episodes of fault displacement have produced new traces. The amount of vertical displacement along active faults has not been uniform neither along the length of the fault nor through time. Greatest fault uplift has occurred along the eastern side of the Ranges on the Wellington Fault. Here, Early Quaternary vertical fault displacements have been greatest in the northeast of the study area and have resulted in the westward tilting of the surface of erosion preserved on the summit of the Range. In contrast, vertical fault displacement has been least in the vicinity of the Manawatu Saddle (see Section 8.3).

Fault activity has continued almost to the present. Much of the Late Quaternary vertical component of faulting has taken place on the Wellington Fault during pre-Ohakean and Ohakean times. On other faults vertical movement ceased prior to Ohakean time. There is no available evidence for fault displacements having occurred in historic time in this area.

### 8.3 DEFORMED REMNANTS OF THE PRE-QUATERNARY EROSION SURFACE

Within the study area there occur remnants of a once extensive erosion surface which had been carved across greywacke bedrock of Triassic-Jurassic age. To the north of the study area at a locality west of Lake Waikaremoana, Late Cretaceous rocks lie unconformably upon Torlesse bedrock (Grindley, 1960). If the erosion surface preserved in the study area is assumed to be a remnant of the same erosion surfaces preserved further to the north, then there is a strong indication that the formation of this surface pre-dates Late Cretaceous time. Rocks of Cretaceous age are not found in the study area, presumably having been totally stripped prior to deposition of the Tertiary deposits. Near Puketitiri (north of the study area), the erosion surface is overlain by Tongaporutuan (Middle Miocene) strata (Grindley, 1960). The oldest known Tertiary deposits found upon this erosion surface in the study area are of Late Opoitian age (Lillie, 1953).

They occur at the point where the erosion surface is structurally lowest, that is, immediately to the north of the Manawatu Gorge within the Manawatu Saddle. There are no known remnants of Tertiary materials upon the erosion surface referred to here as the 'Delaware Ridge' in the north of the study area. Here the presence of marine conglomerates and limestone of Early Nukumaruan age (Moore, 1975) at 700m altitude (T23/652222) in Pohangina Valley suggest that the Delaware Ridge was at least 400-500 metres above sea level at this time.

During Plio-Pleistocene time the erosion surface was warped into "anticlinal" and, in places, unfaulted, elongate, asymmetrical domes to form the Rimutaka, Tararua and Ruahine Ranges. Warping has occurred along both northeast trending longitudinal axes and east-west trending, transverse axes. The latter warps form physiographic "lows", e.g. the saddle north of the Manawatu Gorge that separates the longitudinal domes of the southern Ruahine and the northern Tararua Ranges.

Westward of Masterton to the eastern flank of the Tararua Range gravimetric data indicate that the erosion surface is gently upwarped to meet the domed surface of the Tararua Range, there being no evidence of a tectonic scarp bordering the eastern flank of this section of the Range (Heine, 1962). Such evidence is thought to support the interpretation that the Tararua-Rimutaka 'anticlines' are drag folds due to tectonic buckling as a result of shearing movements along the line of major primary faults (Heine, 1962).

Further to the north, however, the northern tip of the Tararua Range and the southern tip of the Ruahine Range are flanked along their eastern side by the high angle, northeast trending Wellington Fault on which considerable vertical uplift on the west side of the trace has taken place. The eastern flank of the Ranges may therefore be regarded as a tectonic scarp.

The western flank of these Ranges is also bordered by high angle, northeast trending faults on which vertical displacements appear to be predominantly of a reverse sense. Uplift on these faults has been less than that which has occurred on faults bordering the eastern flank of the Ranges. Thus differential fault displacement has occurred to produce a marked asymmetry in the cross-sectional profile of these Ranges (Fig. 8.1). This asymmetry is suggestive of westward tilting of a bedrock block and is best highlighted where remnants of the erosion surface have been preserved, e.g. in the vicinity of the Delaware Ridge (see cross-section E-F on Fig. 8.1). Structures analogous to westward tilted bedrock blocks occur to the east of the Ruahine Range within an asymmetrical depression filled with Tertiary

sediments, the deepest part of the depression lying adjacent to the Ruahine Range. Here, numerous parallel northeast-southwest trending faults traverse the area. Many of these appear to be thrust faults, others appear to be wrench faults showing right lateral movement. A seismic survey in this area indicated a number of structures, generally with long western flanks and short steeply dipping eastern flanks, similar to that described from the southern Ruahine Range (see section 1.5). In most cases eastern closure of these structures was dependent on faulting (Leslie & Hollingsworth, 1972).

"Live" anticlinal structures to the west of and parallel to the Ruahine Range are also asymmetric with similarly short, steep eastern and long, gentle western limbs (Te Punga, 1957). These structures are also likely to be bounded by faults with greatest uplift occurring on faults bordering the eastern flank of these structures. Thus, in contrast to the southern sector of the Tararua Range and the Rimutaka Range, the northern Tararua and the southern Ruahine Ranges are not dome-shaped but represent upthrusted, fault-bounded, westward-tilted bedrock blocks. Nonetheless, the near symmetrical cross-sectional profile of the southern Ruahine Range, in the vicinity of Wharite Trig. (see cross-section C-D on Fig. 8.1), together with the preservation of a surface of marine erosion that plunges westward, southward and eastward at this locality clearly defines this surface where it is least deformed. This structure may reflect an initial warping along both north-south and east-west trending axes which was later faulted along its eastern limb. Greater uplift along the eastern boundary fault relative to the western boundary fault has resulted in the tilting of the erosion surface towards the west. Uplift on the eastern boundary fault has been differential along its length, being greatest in the north of the study area and least in the vicinity of the Manawatu Saddle. Where fault uplift has been greatest the altitude of the Range is higher and the eastern limb of the Range steeper than at localities where uplift has been less. As a consequence, fluvial erosion has had its greatest effect in the northeast of the study area where it has removed all evidence of the erosion surface. Where uplift has been minimal, near the Manawatu Saddle, fluvial dissection is less severe and the surface of erosion is well preserved.

#### 8.4 ORIGIN OF THE MANAWATU GORGE AND A LOCAL ANALOGY

From its source on the eastern flank of the southern Ruahine Range (to the north of the present study area) the Manawatu River follows a southwesterly course for some distance before swinging abruptly towards the west across Tertiary and Holocene deposits to follow an approximate west-northwesterly

course through an axial range, where it is incised within Torlesse bedrock at the Manawatu Gorge.

The position and formation of the Manawatu Gorge have long been the subject of conjecture. The Gorge is found within a physiographically low saddle, known as the Manawatu Saddle, that forms a physiographic boundary between the northern tip of the Tararua Range and the southern tip of the Ruahine Range. Here, the Torlesse bedrock of these Ranges has been warped about two axes; an anticlinal warp about an axis longitudinal to the Ranges and a transverse warp causing the notable sag of the Manawatu Saddle area. The Manawatu Saddle has been a marked structural "low" since Miocene times and has a sequence of Pliocene strata preserved on it that records the existence of an ancient seaway, "The Manawatu Strait" of Lillie (1953). The longitudinal warping at the Saddle involves covering strata of Opoitian to Castlecliffian age and is hence a very late feature, formed by the final uplift of the Range during the Kaikoura Orogeny. The eastern limb of the warp is steeper, due to faulting, than is the longer gentler sloping western limb.

The position of the Manawatu Gorge does not correspond with the maximum depression of the anticlinal axis of the Torlesse bedrock, this being some 3 km to the north of the Gorge. Here the contact between Torlesse bedrock and Plio-Pleistocene marine deposits is only about 200m above sea level.

The Manawatu Gorge has long been regarded as a superposed feature though the exact mode of formation has been variously explained (Ongley, 1935; Cotton, 1942; Lillie, 1953). All explanations, prior to 1935, are examined and criticised by Ongley (1935), from which this brief table has been prepared:

#### PREVIOUS THEORIES ON THE ORIGIN OF THE MANAWATU GORGE

- (1) Before 1905 The antecedent theory: H Hill (referred to in Marshall, 1905).
- (2) 1905-1912 The Puketoi uplift and river-piracy theory: P Marshall.
- (3) 1907 The antecedent theory: D Petrie.
- (4) 1911 The earthquake-rift, uplift and lake theory: H Hill.
- (5) 1914 The (temporary) antecedent theory: P G Morgan.
- (6) 1914 The (technical) antecedent theory: J A Thomson.
- (7) 1912 The Puketoi uplift and lake spillover theory: P Marshall.
- (8) 1922 The anteconsequent theory: C A Cotton.
- (9) 1930 The superposed antecedent theory: G L Adkin.

---

Ongley himself proposed 'The consequent theory'. The latest known attempt to explain the origin of the Manawatu Gorge is that proposed by Piyasin



(1966) called 'The anteconsequent and lake spillover theory'.

It seems reasonable to imagine that with the original cover of marine beds on this country there was no former obstacle present at the structural "high" at the Gorge, that has been a "low" in relation to the rest of the Ruahine and Tararua Ranges since Miocene times. During regional uplift and emergence of the country to the east of the Ranges, a system of drainage was initiated which followed the ancient "Manawatu Strait" being ". . . guided by the first wrinkles of the surface as it emerged from the sea . . ." (Cotton, 1922) and was therefore consequent upon the "Strait". Subsequent down-cutting through the covering Tertiary strata into the underlying Torlesse bedrock gave the Manawatu River a superposed course at the Gorge. This course was antecedent to the localised tectonic uplifting of the Ranges along high angle, northeast striking faults. Adkins' (1930) interpretation of the evidence was that "At the Gorge the Manawatu River may thus be described as having a superposed antecedent course". However, as pointed out by Cotton (1922) and Ongley (1935), the formation of the Manawatu River being consequent on the earlier and antecedent to the later stages of a single series of deforming movements is strictly termed anteconsequent.

#### 8.4.1 THE ANALOGY

The Ruahine and Tararua Ranges are flanked to the east and west by high angle dextral transcurrent faults at which considerable vertical displacements have occurred within Quaternary time (see Chapter 6). The faulted nature of these Ranges suggests that structurally they comprise a horst (Kingma, 1957b) into which the Manawatu River has incised and maintained its course despite subsequent episodes of uplift, predominantly by vertical fault displacement of the Ranges. Taking the above points into account an analogy is drawn between the fault-bound Ruahine-Tararua horst and a similar but much smaller fault-bound structure formed as a result of the vertical fault displacement of part of an extensive terrace surface of Pleistocene age across the path of a previously existing stream.

At approximately 4.5 km to the south of the entrance to the Manawatu Gorge a tilted wedge, comprising a horst and graben, is bounded to the east and west by traces of the Wellington Fault. The wedge has formed between two fault traces from the point at which the principal trace of Wellington Fault bifurcates to where the two traces merge 2 km to the north (Inset E, Map 4). The horst, at the southern end of the tilted wedge, is bound to the east and west by straight and parallel north-striking fault scarps along which other features of tectonic origin also occur (T24/026-031, see

Appendix Va). To the west of the horst a small unnamed stream flows eastward across the north-striking horst into which it has incised a deep, narrow channel. The stream channel immediately to the east and west of the horst drains across a flat lying terrace surface of Pleistocene age into which incision has been minimal (Fig. 6.4). It is interpreted that this stream has maintained its course within the present channel and was antecedent to vertical fault uplift of the horst across its path. The rate of uplift of the horst appears to have been relatively constant, rather than in discrete jumps, as the latter would have resulted in the drainage being deflected either to the north or south along the front of the west-facing fault scarp. The rate of vertical fault displacement, therefore, did not exceed the rate of the downcutting capability of this stream which to date has resulted in the incision of a channel across the horst to a depth of 16 metres. A rate of downcutting and/or vertical fault displacement has not been established for this site as a more precise age for the displaced terrace surface is unavailable.

The above evidence is here considered to reinforce the view that the course of the Manawatu River, across the Ruahine-Tararua Ranges, was antecedent to the major episodes of tectonic uplift of these Ranges, predominantly by vertical fault displacement, during the Kaikoura Orogeny. The Manawatu River therefore maintained a rate of downcutting equivalent to that of the rate of tectonic uplift of these Ranges. Both processes continued well into Late Quaternary time, analagous evidence for which occurs along the trace of Wellington Fault in this area today.

### POTENTIAL RESEARCH

The close proximity of the Ruahine-Tararua Ranges to Massey University provides an ideal opportunity for further research to be carried out in this area. The potential for research topics far exceeds those outlined here and could involve disciplines other than those based upon the earth sciences. The following lines of research are considered to be worthy of consideration as some provide an opportunity for original research in areas where little knowledge is at present available, whilst other lines of research would further extend work carried out in this study.

Large tracts of these Ranges are unmapped. Isolated geologic studies of Torlesse strata within these Ranges indicate that melange terrane is often present. However, the areal distribution, stratigraphic relationships and nature of the contacts between melange and adjacent terranes, particularly in the lowermost portion of the North Island, is poorly understood. In addition, the paucity of fossils in these areas severely limits our interpretation and understanding of the distribution of Torlesse faunal zones. Better definition of faunal zones is likely to ensue from further geological research of the Torlesse in unmapped sectors of these Ranges, particularly in areas where melange terrane is present, because melange terrane tends to yield a disproportionate number of fossils. The discovery of new fossil localities, together with the mapping of melange and adjacent terranes of the Torlesse in these Ranges, hold the key to our understanding of the origin of the Torlesse.

Mapping the Torlesse and, in particular, melange terranes is difficult and is further complicated by the use of a diversity of terms by different authors to describe outcrops of similar appearance. There is, therefore, urgent need for the compilation of a written guide specifically designed to assist with mapping of melange terrane. In order to standardise methods of mapping and use of terminology such a guideline should be designed for use in a New Zealand context and as a supplement to 'Guide to recording of field observations in sedimentary sequences' (Andrews, 1976).

Palaeontological studies of fossil-bearing calcareous conglomerates, calcareous siltstones and cherts hold clues as to the age of allochthonous lithologies. In addition, the association of some fossiliferous cherts with massive volcanic lithologies provides a means of dating the volcanics, thereby clarifying whether the volcanics and associated cherts are of

allochthonous origin or were erupted in the basin of sedimentation contemporaneously with clastic deposition.

Features of tectonic origin, associated with faults in the Tararua Range, have in the past only been sketchily documented. There is scope for the detailed documentation of these features for presentation in the format of the 'Late Quaternary Tectonic Map' series along the lines presented on Map 4 and in Chapter 6 in this study for the southern Ruahine Range.

Within the study area there occur numerous ponds and swamps. Many are likely to contain pollen and wood bearing muds. A significant number of these ponds and swamps have been created by vertical fault displacement in Late Quaternary time and may therefore contain evidence suggestive of the approximate timing of the initial phases of fault displacement.

Alluvial terrace stratigraphy in the vicinity of the eastern flank of the Ruahine and Tararua Ranges is poorly understood. There exists in this area scope for further correlation of terraces over a wider area than was possible in this study. Correlation by pedological comparisons is the recommended approach to further work along these lines. The seemingly wide distribution of the Aokautere Ash and the likelihood of discovering further sites at which wood is preserved enhances the probability that such a line of research will prove to be fruitful.

\*\*\*\*\*